

School of Doctoral Studies in Biological Sciences  
University of South Bohemia in České Budějovice  
Faculty of Science

**Regulation of photosynthetic activity of pigment-  
protein complexes in thylakoid membranes**

Ph.D. Thesis

**Mgr. Eliška Kuthanová**

**Supervisor: Mgr. Radek Kaňa, PhD**

Institute of Microbiology CAS

České Budějovice 2020

This thesis should be cited as:

Kuthanová, E, 2020: Regulation of photosynthetic activity of pigment-protein complexes in thylakoid membranes. Ph.D. Thesis Series, No. 13. University of South Bohemia, Faculty of Science, School of Doctoral Studies in Biological Sciences, České Budějovice, Czech Republic, 175 pp.

### ✿ Annotation

The mechanisms of photoprotection have been examined in the secondary endosymbiotic algae *Chromera velia* and *Rhodomonas salina*. I applied biochemical, physiological and spectroscopical methods to reveal the mechanism of nonphotochemical quenching (NPQ) in native cells and in isolated antenna proteins. The results were compared to the NPQ mechanism already described in higher plants and put to the context within the evolutionary frame of photoprotection.

### ✿ Declaration

Prohlašuji, že svoji disertační práci jsem vypracovala samostatně pouze s použitím pramenů a literatury uvedených v seznamu citované literatury.

Prohlašuji, že v souladu s § 47b zákona č. 111/1998 Sb. v platném znění souhlasím se zveřejněním své disertační práce, a to v úpravě vzniklé vypuštěním vyznačených částí archivovaných Přírodovědeckou fakultou elektronickou cestou ve veřejně přístupné části databáze STAG provozované Jihočeskou univerzitou v Českých Budějovicích na jejich internetových stránkách, a to se zachováním mého autorského práva k odevzdanému textu této kvalifikační práce. Souhlasím dále s tím, aby toutéž elektronickou cestou byly v souladu s uvedeným ustanovením zákona č. 111/1998 Sb. zveřejněny posudky školitele a oponentů práce i záznam o průběhu a výsledku obhajoby kvalifikační práce. Rovněž souhlasím s porovnáním textu mé kvalifikační práce s databází kvalifikačních prací Theses.cz provozovanou Národním registrem vysokoškolských kvalifikačních prací a systémem na odhalování plagiátů.

This thesis originated from a partnership of Faculty of Science, University of South Bohemia, and Institute of Microbiology, CAS (Centre Algatech Třeboň) supporting doctoral studies in the Physiology and Developmental Biology study programme.



Přírodovědecká  
fakulta  
Faculty  
of Science



### **Financial support**

This research project has been supported by the Czech Science Foundation (GAČR) (Grantová agentura České republiky) projects GAČR (19-11494S), GAČR (16-10088S), GAČR (17-02363Y), and by institutional project Algatech Plus (MSMT LO1416) from the Czech Ministry of Education, Youth and Sport.

### **Acknowledgements**

I would like to thank my boss Radek Kaňa for being the calming and cooling element when I got too stressed and for giving me the freedom to develop my skills and abilities. I would also love to thank Erica Belgio for our amazing and inspiring collaboration leading to the majority of my publications. I further thank Roman Sobotka for never kicking me of his office when I needed help with my experiments. I am grateful to Alexander V. Ruban for allowing me to work in one of the leading laboratories in the field. I want to thank my amazing colleagues and office-mates Myriam Canonico, Anna M. Yeates, Aurelie Crepin, Barbora Šedivá, and Grzegorz Konert who motivated me through my studies. Special thanks belong to our secret scientific girl group “Hloupé buchty”, with whom I could share all my thoughts and rough moments. To all the people of Algatech, thank you for having me, thank you for making my work enjoyable, thank you for the amazing and friendly atmosphere and for letting me feel like I am a part of a big family. Last but not least, I want to thank my family for their love, patience and supporting background they have created for me.

## ☼ List of articles and author's contribution

The thesis is based on the following original articles:

- **Kaňa, R., Kotabová, E., Kopečná, J., Trsková, E., Belgio, E., Sobotka, R., and Ruban, A. V.** (2016). Violaxanthin inhibits nonphotochemical quenching in light-harvesting antennae of *Chromera velia*. *FEBS Letters* **590**, 1076-1085. IF = 3.21

*Eliška Kuthanová was responsible for isolation and purification of light harvesting antennas, biochemical characterization, harvesting cells, preparation of extracts for violaxanthin isolation, in vitro experiments with isolated antennas, absorption and 77 K spectra. She discussed the results, prepared the Materials and Methods chapter and commented on the whole manuscript.*

- **Belgio, E., Trsková, E., Kotabová, E., Ewe, D., Prášil, O., and Kaňa, R.** (2018). High light acclimation of *Chromera velia* points to photoprotective NPQ. *Photosynthesis Research* **135**, 263-274. IF = 3.057 (\* Erica Belgio and Eliška Trsková have contributed equally to this work.)

*Eliška Kuthanová was responsible for designing the project, fluorescence induction measurements, size exclusion chromatography and electrophoresis. She discussed the results, analyzed the data, wrote the article and prepared the figures together with Dr. Erica Belgio.*

- **Kuthanová Trsková, E., Belgio, E., Yeates, A. M., Sobotka, R., Ruban, A. V., and Kaňa, R.** (2018). Antenna proton sensitivity determines photosynthetic light harvesting strategy. *Journal of Experimental Botany* **69**, 4483-4493. IF = 5.36

*Eliška was responsible for designing the project, of in vivo and in vitro fluorescence spectroscopy, isolation and purification of antenna proteins and in silico analysis. She discussed the results, wrote the article and prepared the figures together with Dr. Erica Belgio.*

- **Kuthanová Trsková, E., Bína, D., Santabarbara, S., Sobotka, R., Kaňa, R., and Belgio, E.** (2019). Isolation and characterization of CAC antenna proteins and photosystem I supercomplex from the cryptophytic



alga *Rhodomonas salina*. *Physiologia Plantarum* **166**, 309-319. IF (2018) = 3.0

*Eliška Kuthanová was responsible for designing the experiments, for photosystem I and antenna protein isolation and purification, for in vitro quenching and absorption and fluorescence spectroscopy and electrophoretic techniques. She analyzed the data and wrote the article in co-operation with other co-authors.*

- **Kaňa, R., Kotabová, E., Šedivá, B., and Kuthanová Trsková, E.** (2019). Photoprotective strategies in the motile cryptophyte alga *Rhodomonas salina* – role of non-photochemical quenching, ions, photoinhibition and cell motility. *Folia Microbiologica* 64, 691-703.

*Eliška Kuthanová was responsible for cell cultivation and she contributed in writing and finalizing the project in a form of article.*

## **Content**

1. GENERAL INTRODUCTION	1
1.1 Background	1
1.2 An overview of photosynthesis	1
1.3 Light-harvesting antennas of photosystems	4
1.4 Mechanisms of photoprotection and light acclimation	8
1.5 Nonphotochemical quenching – description and detection	14
2. MAIN GOALS	27
3. MATERIALS AND METHODS	33
3.1 Model Organisms	33
3.2 Methods	38
4. OVERVIEW OF MY RESEARCH	41
5. CONCLUSIONS AND FUTURE PROSPECTS	47
6. REFERENCES	57
7. RESEARCH ARTICLES	81
Article I	83
Article II	101
Article III	125
Article IV	145
Article V	161
Curriculum vitae	

### List of abbreviation

- $\beta$ -DDM** = n-Dodecyl- $\beta$ -D-maltoside  
 **$\alpha$ -DDM** = n-Dodecyl- $\alpha$ -D-maltoside  
**CAC** = chlorophyll a/c antenna proteins  
**Chl** = chlorophyll  
**CLH complex** = Chromera light harvesting complex  
**CMC** = critical micellar concentration  
**CN-PAGE** = Clear native polyacrylamide gel electrophoresis  
**ETC** = electron transport chain  
**F<sub>0</sub>** = Minimal fluorescence  
**F<sub>m</sub>** = Maximum fluorescence in dark  
**F<sub>m</sub>'** = Maximal fluorescence during illumination  
**FPLC** = Fast performance liquid chromatography  
**HL** = High light  
**HPLC** = High performance liquid chromatography  
**IEC** = Ion exchange chromatography  
**IEF** = Isoelectric focusing  
**LHC** = Light harvesting complex  
**LHCII** = Light harvesting complex of photosystem II  
**LHCI** = Light harvesting complex of photosystem I  
**NADPH** = Nicotinamide adenine dinucleotide phosphate  
**NPQ** = Nonphotochemical quenching  
**PAM** = pulse amplitude modulated  
**PPCs** = pigment-protein complexes  
**PSI, PSII** = Photosystem I, Photosystem II  
**qE** = Energy dependent quenching  
**qI** = Photoinhibitory quenching  
**qT** = State-transition quenching  
**ROS** = Reactive oxygen species  
**RuBisCO** = Ribulose bisphosphate carboxylase/oxygenase  
**SDS-PAGE** = Polyacrylamide gel electrophoresis with sodium dodecyl sulfate (SDS) as detergent



# **1 General introduction**

## **1.1 Background**

Photosynthesis is one of the most important processes in biology, due to its huge impact on Earth's atmosphere (e.g. by the production of oxygen) and the biosphere in general. Photosynthesis research thus has a long history. The understanding of this fascinating process becomes even more important nowadays, as according to the latest numbers, the world population is estimated to rise close to 10 billion people in the next 30 years. This prediction opens several key issues like the increasing food demand and the need for renewable energy sources that are both connected with photosynthesis. Our understanding of the entire process could thus in the future bring a required increase in the overall crop yield that is crucial for the sustainable development of our planet.

One of the mechanisms which affect yield in crop production is nonphotochemical quenching (NPQ) (see e.g. Kromdijk et al. (2016)). This mechanism protects photosynthetic proteins from damage by reactive oxygen species produced at high light. It dissipates the excessive excitation energy safely as heat. The molecular mechanism of NPQ has been extensively studied mostly in higher plants, however, its detailed mechanism is rather puzzled in many other phototrophs. Therefore, there is a need to study the evolutionary variability of this protective mechanism.

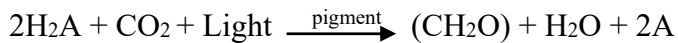
The thesis is based on studies of NPQ in less explored species of algae; cryptophytes, *Rhodomonas salina*, and *Chromera velia* representing photosynthetic alveolate alga. Through insight into the molecular basis of their photoprotection, together with our knowledge of the NPQ mechanism in other model organisms (e.g. higher plants), we can get important information about the possibilities to improve the efficiency of photosynthesis.

## **1.2 An overview of photosynthesis**

The sustainable life on Earth is based on the chemistry of carbon, which is present as three inorganic ionic forms: carbon dioxide (CO<sub>2</sub>), bicarbonate (HCO<sub>3</sub><sup>-</sup>) and carbonate (HCO<sub>3</sub><sup>2-</sup>). These three forms, however,

cannot be used to build organic molecules. First, they need to be reduced with the expense of free energy. The most important process in charge of carbon reduction is photosynthesis.

Photosynthesis converts light energy into the energy of chemical bonds. The whole process can be simplified into the general oxidation-reduction equation:



Note that compound A is the oxygen atom and the process runs under oxygenic conditions in cyanobacteria, prochlorophytes, eukaryotic algae, and higher plants (see e.g. Falkowski and Raven (2007)). Chlorophyll a (Chl *a*) is the main light-harvesting pigment in eukaryotic phototrophs and in prokaryotic cyanobacteria. The pigment (embedded in proteins) is required to catalyze reactions of water oxidation, which results in the production of free molecular oxygen. The oxygenic photosynthesis thus gave rise to the current value of oxygen concentration on Earth.

The overall mechanism of photosynthesis is historically divided into two main series of reactions acting simultaneously (Blankenship, 2002): Light-dependent reactions and light-independent reactions (historically dark reactions). They take place in different parts of chloroplasts, the photosynthetic organelles in eukaryotes. The light reactions occur in thylakoid membranes, whereas carbon fixation in chloroplast stroma (see Figure 1). The light-dependent reactions include light absorption (requiring pigments), charge separation (in reaction centers of photosystem I and II) and subsequent electron flow between redox systems of proteins (cytochrome  $b_6/f$ ) and electron carriers (plastoquinone, plastocyanin). The system of electron transporters is often called an electron transport chain (ETC) (see Figure 1). The redox energy during electron transport in ETC is used to pump protons into the thylakoid lumen. Protons subsequently form a concentration gradient across the thylakoid membrane that is afterward used when protons slide down

through ATP synthase as it is described by the chemiosmotic theory (Mitchell, 1961).

During dark reactions, Calvin-Benson cycle catalyzes the synthesis of triose-phosphate (glyceraldehyde 3-phosphate) and subsequent

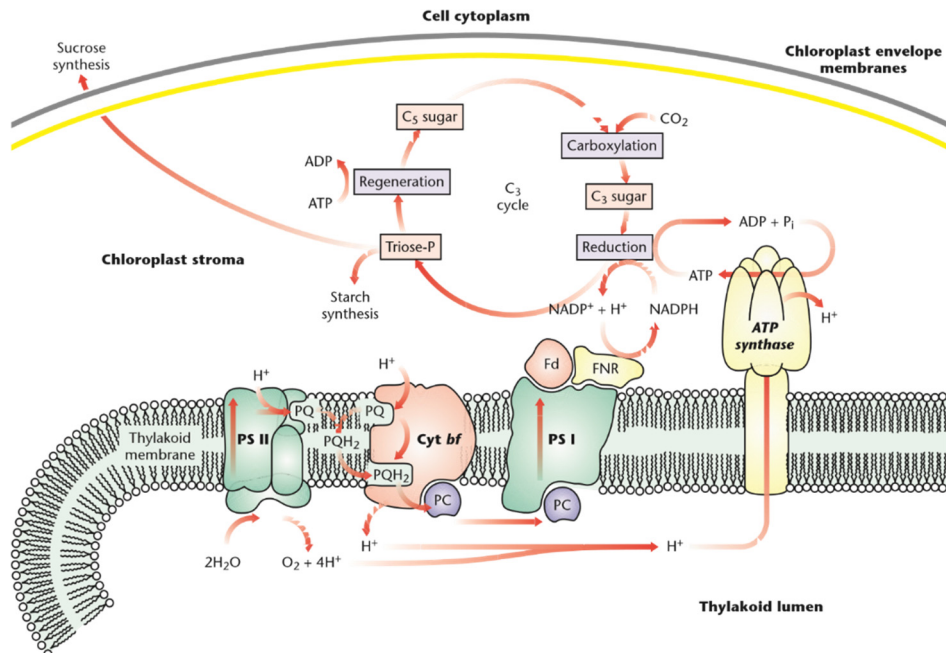


Figure 1: The schematic overview of photosynthesis, its electron transport chain and Calvin-Benson cycle. The light-driven electron flow is coupled to the accumulation of protons in the lumen which is then used for ATP synthesis. The energy stored in ATP and NADPH is then used in the Calvin-Benson cycle, which consists of three stages: carboxylation, reduction, and regeneration. Key: PS II, photosystem II; PS I, photosystem I; PQ and  $PQH_2$ , oxidized and reduced plastoquinone; cyt, cytochrome; PC, plastocyanin; Fd, ferredoxin; FNR, ferredoxin-NADP reductase, Triose-P, triose phosphate;  $C_3$ , three carbon-containing molecule;  $C_5$ , five carbon-containing molecule. Picture from Ort and Whitmarsh (2001)

sucrose/starch synthesis, from the free  $CO_2$  and with the help of light-reactions products – ATP and NADPH. The crucial reaction of the cycle is carboxylation (conversion of 1,5-bisphosphate to two molecules of 3-phosphoglycerate) that is catalyzed by the Earth's most abundant enzyme, ribulose bisphosphate carboxylase/oxygenase – “RuBisCO”. The initial step is followed by the “reduction” step when triose-phosphate is formed and later utilized during gluconeogenesis to produce glucose 6-phosphate.

The whole Calvin-Benson cycle ends with the “regeneration” step when remaining triose-phosphate molecules are used to form ribulose 1,5-bisphosphate (see e.g. (Falkowski and Raven, 2007; Ruban, 2013)).

### **1.3 Light-harvesting antennas of photosystems**

The process of photosynthesis in the two photosystems (PSI, PSII) starts with light absorption by pigments, which are precisely organized in pigment-protein complexes called light-harvesting antennas. Throughout the evolution, antenna proteins have evolved into various antenna systems that are capable of adapting to different light conditions (low light, high light, the light of different spectral compositions, etc.). The antenna systems thus vary considerably among photosynthetic species (see e.g. reviews (Büchel, 2015; Green and Parson, 2003; Green and Pichersky, 1994; Green, 2011; Liu et al., 2008; Liu and Blankenship, 2019)) in contrast to photosystems that are very similar among species (Sobotka et al., 2017). Most of the light-harvesting antennas of oxygenic phototrophs share some common features; they contain chlorophylls (chlorophyll a, b, c) together with different carotenoids (lutein, violaxanthin, zeaxanthin,  $\beta$ -carotene, etc.) that are both covalently bound to protein complexes.

All light-harvesting antenna complexes share properties and fulfill the following crucial functions: i) an increase of the absorption cross-section of photosystems (see e.g. (Ley and Mauzerall, 1982; Nawrocki et al., 2016)); ii) a widening of the spectral range of photosynthetically active irradiation by means of various pigments or proteins with different absorptions (see e.g. (Horton and Ruban, 2005; Horton et al., 2000)).



Two types of antennas can be distinguished based on their position in the membrane (outer vs inner) and interactions with reaction centers: (I) membrane integral antennas and (II) membrane peripheral antennas that are associated with reaction centers via noncovalent interactions (see

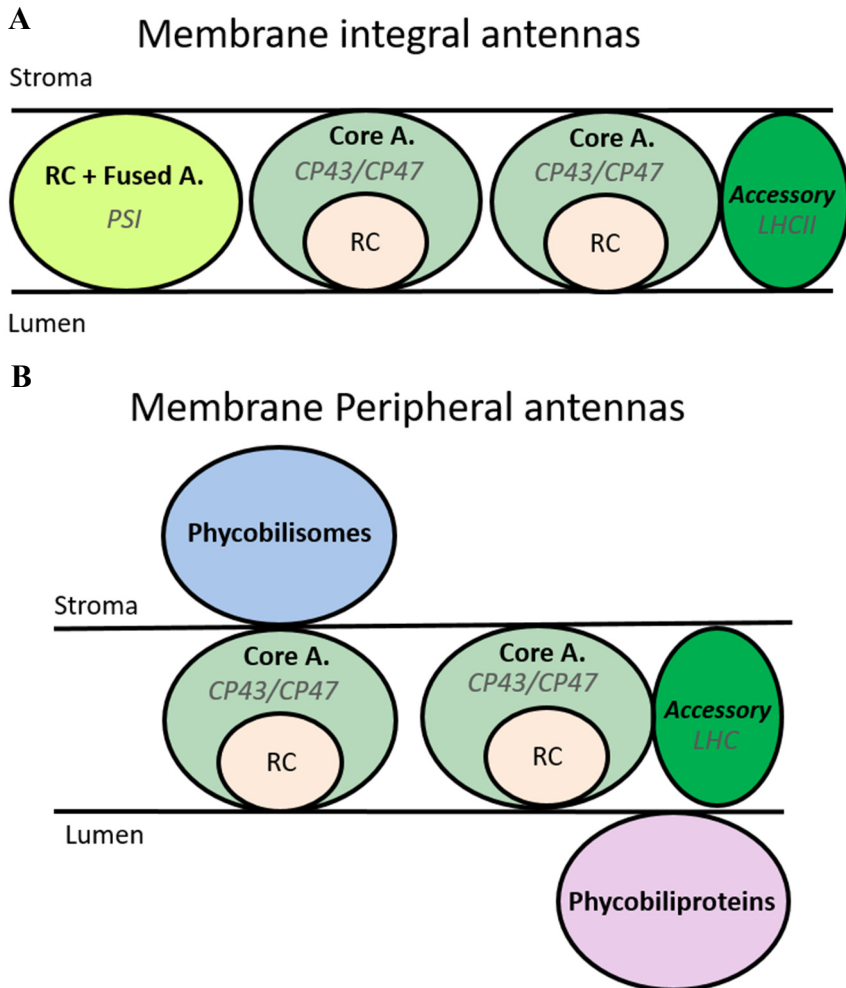


Figure 2: A: Types of membrane integral antennas: Fused antennas are integrated into the reaction center (RC) sharing the same polypeptide, typical example is photosystem I (PSI) RC, Core antennas are closely associated with RC but they do not share the same polypeptide, typical examples are antennas of PSII CP43 and CP47, Accessory antennas are arranged separately from RC and taking various localizations, typical example are LHCII; B: Types of membrane peripheral antennas: Stromal phycobilisomes found in cyanobacteria, red algae and glaucophytes, and luminal phycobiliproteins found in cryptophytes. Picture modified after (Ruban, 2013)

Figure 2). The type (I), the integral antennas are further divided into three subtypes: i) fused antennas, integrated into the reaction center sharing the same polypeptide – e.g. photosystem I reaction center complex which contains two polypeptides binding the photochemically active chlorophyll together with a vast number of Chl *a* molecules serving as light-harvesters (see e.g. (Mazor et al., 2015)); ii) core antennas, associated with reaction centers but not sharing the same polypeptide – e.g. CP43 and CP47 complexes of photosystem II (Alfonso et al., 1994); iii) accessory antennas, which are composed of proteins taking various arrangements and localizations relative to reaction centers – e.g. the main light-harvesting complexes of PSII (LHCII), and of PSI (LHCI). Due to their flexibility and number of possible rearrangements, accessory antennas are, besides light-harvesting, commonly involved in photoprotection (Ruban et al., 2012). A typical example of the latter type, peripheral antennas, are phycobilisomes found in cyanobacteria (Calzadilla et al., 2019; Niedzwiedzki et al., 2019), red algae and glaucophytes (for review see e.g. (Büchel, 2015; Green and Parson, 2003)). These antennas are located in the stromal side of the membrane and they exhibit strict structures of water-soluble phycobiliproteins (Yamanaka et al., 1980; Zhao et al., 2019). Other examples of peripheral antennas are phycobiliproteins found in cryptophytes (Funk et al., 2011; Kaňa et al., 2012) that do not organize into complex structures and are tightly packed in lumen instead (Kaňa et al., 2009).

The majority of eukaryotic photosynthetic organisms have as an accessory antenna the membrane intrinsic pigment-proteins of the Light-harvesting complex (LHC) family (see e.g. (Büchel, 2015; Wolfe et al., 1994)). These proteins are classically formed by three transmembrane  $\alpha$ -helices connected by loops of various sizes. Their pigment content varies based on species, as Chl *a* can be accompanied with Chl *b* or *c* and by a large number of carotenoids (for review see (Büchel, 2015; Büchel, 2019; Engelken et al., 2010)). All accessory LHC proteins are encoded by the nucleus genes. So, LHC apo-proteins need to be transported into

chloroplasts, where they bind chlorophylls and carotenoids (Green and Parson, 2003; Pan et al., 2012). One, two or four-helix antennae proteins from LHC family are usually involved in special functions in photoprotection, e.g. PsbS acting as a pH sensor (see e.g. (Croce, 2015; Mou et al., 2013; Zhang et al., 2013)).

From the evolutionary point of view, genes from the Lhc protein superfamily can be divided into two major groups (Engelken et al., 2010; Koziol et al., 2007): i) “green group” - it codes for Chl *a/b* antennas proteins of PSI (Lhca genes) and PSII (Lhcb genes) from green algae, mosses, and higher plants; ii) red group - genes coding various chlorophyll *a/c* light-harvesting antenna proteins including Lhcf (in dinoflagellates), Lhcr (in cryptophytes and dinoflagellates), Lhcx (the analog of LhcSR from the green lineage) found in some dinoflagellates and Lhcz (in cryptophytes). For a general overview see Figure 3 (Büchel, 2015). This antenna species variability is crucial for aquatic organisms as they are

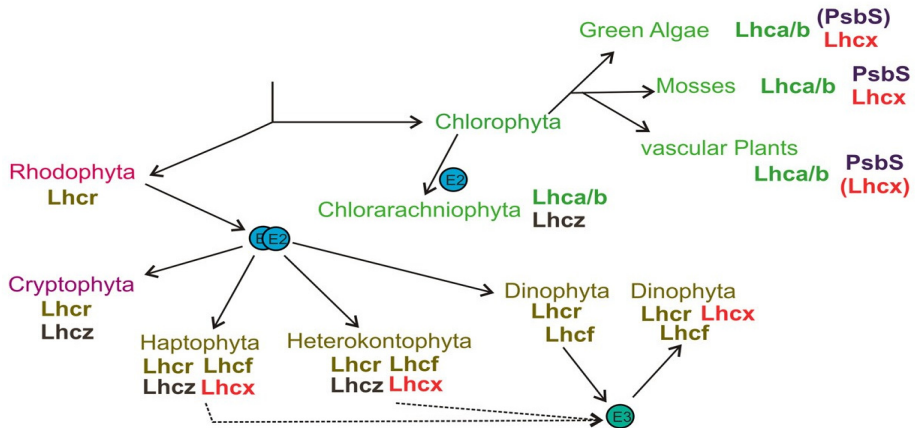


Figure 3: Light harvesting complex (Lhc) proteins in different algal groups and their phylogenetic relationship adapted from (Büchel, 2015). E2, secondary endosymbiosis, E3, tertiary endosymbiosis, brackets indicate that a gene is present but no protein is usually expressed, dotted lines point out alternative routes for tertiary endosymbiosis.

challenged by attenuated light intensities and varying light spectra in higher water depths. As a result of various antenna systems employing different pigments, aquatic organisms are nowadays able to use basically almost the whole range of wavelengths of visible light available from the

sun (see e.g. (Falkowski and Raven, 2007)). This high efficiency in light absorption, however, brings a need to cope with dynamic changes in light intensities as high-light peaks can be harmful to the photosynthetic machinery. From that reason, systems of antenna proteins have been adapted for both efficient light harvesting, and for fast excess light dissipation by mechanisms of photoprotection (for more information in higher plants see (Ruban et al., 1992; Ruban et al., 2012), for diatoms see (Buck et al., 2019; Lavaud et al., 2002b), for recently discovered alveolate *Chromera velia* see (Belgio et al., 2018; Mann et al., 2014)).

#### **1.4 Mechanisms of photoprotection and light acclimation**

Photosynthetic organisms optimize their light-harvesting systems for variability in the incident light to buildup and gain sufficient biomass and energy based on their habitat. In this long-term acclimation (days, weeks) they can modify pigment-protein content (e.g. by a change in the number of light-harvesting units and reaction centers) or pigment content itself (by modification in the concentration of chlorophylls and carotenoids). For instance, leaves in the tree canopy experience various light environment at a different location; it results in different pigment profiles – the shaded/sun leaves are enriched in chlorophyll/xanthophylls (Hansen et al., 2002; Poorter et al., 2009).

However, it is important to note that light intensity in a particular habitat is not constant. Irradiance changes with the position in the forest canopy (shaded leaves vs leaves on direct sunlight (Ruban, 2013)), or in the water column (either turbulent changes in irradiation due to water mixing (Dera and Gordon, 1968; Falkowski et al., 1981)), or due to an active algal movement in the water column (e.g. for cryptophyte algae see (Kaňa et al., 2019)). Irradiance changes also with time, there are either periodical everyday diurnal changes in irradiation or rapid and unpredictable sunlight shading caused by clouds or leaf movement (Kromdijk et al., 2016; Ruban, 2016).

Light-harvesting antennas efficiently collect light and deliver sufficient excitations into reaction centers at various irradiances. The relationship between the absorbed and utilized energy in photosynthesis is depicted in Figure 4. The reaction centers and whole photosynthesis

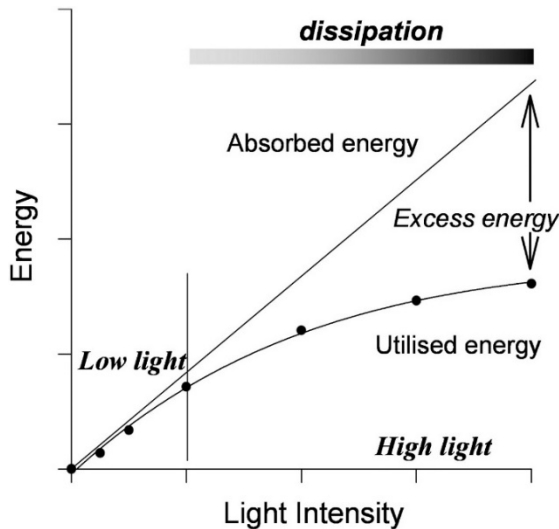


Figure 4: The fate of absorbed light energy and its utilization in photosynthesis. Under low light conditions, the amount of absorbed and utilized energy matches. However, with continuing light absorption, the photosynthetic reaction centers become saturated, which leads to a buildup of potentially harmful excess energy. Figure adapted from (Ruban et al., 2012)

become saturated with increasing light intensity that can lead to the reduction of harmful products like reactive oxygen species - ROS (Goss and Lepetit, 2014; Horton et al., 1996; Johnson et al., 2011; Takahashi and Badger, 2011). ROS can be then fatal to the photosynthetic proteins primarily at the level of PSII. The light-induced PSII degradation is called photoinhibition (in other words, reduction in the number of functional PSII reaction centers, for review

see (Takahashi and Badger, 2011)). It limits overall photosynthetic activity, growth, and productivity. Therefore, photosynthetic organisms have evolved fast PSII repair mechanisms represented by D1 protein turnover (see e.g. (Komenda et al., 2006; Yamamoto et al., 2008)) to deal with the continual damage caused by high PSII sensitivity to high-light.

To cope with fluctuating light intensities, plants and algae evolved an effective network of adaptive mechanisms acting at four levels (adapted from (Li et al., 2009; Long et al., 1994)): i) Light avoidance - on the level of light absorption – it controls the amount of energy absorbed by antennas; ii) Light tolerance – when already absorbed light-energy in the antennas

system is utilized or dissipated; iii) damaged protein turnover, e.g. D1 protein during photoinhibition; iv) the long-term changes in irradiations (days, weeks) that cause acclimation to high light. All these mechanisms (i-iv) are then controlled and triggered differently (see sensing mechanisms in Figure 5). Once the excess light is sensed, the signal is transduced and continuously triggers (with different kinetics) one of these basic physiological responses to high light: light tolerance, light avoidance, light damage (photoinhibition) or light acclimation (summarized in Figure 5). The light tolerance mechanism includes dynamic changes affecting some of the crucial antenna properties, changes in effective absorption cross-section of PSII and fluorescence lifetime. In general, adaptation mechanisms can be distinguished based on their temporal action on Long-

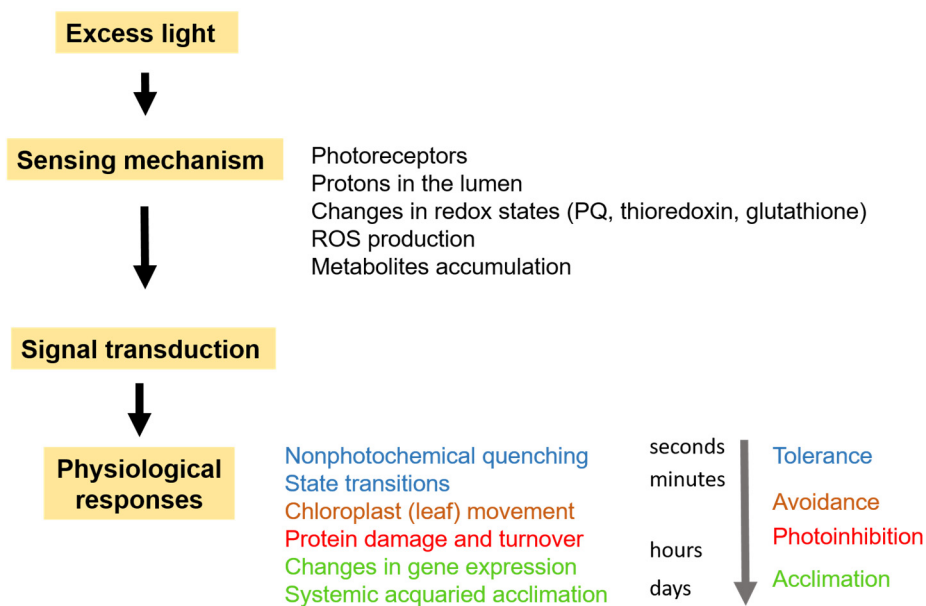


Figure 5: A schematic representation of mechanisms for sensing and responding to excess light modified after (Li et al., 2009), PQ, plastoquinone; ROS, reactive oxygen species. There are 4 basic physiological responses to high-light (Long et al., 1994): light-tolerance, light-avoidance, photoinhibition, acclimation.

term acclimation and Short-term acclimation. The fastest physiological responses are represented by nonphotochemical quenching and state transitions (see section 1.4.1). Later in time, there is light avoidance on the

whole organism level (e.g. adjustment of leaf orientation), on the cellular level (chloroplast movement) or most importantly, the acclimation on the molecular level (a long-term control of chlorophyll content in the membrane connected with the antenna size and with the PSI/PSII ratio (Belgio et al., 2012; Belgio et al., 2014; Belgio et al., 2018; Ruban, 2013)). All the above-mentioned acclimation strategies are discussed in connection to high light stress throughout the following section.

#### **1.4.1 Physiological responses to high light**

**Tolerance:** The short-term acclimation mechanisms allow a tolerance of high/low light. They act as pre-existing regulatory mechanisms triggered by high light, with no effect on gene expression. These mechanisms are rather fast, they occur in seconds/minutes after a sudden change in light intensity (sun flecks, shading by clouds, etc.). The first example of this mechanism is the process of state transitions (for review see (Goldschmidt-Clermont and Bassi, 2015; Mullineaux and Emlyn-Jones, 2004)), firstly observed in green (Bonaventura and Myers, 1969) and red (Murata, 1969) algae. Afterward, it was also found active in cyanobacteria (Mullineaux and Allen, 1990), in higher plants (see e.g. (Nellaepalli et al., 2013; Wientjes et al., 2013a)) and in other secondary endosymbiotic algae, cryptophytes (Cheregi et al., 2015). State transitions can balance an excitation energy distribution between photosystems. Based on the standard model, state transitions functionally re-localize the antennas of PSII either to PSI or leave them uncoupled from photosystems. The process makes use of differences in absorbance spectra of Photosystems, as PSI often contains red-shifted pigments (above 700 nm) that are absent in PSII. State transitions are thus essential to keep the balance between both reaction centers activity in order to optimize the linear electron transport chain. State transitions are usually involved under low light irradiance when light is a limiting factor (reviewed in Mullineaux and Emlyn-Jones (2004)). However, under high light conditions, another quickly-responding phenomenon takes place, the so-called

nonphotochemical quenching of fluorescence (discussed separately in section 1.5).

**Avoidance:** Other short term acclimation strategies lead to light avoidance due to organelle/cell motility. In higher plants, a controlled chloroplast movement takes place in order to optimize the incident light (see e.g. (Suetsugu and Wada, 2007; Wada, 2016)) together with the leaf movement (Feng et al., 2019; Koller, 1990). Chloroplasts are able to move into the shade of other chloroplasts after the blue-light photoreceptors are activated (Cazzaniga et al., 2013). Motile algae, like cryptophytes, exhibit positive and negative phototaxes (Häder et al., 1987) – they move away from the intense light in response to blue and green light receptors (Kaneda and Furuya, 1986; Kaneda and Furuya, 1987). Recently, it has been also suggested that the algal cell rotation around the longitudinal axes might have a photoprotective role as it changes the continual irradiation to periodically fluctuating light (Kaňa et al., 2019).

**Photoinhibition:** Photoinhibition starts with changes on the acceptor side of PSII (Vass, 2012) leading to the degradation of the central subunit of PSII, the D1 protein. The degraded protein is exchanged for the newly synthesized copy in the so-called D1 protein turnover to restore the PSII activity (reviewed in (Li et al., 2009; Yamamoto et al., 2008)). It is important to note that the process of the D1 protein damage occurs at all light intensities, yet the repair mechanisms keep the pace with it. Under saturating light intensities, however, the mechanism fails to keep up with the damage and a net decrease of the photosynthetic rate, the photoinhibitory damage of PSII can be observed (Aro et al., 2005).

The common strategy to avoid photoinhibition in higher plants is reducing the light-harvesting antenna size to decrease the amount of absorbed light energy (Kouřil et al., 2013; Ware et al., 2015a). Algae, in contrast to higher plants, often reduce the number of PSII reaction centers without the change in the antenna size (Belgio et al., 2018). It results in a portion of antennas poorly connected to reaction centers – uncoupled antennas (Behrenfeld et al., 1994; Belgio et al., 2012) that prevent the



photoinhibitory damage of PSII (Belgio et al., 2018; Kaňa et al., 2002). The further mechanism typical rather for algae is the so-called excess capacity of PSII that represents another efficient acclimation strategy (Behrenfeld et al., 1994; Belgio et al., 2018; Kaňa et al., 2002). It allows keeping the maximal photosynthetic rate, the so-called “photosynthetic capacity” (measured either as oxygen evolution or CO<sub>2</sub> assimilation, at saturating light intensity). The excess capacity of PSII is present when the number of PSII is reduced by photoinhibition but photosynthetic capacity remains unchanged. It has been rationalized by the increase in PSII turnover (Behrenfeld et al., 1998; Kaňa et al., 2002).

**Acclimation and adaptation:** Long-term acclimation mechanisms are connected with the development and regulation of gene expression, which can take from days to weeks and usually results in changes in composition and structure on the membrane level. The typical examples are fine-tuning of PSI/PSII ratio (Walters, 2005), changes in effective antenna size of photosystems (see e.g. (Havelková-Doušová et al., 2004; Kagawa et al., 2001)) or the number of reaction center units in total (Belgio et al., 2018). For example, high light treatment in higher plants usually increases Photosystem I/Photosystem II ratio (Boardman, 1977; Kendrick and Kronenberg, 1994), reduces total chlorophyll content (see e.g. (Oguchi et al., 2003; Pyke, 2009) – this is often connected with smaller effective antenna size of PSII (Anderson and Osmond, 2001; Anderson et al., 1988; Morosinotto et al., 2006; Pesaresi et al., 2009; Wientjes et al., 2013b). However, the reduction in the effective antenna size at high light is not a universal principle for all organisms as especially aquatic organisms react differently to high-light (HL) (see for diatoms (Behrenfeld et al., 1998), for green algae (Bonente et al., 2012; Havelková-Doušová et al., 2004), or in other algae (e.g. *Chromera velia* (Belgio et al., 2018))). For overall species variability in the changes in antenna size, see the review (Falkowski and Owens, 1980) for algae and (Kouřil et al., 2012) for comparison with higher plants. Another interesting example of long-term acclimation is present in colonial algae; they need to optimize their overall

antennae system, in contrast to single cellular species. Therefore, they often display larger and more spatially heterogeneous colonies, where cells that are deeper inside have increased pigmentation and larger antenna system due to overcoming self-shading (van den Berg et al., 2019; Wobbe et al., 2016).

### **1.5 Nonphotochemical quenching – description and detection**

Nonphotochemical quenching (NPQ) of Chl *a* fluorescence represents one of the most common and the fastest mechanism of tolerance to high light (see the previous chapter). It is a rapidly responding mechanism of photoprotection, in which the excess light energy absorbed by pigments is safely dissipated as heat. The term quenching results from the fact that it is often measured as a decrease in quantum yield of Chl *a* fluorescence. Therefore, it has been defined as a so-called nonphotochemical Chl *a* fluorescence quenching. Currently, also some other methods of NPQ detection based on fluorescence life-time (see e.g. (Johnson et al., 2010; Kaňa et al., 2016; Miloslavina et al., 2009)) and measurements of isolated proteins *in vitro* in detergent micelles (Belgio et al., 2013; Kuthanová Trsková et al., 2018; Petrou et al., 2014) are commonly used.

NPQ operates in different organisms including higher plants, various algae, and also in cyanobacteria (Büchel, 2014; Demmig-Adams et al., 2014; Finazzi and Minagawa, 2014; Ruban and Murchie, 2012). Even though there are many similarities in NPQ regulations for different species (e.g. triggering by pH), there are also some species-specific features of NPQ (e.g. location either in antennas or in reaction centrum). Although numerous studies have been already performed, our knowledge of the general features of NPQ mechanisms is still rather puzzled as most of the studies have been focused on only a few model organisms: higher plants, green algae (most often represented by *Chlamydomonas*, see e.g. (Tian et al., 2019) and section 1.5.2) and diatoms (see section 1.5.2). The overall understanding of NPQ in other algae formed by secondary

endosymbiosis like cryptophytes and an evolutionary interesting alveolate alga *Chromera velia*, both used in this thesis as model organisms, is much worse.

The NPQ mechanism is usually studied based on the changes in variable fluorescence by means of pulse amplitude modulated (PAM) Chl *a* fluorescence *in vivo*. A typical measuring protocol is depicted in Figure 6 (see e.g. (Belgio et al., 2018; Kuthanová Trsková et al., 2018; Müller et al., 2001; Ruban, 2016). NPQ is often kinetically divided into two or even more components (Figure 6) based on fluorescence recovery in dark: the fast component often called qE - the high energy quenching; slowly reversible component – often called photoinhibitory (qI) or sustained quenching. NPQ can be then calculated based on Stern-Volmer equation for concentration quenching of fluorescence according to the following formula

$$\text{NPQ} = (\text{Fm} - \text{Fm}') / \text{Fm}'.$$

The fast reversible NPQ - qE is a major type of NPQ in plants caused by  $\Delta\text{pH}$  (Horton et al., 1996). It contrasts to slowly reversible photoinhibitory quenching (Ruban and Horton, 1995) which is rather ambiguous, highly complex component that is hard to interpret, (Nilkens et al., 2010; Ware et al., 2015b). We need to note that the above-mentioned definition perfectly fits for higher plants and green algae where fast reversibility of qE is connected with its fast triggering. On the contrary, this is not fully correct in many other secondary endosymbiotic algae like diatoms (Ruban et al., 2004) and recently discovered *Chromera velia* (Kotabová et al., 2011). In these organisms, NPQ can be rapidly induced, but it is only very slowly reversible. The mechanism has been defined as the so-called NPQ lock (Belgio et al., 2018; Kuthanová Trsková et al., 2018; Ruban et al., 2004). Therefore, the more general term “NPQ” is used

throughout my thesis instead of qE (which has been defined rather for higher plants).

The mechanism of NPQ has been often studied in isolated pigment-protein complexes (PPC) *in vitro* (Ruban et al., 1994b). Protons are considered to be the main trigger of the NPQ mechanism in light-harvesting antenna. In order to decompose the effect of protons on antennas itself, the technique of *in vitro* Chl *a* fluorescence quenching of light-harvesting antenna proteins has been developed (Ruban et al.,

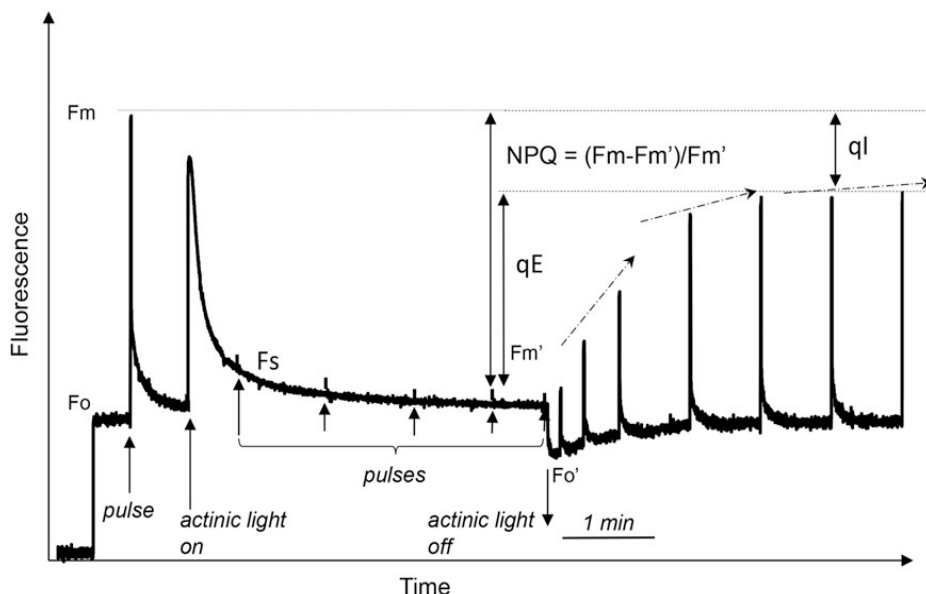


Figure 6: A typical fluorescence induction trace obtained with a higher plant *Arabidopsis thaliana* adapted from Ruban (2016). The major parts of the protocol are marked with arrows. Under weak measuring light, minimal fluorescence ( $F_o$ ) is detected. Subsequently, all the reaction centers of PSII become closed by high-intensity pulse of light and a maximum level of fluorescence in dark is observed ( $F_m$ ). A following continuous illumination with moderately excess light leads to the decrease in fluorescence yield caused by both photochemical and nonphotochemical quenching.  $F_s$  = steady-state fluorescence level;  $F_m'$  = maximum fluorescence during actinic light illumination. The formula for NPQ is indicated. Energetic quenching, qE in higher plants, is a major, quickly reversible component of NPQ. Inhibitory quenching, qI, is a minor, slowly reversible NPQ component.

1994a). The method is based on the detection of Chl *a* fluorescence in isolated antennas solubilized in a detergent (close to critical micellar concentration - CMC). For samples below CMC simple acidification of

antenna solution (solubilized in detergent) induces quenching of Chl *a* fluorescence (see Figure 7). It has been shown that this type of fluorescence quenching in antennas shares some characteristic features with the nonphotochemical quenching of chlorophyll *a* fluorescence as defined for native cells (Belgio et al., 2013; Petrou et al., 2014; Ruban et al., 1994a). The following similarities can be listed: i) the fluorescence quenching is pH-dependent (Petrou et al., 2014; Ruban et al., 1994a); ii) it is connected with the aggregation/oligomerization of the antenna proteins as dilution of detergent results in fluorescence decrease (Kuthanová Trsková et al., 2018); iii) the fluorescence quenching is reversible, the addition of the detergent in the sample results in the original fluorescence value (Belgio et al., 2013; Ruban et al., 1994a); iv) the dilution does not

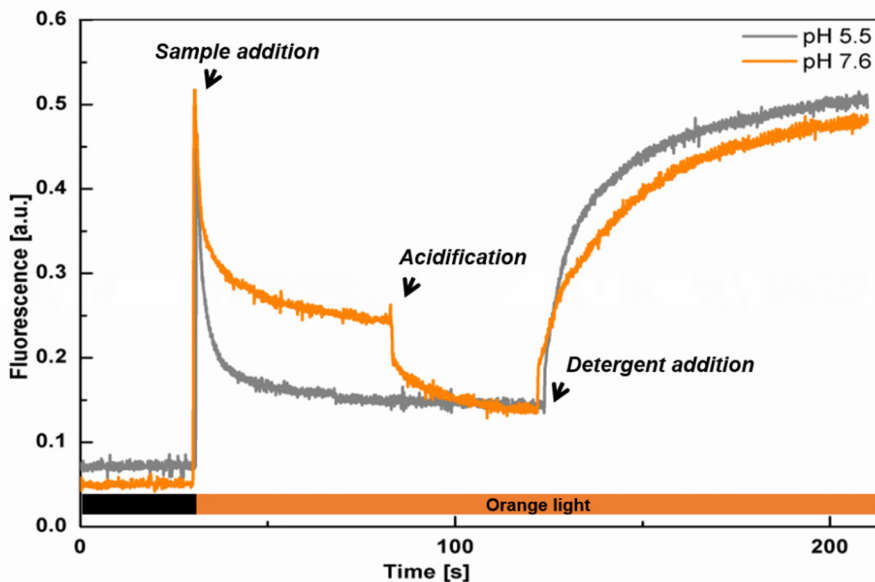


Figure 7: Chlorophyll *a* fluorescence quenching in isolated antennas in detergent micelles. After the antenna addition, detergent is diluted which results in changes in protein structure (aggregation/oligomerization) accompanied by decrease in chlorophyll *a* fluorescence that is fully reversible upon detergent addition.

cause any pigment release (fluorescence and absorption spectra are the same) (Ruban et al., 1994a), v) the addition of carotenoids results in the changes in fluorescence (Kaňa et al., 2016; Ruban et al., 1994a). These above-mentioned similarities between NPQ *in vivo* and Chl *a* fluorescence

quenching in isolated antennas justified the application of this technique to study the quenching properties of isolated antenna complexes. It is also possible to qualitatively compare the *in vitro* method with PAM method in intact cells/chloroplasts used for calculation of NPQ. This method has been already successfully used for various antennas systems – see (Belgio et al., 2013; Ruban et al., 1994b; Wentworth et al., 2000) for Chl *a/b* containing antennas from higher plants, (Kaňa et al., 2012) for Chl *a/c* containing antennas from cryptophytes, and for Chl *a* containing antennas from *Chromera velia* (Kuthanová Trsková et al., 2018). It was also used to test the properties of CP43 which was proven to be not sensitive to acidification (Ruban et al., 1998).

### **1.5.1 Molecular mechanisms and regulation of NPQ**

The most commonly accepted theory states that NPQ in higher plants and green algae resides in the light-harvesting antennas which change their conformation responding to this  $\Delta\text{pH}$  (Horton et al., 1996; Peers et al., 2009; Ruban et al., 2012), although some additional theories suggest quenching in the reaction center (Bruce et al., 1997; Ivanov et al., 2008; Nicol et al., 2019) that is probably more important in extremophilic organisms (Krupnik et al., 2013). For the rest of this thesis, I will only concentrate on the light-harvesting antenna-type quenching. The antennas *in vivo* respond to pH either directly through the protonation of amino acid residues at their luminal side (see e.g. (Belgio et al., 2013; Kuthanová Trsková et al., 2018; Petrou et al., 2014)), or indirectly, through the pH-dependent de-epoxidation of xanthophylls that triggers/facilitates NPQ (Johnson et al., 2010). The xanthophyll cycle pigments act as an NPQ modulator, allosteric factor, together with PsbS protein (a  $\Delta\text{pH}$  sensor) that accelerates both fluorescence quenching and recovery (Croce, 2015; Johnson and Ruban, 2010).

The molecular mechanism of NPQ can be studied from different perspectives starting from triggering mechanism, location (site of NPQ), allosteric regulators and quenching pigments. The general NPQ scenario in antennas of higher plants and our species of interest, *Chromera velia* and *Rhodomonas salina* (for more information see section 3.1), is presented in Figure 8.

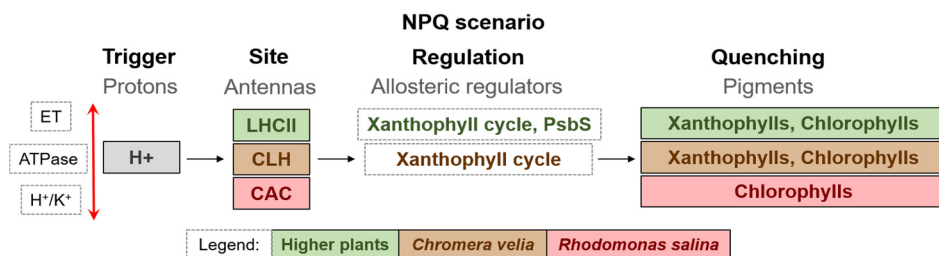


Figure 8: The proposed scenario of the NPQ mechanism in antennas modified after (Ruban and Murchie, 2012). The trigger of NPQ are protons in the lumen which are regulated by electron transport (ET), the function of ATPase and H<sup>+</sup>/K<sup>+</sup> specific antiporters. The protons react either directly with antennas or through allosteric regulators (xanthophyll cycle). Nonphotochemical quenching occurs thanks to pigments, xanthophylls, and chlorophylls. The main differences between species of interest of this thesis are depicted; CLH = Chromera light-harvesting complex, CAC = chlorophyll a/c antennas of *R. salina*

The currently most common model of NPQ in antennas of eukaryotic phototrophs **proposes that lumen acidification is a key factor for triggering of nonphotochemical quenching. Low lumen pH induces antenna protonation** that leads to conformational changes and aggregation/oligomerization followed by energy dissipation. The previous research (see e.g. (Ballottari et al., 2016; Ruban et al., 1998)) showed that the sensors of the  $\Delta\text{pH}$  are negatively charged residues (Asp and Glu) located mainly in the luminal loop of the antenna protein and in the C-terminus (Walters et al., 1996). These residues become neutral upon protonation subsequently making the whole protein structure more hydrophobic and easier to aggregate. Several types of antennas were already tested *in vitro* (Gundermann and Büchel, 2012; Kaňa et al., 2012; Kuthanová Trsková et al., 2018), however, the protonable residues are mostly identified only in the green lineage (see e.g. (Ballottari et al., 2016;

Li et al., 2004; Liguori et al., 2013)) with exception of alveolate alga *C. velia* (Kuthanová Trsková et al., 2018).

**Allosteric regulators of NPQ – Xanthophylls:** There are different types of light-induced xanthophyll cycles in different organisms: i) Violaxanthin — zeaxanthin cycle in higher plants, green algae, chromerids, eustigmatophytes, chrysophytes, phaeophyceae, and raphidophytes; ii) Diadinoxanthin – diatoxanthin cycle in diatoms, dinophytes, and haptophytes; iii) Lutein cycle involving lutein-5,6, epoxidase observed in cuscuta species (Bungard et al., 1999). Lutein is indeed another xanthophyll with known function in NPQ also in other higher plants ((Pogson, 2000); for review see (Goss and Lepetit, 2014)). The overall mechanism of how particular xanthophylls affect NPQ is still an open question. They can act directly as quenchers, or indirectly from the outside of the antennas proteins (Croce, 2015; Kaňa et al., 2016; Xu et al., 2015). The indirect effect of xanthophylls on NPQ could be caused by their hydrophobic/hydrophilic interaction with membrane lipids or with membrane proteins (Johnson et al., 2010; Ruban and Johnson, 2010). By experimental studies, it was confirmed that xanthophylls modulate membrane fluidity and permeability to ions (Gruszecki and Sielewiesiuk, 1991). Moreover, they can act as modulators of tertiary protein structure, they modulate membrane protein function (Ruban and Johnson, 2010), and they are crucial for photosynthetic membrane protein assembly (Phillip et al., 2002).

Photosynthetic light harvesting-antennas typically contain several xanthophylls, therefore, their direct effect on the NPQ value has been often proposed (Holt et al., 2005). The hydrophobic xanthophylls (e.g. zeaxanthin) accelerate the development of NPQ on light but slow down its relaxation in dark. In fact, hydrophobicity of xanthophylls is a crucial parameter affecting directly both the amplitude and kinetics of NPQ (Johnson et al., 2010). Considering indirect, regulatory allosteric role, the highly hydrophobic pigment (e.g. zeaxanthin) makes antennas more dehydrated, which subsequently shifts their pH sensitivity to higher pH –



making them ready to quench. On the contrary, hydrophilic xanthophylls (e.g. violaxanthin) act rather as quenching inhibitor (Gundermann and Büchel, 2008; Kaňa et al., 2016; Kotabová et al., 2011; Ocampo-Alvarez et al., 2013; Ruban et al., 1994b).

**Allosteric regulators of NPQ – the PsbS protein:** The PsbS protein is another NPQ allosteric modulator (Croce, 2015), which is present only in higher plants (Fan et al., 2015; Roach and Krieger-Liszkay, 2012), mosses (together with LHCSR protein (Alboresi et al., 2010; Gerotto et al., 2011)) and some green algae (Mou et al., 2013; Zhang et al., 2013). It does not specifically bind pigments and possesses a dimeric structure that is more stable at low pH (Fan et al., 2015). The molecular mechanism of action and localization of PsbS is still not fully clear. It has been proposed that the acidified PsbS protein changes its conformation in a way similar to the NPQ-switch in antennas; it makes these antenna proteins more sensitive to protonation (Croce, 2015; Ruban et al., 2012). Alternatively, PsbS could lead to an increase in the fluidity of the membrane, accelerating the re-organization of the photosystem II macrostructure that is necessary for the induction of NPQ (Goral et al., 2012).

It is important to note that reversible NPQ can be formed in several organisms even without the allosteric regulators like PsbS or zeaxanthin. For instance cryptophytes, secondary endosymbiotic algae, exhibit “qE” type of NPQ even without the presence of any xanthophyll cycle (Kaňa et al., 2019; Kaňa et al., 2012; Kuthanová Trsková et al., 2019). It is worth noting that the slowly reversible, and  $\Delta$ pH-sensitive NPQ can be found also in plant mutants without PsbS however with very slow kinetics (Johnson et al., 2011). Further, NPQ can be stimulated by the addition of chemicals providing protons, e.g. diaminodurene (Ruban et al., 2012). It suggests that the main role of PsbS in higher plants is facilitating the fast changes in NPQ (Ruban et al., 2012).

**Quenching mechanism:** The scientific chase to find quenchers during the fast qE mechanism of NPQ has brought results that proposed

various mechanisms requiring different pigments (e.g. zeaxanthin, lutein, chlorophyll) as a physical quenchers of the excitation energy (see e.g. (Demmig-Adams, 1990; Holt et al., 2005; Phillip et al., 2002; Ruban et al., 2007). In principle, four physical mechanisms of nonphotochemical quenching of excited chlorophyll states have been proposed: 1) quenching of the Chl *a* excited state via electron transfer to carotenoid (Holt et al., 2005), 2) Energy transfer quenching – through transfer of energy from Chl *a* to carotenoid (Duffy and Ruban, 2015; Ruban et al., 2007), 3) Quenching due to excitonic interactions between Chl *a* and carotenoid (Bode et al., 2009); 4) Quenching due to excitation energy transfer from chlorophylls to a dark state of carotenoid (lutein) (Mascoli et al., 2019). Despite the intensive research on this topic, there is still no conclusive model of the final quencher/quenching mechanism. Moreover, the research on the quenching mechanism is often hampered by the great diversity of photosynthetic species and their antennas/pigment systems as it is described in the following paragraph.

### 1.5.2 NPQ in algal kingdom

There are only a few typical algae used as model organisms to explore the NPQ mechanism, namely *Chlamydomonas reinhardtii* for green algae, and diatom algae *Phaeodactylum tricoratum* or *Thalassiosira pseudonana*. Therefore, in the following section, NPQ mechanisms/features in these algal groups will be summarized more specifically.

**Green algae:** To some extent, green algae have a very similar NPQ mechanism in comparison to higher plants. It depends on the lumen acidification and on changes in the structure of antenna proteins (reviewed in (Goss and Lepetit, 2014)). Interestingly, there is a lack of the proposed low pH sensor typical for higher plants, PsbS, in many green algae, although the responsible gene is present (Büchel, 2015); exception is represented by green alga *Ulva linza* (Zhang et al., 2013) or *Chlamydomonas reinhardtii*, in which it has been suggested that the role

of PsbS in physiologically relevant growth conditions might be more prominent than previously thought (Nawrocki et al., 2020). Functional NPQ in green alga requires rather other proteins - LHCSR (**L**ight-**H**arvesting **C**omplex **S**tress-**R**elated, see e.g. (Girolomoni et al., 2019; Peers et al., 2009)) that are expressed under blue (Gabilly et al., 2019) or high light (Peers et al., 2009). Some green algae exhibit NPQ only under specific conditions; biofilm-forming algae exhibit substantial NPQ capacity only in low light. Interestingly, under high light, NPQ amplitude increases, but its kinetics is unchanged in colonial algae (van den Berg et al., 2019). One of the last differences between higher plant and green algal NPQ comes from the function of the xanthophyll cycle pigments. NPQ in some green algae is modulated by the xanthophyll cycle, whereas in other green algal species (e.g. *Chlorella*, *Scenedesmus*, *Pedinomonas minor*, *Chlamydomonas reinhardtii*, etc.), violaxanthin is not de-epoxidized or its de-epoxidation state is not related to the formation of NPQ (Goss et al., 2015; Masojidek et al., 2004; Masojidek et al., 1999).

**Diatoms:** Diatom algae possess secondary endosymbiotic chloroplasts that originated from a red algal ancestor (Keeling, 2013). They are the main model organism for NPQ research from the red clade of photosynthesis. They contain different types of light-harvesting antenna proteins in comparison to green plants/algae (see Figure 3), the so-called fucoxanthin-chlorophyll *a/c* proteins (FCPs), together with stress-related proteins (similar to LHCSR) from the LHCX family (Büchel, 2015). Further, their xanthophyll cycle pigments differ from higher plants and green algae: there is a diadinoxanthin cycle in which diatoxanthin is formed from diadinoxanthin (Büchel, 2015; Büchel, 2019). Diatoms display a great capacity to rapidly inducible energetic quenching (see e.g. (Lavaud et al., 2002a; Lavaud et al., 2002b; Ting and Owens, 1994)) that is however only slowly reversible in dark due to the so-called NPQ lock (Ruban et al., 2004). NPQ is, similarly to higher plants, dependent and mutually controlled by several factors: lumen acidification (Lavaud and Kroth, 2006), a xanthophyll cycle, presence of LHCX proteins (Lepetit et

al., 2017), and aggregation/oligomerization of FCP antennas (see e.g. (Buck et al., 2019; Hao et al., 2018; Lavaud et al., 2002a)). It is important to note, however, that there is no PsbS protein required for NPQ (Giovagnetti and Ruban, 2018). Further, a pennate diatom, *Phaeodactylum tricornutum*, grown under the intermittent light regime, is capable of so-called “super quenching”: its NPQ is five times larger compared to higher plants (Ruban et al., 2004). As diatoms live in different aquatic habitats with various light inputs, there is species variability also in their NPQ features, especially between centric and pennate diatoms (Lavaud and Lepetit, 2013). For example, when compared to widely studied pennate diatom *P. tricornutum*, a centric diatom *Skeletonema costatum* shows approximately two times lower NPQ extent due to different organizations of FCP antennas and LHCX proteins and the possibly lower amount of diatoxanthin involved in NPQ (Lavaud and Lepetit, 2013).

**NPQ mechanism/regulation in other algal groups:** Except for the most common model organisms (plants, green algae, diatoms) there are several other species mostly belonging to the red clade of algae (algae with red algal ancestor) for which we have only fragmental knowledge on NPQ (see review (Goss and Lepetit, 2014)). For example, this is the case of red algae (Rhodophyta), eukaryotic algae containing phycobilisomes similar to cyanobacteria. The mechanism of NPQ in red algae, in general, is still questionable (Delphin et al., 1996), even though pieces of evidence now point to reaction center quenching (Krupnik et al., 2013). Considering the role of xanthophylls, different red algal species have different xanthophyll profiles with either lutein or zeaxanthin as the main carotenoids (Schubert et al., 2006). Even though the presence of the epoxy-carotenoids points at their involvement in photoprotection, the interconversion of xanthophyll cycle pigments was found only in Gracilariales species with no evidence for their photoprotective role (Andersson et al., 2006; Ursi, 2003). Several other algae have been only partially studied; it includes chrysophytes (golden algae) with NPQ dependent on violaxanthin cycle (Tanabe et al., 2011), brown algae with NPQ associated only with the formation of

zeaxanthin (Garcia-Mendoza et al., 2011; Ocampo-Alvarez et al., 2013) or dinophytes with NPQ dependent on the diadinoxanthin cycle (Brown et al., 1999; Warner and Berry-Lowe, 2006).

Two species from the red lineage are important for my thesis: *Chromera velia* from alveolates and cryptophyte alga *Rhodomonas salina*. They both are secondary endosymbiotic algae with unusual NPQ mechanisms (for details on their NPQ mechanism see section 3.1). *C. velia* exhibits an effective and fast inducible NPQ dependent on the violaxanthin cycle (see e.g. (Kaňa et al., 2016; Kotabová et al., 2011; Quigg et al., 2012) and chapter 3.1.1). *R. salina* is specific in the way that it does not possess any xanthophyll cycle, yet still shows rapidly inducible and reversible NPQ (see e.g. (Cheregi et al., 2015; Kaňa et al., 2019; Kaňa et al., 2012) and chapter 3.1.2.).



## 2 Main goals

Aquatic photosynthetic organisms have to cope with dynamic changes in light intensities which directly influence the process of photosynthesis. The overall aim of this thesis was to study the mechanism of regulation of photosynthetic activity of thylakoid membrane pigment-protein complexes at the level of light-harvesting processes. I focused on the mechanisms of photoprotection in these complexes in algae from the red clade of photosynthesis; the data were also compared with mechanisms observed in the land plants.

My research was based on an assumption that these algae, although being evolutionary distant, share some common features in their photoprotective mechanisms. In order to address this hypothesis, I carried out experiments that were divided as follows: (a) **Algal physiology** and photoprotection – to analyze the photoprotective behavior of live cells under different light conditions and with uncouplers; (b) **Study on isolated pigment-proteins complexes** – to isolate native photosynthetic complexes (photosystems, light-harvesting antennas), characterize their pigment and protein composition, intactness and mechanisms of protective quenching *in vitro*; (c) ***In silico* study** – to exploit the bioinformatics tools for the prediction of algal protein structure and the theoretical effect of pH *in silico* based on known aminoacid composition.

### Specific goals:

**Goal 1: Improve and optimize the current methods for the isolation of pure, functional algal pigment-protein complexes (PPCs); characterize their function with respect to the NPQ mechanism.**

Isolation of pure and intact pigment-protein complexes is a crucial step for any *in vitro* study. Although the traditional biochemical methods have been already successfully adapted by many authors for the isolation of membrane proteins from higher plant thylakoids, the situation is

different in algae. This is probably due to the peculiar structure of their thylakoids, the lack of grana-stroma heterogeneity and the problems with cell disruption. I have tested different methods of cell disruption and membrane solubilization (**A**), isolation of PPCs (**B**), and biochemical characterization (**C**) from two selected algal species, *Chromera velia* and *Rhodomonas salina*.

**A:** The proper conditions of cell disruption were tested: the number of breaking cycles, various buffers, pH and ionic composition. Moreover, the different types of detergents were tested: dodecyl- $\beta$ -maltoside ( $\beta$ -DM), dodecyl- $\alpha$ -maltoside ( $\alpha$ -DM), Triton X-100 in various concentrations.

**B:** Several biochemical techniques were tested to isolate pure and active pigment-protein complexes, namely light-harvesting antennas and photosystems. The applied techniques included: sucrose gradient density centrifugation (separation based on density and the molecular weight of complexes), size exclusion gel chromatography (separation based on physical size of complexes), ion-exchange chromatography IEC (separation based on electrical charges of complexes) and preparative isoelectric focusing (separation based on isoelectric points).

**C:** The isolated PPCs, especially light-harvesting antennas, were characterized spectroscopically (absorption spectroscopy, room/low-temperature fluorescence spectroscopy, fluorescence lifetime measurements, fluorescence quenching *in vitro*) and biochemically (clear native electrophoresis (CN-PAGE), SDS-PAGE). HPLC was used to monitor the pigment composition of isolated PPCs and for the isolation of pigments.

The experimental outcomes of goal 1 were used in Articles I, II, III, and IV directly connected with the topic of the thesis, together with my other co-authored publications (Belgio et al., 2017; Sobotka et al., 2017; West et al., 2016) that do not deal with the mechanism of photoprotection, and are, therefore, not included in the thesis.



## **Goal 2: Estimate the effect of xanthophylls on *Chromera velia* NPQ *in vivo* and *in vitro***

Xanthophylls are considered as the main allosteric regulators of NPQ. Nonphotochemical quenching in plants and many algal strains is often accompanied by the light-dependent cycling of the xanthophyll pigments. However, the overall molecular mechanism of the action of xanthophylls is still a matter of discussion, as it was proposed that they can act either directly (in proteins) as quenchers or indirectly through some allosteric regulations that transform the PSII antenna proteins from an unquenched to a quenched state. It is generally accepted that the deepoxidized/epoxidized xanthophylls stimulate/inhibit NPQ. Within goal 2, we wanted to compare the effect of naturally formed xanthophylls *in vivo* with the effect induced when they are mixed with isolated light-harvesting antennas *in vitro*. Therefore, we isolated two xanthophyll pigments, violaxanthin (from *Chromera velia*) and zeaxanthin (from *Cyanidioschyzon merolae*). The *in vitro* effect was then studied by the analysis of Chl *a* fluorescence quenching for which the xanthophylls were mixed with isolated antennas (see chapter 3.2). To study the same effect of xanthophylls during natural and *in vivo* accumulation at high-light, we pre-treated the photosynthetic material (chloroplasts from *Spinacia oleracea* and algal culture of *Chromera velia*) under different light conditions to tune the number of pigments. Farther, these samples with different xanthophylls composition were then used to explore the differences in NPQ kinetics and absolute values caused by xanthophylls.

The outcomes of goal 2 are summarized in Articles I and III. Moreover, isolated alloxanthin was also used in the article (West et al., 2016) which is not directly connected with the topic of the thesis.

## **Goal 3: Examine the effect of high light growth on photoprotection and photosynthetic apparatus in *Chromera velia***

It is known that the photosynthetic apparatus can adapt its growth to different light conditions. We wanted to address the mechanism of

photoprotection in *Chromera velia* with respect to the changes in structure and composition of thylakoid membrane pigment-protein complexes grown at low/high light. It has been previously shown that *C. velia* is very flexible in adapting to different light conditions (Kotabová et al., 2014; Kotabová et al., 2011; Quigg et al., 2012). For our experiments, *C. velia* was grown under continuous light of 20 and 200  $\mu\text{mol}\cdot\text{m}^{-2}\cdot\text{s}^{-1}$ . The two differently grown cultures were then characterized considering PPCs compositions (number of photosystems and light-harvesting proteins) and their ability for photoprotection *in vivo*. The mechanisms of photoprotection (photoinhibition, NPQ) were estimated based on the biochemistry and the determination of the variations of Chl *a* fluorescence and oxygen evolution. Via combining all the above-mentioned methods, it was possible to compare the mechanisms of long-term high light acclimation (i.e. growth on high light) with the effect of short high-light treatment on photosynthesis and photoprotection in *C. velia*. The data were put into the wider context of the same processes known for higher plants.

The outcome of goal 3 is summarized in Article II.

#### **Goal 4: Compare the role of lumen acidification in triggering NPQ in *Chromera velia* and in the land plants (*Spinacia oleracea*)**

Based on the standard model, nonphotochemical quenching is triggered by lumen acidification that causes protonation of light-harvesting antenna proteins (Belgio et al., 2013). There are almost no direct data showing interspecies variability in the sensitivity of the light-harvesting antenna proteins to protonation. However, there seem to be differences in the ability of trans-thylakoid  $\Delta\text{pH}$  to trigger NPQ *in vivo* (Finazzi et al., 2006). In addition, based on *in vitro* studies it has been proposed that only chlorophyll *a/b* antennas are able to be reversibly protonated (Miloslavina et al., 2009; Ruban et al., 1994a), but the same effect is questionable in chlorophyll *a/c* containing antennas of diatoms (Lavaud and Kroth, 2006; Lavaud et al., 2002a). Within goal 4, we wanted to test the sensitivity of antenna proteins for acidification directly with isolated antennas of

*Chromera velia* (CLH) and in higher plants LHCII from *S. oleracea*. For this purpose, CLH and LHCII proteins were isolated and used to study the effect of antenna pH sensitivity on the overall mechanism of photoprotection. The *in vitro* experiments were further supported by *in vivo* experiments with native cells (or chloroplast) and by *in silico* analysis of CLH and LHCII proteins.

The outcome of goal 4 was summarized in Articles II and III.

### **Goal 5: Study on the composition of pigment-proteins and photoprotective strategies in cryptophytic alga *Rhodomonas salina***

Cryptophytes are an exceptional group of algae in many ways; they display flexible and effective NPQ not dependent on the xanthophyll cycle (Kaňa et al., 2012) they have active state transitions at stationary growth phase (Cheregi et al., 2015) and most importantly, they carry a unique combination of light-harvesting systems combining phycobiliproteins and chlorophyll a/c (CAC) antennas (Green and Parson, 2003). The proper characteristics of cryptophyte light-harvesting antennas, characterization of the activity of their photosystems (especially PSI) and details on photoprotective strategies were missing in the literature. For that reason, we combined *in vivo* (physiological and biophysical) and biochemical as well as other *in vitro* methods to address these questions.

First, I have optimized a biochemical method (a combination of sucrose gradient density centrifugation with ion-exchange chromatography) for the isolation of intact light-harvesting antennas. The resulting complexes were then characterized by means of absorption and fluorescence spectroscopy, HPLC, and gel electrophoresis. The isolated CAC proteins were subjected to *in vitro* quenching analysis (see chapter 3.2). The *in vitro* method was then combined with other physiological experiments *in vivo* to address general photoprotective strategy in cryptophytes.

The outcome of goal 5 was summarized in Articles IV and V.



### 3 Material and Methods

#### 3.1 Model Organisms

Two secondary endosymbiotic algal species belonging to Chromalveolates were studied during my PhD project: *Chromera velia*, colpodellid alga possessing a very efficient and simple photosynthetic system, and *Rhodomonas salina*, a cryptophyte alga showing a special mechanism of nonphotochemical quenching without any xanthophyll cycle. As a control, most measurements were done also with chloroplasts of *Spinacia oleracea*, a well-characterized higher plant model organism for studying photoprotection. In the following sections, some key and important features of our model algal species are mentioned.

##### 3.1.1 *Chromera velia*

*Chromera velia* is a unicellular alveolate alga (Figure 9) isolated from a stony coral (*Plesiastrea versipora*) near the eastern coast of Australia (Moore et al., 2008). It is a close relative of apicomplexan parasites (organisms that possess unpigmented chloroplast, the apicoplast). Therefore, it constitutes an interesting evolutionarily link between

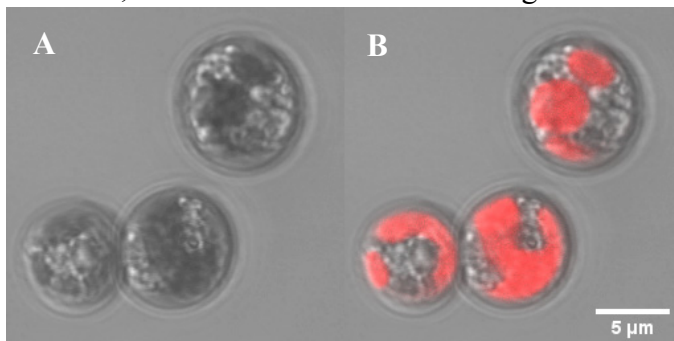


Figure 9: Typical spherical type of *Chromera velia* cells recorded using Zeiss LSM 880. Panel A: Transmission picture of *C. velia* cells. B: The location of chlorophyll a detected by excitation 488 nm/emission 696-758 nm in the cells is shown by red colour.

photosynthetic organisms and heterotrophic apicomplexan parasites. The life cycle of *C. velia* involves three distinct life stages: i) the spherical, coccoid form (Figure 9) represents immotile but dividing cells and is the predominant type of cells used for our measurements; ii) if the culture is stationary and grown under

low light, the flagellate form occurs; iii) when there is an unfavorable environment, it is found in cystic form, which can withstand harsh conditions for a long time (Oborník et al., 2011). Evidence suggested that *C. velia* can be endosymbiotic in coral larvae (Cumbo et al., 2013); however, it can also become parasitic, a transition accompanied by the formation of organelles needed for invasion into the host (Oborník et al., 2016).

The chloroplasts of *C. velia* are bound by four membranes and contain four major pigments: chlorophyll a, violaxanthin, zeaxanthin and an isofucoxanthin-like carotenoid. These chloroplasts are thus supposed to originate from a secondary (at least) endosymbiotic event (Janouškovec et al., 2010). It is important to note that CLH are nuclear-encoded as is the case for most antenna proteins, and they exhibit different evolutionary origin when compared to proteins encoded in the chloroplast. The research with EST sequences provided data suggesting that *C. velia* contains peptide sequences closely related mostly to diatoms, brown algae and dinoflagellates (Pan et al., 2012), suggesting possible horizontal gene transfers from these algae.

The chloroplasts of *C. velia* lack any additional chlorophylls (e.g. chlorophyll b or c) and use only the primitive type of RuBisCO. Despite this simplicity, it exhibits a highly efficient and versatile photosynthetic system (Kotabová et al., 2011; Quigg et al., 2012) with protective nonphotochemical quenching (Kotabová et al., 2011). *C. velia* NPQ shares similarities with higher plants mechanism (the presence of violaxanthin cycle) on one side (Belgio et al., 2018; Kotabová et al., 2011; Quigg et al., 2012), and with diatoms (e.g. variable fluorescence below minimal fluorescence and the presence of “NPQ lock” (Ruban et al., 2004)) on the other. Interestingly, although *C. velia* is proposed to be a facultative symbiont (Cumbo et al., 2013) usually found at depths of at most 5 meters, it is able to acclimate to a wide range of light intensities under laboratory conditions and tends to perform photosynthesis in maximal rates under numerous different growth conditions (Kotabová et al., 2014; Quigg et al.,

2012). There are several reasons for this wide light-acclimation ability, including i) photorespiration (Quigg et al., 2012); ii) efficient NPQ (Kotabová et al., 2011) that can avoid photoinhibition (Belgio et al., 2018); iii) high CO<sub>2</sub> assimilation rates (especially under sinusoidal light regime) that are enabled by activation of the oxygen-consuming mechanism helping to maintain anoxygenic conditions necessary for RuBisCO type II (Quigg et al., 2012). As a consequence, the water/water cycle has been suggested to be active in *C. velia* (Quigg et al., 2012). Indeed, this has been indirectly confirmed by the presence of a high amount of PSI accompanied by superoxidismutases, enzymes for scavenging the reactive oxygen species (Sobotka et al., 2017); iv) High light acclimation is accompanied with the strong increase in violaxanthin pool, which is either free or localized in the membrane and modulates NPQ (Belgio et al., 2018; Mann et al., 2014); v) *C. velia* can synthesize red-shifted antenna very quickly to improve light harvesting under far-red light (Kotabová et al., 2014).

### **3.1.2 Rhodomonas salina**

The second model organism in my thesis is represented by the motile marine cryptophytic alga *Rhodomonas salina* (see Figure 10). The alga is usually found in estuarine, highly eutrophic areas Hammer et al. (2002), where it can form blooms, however not connected to excretion of harmful substances (Al-Najjar et al., 2007). Cryptophytes have a unique photosynthetic system, as they use both phycobiliproteins and chlorophyll a/c (CAC) antenna proteins for efficient light harvesting. Therefore, cryptophytes constitute the evolutionary intermediates between red algae containing phycobiliproteins but no chlorophyll c, and diatoms that contain chlorophyll c but no phycobiliproteins (see e.g. Armbrust et al. (2004)).

Phycobiliproteins are formed either by phycoerythrin or by phycocyanin (it is species-dependent) and they do not organize into the typical phycobilisomes known in red algae and in cyanobacteria (Green et al., 2003; Overkamp et al., 2014). They are located exclusively in the thylakoid lumen (Kaňa et al., 2009). The second light-harvesting system is

composed of cryptophytic equivalents of LHC known in other algae, CAC antennas. These proteins are membrane intrinsic and they are formed by three  $\alpha$ -helices, that are, however, distinct from the chlorophyll a/b binding antennas of green algae and higher plants (LHC), but also differ from chlorophyll c antennas of chromalveolates including peridinin-chlorophyll proteins (PCP proteins) of dinoflagellates and the fucoxanthin-chlorophyll antennas (FCP proteins) of diatoms (Kaňa et al., 2012).

Several studies have provided evidence that these CAC proteins are involved in the adaptations to even extreme low light conditions (see e.g. (Gervais, 1997)). However, cryptophytes also make use of other mechanisms to overcome light-limited conditions as well. The first of them is their active flagellar motion connected to phototaxis that would allow them to move between light-limiting and light-saturating water layers. Interestingly, it has been suggested that algal cell rotation around longitudinal axes changes continual irradiation to intermittent light that can protect cells against excessive irradiation (Kaňa et al., 2019). The second

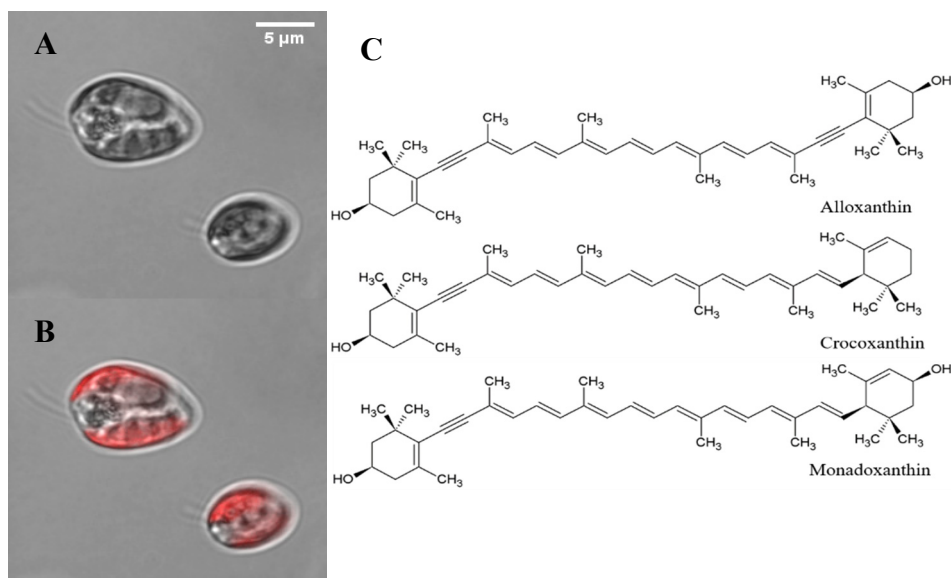


Figure 10: Cells of *Rhodomonas salina* recorded using confocal Zeiss LSM 880. Panel A: The transmission picture *R. salina*. B: The location of chlorophyll *a* detected by excitation 488 nm/emission 696-758 nm in the cells is shown by red colour. C: The overall scheme of the three unusual triple bonds carotenoids from *R. salina*.



one, still controversial, is an idea of mixotrophy occurring in these species (see e.g. (Gervais, 1997; Salonen and Jokinen, 1988)).

The nonphotochemical quenching in cryptophytes exhibits special features as well (Kaňa, 2018). Cryptophytes represent so far the only known type of algae that displays effective NPQ (Kaňa et al., 2012; Kuthanová Trsková et al., 2019) which can be exchanged for state transitions depending on the growth stage (Cheregi et al., 2015). Moreover, NPQ is not accompanied by the cycling of any xanthophyll cycle (Funk et al., 2011; Kaňa et al., 2012), even though the NPQ kinetics show similar features, being rapid and reversible, as energetic quenching in higher plants and was shown to be modulated by  $\text{Ca}^{2+}$  fluxes (Kaňa et al., 2019). Concerning the photosynthetic apparatus itself, it has been shown, at the molecular level, that cryptophytic PSI binds the so-called red chlorophyll forms (opposite to e.g. *C. velia* which was shown not to bind them (Belgio et al., 2017)). Finally, next to Chl *a* and *c*, *R. salina* carries unusual carotenoids with triple bonds in their structures (see Figure 10). Alloxanthin is the major carotenoid with two triple bonds and is the only known carotene with two triple bonds in photosynthetic organisms (West et al., 2016). Crocoxanthin and monadoxanthin are additional less abundant carotenes (Kaňa et al., 2012; Kuthanová Trsková et al., 2019) with one more triple bond. All these three carotenoids possess special spectroscopic features due to their molecular structure and they are present in native CAC antennas (Kaňa et al., 2012). However, the molecular function of crocoxanthin and monadoxanthin remains unknown, and only recently alloxanthin was identified as a possible light harvester in *R. salina* (West et al., 2016).

## 3.2 Methods

**Culture cultivation:** *Chromera velia* (strain RM12) and *Rhodomonas salina* (strain CCAP 978/27) cultures were grown in artificial seawater medium with additional f/2 nutrients (Guillard and Ryther, 1962) in 450 ml glass tubes kept in the temperature-controlled baths. Cells were continually bubbled with air and illuminated by dimmable fluorescence tubes light with different light regimes: *C. velia* cells were grown in a continuous light regime with either  $200 \mu\text{mol m}^{-2} \text{s}^{-1}$  or  $20 \mu\text{mol m}^{-2} \text{s}^{-1}$  ( $t = 28^\circ\text{C}$ ) and *R. salina* was grown under  $35 \mu\text{mol photons m}^{-2}\text{s}^{-1}$  (day-night cycle 12/12 h) at  $18^\circ\text{C}$ . All the *in vivo* experiments and culture harvesting were performed in the exponential growth phase to ensure the reproducibility of the results. For more information, see articles I, II, III and IV.

**Membrane preparation:** A successful study of membrane proteins requires a mild method for thylakoid membrane isolation and solubilization without destroying the pigment-protein complexes. The thylakoid membrane preparations from algal cells are even more challenging as they commonly possess hard cell walls that need to be safely removed. We homogenize our algal cells using glass beads in an optimized buffer followed by solubilization using dodecyl-maltoside. For more information, see Articles I, II, III and IV.

Instrumentation: Mini Bead Beater (BioSpec, USA).

**Antenna isolation:** Isolation of native complexes from algal species is usually hampered by the fact that no standardized methods are available for their purification. Moreover, algae often possess structural differences making the isolation more challenging. Several techniques working properly in higher plants result in contaminants in isolates and affected supercomplex integrities. For our purposes, we used several isolation techniques with optimized detergent concentrations: Sucrose

gradient ultracentrifugation (for more information, see Articles I, III and IV), gel chromatography (for more information, see Article II) and ion-exchange chromatography (for more information, see Article IV).

Instrumentation: L8-M ultracentrifuge (Beckmann, USA), FPLC system (Pharmacia, Biotech, Sweden).

***In vivo* chlorophyll *a* fluorescence quenching – the measurement of variable fluorescence:** To address the mechanism of photoprotection in our species of interest, we needed to employ the variable fluorescence measurements (for more information, see Figure 6 and chapter 1.5) in algal cultures and higher plant chloroplasts. NPQ is then calculated according to formula.

$$\text{NPQ} = (\text{Fm} - \text{Fm}') / \text{Fm}'.$$

Instrumentation: FL 3000 fluorometer (PSI, Czech), Dual PAM 100 Fluorometer (Walz, Germany).

**Chlorophyll *a* fluorescence quenching in isolated antennas:** We tested the mechanism of NPQ by the method of chlorophyll *a* fluorescence quenching in isolated antennas. In higher plants, and many algae, NPQ is considered to be localized mostly in accessory PSII antennas. The hypothesis that the *in vivo* antennas aggregation/oligomerization is a mechanism behind NPQ has been widely supported by several facts: i) similarities in quenching kinetics between isolated antennas and intact chloroplasts (see e.g. (Johnson and Ruban, 2009; Kuthanová Trsková et al., 2018)); ii) plants with the majority of LHCII antennas removed display highly reduced NPQ (Havaux et al., 2000); iii) isolated antennas react to cross-linkers, and several ions in a similar way as NPQ *in vivo* (see e.g. (Johnson and Ruban, 2009; Kaňa and Govindjee, 2016)). We wanted to test the effect of pH, xanthophylls and detergent concentration on still unexplored antennas of our species of interest. For more information, see section 1.5 and Articles I, II, III and IV

Instrumentation: FL 3000 fluorometer (PSI, Czech), Dual PAM 100 Fluorometer (Walz, Germany).

**Gel electrophoresis:** We used the standard electrophoretic technique – SDS – PAGE (for more information, see Articles I, II, III, IV). Further, the clear-native gel electrophoresis was employed which allowed us to study native oligomerization state and total content of our complexes. For more information, see Articles III and IV.

Instrumentation: Mini – Protean Cell (Bio-Rad, USA), PAGE apparatus PROTEAN II xi Cell (Bio-Rad, USA), PowerPac HV High-Voltage (Bio-Rad, USA).

**Absorption spectroscopy:** We used room-temperature absorption spectroscopy to study the intactness and the pigment composition of our isolated material. For more information, see Articles I, II, III and IV.

Instrumentation: Unicam UV /VIS 500 spectrometer (Thermo spectronic, UK).

**Fluorescence steady-state spectroscopy:** Low-temperature fluorescence spectroscopy was used to check the sample intactness, characterization and composition. For more information, see Articles I, II, III and IV.

Instrumentation: Aminco–Bowman Series 2 spectrofluorometer (Thermo Fisher Scientific, USA).

## 4 Overview of my research

My thesis is based on five published articles directly connected with the mechanism of photoprotection defined as NPQ; some from my side results obtained in the Goal I (“*Optimization of PPCs isolations from alga strains*”) are not discussed directly in my thesis (see (Belgio et al., 2017; Sobotka et al., 2017; West et al., 2016)) as they are not directly connected with the regulation of light-harvesting efficiency. Article I focuses on the effect of violaxanthin onto nonphotochemical quenching in isolated CLH antennas of *Chromera velia*, violaxanthin has been defined as an inhibitor of NPQ. Article II describes the process of *C. velia* acclimation to high light (HL) and its connection with the photoprotective mechanism of NPQ and with photoinhibition. Article III compares the sensitivity of CLH (from *C. velia*) and LHCII antenna (from *Spinacia oleracea*) for protonation; the process has been recognized as the key factor determining the light-harvesting strategy in these two organisms and the data are put in the wider context of their xanthophyll compositions. Article IV describes the methodology for isolation of native pigment-protein complexes in cryptophyte alga *Rhodomonas salina*, the basic properties of light-harvesting antennas are also studied. Finally, article V describes the overall photoprotective strategies in motile cryptophyte alga of *R. salina*.

### Article I

*Violaxanthin inhibits nonphotochemical quenching in light-harvesting antennae of Chromera velia.*

Nonphotochemical quenching is a photoprotective mechanism that is most often placed in light-harvesting antennas. It is triggered by low pH in the thylakoid lumen and it is modulated by the xanthophyll cycle, namely violaxanthin de-epoxidation to zeaxanthin. In this study, we tested the effect of violaxanthin on the extent of NPQ in isolated CLH antenna from *Chromera velia*. We reported that naturally present violaxanthin in

isolated CLH antennas reduces the fluorescence quenching; a higher amount of violaxanthin in isolated fraction of CLH resulted in lower quenching. It contrasts with the effect of zeaxanthin that acts in the opposite direction. Further, we have pointed out that the same correlation between the amount of violaxanthin in light-harvesting proteins and their quenching is also visible in isolated higher plant LHCII antennas. All these data have indicated an inhibitory role of violaxanthin on NPQ; It also points out to the fact that violaxanthin needs to be removed from the antenna protein vicinity to reach maximal NPQ.

## **Article II**

*High light acclimation of *Chromera velia* points to photoprotective NPQ.*

The acclimation of photosynthetic organisms to the different light regimes is usually accompanied by changes in structure and in the composition of the pigment-proteins complexes in the thylakoid membrane. In this study, we compared the low light (LL) and high light (HL) grown *C. velia* cells. We found a rather unusual physiological response of *C. velia* to growth on HL. HL cells showed severe changes in PPCs composition of the thylakoid membrane resembling higher plant thylakoid treated by lincomycin (chloroplast inhibitor of PSII synthesis) (Belgio et al., 2012). The HL *C. velia* culture reduced the number of PSII but kept similar antenna content to LL *C. velia* culture; it contrasted with the typical higher plant acclimation to HL causing the reduction in the antenna content. The increased number in CLH per PSII resulted in partial uncoupling of CLH from PSII and enhanced NPQ. Interestingly, the reduced number of PSII reaction centers was not connected with photoinhibition. That was, in fact, minimized under HL thanks to a lower PSII content. *C. velia* cells were thus protected mostly by effective NPQ located in the CLH antennas.

### Article III

*Antenna proton sensitivity determines photosynthetic light harvesting strategy.*

In this study, we compared the light-harvesting strategies and photoprotection mechanisms in the *C. velia* alga with the well-studied land plant model organism, *Spinach oleracea*. NPQ formation/relaxation kinetics are usually said to be dependent on the pH and xanthophyll composition. However, *Chromera velia* displays a constitutively fast formation rate of NPQ on the light that is independent of the xanthophyll pigments composition. It contrasts with higher plant behavior of NPQ formation, where high-light grown plants exhibit a faster NPQ rate of formation because of the zeaxanthin formation. Our *in vitro* results with *C. velia* together with the *in silico* studies showed that the constitutively fast formation rate of NPQ on light is an intrinsic property of the Chromera light-harvesting complexes (CLHs), related to the structure and amino acid composition of CLH proteins. Based on *in vitro* pH titration experiments (see Chapter 3.2, Chlorophyll a fluorescence quenching in isolated antennas) with isolated CLH we showed that these antenna proteins are more sensitive to protons in comparison to plant LHCII; the pKa value for CLH is shifted by 0.5 units to higher pH values. In line with this, our *in silico* calculations proved that CLH also contains additional easily protonable amino acid residues on their luminal side. We propose that organisms with antenna proteins intrinsically more sensitive to protons, such as *C. velia*, carry a relatively high concentration of violaxanthin to improve their light-harvesting ability. In contrast, higher plants need less violaxanthin per chlorophyll because LHCII proteins are more efficient light harvesters and instead require co-factors such as zeaxanthin and PsbS to accelerate and enhance quenching.

## Article IV

*Isolation and characterization of CAC antenna proteins and photosystem I supercomplex from the cryptophytic alga Rhodomonas salina.*

All the *in vitro* methods and spectroscopic characterization of pigment-protein complexes are usually hampered by their purity and by intactness. This is especially true for the chlorophyll *a/c* type of antennas that are considered to be rather sensitive and easy to damage by isolating procedures (see e.g. Büchel (2003)). In this article, we described an improved method for isolation of chlorophyll *a/c* light-harvesting antennas (CAC) and also pure PSI supercomplex from a cryptophyte alga, *Rhodomonas salina*. We combined the sucrose density gradient with ion-exchange chromatography to that allowed us to obtain pure native CAC antennas. The pure antennas were subsequently used to study *in vitro* quenching (see Chlorophyll *a* fluorescence quenching in isolated antennas in chapter 3.2). The method showed that protein aggregation/oligomerization is a plausible mechanism behind nonphotochemical quenching in *R. salina*. Moreover, a functional photosystem I supercomplex has been purified by sucrose gradient as a side-product of antenna isolation. The isolated PSI from *R. salina* showed a remarkably fast photochemical trapping rate, comparable with previously reported rates in PSI from other secondary endosymbiotic algae, *Chromera velia* and *Phaeodactylum tricornutum* (Belgio et al., 2017).

## Article V

*Photoprotective strategies in the motile cryptophyte alga Rhodomonas salina – role of non-photochemical quenching, ions, photoinhibition and cell motility.*

Cryptophytes are secondary endosymbiotic algae that possess, together with chlorophyll *a/c* antennas inside thylakoids, an additional light-harvesting system of phycobiliproteins situated in the thylakoid lumen. These algae display pH-dependent nonphotochemical quenching



similar to energetic quenching in higher plants, that is, however, not dependent on any xanthophyll cycle (Kaňa et al., 2012). In this article, we investigated the photoprotective strategies in the cryptophyte representative, *Rhodomonas salina*. At first, based on the treatment with selective ion inhibitors (diltiazem and non-actin), we concluded that the initial fast phase of NPQ is sensitive to monovalent and divalent cations. Further, the motile *R. salina* cells exposed to high light displayed a lower level of PSII photoinhibition in comparison to the immotile, planktonic representative of diatoms, *Phaeodactylum tricorutum*. Therefore, we investigated a possible role of algal motility in the reduced photoinhibition in *R. salina*. We found out that high light exposure increased cell velocity by almost 25% percent. We suggested that algal cell rotation around longitudinal axes can transform the continual irradiation to periodically fluctuating light. Based on these findings, we proposed that algal cell motility could represent yet another photoprotective strategy.



## 5 Conclusion and future prospects

Photosynthetic organisms inhabit almost all environments on Earth including fresh and marine waters, soils, muds, snow, and hypersaline environments (see e.g. (Blankenship, 2002; Falkowski and Raven, 2007; Lee, 2008)). The major limiting factor in many environments is the incoming light input: phototrophs are exposed to periods of sometimes limiting, sometimes largely excessive irradiations. The latter can be then fatal to the thylakoid pigment-proteins as they can be damaged by reactive oxygen species (Roach and Krieger-Liszkay, 2019). The overall aim of this thesis was to investigate the mechanism of photoprotection of these pigment-protein complexes (PPCs) with the main focus on nonphotochemical quenching in light-harvesting antenna. As model organisms, we selected two marine algal species from the red clade of photosynthesis, *Rhodomonas salina* and *Chromera velia*. Our findings were compared with well-studied higher plants model organism, *Spinacia oleracea*.

Initially, I had to improve and optimize the current biochemical methods for the isolation of pure, functional algal PPCs. The successful fulfilling of this goal was crucial for my further experiments on the NPQ mechanism. When I started, there was no widely applicable method for isolation of thylakoid membrane PPCs from these algal species in our laboratory. The goal was accomplished by testing several homogenizing conditions, detergent systems, buffers, and isolation techniques. At the end of this phase, I managed to optimize all the necessary methods for isolation of pure light-harvesting antennas from these algal species. As a side result, I also isolated pure photosystem I (PSI) supercomplexes for both model organisms. The isolated antenna complexes from *C. velia* and *R. salina* were biochemically and spectroscopically characterized and used for further analysis of NPQ mechanism. The data was published in 4 articles that I co-authored (Belgio et al., 2018; Kaňa et al., 2016; Kuthanová Trsková et al., 2018; Kuthanová Trsková et al., 2019). The isolated PSI

supercomplexes were used to study the efficiency of PSI photochemical trapping (Belgio et al. (2017), and detailed structure of *C. velia* PSI (Sobotka et al., 2017). In the latter work, we found out that *C. velia* PSI supercomplex contains bound superoxide dismutases to cope with the oxidative damage (Sobotka et al., 2017). These data are however not discussed in the frame of my thesis as they are not directly connected with the main topic. Thanks to the optimization of cell disruption and pigment extraction, we also managed to isolate pure pigments (violaxanthin from *C. velia*, zeaxanthin from the red alga *Cyanisioschyzon merolae*, and alloxanthin from *R. salina*), which were further used in two studies (Kaňa et al., 2016; West et al., 2016).

With the optimization of biochemical methods (Goal I), I started exploring NPQ mechanism *in vivo* and *in vitro* (Goals II-IV). Initially, I tried to estimate the allosteric role of xanthophylls on algal NPQ. This part of my work has been based on the known fact that xanthophyll cycle pigments are able to modulate NPQ and they affect the structure of antenna complexes in general (Ruban and Johnson, 2010). The typical model of NPQ in higher plants states that zeaxanthin enhances steady-state value of NPQ. It also accelerates the rate of NPQ triggering upon illumination when it is already present as a result of a previous irradiation (Ruban et al., 1994b). We wanted to establish the effect of xanthophylls on NPQ in our model organisms. Firstly, the effect of violaxanthin in *C. velia* has been studied (Kaňa et al., 2016). It was known from the previous studies (Tichý et al., 2013) that CLH (Chomera light-harvesting complex) is naturally rich in violaxanthin. The ratio of Vio/Chl in native cells varies between 1 : 3 to 1 : 4 in the cells grown in high and low light, respectively (Quigg et al., 2012). Based on our study (see Article I (Kaňa et al., 2016)), we concluded that violaxanthin reduces NPQ in isolated CLH; this xanthophyll thus works as an inhibitor of NPQ. The result implied that violaxanthin needs to be removed from the protein vicinity to reach the maximal NPQ (Kaňa et al., 2016). Our conclusion was in line with the published results showing the indirect effect of zeaxanthin on stimulation of NPQ (Xu et al., 2015).

We do not know the precise molecular mechanisms behind this indirect effect of xanthophylls on NPQ so far. One may speculate that it can be connected with the changes in the antenna structure in the presence of particular xanthophylls of different chemical properties, hydrophilic or hydrophobic (Johnson et al., 2010). Violaxanthin, as a hydrophilic xanthophyll, makes the protein structure less dehydrated which can lead to the inhibition of excited states quenching by preventing the closer chlorophyll–chlorophyll or chlorophyll–xanthophyll interactions (Ruban and Johnson, 2010). The opposite effect can then be expected from hydrophobic zeaxanthin. Moreover, the same stimulatory or inhibitory effect of xanthophylls on quenching of Chl *a* fluorescence is also visible in isolated antenna proteins when they are studied in detergent micelles (for the methods see chapter 3.2 and (Kuthanová Trsková et al., 2018)). When violaxanthin is added into the reaction mixture of isolated antennas in micelles, the addition clearly inhibits quenching of Chl *a* fluorescence (see (Ruban et al., 1994a) for LHCII, and supplementary data from (Kaňa et al., 2016) for CLH). However, to understand this phenomenon, additional precise biochemical and *in silico* analysis methods are required to be applied in the future. The most promising of them might be the *in vitro* system of antennas in proteoliposomes (Akhtar et al., 2019; Wilk et al., 2013) that would, possibly, better mimic the native conditions in thylakoids.

We have also discussed the importance of different xanthophyll content in *C. velia* (in comparison to higher plants) in light of broader evolutionary consequences. Based on our findings (Kuthanová Trsková et al., 2018), we proposed that higher plants LHCII proteins are efficient light harvesters (i.e. these antennas are ready to harvest light) and they need less hydrophilic violaxanthin per chlorophyll. However, they require co-factors such as hydrophobic zeaxanthin and PsbS to accelerate and enhance quenching. Whereas organisms with antennas not that efficient in light harvesting (i.e. antennas ready to be switched into the quenched state), such as CLH from *C. velia*, have to carry a high concentration of free (lipid

phase) violaxanthin to improve their light-harvesting (Kuthanová Trsková et al., 2018). The future studies need to address the relevance of this model also in other model alga like diatoms as the high carotenoid content in CLH antennas resembles their carotenoid-rich FCP antennas (Joshi-Deo et al., 2010). The presence of loosely-bound xanthophyll molecules seems to be a unique feature mostly for red-clade algae. In diatoms, the presence of lipid-phase hydrophilic xanthophyll (diadinoxanthin) has been shown (Goss et al., 2010) and the existence of loosely-bound violaxanthin in CLH antennas has been already discussed previously for *C. velia* (Bína et al., 2014; Kuthanová Trsková et al., 2018). All this is in line with the fact that violaxanthin has the lowest interaction strength among all of the other carotenoids (Ruban et al., 1999). In contrast to red-clade algae, the presence of lipid-phase violaxanthin (unbound to proteins) in higher plants thylakoids seems to be rather minimal (Dall'Osto et al., 2010). However, the presence of xanthophylls weakly bound to the proteins/in the lipid phase seems to have no effect on NPQ kinetics *in vivo*. In Article III (Kuthanová Trsková et al., 2018), we showed that *C. velia*, on the contrary to higher plants, possesses a constitutively higher rate of light-induced triggering of NPQ, because CLH antenna are much more sensitive to protonation than LHCII. The rate is not dependent on the presence of zeaxanthin formed by previous light cycle, which is the typical phenomenon observed in higher plants (Ruban et al., 1994b).

The above-mentioned knowledge about xanthophylls was also implemented in a more general model of *C. velia* photoprotection and long-term photo-acclimation (Goal III). In fact, as the typical natural habitat of *C. velia* is still not fully clear, we do not know how often this alga is exposed to periods of high light. Previous works suggested that it could live either closely associated with corals, experiencing only moderate light intensities, or it can be found as a free-living planktonic alga in the ocean, where it can often experience light intensities of up to  $1000 \mu\text{mol m}^{-2} \text{s}^{-1}$  (Oborník et al., 2011). This may be the reason for its very efficient photosynthesis at a relatively broad range of intensities and

for effective photoprotection (Kotabová et al., 2011; Quigg et al., 2012). We have explored this adaptability of *C. velia* in more detail. Based on our physiological and biochemical analysis, we figured out that *C. velia* cells grown under relatively high light ( $200 \mu\text{mol m}^{-2} \text{s}^{-1}$ ) exhibit no severe effect on photosynthesis, as summarized in Article II (Belgio et al., 2018). Even much higher light intensities (above  $500 \mu\text{mol m}^{-2} \text{s}^{-1}$ ) were needed in our case to saturate the photosynthetic chain. Further, high light-grown cells displayed enhanced NPQ connected with severe changes in the PPCs composition in the thylakoid membrane. We observed lowered PSII content in HL (in comparison to LL) accompanied by unchanged amount of CLH antenna. The antennas in HL cells were then partially uncoupled from PSII and the decrease in PSII content was compensated by the excess photosynthetic capacity of PSII (Behrenfeld et al., 1998; Kaňa et al., 2002). Both these processes then guaranteed efficient photosynthesis under high light in *C. velia*. Our data thus further explain why *C. velia* can be considered as a simple system with high efficiency at both HL and LL grown conditions. The molecular mechanisms underlying the trigger and control of this unusual HL acclimation (i.e. maintaining antennas and reducing PSII content) still have to be elucidated.

Apart from the role of xanthophylls on NPQ, I also focused on the effect of lumen acidification in NPQ triggering in *Chromera velia* and the land plants (represented by *Spinacia oleracea*) (see Article III (Kuthanová Trsková et al., 2018) and Goal IV). We know that NPQ in *C. velia* is pH-dependent (Kotabová et al., 2011) similarly to higher plants (Ruban et al., 1992). Farther, PsbS protein is not present in this organism (Belgio et al., 2018). Therefore, I wanted to characterize the sensitivity of *Chromera* light-harvesting antennas (CLH) to protons in comparison to LHCII proteins from *S. oleracea*. We know that, during NPQ, low pH is sensed by protonable lumenal amino acid residues of antenna proteins (Belgio et al., 2013). From our *in vitro* quenching experiments in detergent micelles (see chapter 3.2) we were able to quantitatively estimate a pH-dependency of quenching in both types of these antennas. Their actual pH sensitivity

was different, as CLH showed higher proton sensitivity with pKa shifted by 0.5 to higher values in comparison to LHCII (see Figure 11 for further details). The *in vitro* results also explained the faster rate of NPQ formation after irradiation (e.g. during transition from dark to light) in native cells of *C. velia*. In summary, CLH switched into a dissipative quenched state more easily than LHCII *in vivo* and *in vitro*. These results were further supported by *in silico* analysis that confirmed more sensitive protonable residues in CLH. Following our previous findings on the effect of carotenoids, we proposed a combined hypothesis that the sensitivity of antenna for acidification affects overall photoprotective strategy in particular organisms. Phototrophs containing antennas more sensitive to protons (e.i. antennas that are ready to quench), simultaneously carry also a relatively higher concentration of hydrophilic xanthophyll (violaxanthin) as

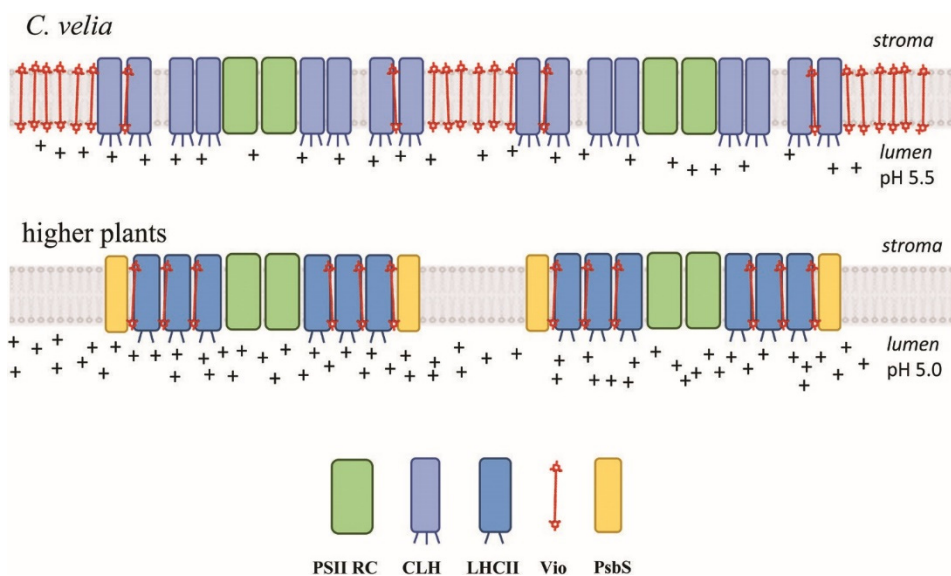


Figure 11: Scheme showing the different light-harvesting strategies of *C. velia* and higher plants. The *C. velia* thylakoid membrane carries CLH proteins that are ‘natural quenchers’ with three protonable lumen-facing residues (indicated by small protrusions). The membrane is highly enriched in unbound, ‘anti-quenching’, violaxanthin pigments, and PsbS protein is absent. The higher plant thylakoid membrane supports the LHCII protein, a ‘natural light harvester’ with two protonable lumen-facing residues. PsbS protein is required for effective quenching, and the amount of unbound violaxanthin in the membrane is negligible. The scheme does not represent real stoichiometries/proportions. For more details, see (Kuthanová Trsková et al., 2018)



quenching inhibitor to improve their light-harvesting ability. On the other hand, organisms with less free/loosely bound violaxanthin (e.g. higher plants) contain light-harvesting proteins (LHCII) that are more efficient light harvesters as they have lower pKa to trigger NPQ. The scheme showing these two light-harvesting strategies is presented in Figure 11.

In the final part of my research (goal V) I studied the composition of photosynthetic apparatus and photoprotective strategies in my second model organism, the cryptophyte alga *Rhodomonas salina*. First, I optimized the method for isolation of pure and intact pigment-protein complexes from *R. salina*, namely chlorophyll a/c antennas (CAC) and PSI supercomplex (data are summarized in the Article IV (Kuthanová Trsková et al., 2019)). The isolated PSI supercomplex was then used to study the efficiency of PSI photochemical trapping (Kuthanová Trsková et al., 2019). In parallel, we proved that CAC antenna proteins acted similarly to higher plant antennas when subjected to *in vitro* quenching analysis. The detergent removal induced changes in the relative distances and positions of pigments leading to the formation of quenching sites in these antennas. The photoprotective strategies of *R. salina* were further studied also *in vivo* (see Article V (Kaňa et al., 2019)). Based on the study, we newly concluded that the fastest part of protective NPQ seems to be sensitive to monovalent and divalent cations. This is another factor next to the previously known effect of pH on NPQ triggering in cryptophytes (Kaňa et al., 2012). Moreover, the data suggested that the algal cell rotation in this motile alga might change the continual irradiation to periodically fluctuating light and this movement, together with the light-induced increase in cell velocity could in general act as another photoprotective mechanism of high light avoidance.

Thanks to our work, together with previous data, the current knowledge on the mechanism of photoprotection in cryptophytes can be summarized as follows: 1) Cryptophytes exhibit pH-dependent NPQ (Kaňa et al., 2012) that resembles quickly recovering qE type quenching of higher plants; 2) Their CAC antennas reacts to pH *in vitro* (Kaňa et al.,

2012); 3) The antenna aggregation/oligomerization induces quenching (Kuthanová Trsková et al., 2019); 4) Cryptophytes use state transitions as a form of photoprotection during the exponential growth phase (Cheregi et al., 2015); 5) Their NPQ is not accompanied by the cycling of xanthophyll cycle pigments (Kaňa et al., 2012), and *R. salina* contains unusual triple bond carotenoids (Kuthanová Trsková et al., 2019; West et al., 2016); 6) Cryptophytes' photoprotection does not involve any effect of a single helix LHC-like proteins (Funk et al., 2011); 7) Ions have pronounced effect on the fast phase of NPQ (Kaňa et al., 2019); 8) Algal cell motility was proposed as a photoprotective strategy of HL avoidance (Kaňa et al., 2019).

A similar model of photoprotective strategies can be also summarized for *C. velia* into following points: 1) NPQ is pH-sensitive and photoprotective (Belgio et al., 2018; Kotabová et al., 2011); 2) *C. velia* shows unusual acclimation strategy to high light, as it keeps the same number of light-harvesting antennas and limits the number of active photosystem II reaction centers on high light (Belgio et al., 2018); 3) The mechanism of high light acclimation tries to avoid the presence of photoinhibition, reducing PSII content is a “surviving” strategy to avoid PSII photodamage as several indispensable assembly factor proteins for PSII (known as Ycf48/Hcf136, Psb27 and Psb28) are missing (Belgio et al., 2018) 4) The quenching in *C. velia* is located in CLH complexes as confirmed by several studies (Kaňa et al., 2016; Kuthanová Trsková et al., 2018); 5) Long-term high light acclimation results in the presence of uncoupled/weakly coupled antennas that reduces the energy transfer to reaction center (Belgio et al., 2018); 6) CLH antenna are highly sensitive to protons, which makes them ready to quench (Kuthanová Trsková et al., 2018); 6) So far there are no indications of regulation of light-harvesting by state transitions; 7) The fast NPQ present in *C. velia* is slowly reversible (Kuthanová Trsková et al., 2018) and similar to the so-called NPQ lock found in diatoms (Ruban et al., 2004), therefore *C. velia* NPQ cannot be considered as a displaying the classical, fast reversible qE type quenching

typical for higher plants; 8) *C. velia* can synthesize red-shifted chlorophyll antenna protein after a few days under low white (Lukes et al., 2019) or red light (Kotabová et al., 2014), which helps to overcome shading effects; 9) Native PSI supercomplex contains superoxide dismutases, enzymes for scavenging the reactive oxygen species (Sobotka et al., 2017).

In conclusion, the two secondary endosymbiotic algae I used in my study turned out to be useful model organisms with NPQ features that are unique in comparison to higher plant models. Results that I have obtained and published during my study helped to better understand the fine-tuning and regulation of algal NPQ. It has also shown the general importance of this photoprotective mechanism among different algal species. Nevertheless, the complete understanding of all the processes accompanying NPQ and its actual impact on the final crop production (Kromdijk et al., 2016) is still a long-term task for researchers around the world. I hope my work sets the background and provides useful data for future successful studies in this field.



## 6 References

- Akhtar, P., Görföl, F., Garab, G., and Lambrev, P. H. (2019). Dependence of chlorophyll fluorescence quenching on the lipid-to-protein ratio in reconstituted light-harvesting complex II membranes containing lipid labels. *Chemical Physics* **522**, 242-248.
- Al-Najjar, T., Badran, M., Richter, C., Meyerhöfer, M., and Sommer, U. (2007). "Seasonal dynamics of phytoplankton in the Gulf of Aqaba, Red Sea."
- Alboresi, A., Gerotto, C., Giacometti, G. M., Bassi, R., and Morosinotto, T. (2010). *Physcomitrella patens* mutants affected on heat dissipation clarify the evolution of photoprotection mechanisms upon land colonization. *Proceedings of the National Academy of Sciences of the United States of America* **107**, 11128-11133.
- Alfonso, M., Montoya, G., Cases, R., Rodriguez, R., and Picorel, R. (1994). Core Antenna Complexes, CP43 and CP47, of Higher Plant Photosystem II. Spectral Properties, Pigment Stoichiometry, and Amino Acid Composition. *Biochemistry* **33**, 10494-10500.
- Anderson, J., and Osmond, B. (2001). Sun-shade responses: Compromises between acclimation and photoinhibition. In "Photoinhibition" (D. Kyle, B. Osmond and C. Arntzen, eds.). Elsevier, Amsterdam.
- Anderson, J. M., Chow, W. S., and Goodchild, D. J. (1988). Thylakoid Membrane Organization in Sun/Shade Acclimation. *Australian Journal of Plant Physiology* **15**, 11-26.
- Andersson, M., Schubert, H., Pedersén, M., and Snoeijs, P. (2006). Different patterns of carotenoid composition and photosynthesis acclimation in two tropical red algae. *Marine Biology* **149**, 653-665.
- Armbrust, E. V., Berges, J. A., Bowler, C., Green, B. R., Martinez, D., Putnam, N. H., Zhou, S., Allen, A. E., Apt, K. E., Bechner, M., Brzezinski, M. A., Chaal, B. K., Chiovitti, A., Davis, A. K., Demarest, M. S., Detter, J. C., Glavina, T., Goodstein, D., Hadi, M. Z., Hellsten, U., Hildebrand, M., Jenkins, B. D., Jurka, J., Kapitonov, V. V., Kroger, N., Lau, W. W., Lane, T. W., Larimer, F. W., Lippmeier, J. C., Lucas, S., Medina, M., Montsant, A.,

- Obornik, M., Parker, M. S., Palenik, B., Pazour, G. J., Richardson, P. M., Rynearson, T. A., Saito, M. A., Schwartz, D. C., Thamtrakoln, K., Valentin, K., Vardi, A., Wilkerson, F. P., and Rokhsar, D. S. (2004). The genome of the diatom *Thalassiosira pseudonana*: ecology, evolution, and metabolism. *Science* **306**, 79-86.
- Aro, E. M., Suorsa, M., Rokka, A., Allahverdiyeva, Y., Paakkanen, V., Saleem, A., Battchikova, N., and Rintamaki, E. (2005). Dynamics of photosystem II: a proteomic approach to thylakoid protein complexes. *Journal of Experimental Botany* **56**, 347-356.
- Ballottari, M., Truong, T. B., De Re, E., Erickson, E., Stella, G. R., Fleming, G. R., Bassi, R., and Niyogi, K. K. (2016). Identification of pH-sensing Sites in the Light Harvesting Complex Stress-related 3 Protein Essential for Triggering Non-photochemical Quenching in *Chlamydomonas reinhardtii*. *The Journal of Biological Chemistry* **291**, 7334-46.
- Behrenfeld, M. J., Lee, H., and Small, L. F. (1994). Interactions between nutritional-status and long-term responses to ultraviolet-b radiation stress in a marine diatom. *Marine Biology* **118**, 523-530.
- Behrenfeld, M. J., Prášil, O., Kolber, Z. S., Babin, M., and Falkowski, P. G. (1998). Compensatory changes in Photosystem II electron turnover rates protect photosynthesis from photoinhibition. *Photosynth Res* **58**, 259-268.
- Belgio, E., Duffy, C. D., and Ruban, A. V. (2013). Switching light harvesting complex II into photoprotective state involves the lumen-facing apoprotein loop. *Phys Chem Chem Phys* **15**, 12253-61.
- Belgio, E., Johnson, M. P., Juric, S., and Ruban, A. V. (2012). Higher plant photosystem II light-harvesting antenna, not the reaction center, determines the excited-state lifetime-both the maximum and the nonphotochemically quenched. *Biophys J* **102**, 2761-71.
- Belgio, E., Kapitonova, E., Chmeliov, J., Duffy, C. D. P., Ungerer, P., Valkunas, V., and Ruban, A. V. (2014). Economic photoprotection

- in photosystem II that retains a complete light-harvesting system with slow energy traps. *Nature Communications* **5**, 8.
- Belgio, E., Santabarbara, S., Bína, D., Trsková, E., Herbstová, M., Kaňa, R., Zucchelli, G., and Prášil, O. (2017). High photochemical trapping efficiency in Photosystem I from the red clade algae *Chromera velia* and *Phaeodactylum tricornutum*. *Biochim Biophys Acta* **1858**, 56-63.
- Belgio, E., Trskova, E., Kotabova, E., Ewe, D., Prasil, O., and Kana, R. (2018). High light acclimation of *Chromera velia* points to photoprotective NPQ. *Photosynthesis Research* **135**, 263-274.
- Bína, D., Gardian, Z., Herbstová, M., Kotabová, E., Koník, P., Litvín, R., Prášil, O., Tichý, J., and Vácha, F. (2014). Novel type of red-shifted chlorophyll a antenna complex from *Chromera velia*: II. Biochemistry and spectroscopy. *Biochimica et Biophysica Acta* **1837**, 802-10.
- Blankenship, R. E. (2002). "Molecular Mechanisms of Photosynthesis," Blackwell Science Ltd, Oxford.
- Boardman, N. K. (1977). Comparative Photosynthesis of Sun and Shade Plants. *Annual Review of Plant Physiology and Plant Molecular Biology* **28**, 355-377.
- Bode, S., Quentmeier, C. C., Liao, P.-N., Hafi, N., Barros, T., Wilk, L., Bittner, F., and Walla, P. J. (2009). On the regulation of photosynthesis by excitonic interactions between carotenoids and chlorophylls. *Proceedings of the National Academy of Sciences* **106**, 12311-12316.
- Bonaventura, C., and Myers, J. (1969). Fluorescence and oxygen evolution from *Chlorella pyrenoidosa*. *Biochimica et Biophysica Acta (BBA) - Bioenergetics* **189**, 366-383.
- Bonente, G., Pippa, S., Castellano, S., Bassi, R., and Ballottari, M. (2012). Acclimation of *Chlamydomonas reinhardtii* to Different Growth Irradiances. *Journal of Biological Chemistry* **287**, 5833-5847.
- Brown, B., Ambarsari, I., Warner, M., Fitt, W., Dunne, R., Gibb, S., and Cummings, D. (1999). Diurnal changes in photochemical efficiency and xanthophyll concentrations in shallow water reef

- corals: evidence for photoinhibition and photoprotection. *Coral Reefs* **18**, 99-105.
- Bruce, D., Samson, G., and Carpenter, C. (1997). The origins of nonphotochemical quenching of chlorophyll fluorescence in photosynthesis. Direct quenching by P680+ in photosystem II enriched membranes at low pH. *Biochemistry* **36**, 749-55.
- Büchel, C. (2003). Fucoxanthin-chlorophyll proteins in diatoms: 18 and 19 kDa subunits assemble into different oligomeric states. *Biochemistry* **42**, 13027-13034.
- Büchel, C. (2014). Fucoxanthin-Chlorophyll-Proteins and Non-Photochemical Fluorescence Quenching of Diatoms. In "Non-Photochemical Quenching and Energy Dissipation in Plants, Algae and Cyanobacteria" (B. Demmig-Adams, G. Garab, W. Adams and Govindjee, eds.), Vol. 40, pp. 259-275. Springer, Dordrecht.
- Büchel, C. (2015). Evolution and function of light harvesting proteins. *Journal of Plant Physiology* **172C**, 62-75.
- Büchel, C. (2019). Light harvesting complexes in chlorophyll c-containing algae. *Biochimica et Biophysica Acta (BBA) - Bioenergetics*, 148027.
- Buck, J., Sherman, J., Bartulos, C., Serif, M., Halder, M., Henkel, J., Falciatore, A., Lavaud, J., Gorbunov, M., Kroth, P., Falkowski, P., and Lepetit, B. (2019). Lhex proteins provide photoprotection via thermal dissipation of absorbed light in the diatom *Phaeodactylum tricorutum*. *Nature Communications* **10**, 1234567890.
- Bungard, R., Ruban, A., Hibberd, J., Press, M., Horton, P., and Scholes, J. (1999). Unusual carotenoid composition and a new type of xanthophyll cycle in plants. *Proceedings of the National Academy of Sciences of the United States of America* **96**, 1135-1139.
- Calzadilla, P. I., Muzzopappa, F., Setif, P., and Kirilovsky, D. (2019). Different roles for ApcD and ApcF in *Synechococcus elongatus* and *Synechocystis* sp. PCC 6803 phycobilisomes. *Biochimica Et Biophysica Acta-Bioenergetics* **1860**, 488-498.
- Cazzaniga, S., Dall' Osto, L., Kong, S. G., Wada, M., and Bassi, R. (2013). Interaction between avoidance of photon absorption, excess energy



- dissipation and zeaxanthin synthesis against photooxidative stress in Arabidopsis. *The Plant Journal* **76**, 568-79.
- Cheregi, O., Kotabová, E., Prášil, O., Schröder, W., Kaňa, R., and Funk, C. (2015). Presence of state transitions in the cryptophyte alga *Guillardia theta*. *J Exp Bot* **66**, 6461-6470.
- Croce, R. (2015). PsbS is the plants' pick for sun protection. *Nat Struct Mol Biol* **22**, 650-2.
- Cumbo, V. R., Baird, A. H., Moore, R. B., Negri, A. P., Neilan, B. A., Salih, A., van Oppen, M. J., Wang, Y., and Marquis, C. P. (2013). *Chromera velia* is endosymbiotic in larvae of the reef corals *Acropora digitifera* and *A. tenuis*. *Protist* **164**, 237-44.
- Dall'Osto, L., Cazzaniga, S., Havaux, M., and Bassi, R. (2010). Enhanced photoprotection by protein-bound vs free xanthophyll pools: a comparative analysis of chlorophyll b and xanthophyll biosynthesis mutants. *Mol Plant* **3**, 576-93.
- Delphin, E., Duval, J. C., Etienne, A. L., and Kirilovsky, D. (1996). State transitions or delta pH-dependent quenching of photosystem II fluorescence in red algae. *Biochemistry* **35**, 9435-45.
- Demmig-Adams, B. (1990). Carotenoids and photoprotection in plants: A role for the xanthophyll zeaxanthin. *Biochimica et Biophysica Acta - Bioenergetics* **1020**, 1-24.
- Demmig-Adams, B., Garab, G., Adams Iii, W., and Govindjee (2014). "Non-Photochemical Quenching and Energy Dissipation in Plants, Algae and Cyanobacteria," Springer, Dordrecht.
- Dera, J., and Gordon, H. (1968). Light field fluctuations in the photic zone. *Limnol. Oceanogr* **13**, 697-699.
- Duffy, C. D., and Ruban, A. V. (2015). Dissipative pathways in the photosystem-II antenna in plants. *J Photochem Photobiol B* **152**, 215-26.
- Engelken, J., Brinkmann, H., and Adamska, I. (2010). Taxonomic distribution and origins of the extended LHC (light-harvesting complex) antenna protein superfamily. *BMC Evolutionary Biology* **10**.

- Falkowski, P., Owens, T., Ley, A., and Mauzerall, D. (1981). Effects of Growth Irradiance Levels on the Ratio of Reaction Centers in Two Species of Marine Phytoplankton *Plant Physiol* **68**, 969-973.
- Falkowski, P. G., and Owens, T. G. (1980). Light-Shade Adaptation - 2 Strategies in Marine-Phytoplankton. *Plant Physiology* **66**, 592-595.
- Falkowski, P. G., and Raven, J. A. (2007). "Aquatic Photosynthesis," 2nd/Ed. Princeton University Press, New Jersey.
- Fan, M., Li, M., Liu, Z., Cao, P., Pan, X., Zhang, H., Zhao, X., Zhang, J., and Chang, W. (2015). Crystal structures of the PsbS protein essential for photoprotection in plants. *Nature Structural & Molecular Biology* **22**, 729-U115.
- Feng, L., Raza, M. A., Li, Z., Chen, Y., Khalid, M. H. B., Du, J., Liu, W., Wu, X., Song, C., Yu, L., Zhang, Z., Yuan, S., Yang, W., and Yang, F. (2019). The Influence of Light Intensity and Leaf Movement on Photosynthesis Characteristics and Carbon Balance of Soybean. *Frontiers in plant science* **9**, 1952-1952.
- Finazzi, G., Johnson, G. N., Dall'Osto, L., Zito, F., Bonente, G., Bassi, R., and Wollman, F. A. (2006). Nonphotochemical quenching of chlorophyll fluorescence in *Chlamydomonas reinhardtii*. *Biochemistry* **45**, 1490-8.
- Finazzi, G., and Minagawa, J. (2014). High light acclimation in green microalgae. In "Non-Photochemical Quenching and Energy Dissipation in Plants, Algae and Cyanobacteria" (B. Demmig-Adams, W. W. Adams, G. Garab and Govindjee, eds.). Springer Netherlands.
- Funk, C., Alami, M., Tibiletti, T., and Green, B. R. (2011). High light stress and the one-helix LHC-like proteins of the cryptophyte *Guillardia theta*. *Biochim Biophys Acta* **1807**, 841-6.
- Gabilly, S. T., Baker, C. R., Wakao, S., Crisanto, T., Guan, K., Bi, K., Guet, E., Guadagno, C. R., and Niyogi, K. K. (2019). Regulation of photoprotection gene expression in *Chlamydomonas* by a putative E3 ubiquitin ligase complex and a homolog of CONSTANS. *Proceedings of the National Academy of Sciences* **116**, 17556-17562.

- Garcia-Mendoza, E., Ocampo-Alvarez, H., and Govindjee (2011). Photoprotection in the brown alga *Macrocystis pyrifera*: Evolutionary implications. *Journal of Photochemistry and Photobiology B-Biology* **104**, 377-385.
- Gerotto, C., Alboresi, A., Giacometti, G. M., Bassi, R., and Morosinotto, T. (2011). Role of PSBS and LHCSR in *Physcomitrella patens* acclimation to high light and low temperature. *Plant, Cell & Environment* **34**, 922-32.
- Gervais, F. (1997). Light-dependent growth, dark survival, and glucose uptake by cryptophytes isolated from a freshwater chemocline. *Journal of Phycology* **33**, 18-25.
- Giovagnetti, V., and Ruban, A. V. (2018). The evolution of the photoprotective antenna proteins in oxygenic photosynthetic eukaryotes. *Biochem Soc Trans* **46**, 1263-1277.
- Girolomoni, L., Cazzaniga, S., Pinnola, A., Perozeni, F., Ballottari, M., and Bassi, R. (2019). LHCSR3 is a nonphotochemical quencher of both photosystems in *Chlamydomonas reinhardtii*. *Proceedings of the National Academy of Sciences of the United States of America* **116**, 4212-4217.
- Goldschmidt-Clermont, M., and Bassi, R. (2015). Sharing light between two photosystems: mechanism of state transitions. *Current Opinion in Plant Biology* **25**, 71-78.
- Goral, T. K., Johnson, M. P., Duffy, C. D., Brain, A. P., Ruban, A. V., and Mullineaux, C. W. (2012). Light-harvesting antenna composition controls the macrostructure and dynamics of thylakoid membranes in *Arabidopsis*. *Plant J* **69**, 289-301.
- Goss, R., and Lepetit, B. (2014). Biodiversity of NPQ. *Journal of Plant Physiology* **172**, 13-32.
- Goss, R., Lepetit, B., Volke, D., Gilbert, M., and Wilhelm, C. (2010). Evidence for the existence of one antenna-associated, lipid-dissolved and two protein-bound pools of diadinoxanthin cycle pigments in diatoms. *Plant Physiology* **154**, 1905-20.
- Goss, R., Quaas, T., Berteotti, S., Ballottari, M., Flieger, K., Bassi, R., and Wilhelm, C. (2015). Non-photochemical quenching and

- xanthophyll cycle activities in six green algal species suggest mechanistic differences in the process of excess energy dissipation. *Journal of Plant Physiology* **172**, 92-103.
- Green, B., and Parson, W. (2003). "Light-Harvesting Antennas in Photosynthesis," Kluwer Academic Publishers, Dordrecht, The Netherlands.
- Green, B., and Pichersky, E. (1994). Hypothesis for the evolution of three-helix Chl a/b and Chl a/c light-harvesting antenna proteins from two-helix and four-helix ancestors. *Photosynthesis Research* **39**, 149-162.
- Green, B. R. (2011). After the primary endosymbiosis: an update on the chromalveolate hypothesis and the origins of algae with Chl c. *Photosynth Res* **107**, 103-15.
- Green, B. R., Anderson, J. M., and Parson, W. W. (2003). Photosynthetic Membranes and Their Light-Harvesting Antennas. In "Light-Harvesting Antennas in Photosynthesis" (B. R. Green and W. W. Parson, eds.), pp. 1-28. Springer Netherlands, Dordrecht.
- Gruszecki, W., and Siewiewiesiuk, J. (1991). Galactolipid multibilayers modified with xanthophylls: orientational and diffractometric studies. *Biochim Biophys Acta* **1069**, 21-26.
- Guillard, R. R., and Ryther, J. H. (1962). Studies of marine planktonic diatoms I. *Cyclotella nana* Hustedt and *Detonula confervacea* (Cleve) Gran. *Canadian Journal of Microbiology* **8**, 229-239.
- Gundermann, K., and Büchel, C. (2008). The fluorescence yield of the trimeric fucoxanthin-chlorophyll-protein FCPa in the diatom *Cyclotella meneghiniana* is dependent on the amount of bound diatoxanthin. *Photosynthesis Research* **95**, 229-235.
- Gundermann, K., and Büchel, C. (2012). Factors determining the fluorescence yield of fucoxanthin-chlorophyll complexes (FCP) involved in non-photochemical quenching in diatoms. *Biochimica Et Biophysica Acta-Bioenergetics* **1817**, 1044-1052.
- Häder, D.-P., Rhiel, E., and Wehrmeyer, W. (1987). Phototaxis in the marine flagellate *Cryptomonas maculata*. *Journal of Photochemistry and Photobiology B: Biology* **1**, 115-122.

- Hammer, A., Schumann, R., and Schubert, H. (2002). "Light and temperature acclimation of *Rhodomonas salina* (Cryptophyceae): Photosynthetic performance."
- Hansen, U., Fiedler, B., and Rank, B. (2002). Variation of pigment composition and antioxidative systems along the canopy light gradient in a mixed beech/oak forest: a comparative study on deciduous tree species differing in shade tolerance. *Trees* **16**, 354-364.
- Hao, T.-B., Jiang, T., Dong, H.-P., Ou, L.-J., He, X., and Yang, Y.-F. (2018). Light-harvesting protein Lhcx3 is essential for high light acclimation of *Phaeodactylum tricornutum*. *AMB Express* **8**, 174-174.
- Havaux, M., Bonfils, J. P., Lutz, C., and Niyogi, K. K. (2000). Photodamage of the photosynthetic apparatus and its dependence on the leaf developmental stage in the npq1 Arabidopsis mutant deficient in the xanthophyll cycle enzyme violaxanthin de-epoxidase. *Plant Physiol* **124**, 273-84.
- Havelková-Doušová, H., Prášil, O., and Behrenfeld, M. (2004). Photoacclimation of *Dunaliella tertiolecta* (Chlorophyceae) under fluctuating irradiance. *Photosynthetica* **42**, 273-281.
- Holt, N. E., Zigmantas, D., Valkunas, L., Li, X. P., Niyogi, K. K., and Fleming, G. R. (2005). Carotenoid cation formation and the regulation of photosynthetic light harvesting. *Science* **307**, 433-6.
- Horton, P., and Ruban, A. (2005). Molecular design of the photosystem II light-harvesting antenna: photosynthesis and photoprotection. *J Exp Bot* **56**, 365-73.
- Horton, P., Ruban, A. V., and Walters, R. G. (1996). Regulation of light harvesting in green plants *Annu Rev Plant Physiol Plant Mol Biol* **47**, 655-684.
- Horton, P., Ruban, A. V., and Wentworth, M. (2000). Allosteric regulation of the light-harvesting system of photosystem II. *Philos. Trans. R. Soc. Lond. Ser. B-Biol. Sci.* **355**, 1361-1370.

- Ivanov, A. G., Sane, P. V., Hurry, V., Oquist, G., and Huner, N. P. (2008). Photosystem II reaction centre quenching: mechanisms and physiological role. *Photosynth Res* **98**, 565-74.
- Janouškovec, J., Horák, A., Oborník, M., Lukeš, J., and Keeling, P. J. (2010). A common red algal origin of the apicomplexan, dinoflagellate, and heterokont plastids. *Proceedings of the National Academy of Sciences of the United States of America* **107**, 10949-54.
- Johnson, M. P., Goral, T. K., Duffy, C. D., Brain, A. P., Mullineaux, C. W., and Ruban, A. V. (2011). Photoprotective energy dissipation involves the reorganization of photosystem II light-harvesting complexes in the grana membranes of spinach chloroplasts. *Plant Cell* **23**, 1468-79.
- Johnson, M. P., and Ruban, A. V. (2009). Photoprotective energy dissipation in higher plants involves alteration of the excited state energy of the emitting chlorophyll(s) in the light harvesting antenna II (LHCII). *J Biol Chem* **284**, 23592-601.
- Johnson, M. P., and Ruban, A. V. (2010). Arabidopsis plants lacking PsbS protein possess photoprotective energy dissipation. *Plant J* **61**, 283-9.
- Johnson, M. P., Zia, A., Horton, P., and Ruban, A. V. (2010). Effect of xanthophyll composition on the chlorophyll excited state lifetime in plant leaves and isolated LHCII. *Chemical Physics* **373**, 23-32.
- Joshi-Deo, J., Schmidt, M., Gruber, A., Weisheit, W., Mittag, M., Kroth, P. G., and Büchel, C. (2010). Characterization of a trimeric light-harvesting complex in the diatom *Phaeodactylum tricornutum* built of FcpA and FcpE proteins. *Journal of experimental botany* **61**, 3079-3087.
- Kagawa, T., Sakai, T., Suetsugu, N., Oikawa, K., Ishiguro, S., Kato, T., Tabata, S., Okada, K., and Wada, M. (2001). Arabidopsis NPL1: a phototropin homolog controlling the chloroplast high-light avoidance response. *Science* **291**, 2138-41.

- Kaňa, R. (2018). Application of spectrally resolved fluorescence induction to study light-induced nonphotochemical quenching in algae. *Photosynthetica* **56**, 132-138.
- Kaňa, R., and Govindjee (2016). Role of Ions in the Regulation of Light-Harvesting. *Frontiers in Plant Science* **7**.
- Kaňa, R., Kotabová, E., Kopečná, J., Trsková, E., Belgio, E., Sobotka, R., and Ruban, A. V. (2016). Violaxanthin inhibits nonphotochemical quenching in light-harvesting antennae of *Chromera velia*. *FEBS Lett* **590**, 1076-1085.
- Kaňa, R., Kotabová, E., Šedivá, B., and Kuthanová Trsková, E. (2019). Photoprotective strategies in the motile cryptophyte alga *Rhodomonas salina* – role of non-photochemical quenching, ions, photoinhibition and cell motility. *Folia Microbiologica* **64**, 691-703.
- Kaňa, R., Kotabová, E., Sobotka, R., and Prášil, O. (2012). Non-photochemical quenching in cryptophyte alga *Rhodomonas salina* is located in chlorophyll a/c antennae. *PLoS One* **7**, e29700.
- Kaňa, R., Lazár, D., Prášil, O., and Naus, J. (2002). Experimental and theoretical studies on the excess capacity of Photosystem II. *Photosynth Res* **72**, 271-284.
- Kaňa, R., Prášil, O., and Mullineaux, C. W. (2009). Immobility of phycobilins in the thylakoid lumen of a cryptophyte suggests that protein diffusion in the lumen is very restricted. *FEBS Lett* **583**, 670-674.
- Kaneda, H., and Furuya, M. (1986). Temporal Changes in Swimming Direction during the Phototactic Orientation of Individual Cells in *Cryptomonas* sp. *Plant and Cell Physiology* **27**, 265-271.
- Kaneda, H., and Furuya, M. (1987). Effects of the Timing of Flashes of Light during the Course of Cellular Rotation on Phototactic Orientation of Individual Cells of *Cryptomonas*. *Plant Physiol* **84**, 178-81.
- Keeling, P. J. (2013). The Number, Speed, and Impact of Plastid Endosymbioses in Eukaryotic Evolution. *Annual Review of Plant Biology* **64**, 583-607.

- Kendrick, R., and Kronenberg, G. (1994). "Photomorphogenesis in plants," 2nd/Ed. Kluwer Academic Publishers, The Netherlands.
- Koller, D. (1990). Light-driven leaf movements\*. *Plant, Cell & Environment* **13**, 615-632.
- Komenda, J., Barker, M., Kuvikova, S., de Vries, R., Mullineaux, C. W., Tichy, M., and Nixon, P. J. (2006). The FtsH protease slr0228 is important for quality control of photosystem II in the thylakoid membrane of *Synechocystis* sp. PCC 6803. *J Biol Chem* **281**, 1145-51.
- Kotabová, E., Jarešová, J., Kaňa, R., Sobotka, R., Bína, D., and Prášil, O. (2014). Novel type of red-shifted chlorophyll alpha antenna complex from *Chromera velia*. I. Physiological relevance and functional connection to photosystems. *Biochimica Et Biophysica Acta-Bioenergetics* **1837**, 734-743.
- Kotabová, E., Kaňa, R., Jarešová, J., and Prášil, O. (2011). Non-photochemical fluorescence quenching in *Chromera velia* is enabled by fast violaxanthin de-epoxidation. *FEBS Letters* **585**, 1941-5.
- Kouřil, R., Dekker, J. P., and Boekema, E. J. (2012). Supramolecular organization of photosystem II in green plants. *Biochimica Et Biophysica Acta-Bioenergetics* **1817**, 2-12.
- Kouřil, R., Wientjes, E., Bultema, J. B., Croce, R., and Boekema, E. J. (2013). High-light vs. low-light: Effect of light acclimation on photosystem II composition and organization in *Arabidopsis thaliana*. *Biochimica Et Biophysica Acta-Bioenergetics* **1827**, 411-419.
- Koziol, A. G., Borza, T., Ishida, K.-I., Keeling, P., Lee, R. W., and Durnford, D. G. (2007). Tracing the Evolution of the Light-Harvesting Antennae in Chlorophyll *a*/*b*-Containing Organisms. *Plant Physiology* **143**, 1802-1816.
- Kromdijk, J., Glowacka, K., Leonelli, L., Gabilly, S. T., Iwai, M., Niyogi, K. K., and Long, S. P. (2016). Improving photosynthesis and crop productivity by accelerating recovery from photoprotection. *Science* **354**, 857-861.



- Krupnik, T., Kotabova, E., van Bezouwen, L. S., Mazur, R., Garstka, M., Nixon, P. J., Barber, J., Kana, R., Boekema, E. J., and Kargul, J. (2013). A reaction center-dependent photoprotection mechanism in a highly robust photosystem II from an extremophilic red alga, *Cyanidioschyzon merolae*. *J Biol Chem* **288**, 23529-42.
- Kuthanová Trsková, E., Belgio, E., Yeates, A. M., Sobotka, R., Ruban, A. V., and Kaňa, R. (2018). Antenna proton sensitivity determines photosynthetic light harvesting strategy. *J Exp Bot* **69**, 4483-4493.
- Kuthanová Trsková, E., Bína, D., Santabarbara, S., Sobotka, R., Kaňa, R., and Belgio, E. (2019). Isolation and characterization of CAC antenna proteins and photosystem I supercomplex from the cryptophytic alga *Rhodomonas salina*. *Physiologia Plantarum* **166**, 309-319.
- Lavaud, J., and Kroth, P. G. (2006). In diatoms, the transthylakoid proton gradient regulates the photoprotective non-photochemical fluorescence quenching beyond its control on the xanthophyll cycle. *Plant Cell Physiol* **47**, 1010-6.
- Lavaud, J., and Lepetit, B. (2013). An explanation for the inter-species variability of the photoprotective non-photochemical chlorophyll fluorescence quenching in diatoms. *Biochim Biophys Acta* **1827**, 294-302.
- Lavaud, J., Rousseau, B., and Etienne, A. (2002a). In diatoms, a transthylakoid proton gradient alone is not sufficient to induce a non-photochemical fluorescence quenching. *FEBS Lett* **523**, 163-166.
- Lavaud, J., Rousseau, B., van Gorkom, H., and Etienne, A. (2002b). Influence of the Diadinoxanthin Pool Size on Photoprotection in the Marine Planktonic Diatom *Phaeodactylum tricornutum*. *Plant Physiol* **129**, 1398-1406.
- Lee, R. E. (2008). "Phycology," 4/Ed. Cambridge University Press, Cambridge.
- Lepetit, B., Gelin, G., Lepetit, M., Sturm, S., Vugrinec, S., Rogato, A., Kroth, P. G., Falciatore, A., and Lavaud, J. (2017). The diatom *Phaeodactylum tricornutum* adjusts nonphotochemical

- fluorescence quenching capacity in response to dynamic light via fine-tuned Lhcx and xanthophyll cycle pigment synthesis. *New Phytol* **214**, 205-218.
- Ley, A. C., and Mauzerall, D. C. (1982). Absolute absorption cross-sections for Photosystem II and the minimum quantum requirement for photosynthesis in *Chlorella vulgaris*. *Biochimica et Biophysica Acta (BBA) - Bioenergetics* **680**, 95-106.
- Li, X. P., Gilmore, A. M., Caffarri, S., Bassi, R., Golan, T., Kramer, D., and Niyogi, K. K. (2004). Regulation of photosynthetic light harvesting involves intrathylakoid lumen pH sensing by the PsbS protein. *Journal of Biological Chemistry* **279**, 22866-22874.
- Li, Z. R., Wakao, S., Fischer, B. B., and Niyogi, K. K. (2009). Sensing and Responding to Excess Light. *Annual Review of Plant Biology* **60**, 239-260.
- Liguori, N., Roy, L. M., Opacic, M., Durand, G., and Croce, R. (2013). Regulation of Light Harvesting in the Green Alga *Chlamydomonas reinhardtii*: The C-Terminus of LHCSR Is the Knob of a Dimmer Switch. *Journal of the American Chemical Society* **135**, 18339-18342.
- Liu, C., Zhang, Y., Cao, D., He, Y., Kuang, T., and Yang, C. (2008). Structural and functional analysis of the antiparallel strands in the lumenal loop of the major light-harvesting chlorophyll a/b complex of photosystem II (LHCIIb) by site-directed mutagenesis. *J Biol Chem* **283**, 487-95.
- Liu, H., and Blankenship, R. E. (2019). On the interface of light-harvesting antenna complexes and reaction centers in oxygenic photosynthesis. *Biochim Biophys Acta Bioenerg* **1860**, 148079.
- Long, S., Humphries, S., and Falkowski, P. (1994). Photoinhibition of Photosynthesis in Nature. *Annual Review of Plant Physiology and Plant Molecular Biology* **45**, 633-662.
- Lukes, M., Giordano, M., and Prasil, O. (2019). The effect of light quality and quantity on carbon allocation in *Chromera velia*. *Folia Microbiol (Praha)* **64**, 655-662.

- Mann, M., Hoppenz, P., Jakob, T., Weisheit, W., Mittag, M., Wilhelm, C., and Goss, R. (2014). Unusual features of the high light acclimation of *Chromera velia*. *Photosynthesis Research*.
- Mascoli, V., Liguori, N., Xu, P., Roy, L. M., van Stokkum, I. H. M., and Croce, R. (2019). Capturing the Quenching Mechanism of Light-Harvesting Complexes of Plants by Zooming in on the Ensemble. *Chem* **5**, 2900-2912.
- Masojidek, J., Kopecky, J., Koblizek, M., and Torzillo, G. (2004). The xanthophyll cycle in green algae (chlorophyta): its role in the photosynthetic apparatus. *Plant Biol (Stuttg)* **6**, 342-9.
- Masojidek, J., Torzillo, G., Koblizek, M., Kopecky, J., Bernardini, P., Sacchi, A., and Komenda, J. (1999). Photoadaptation of two members of the Chlorophyta (*Scenedesmus* and *Chlorella*) in laboratory and outdoor cultures: changes in chlorophyll fluorescence quenching and the xanthophyll cycle. *Planta* **209**, 126-35.
- Mazor, Y., Borovikova, A., and Nelson, N. (2015). The structure of plant photosystem I super-complex at 2.8 Å resolution. *eLife* **4**, e07433-e07433.
- Miloslavina, Y., Grouneva, I., Lambrev, P. H., Lepetit, B., Goss, R., Wilhelm, C., and Holzwarth, A. R. (2009). Ultrafast fluorescence study on the location and mechanism of non-photochemical quenching in diatoms. *Biochimica et Biophysica Acta (BBA) - Bioenergetics* **1787**, 1189-1197.
- Mitchell, P. (1961). Coupling of Phosphorylation to Electron and Hydrogen Transfer by a Chemi-Osmotic type of Mechanism. *Nature* **191**, 144-148.
- Moore, R. B., Oborník, M., Janouškovec, J., Chrudimský, T., Vancová, M., Green, D. H., Wright, S. W., Davies, N. W., Bolch, C. J., Heimann, K., Šlapeta, J., Hoegh-Guldberg, O., Logsdon, J. M., and Carter, D. A. (2008). A photosynthetic alveolate closely related to apicomplexan parasites. *Nature* **451**, 959-63.
- Morosinotto, T., Bassi, R., Frigerio, S., Finazzi, G., Morris, E., and Barber, J. (2006). Biochemical and structural analyses of a higher plant

- photosystem II supercomplex of a photosystem I-less mutant of barley - Consequences of a chronic over-reduction of the plastoquinone pool. *Febs Journal* **273**, 4616-4630.
- Mou, S., Zhang, X., Dong, M., Fan, X., Xu, J., Cao, S., Xu, D., Wang, W., and Ye, N. (2013). Photoprotection in the green tidal alga *Ulva prolifera*: role of LHCSR and PsbS proteins in response to high light stress. *Plant Biology (Stuttg)* **15**, 1033-9.
- Müller, P., Li, X. P., and Niyogi, K. K. (2001). Non-photochemical quenching. A response to excess light energy. *Plant Physiology* **125**, 1558-1566.
- Mullineaux, C. W., and Allen, J. F. (1990). State 1-State 2 transitions in the cyanobacterium *Synechococcus* 6301 are controlled by the redox state of electron carriers between Photosystems I and II. *Photosynthesis Research* **23**, 297-311.
- Mullineaux, C. W., and Emlyn-Jones, D. (2004). State transitions: an example of acclimation to low-light stress. *Journal of Experimental Botany* **56**, 389-393.
- Murata, N. (1969). Control of excitation transfer in photosynthesis I. Light-induced change of chlorophyll a fluorescence in *Porphyridium cruentum*. *Biochimica et Biophysica Acta (BBA) - Bioenergetics* **172**, 242-251.
- Nawrocki, W. J., Liu, X., and Croce, R. (2020). *Chlamydomonas reinhardtii* exhibits de facto constitutive NPQ capacity in physiologically relevant conditions. *Plant Physiology*, pp.00658.2019.
- Nawrocki, W. J., Santabarbara, S., Mosebach, L., Wollman, F.-A., and Rappaport, F. (2016). State transitions redistribute rather than dissipate energy between the two photosystems in *Chlamydomonas*. *Nature Plants* **2**, 16031.
- Nellaepalli, S., Zsiros, O., Kovács, L., Venkateswarlu, Y., Rao, M. N., Mohanty, P., and Subramanyam, R. (2013). State Transition Mechanism in *Arabidopsis Thaliana*: Biophysical and Proteomic Studies. pp. 398-401. Springer Berlin Heidelberg, Berlin, Heidelberg.

- Nicol, L., Nawrocki, W. J., and Croce, R. (2019). Disentangling the sites of non-photochemical quenching in vascular plants. *Nature Plants* **5**, 1177-1183.
- Niedzwiedzki, D. M., Bar-Zvi, S., Blankenship, R. E., and Adir, N. (2019). Mapping the excitation energy migration pathways in phycobilisomes from the cyanobacterium *Acaryochloris marina*. *Biochimica Et Biophysica Acta-Bioenergetics* **1860**, 286-296.
- Nilkens, M., Kress, E., Lambrev, P., Miloslavina, Y., Müller, M., Holzwarth, A. R., and Jahns, P. (2010). Identification of a slowly inducible zeaxanthin-dependent component of non-photochemical quenching of chlorophyll fluorescence generated under steady-state conditions in *Arabidopsis*. *Biochimica et Biophysica Acta* **1797**, 466-75.
- Oborník, M., Kručinská, J., and Esson, H. (2016). Life cycles of chromerids resemble those of colpodellids and apicomplexan parasites. *Perspectives in Phycology* **3**, 21-27.
- Oborník, M., Vancová, M., Lai, D. H., Janouškovec, J., Keeling, P. J., and Lukeš, J. (2011). Morphology and ultrastructure of multiple life cycle stages of the photosynthetic relative of apicomplexa, *Chromera velia*. *Protist* **162**, 115-30.
- Ocampo-Alvarez, H., Garcia-Mendoza, E., and Govindjee (2013). Antagonist effect between violaxanthin and de-epoxidated pigments in nonphotochemical quenching induction in the qE deficient brown alga *Macrocystis pyrifera*. *Biochimica Et Biophysica Acta-Bioenergetics* **1827**, 427-437.
- Oguchi, R., Hikosaka, K., and Hirose, T. (2003). Does the photosynthetic light-acclimation need change in leaf anatomy? *Plant Cell and Environment* **26**, 505-512.
- Ort, D. R., and Whitmarsh, J. (2001). Photosynthesis. In "Encyclopedia of Life Sciences". John Wiley & Sons.
- Overkamp, K. E., Gasper, R., Kock, K., Herrmann, C., Hofmann, E., and Frankenberg-Dinkel, N. (2014). Insights into the biosynthesis and assembly of cryptophycean phycobiliproteins. *J Biol Chem* **289**, 26691-707.

- Pan, H., Slapeta, J., Carter, D., and Chen, M. (2012). Phylogenetic analysis of the light-harvesting system in *Chromera velia*. *Photosynthesis Research* **111**, 19-28.
- Peers, G., Truong, T. B., Ostendorf, E., Busch, A., Elrad, D., Grossman, A. R., Hippler, M., and Niyogi, K. K. (2009). An ancient light-harvesting protein is critical for the regulation of algal photosynthesis. *Nature* **462**, 518-U215.
- Pesaresi, P., Scharfenberg, M., Weigel, M., Granlund, I., Schroeder, W. P., Finazzi, G., Rappaport, F., Masiero, S., Furini, A., Jahns, P., and Leister, D. (2009). Mutants, Overexpressors, and Interactors of Arabidopsis Plastocyanin Isoforms: Revised Roles of Plastocyanin in Photosynthetic Electron Flow and Thylakoid Redox State. *Molecular Plant* **2**, 236-248.
- Petrou, K., Belgio, E., and Ruban, A. V. (2014). pH sensitivity of chlorophyll fluorescence quenching is determined by the detergent/protein ratio and the state of LHCII aggregation. *Biochim Biophys Acta* **1837**, 1533-1539.
- Phillip, D., Hobe, S., Paulsen, H., Molnar, P., Hashimoto, H., and Young, A. J. (2002). The binding of Xanthophylls to the bulk light-harvesting complex of photosystem II of higher plants. A specific requirement for carotenoids with a 3-hydroxy-beta-end group. *J Biol Chem* **277**, 25160-9.
- Pogson, B. R., HM (2000). Genetic manipulation of carotenoid biosynthesis and photoprotection. *Philosophical Transactions of the Royal Society of London Series B - Biological Sciences* **355**, 1395-1403.
- Poorter, H., Niinemets, Ü., Poorter, L., Wright, I. J., and Villar, R. (2009). Causes and consequences of variation in leaf mass per area (LMA): a meta-analysis. *New Phytologist* **182**, 565-588.
- Pyke, K. (2009). "Plastid Biology," Cambridge Univ Press, Cambridge.
- Quigg, A., Kotabová, E., Jarešová, J., Kaňa, R., Šetlík, J., Šedivá, B., Komárek, O., and Prášil, O. (2012). Photosynthesis in *Chromera velia* represents a simple system with high efficiency. *PLoS One*, <https://doi.org/10.1371/journal.pone.0047036>.

- Roach, T., and Krieger-Liszkay, A. (2012). The role of the PsbS protein in the protection of photosystems I and II against high light in *Arabidopsis thaliana*. *Biochimica et Biophysica Acta (BBA) - Bioenergetics* **1817**, 2158-2165.
- Roach, T., and Krieger-Liszkay, A. (2019). Photosynthetic Regulatory Mechanisms for Efficiency and Prevention of Photo-Oxidative Stress. In "Annual Plant Reviews online" (J. Roberts, ed.), pp. 273-306. John Wiley & Sons.
- Ruban, A. (2013). "The Photosynthetic Membrane," John Wiley & Sons, Ltd., United Kingdom.
- Ruban, A., Lavaud, J., Rousseau, B., Guglielmi, G., Horton, P., and Etienne, A. (2004). The super-excess energy dissipation in diatom algae: comparative analysis with higher plants. *Photosynthesis Research* **82**, 165-175.
- Ruban, A., Rees, D., Pascal, A. A., and Horton, P. (1992). Mechanism of  $\Delta pH$ -dependent dissipation of absorbed excitation energy by photosynthetic membranes. II. The relationship between LHCII aggregation in vitro and qE in isolated thylakoids. *Biochim Biophys Acta* **1102**, 39-44.
- Ruban, A. V. (2016). Nonphotochemical Chlorophyll Fluorescence Quenching: Mechanism and Effectiveness in Protecting Plants from Photodamage. *Plant physiology* **170**, 1903-1916.
- Ruban, A. V., Berera, R., Iliaia, C., van Stokkum, I. H., Kennis, J. T., Pascal, A. A., van Amerongen, H., Robert, B., Horton, P., and van Grondelle, R. (2007). Identification of a mechanism of photoprotective energy dissipation in higher plants. *Nature* **450**, 575-8.
- Ruban, A. V., and Horton, P. (1995). An Investigation of the Sustained Component of Nonphotochemical Quenching of Chlorophyll Fluorescence in Isolated Chloroplasts and Leaves of Spinach. *Plant physiol* **108**, 721-726.
- Ruban, A. V., and Johnson, M. P. (2010). Xanthophylls as modulators of membrane protein function. *Arch Biochem Biophys* **504**, 78-85.

- Ruban, A. V., Johnson, M. P., and Duffy, C. D. (2012). The photoprotective molecular switch in the photosystem II antenna. *Biochim Biophys Acta* **1817**, 167-81.
- Ruban, A. V., Lee, P. J., Wentworth, M., Young, A. J., and Horton, P. (1999). Determination of the stoichiometry and strength of binding of xanthophylls to the photosystem II light harvesting complexes. *J Biol Chem* **274**, 10458-65.
- Ruban, A. V., and Murchie, E. H. (2012). Assessing the photoprotective effectiveness of non-photochemical chlorophyll fluorescence quenching: a new approach. *Biochim Biophys Acta* **1817**, 977-82.
- Ruban, A. V., Pesaresi, P., Wacker, U., Irrgang, K. D. J., Bassi, R., and Horton, P. (1998). The relationship between the binding of dicyclohexylcarbodiimide and quenching of chlorophyll fluorescence in the light-harvesting proteins of photosystem II. *Biochemistry* **37**, 11586-11591.
- Ruban, A. V., Young, A., and Horton, P. (1994a). Modulation of chlorophyll fluorescence quenching in isolated light-harvesting complex of Photosystem II. *Biochimica Et Biophysica Acta-Bioenergetics* **1186**, 123-127.
- Ruban, A. V., Young, A. J., Pascal, A. A., and Horton, P. (1994b). The Effects of Illumination on the Xanthophyll Composition of the Photosystem II Light-Harvesting Complexes of Spinach Thylakoid Membranes. *Plant Physiol* **104**, 227-234.
- Salonen, K., and Jokinen, S. (1988). Flagellate grazing on bacteria in a small dystrophic lake. *Hydrobiologia* **161**, 203-209.
- Schubert, N., García-Mendoza, E., and Pacheco-Ruiz, I. (2006). Carotenoid composition of marine red algae 1 *Journal of Phycology* **42**, 1208-1216.
- Sobotka, R., Esson, H. J., Konik, P., Trskova, E., Moravcova, L., Horak, A., Dufkova, P., and Obornik, M. (2017). Extensive gain and loss of photosystem I subunits in chromerid algae, photosynthetic relatives of apicomplexans. *Sci Rep* **7**, 13214.



- Suetsugu, N., and Wada, M. (2007). Chloroplast photorelocation movement mediated by phototropin family proteins in green plants. *Biol Chem* **388**, 927-35.
- Takahashi, S., and Badger, M. R. (2011). Photoprotection in plants: a new light on photosystem II damage. *Trends in Plant Science* **16**, 53-60.
- Tanabe, Y., Shitara, T., Kashino, Y., Hara, Y., and Kudoh, S. (2011). Utilizing the Effective Xanthophyll Cycle for Blooming of *Ochromonas smithii* and *O. itoi* (Chrysophyceae) on the Snow Surface. *PLoS One* **6**.
- Tian, L., Nawrocki, W. J., Liu, X., Polukhina, I., van Stokkum, I. H. M., and Croce, R. (2019). pH dependence, kinetics and light-harvesting regulation of nonphotochemical quenching in *Chlamydomonas*. *Proceedings of the National Academy of Sciences* **116**, 8320-8325.
- Tichý, J., Gardian, Z., Bina, D., Koník, P., Litvín, R., Herbstová, M., Pain, A., and Vácha, F. (2013). Light harvesting complexes of *Chromera velia*, photosynthetic relative of apicomplexan parasites. *Biochimica et Biophysica Acta* **1827**, 723-9.
- Ting, C. S., and Owens, T. G. (1994). The Effects of Excess Irradiance on Photosynthesis in the Marine Diatom *Phaeodactylum tricornutum*. *Plant Physiology* **106**, 763.
- Ursi, S. (2003). Intraspecific variation of photosynthesis, respiration and photoprotective carotenoids in *Gracilaria birdiae* (Gracilariales: Rhodophyta). *Marine biology* v. **142**, pp. 997-1007-2003 v.142 no.5.
- van den Berg, T. E., Chukhutsina, V. U., van Amerongen, H., Croce, R., and van Oort, B. (2019). Light Acclimation of the Colonial Green Alga *Botryococcus braunii* Strain Showa. *Plant Physiology* **179**, 1132-1143.
- Vass, I. (2012). Molecular mechanisms of photodamage in the Photosystem II complex. *Biochim Biophys Acta* **1817**, 209-17.
- Wada, M. (2016). Chloroplast and nuclear photorelocation movements. *Proceedings of the Japan Academy. Series B, Physical and biological sciences* **92**, 387-411.

- Walters, R. G. (2005). Towards an understanding of photosynthetic acclimation. *Journal of Experimental Botany* **56**, 435-447.
- Walters, R. G., Ruban, A. V., and Horton, P. (1996). Identification of proton-active residues in a higher plant light-harvesting complex. *Proc Natl Acad Sci U S A* **93**, 14204-9.
- Ware, M. A., Belgio, E., and Ruban, A. V. (2015a). Photoprotective capacity of non-photochemical quenching in plants acclimated to different light intensities. *Photosynth Res* **126**, 261-274.
- Ware, M. A., Giovagnetti, V., Belgio, E., and Ruban, A. V. (2015b). PsbS protein modulates non-photochemical chlorophyll fluorescence quenching in membranes depleted of photosystems. *Journal of Photochemistry and Photobiology B: Biology* **152, Part B**, 301-307.
- Warner, M. E., and Berry-Lowe, S. (2006). Differential xanthophyll cycling and photochemical activity in symbiotic dinoflagellates in multiple locations of three species of Caribbean coral. *Journal of Experimental Marine Biology and Ecology* **339**, 86-95.
- Wentworth, M., Ruban, A. V., and Horton, P. (2000). Chlorophyll fluorescence quenching in isolated light harvesting complexes induced by zeaxanthin. *FEBS Lett* **471**, 71-4.
- West, R., Kesan, G., Trsková, E., Sobotka, R., Kaňa, R., Fuciman, M., and Polívka, T. (2016). Spectroscopic properties of the triple bond carotenoid alloxanthin. *Chem Phys Lett* **653**, 167-172.
- Wientjes, E., Drop, B., Kouril, R., Boekema, E. J., and Croce, R. (2013a). During state 1 to state 2 transition in *Arabidopsis thaliana*, the photosystem II supercomplex gets phosphorylated but does not disassemble. *J Biol Chem* **288**, 32821-6.
- Wientjes, E., van Amerongen, H., and Croce, R. (2013b). Quantum Yield of Charge Separation in Photosystem II: Functional Effect of Changes in the Antenna Size upon Light Acclimation. *Journal of Physical Chemistry B* **117**, 11200-11208.
- Wilk, L., Grunwald, M., Liao, P. N., Walla, P. J., and Kuhlbrandt, W. (2013). Direct interaction of the major light-harvesting complex II and PsbS in nonphotochemical quenching. *Proceedings of the*

- National Academy of Sciences of the United States of America* **110**, 5452-5456.
- Wobbe, L., Bassi, R., and Kruse, O. (2016). Multi-Level Light Capture Control in Plants and Green Algae. *Trends Plant Sci* **21**, 55-68.
- Wolfe, G. R., Cunningham, F. X., Durnfordt, D., Green, B. R., and Gantt, E. (1994). Evidence for a common origin of chloroplasts with light-harvesting complexes of different pigmentation. *Nature* **367**, 566-568.
- Xu, P., Tian, L., Kloz, M., and Croce, R. (2015). Molecular insights into Zeaxanthin-dependent quenching in higher plants. *Sci Rep* **5**, 13679.
- Yamamoto, Y., Aminaka, R., Yoshioka, M., Khatoon, M., Komayama, K., Takenaka, D., Yamashita, A., Nijo, N., Inagawa, K., Morita, N., Sasaki, T., and Yamamoto, Y. (2008). Quality control of photosystem II: impact of light and heat stresses. *Photosynth Res* **98**, 589-608.
- Yamanaka, G., Glazer, A. N., and Williams, R. C. (1980). Molecular architecture of a light-harvesting antenna - comparison of wild-type and mutant *synechococcus-6301* phycobilisomes *Journal of Biological Chemistry* **255**, 1004-1010.
- Zhang, X., Ye, N., Mou, S., Xu, D., and Fan, X. (2013). Occurrence of the PsbS and LhcSR products in the green alga *Ulva linza* and their correlation with excitation pressure. *Plant Physiol Biochem* **70**, 336-41.
- Zhao, M. R., Sun, L., Fu, X. J., and Chen, M. (2019). Phycoerythrin-phycoerythrin aggregates and phycoerythrin aggregates from phycobilisomes of the marine red alga *Polysiphonia urceolata*. *International Journal of Biological Macromolecules* **126**, 685-696.



## RESEARCH ARTICLES



ARTICLE I

**Violaxanthin inhibits nonphotochemical quenching in light-harvesting antennae of *Chromera velia***

Kaňa, R., Kotabová, E., Kopečná, J., Trsková, E., Belgio, E., Sobotka, R.,  
and Ruban, A. V.

(2016)

*FEBS Letters* **590**, 1076-1085. IF = 3.21





## Violaxanthin inhibits nonphotochemical quenching in light-harvesting antenna of *Chromera velia*

Radek Kaňa<sup>1,2</sup>, Eva Kotabová<sup>1,2</sup>, Jana Kopečná<sup>1</sup>, Eliška Trsková<sup>1,2</sup>, Erica Belgio<sup>1,3</sup>, Roman Sobotka<sup>1,2</sup> and Alexander V. Ruban<sup>3</sup>

1 Institute of Microbiology, Academy of Sciences of the Czech Republic, Třeboň, Czech Republic

2 Faculty of Sciences, University of South Bohemia, České Budějovice, Czech Republic

3 School of Biological and Chemical Sciences, Queen Mary University of London, UK

### Correspondence

R. Kaňa, Institute of Microbiology, Academy of Sciences of the Czech Republic, Opatovický mlýn, 379 81 Třeboň, Czech Republic

Fax: +420 384340415

Tel: +420 384340436

E-mail: kana@alga.cz

(Received 27 November 2015, revised 24 February 2016, accepted 26 February 2016, available online 4 April 2016)

doi:10.1002/1873-3468.12130

Edited by Richard Cogdell

**Non-photochemical quenching (NPQ) is a photoprotective mechanism in light-harvesting antennae. NPQ is triggered by chloroplast thylakoid lumen acidification and is accompanied by violaxanthin de-epoxidation to zeaxanthin, which further stimulates NPQ. In the present study, we show that violaxanthin can act in the opposite direction to zeaxanthin because an increase in the concentration of violaxanthin reduced NPQ in the light-harvesting antennae of *Chromera velia*. The correlation overlapped with a similar relationship between violaxanthin and NPQ as observed in isolated higher plant light-harvesting complex II. The data suggest that violaxanthin in *C. velia* can act as an inhibitor of NPQ, indicating that violaxanthin has to be removed from the vicinity of the protein to reach maximal NPQ.**

**Keywords:** *Chromera velia*; light-harvesting antennae; nonphotochemical quenching; photoprotection; violaxanthin; zeaxanthin

Photosynthetic organisms use light as a main source of energy. The efficiency of conversion of light into chemical energy is a precisely controlled process requiring the functional connection of a number of light-harvesting pigment–protein complexes (known as photosynthetic antenna) to the photosynthetic reaction center. Under optimal light conditions, these pigment–proteins can efficiently collect light for photochemistry. However, during periods of excessive irradiation, absorbed light energy in antenna complexes can be safely dissipated into heat [1] via a photoprotective mechanism termed non-photochemical quenching NPQ [2]. Factors regulating NPQ are closely related to variability in species dependence on the type of light-harvesting antennae present in particular phototrophs [3]. In the outer membrane-bound phycobiliproteins, NPQ

proceeds via a pH-independent mechanism (see NPQ in PBsomes of cyanobacteria) [4] or it can be even negligible (no NPQ in phycoerythrins of cryptophytes) [5]. Except for evolutionary older cyanobacterial high-light inducible proteins (e.g. HliD protein) that are in a fixed quenching state [6], NPQ in the other membrane-spanning light-harvesting antennae is usually controlled (stimulated) by an increase in lumen acidification. The sensitivity of NPQ to the lumen pH is tuned by several allosteric regulators affecting the sensitivity of light-harvesting complexes (LHCs) to lumen acidification. These allosteric regulators include small membrane proteins such as Psbs in higher plants [7], or a stress-related light harvesting complex (LhcSR protein) in green algae [8], mosses [9] and in diatoms [10]. Xanthophylls are other compounds involved in the

### Abbreviations

Chl, chlorophyll; CLH, *Chromera velia* light-harvesting; DM, *N*-dodecyl- $\beta$ -D-maltoside;  $F_M$ , maximal variable fluorescence in the dark;  $F_M'$ , maximal variable fluorescence on light; LHC, light-harvesting complex; NPQ, nonphotochemical quenching; PSI (II), photosystem I (II); PSI-LHCr, photosystem I with bound light-harvesting complexes; Vio, violaxanthin.

regulation of NPQ sensitivity to lumen pH and therefore are important for photoprotection [11]. The correlation between de-epoxidation of certain xanthophylls and enhancement of NPQ has been already observed in higher plants [12] and diatoms [13], as well as recently in *Chromera velia* [14], which is a newly discovered algae that belongs to colpodellids [15]. An exception for algae appears to comprise cryptophytes without a xanthophyll cycle [5,16] and red algae where the role of xanthophylls in the mechanism of photoprotection is still questionable [17,18]. The molecular mechanism of photoprotection by de-epoxidized xanthophylls such as zeaxanthin is still a matter of discussion. It was proposed that they have a direct quenching role (e.g. by zeaxanthin) [19] or, alternatively, they may act indirectly through allosteric regulation of NPQ in light-harvesting antenna via binding to a specific site [20] or from the outside of a protein without any specific interaction with antennae [21]. Indeed, all of the xanthophylls can act as modulators of membrane protein function [22]. It has been proposed that the hydrophobic nature of de-epoxidized xanthophylls such as zeaxanthin makes the protein structure more compact, leading to protein dehydration. This, in turn, promotes closer pigment–pigment interactions that result in a shortening of fluorescence lifetime and hence NPQ [23].

The effect of epoxidized xanthophylls on NPQ has been studied in less detail [22–24]. In the present study, we explored the effect of various amounts of naturally present violaxanthin on NPQ in isolated *C. velia* light-harvesting (CLH) antenna complexes. The fluorescence lifetime measurements show a strong anti-correlation between the extent of NPQ and the violaxanthin to chlorophyll (Vio/Chl) ratio in these antennae. The inhibitory effect of violaxanthin on fluorescence quenching has been confirmed directly by an artificial mixing of additional violaxanthin with CLH antennae reducing NPQ. These data match the same anti-correlation observed in chlorophyll *a/b* antenna complexes isolated from higher plants [24]. We suggest that violaxanthin functions as an inhibitor of NPQ in *C. velia*, as has already been indicated in higher plants [24]. We propose that NPQ in *C. velia* requires not only violaxanthin de-epoxidation to zeaxanthin, but also removal of violaxanthin from the close vicinity of LHCs.

## Materials and methods

### Alga growth

The *C. velia* strain RM 12 originally isolated from the stony coral *Plesiastrea versipora* in Sydney Harbour [25],

was obtained from Professor M. Oborník (University of South Bohemia). The strain was grown at 28 °C in artificial seawater medium with supplementation of *f*/2 nutrients as described previously [14]. Cells were kept in aerated glass tubes in semi-continuous batch growth with 24 h of irradiation by fluorescence tubes ( $100 \mu\text{mol}\cdot\text{m}^{-2}\cdot\text{s}^{-1}$ ). All physiological measurements were performed with culture harvested in the late exponential phase.

### Chlorophyll fluorescence lifetime

Time-correlated single photon counting measurements were performed on a FluoTime 200 fluorometer (PicoQuant, Berlin, Germany) as described previously [22,26]. Excitation at a 10 MHz repetition rate was provided by a 470 nm laser diode, and its intensity was carefully adjusted to completely close all photosystem (PS)II reaction centers without causing photoinhibitory quenching of maximal variable fluorescence in the dark ( $F_M$ ) and to be far below the onset of singlet–singlet exciton annihilation. The instrumental response function was during the first 50 ps. Fluorescence was detected at 682 nm with a 2 nm slit width.

Native cells of *C. velia* were either treated with  $100 \mu\text{M}$   $\text{NH}_4\text{Cl}$  in the dark to completely inhibit NPQ, or kept untreated for 4 min under white light ( $300 \mu\text{mol}\cdot\text{m}^{-2}\cdot\text{s}^{-1}$ ) to induce NPQ. Fluorescence lifetimes of isolated CLH complexes were measured either in a light-harvesting state [ $800 \mu\text{M}$  *N*-dodecyl- $\beta$ -D-maltoside (DM), 20 mM Hepes, pH 7.8] or in a quenched state induced by a reduction in DM concentration ( $8 \mu\text{M}$  DM, pH 5.5). The same quenching yield was obtained when detergent was reduced by 3 min of incubation with  $80 \text{ mg}\cdot\text{mL}^{-1}$  Bio-Beads (SM-2; Bio-Rad, Hercules, CA, USA) in low pH (5.5) medium. Fluorescence lifetime decay kinetics were analyzed by FLUORFIT (PicoQuant) and chi-squared was used as a good-fit indicator. The intensity-weighted average lifetimes ( $\tau$ ) were used for further analysis. NPQ in native cells and in the light-harvesting antennae was calculated based on Stern–Volmer formalisms as  $\text{NPQ} = \tau/\tau' - 1$  where  $\tau'$  and  $\tau$  represent the intensity-weighted average lifetimes for a sample in the quenched and nonquenched states, respectively.

### 77K fluorescence

77K fluorescence emission spectra were measured using an Aminco–Bowman Series 2 spectrofluorometer (Thermo Fisher Scientific, Waltham, MA, USA) as described previously [27]. The excitation was at 435 nm with a 4 nm slit width.

### Isolation of *Chromera velia* antenna proteins

To isolate antenna complexes cells of *C. velia* (0.5 L with  $A_{750} = \sim 0.5$ ), cells were washed and resuspended in 1.5 mL of the working buffer containing 25 mM Hepes (pH 7.8).

The resuspended cells were mixed with 0.5 mL of glass beads (0.1–0.2 mm in diameter) in a 2 mL Eppendorf tube and broken using Mini-BeadBeater (BioSpec Products, Inc., Bartlesville, OK, USA) (eight shaking cycles, 10 s each with 2 min breaks for cooling the suspension on ice). Membranes were separated from the cell extract by centrifugation (40 000 *g* for 20 min) and solubilized with DM (2%, DM/chlorophyll = 20 w/w for 1 h on ice). Antenna proteins were isolated by ultracentrifugation (141 000 *g* for 18 h) in a 5–20% gradient of sucrose in the working buffer containing 0.04% DM. Obtained fractions from sucrose gradient were analyzed by Tricine-SDS-electrophoresis according to Schaegger [28].

### Pigment extraction and analysis

Pigment analysis of cells was carried out as described previously [14]. Pigment from protein complexes was extracted in 100% methanol, centrifuged and the supernatant used for HPLC analysis on a 1200 chromatography HPLC system (Agilent Technologies Inc., Santa Clara, CA, USA) and the eluted pigments were quantified at  $A_{440}$  [14,29].

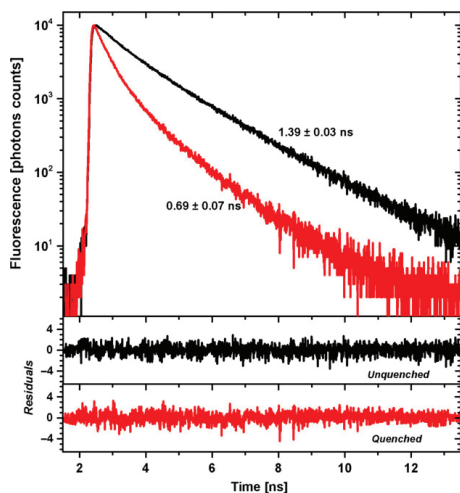


**Fig. 1.** Chlorophyll fluorescence lifetime decays of *Chromera velia*. The light harvesting state with maximal fluorescence  $F_M$  induced in the presence of 100  $\mu\text{M}$   $\text{NH}_4\text{Cl}$  is shown in black; the photoprotective quenched state induced by 5 min of treatment at 300  $\mu\text{mol}\cdot\text{m}^{-2}\cdot\text{s}^{-1}$  is shown red. The intensity weighted mean  $\pm$  SD fluorescence lifetime ( $n = 6$ ) is also shown. The panels with residuals display the difference between the three exponential fit and the experimental data used for estimation of average fluorescence lifetime.

## Results

### Fluorescence lifetime analysis in NPQ state in native cells of *Chromera velia*

NPQ in native *C. velia* cells was studied by fluorescence lifetime measurements. Fluorescence decay kinetics were measured under unquenched ( $F_M$  state, brought about by addition of  $\text{NH}_4\text{Cl}$ ) and quenched conditions induced by high light (Fig. 1). In both cases, three exponential decays were sufficient to optimally fit the experimental data (see minimal residual in Fig. 1). The intensity-weighted average lifetime ( $\tau$ ) thus obtained (see also Materials and methods) was then used for further analysis. Its value for *C. velia* cells in  $F_M$  state (i.e. nonquenched) was approximately 1.39 ns, which is comparable with that of diatoms [30] but somewhat shorter than values usually observed in *Arabidopsis* (~ 1.8–2 ns) [22,26]. High-light illumination shortened the fluorescence lifetime ( $\tau'$  at  $F_M'$  state) to approximately 0.69 ns as a result of the onset of NPQ in native cells [14]. The NPQ value (defined as  $\tau/\tau' - 1$ ; see also Materials and methods) in this experiment was 1.02 (Table 1), which is very close to the values previously reported in *C. velia* grown under similar conditions [29].

### Isolation and characterization of antenna complexes from *Chromera velia*

The LHCs of *C. velia* were isolated by DM solubilization of membranes followed by ultracentrifugation on a sucrose density gradient (Fig. 2). Photosynthetic complexes separated into three main bands: top (fractions 1–3), middle (PSI, PSII supercomplexes, supercomplexes – S.C.) and low (PSI with bound antenna complexes, PSI-LHCr); see Tichy *et al.* [31]. Three upper fractions (fractions 1–3 of Fig. 2) were further characterized by SDS/PAGE (Fig. 2B) and by spectroscopy (Figs S1 and S2). The CLH proteins described previously (with molecular weights in the range 19–25 kDa) [31,32] were found to be dominant in all three fractions (see asterisk in Fig. 2B). Absorption and 77K fluorescence spectroscopy (Figs S1 and S2) further supported the identification of fractions 1–3 as antenna complexes.

The pigment composition of fractions 1–3 was determined by HPLC. This analysis revealed the presence of three main pigments for this alga [14,29]: chlorophyll *a* (approximately 50%), isofucoxanthin (approximately 30%) and violaxanthin (approximately 10%) (Table 2). There was no zeaxanthin detected because we used dark-adapted cells to avoid de-epoxidation of violaxanthin into zeaxanthin [14]. The relative concentration of

**Table 1.** Comparison of average fluorescence lifetimes from *Chromera vera* live cells and isolated antenna fractions at  $F_M$  and  $F_M'$ .

	Fraction 1	Fraction 2	Fraction 3	Cells
$\tau_{\text{unquenched}}$ (ns)	$3.90 \pm 0.02$	$3.59 \pm 0.02$	$3.58 \pm 0.02$	$1.39 \pm 0.03$
$\tau_{\text{quenched}}$ (ns)	$2.39 \pm 0.11$	$1.82 \pm 0.09$	$1.43 \pm 0.09$	$0.69 \pm 0.07$
NPQ	$0.63 \pm 0.08$	$0.97 \pm 0.10$	$1.51 \pm 0.16$	$1.02 \pm 0.22$

Detergent-solubilized antenna complexes were separated on a sucrose density gradient, harvested and measured in  $F_M$  and  $F_M'$  states.  $\tau_{\text{unquenched}}$  represents the light harvesting state at high DM concentration (800  $\mu\text{M}$  DM, pH 7.5), whereas  $\tau_{\text{quenched}}$  is the photoprotective quenched state induced by removal of DM with Bio-Beads, and acidification (pH 5.5).  $\tau_{\text{unquenched}}$  in native cells reflects the light harvesting state with maximal fluorescence  $F_M$  induced by 100  $\mu\text{M}$   $\text{NH}_4\text{Cl}$ , whereas  $\tau_{\text{quenched}}$  is the photoprotective quenched state after 5 min under 300  $\mu\text{mol}\cdot\text{m}^{-2}\cdot\text{s}^{-1}$  light. The intensity weighted fluorescence lifetime represents the mean  $\pm$  SD ( $n = 6$ ). The NPQ value was defined as  $\tau/\tau' - 1$  (see also Materials and methods).

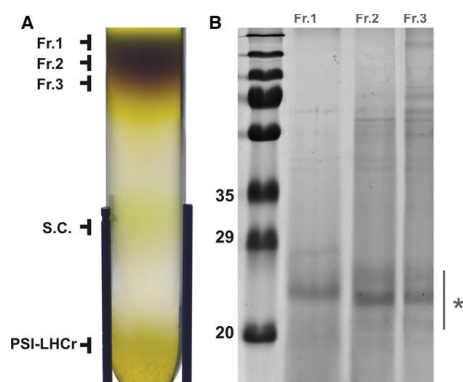


**Fig. 2.** Isolation and characterization of light-harvesting antenna complexes of *Chromera velia*. (A) Sucrose gradient (5–20%) separation of light-harvesting complexes (fractions 1–3) from PSI and II supercomplexes (S.C.) and PSI-LHCr band. (B) SDS/PAGE of fractions 1–3 from (A). Molecular weights of used standards are marked; the typical position of *Chromera* light harvesting proteins is indicated by an asterisk.

chlorophyll *a* and isofucoaxanthin was similar in all three fractions. By contrast, the concentration of violaxanthin varied significantly (Table 2 and Fig. S3). The data clearly showed that fraction 1 was enriched by violaxanthin and also that its abundance was lower in fraction 2 and further decreased in fraction 3 (Table 2). These differing amounts of violaxanthin in the three antennae fractions enabled us to study the effect of violaxanthin on NPQ in CLH antenna complexes.

#### NPQ in the isolated antenna complexes is inhibited by violaxanthin content

NPQ in isolated complexes of *C. velia* was measured by fluorescence lifetimes decays (Fig. 3). The intensity-weighted average fluorescence lifetime ( $\tau$ ) of CLH

**Table 2.** Relative pigment content in intact cells of *C. velia* and in their isolated light-harvesting antenna complexes (fractions 1–3).

	Chlorophyll <i>a</i> /total pigment (molar ratio, %)	Violaxanthin/chlorophyll <i>a</i> (molar ratio, %)	Isofucoxanthin/chlorophyll <i>a</i> (molar ratio, %)	$\beta$ -carotene/chlorophyll <i>a</i> (molar ratio, %)
Fraction 1	$50.1 \pm 1.2$	$33.6 \pm 0.8$	$64.7 \pm 2.9$	$1.2 \pm 0.8$
Fraction 2	$54.2 \pm 1.0$	$20.5 \pm 0.5$	$63.2 \pm 2.7$	$0.8 \pm 0.1$
Fraction 3	$56.3 \pm 0.2$	$17.1 \pm 0.2$	$59.9 \pm 0.3$	$0.5 \pm 0.4$
Cells	42.4	57.9	71.5	6.4

Pigments were extracted from cells and antenna fractions with methanol, separated and quantified by HPLC. Data represent the molar ratio pigment content relative to total pigments or to total chlorophyll *a* (see description). Pigment analysis and protein isolation were performed in dark-adapted cells; therefore, no zeaxanthin has been detected [14].

complexes in a nonquenched state (high DM concentration) was approximately 3.9 ns for fraction 1 or 3.6 ns for fractions 2 and 3 (Table 1). Solubilization of antenna complexes therefore induced an increase in the fluorescence lifetime ( $F_M$ ) by more than three-fold compared to the native state, ranging from 1.4 to 3.6–3.9 ns (Fig. 1). A similar increase in fluorescence lifetime in detergent-solubilized antennae was shown for antenna complexes from higher plants or diatoms [26,30]; this was rationalized by antennae aggregation *in vivo* that is minimal in the detergent-solubilized system [26] or by antennae perturbations as a result of a detergent-aqueous environment [33,34]. Quenching of the antenna fractions was induced *in vitro* using a method described previously [35–37] (Fig. S4). The CLH complexes in a quenched state possessed a reduced fluorescence lifetime. The lifetime in the quenched state was different for all three antenna complexes, which was also reflected by different levels of NPQ calculated from the lifetimes (Table 1). To

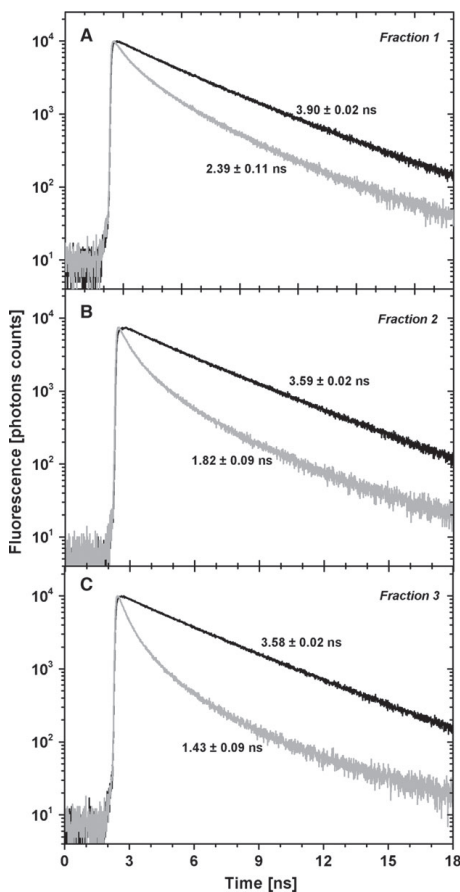


**Fig. 3.** Chlorophyll fluorescence lifetime decays in different light-harvesting complexes of *Chromera velia*. The light harvesting (unquenched) state (in the presence of 800  $\mu\text{M}$  DM, pH 7.5) is shown in black; the photoprotective (quenched) state (in the presence of low DM after treatment with Bio-Beads, pH 5.5) is shown in grey. Panel A, B and C represent chlorophyll fluorescence lifetime decays of isolated antennae protein complexes from fraction 1, 2 and 3 respectively (see Fig. 1 and Table 2 for their protein and pigment composition). The intensity weighted mean  $\pm$  SD fluorescence lifetime of each decay ( $n = 6$ ) is also shown.

understand the origin of these changes, NPQ in fractions 1–3 was compared with the relative violaxanthin content. The NPQ value for particular CLH fractions (Table 1) was plotted over the relative concentration of violaxanthin (Table 2) and this relationship is shown in Fig. 4. There was a clear decrease in NPQ

with an increasing concentration of violaxanthin (Fig. 4). The higher concentration of violaxanthin in CLH from fraction 1 resulted in a smaller NPQ and vice versa. This result indicates the inhibitory effect of violaxanthin on NPQ in native light-harvesting proteins of *C. velia*. The inhibitory effect of violaxanthin on NPQ has also been confirmed directly by the artificial addition of 5  $\mu\text{M}$  violaxanthin into isolated CLH antennae (Fig. 4, insert). The additional violaxanthin reduced the observed NPQ by approximately 35%. The effect observed in *C. velia* CLH with naturally high violaxanthin has been explored further, and the data obtained (Tables 1 and 2) were compared with the inhibitory effect of violaxanthin on NPQ in LHCs from higher plants (LHCII antennae) [24]. All of these data taken together show a similar relationship between violaxanthin content and NPQ: antenna complexes with a relatively higher violaxanthin concentration had a smaller NPQ. This nonlinear correlation is valid for both violaxanthin when artificially added just before the NPQ measurements (see LHCII data in Ruban *et al.* [24]), as well as for violaxanthin in native CLH antenna complexes from *C. velia* containing variable amounts of violaxanthin [14,29]. These data allow us to suggest that violaxanthin has an inhibitory effect on NPQ in *C. velia*, and they also indicate that the maximum NPQ *in vivo* requires the removal of violaxanthin from the protein moiety.

## Discussion

*Chromera velia* represents a simple photosynthetic model system with light-harvesting antennas lacking accessory chlorophylls [29]. This alga is photoprotected by NPQ triggered by lumen acidification and amplified by a fast violaxanthin de-epoxidation into zeaxanthin [14]. In the present study, we have shown that the formation of NPQ *in vivo* results in a shortening of the chlorophyll fluorescence lifetime of cells from 1.39 ns to 0.69 ns (Table 1), which is representative of lifetimes not far from those displayed *in vivo* by higher plants [26]. NPQ in *C. velia* appears to have some features similar to higher plants. It has already been shown to comprise a  $\Delta\text{pH}$ -dependent process [14]; in the present study, we show that fluorescence quenching in CLH complexes can be induced by a decrease in the amount of detergent *in vitro* and by acidification (Fig. 4, insert, and Fig. S4). To resolve the particular importance of these NPQ triggering conditions (low pH, low detergent concentration), more detailed experiments are required because the effects are not fully separate; the decrease in detergent/protein ratio is able to increase the sensitivity of pH-induced quenching [37]. It is also

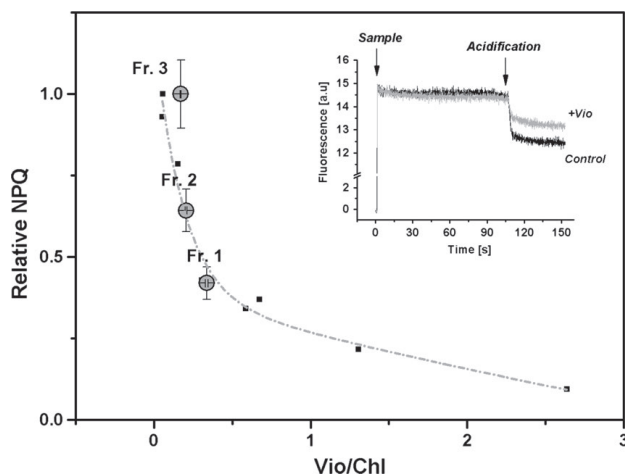


**Fig. 4.** The relative inhibition of chlorophyll fluorescence quenching in isolated antenna complexes by violaxanthin. Black points represent inhibition of chlorophyll fluorescence quenching in isolated LHCIIb from spinach [24] when violaxanthin was added to the incubation medium before the addition of LHCII. Grey cycles represent the same inhibition of quenching in light-harvesting antennas complexes isolated from *Chromera velia*, fractions 1–3 (for their NPQ, see Fig. 2 and Table 1). Violaxanthin from light-harvesting antennas of *C. velia* represent its native fraction detected after sucrose gradient isolation (Table 2). For a comparison of LHCIIb complexes with the high capacity of photoprotection (maximal NPQ = 3.5) [24] with *C. velia* antennas of much lower NPQ (NPQ = 1.51) (Table 1), the presented NPQ is relative with normalization to the NPQ maxima at low Vio/Chl. The insert present the inhibitory effect of free violaxanthin on NPQ in isolated CLH fraction no. 1. Quenching was induced by injection of CHL complexes in a buffer (pH 7.8) containing low detergent (6  $\mu\text{M}$  final concentration DM) (left arrow). The second arrow indicates the time when the pH of the medium was changed from 7.8 to 5.5 by the addition of small drops of HCl (see acidification). The black line represent control samples (no violaxanthin addition, see 'Control'); the gray line represents the antenna sample previously mixed with additional violaxanthin (5  $\mu\text{M}$  final concentration). Data represent typical curves (for more data, see Fig. S5). Violaxanthin was purified as described in the Supporting information (Data S1).

worth checking for the presence of protonable residues in CLH, as already shown for higher plant LHCs [35,38].

We have demonstrated an inhibitory effect of artificially added violaxanthin on NPQ in isolated CLH antennae (Fig. 4, insert). The data are in line with previous experiments carried out with LHCII antennae of higher plants [24,39]. The same inhibitory effect has been also shown in isolated CLH antennae of *C. velia*, which were naturally rich in violaxanthin (the Vio/Chl ratio varies between 1 : 3 in the cells grown in high light to 1 : 4 in those grown in low light) [29] (Fig. 4). The high carotenoid content in CLH antennae (Table 2) resembles the carotenoid-rich FCP antennae from diatoms [40] and contrasts with plant LHCII antenna where the amount of carotenoid including violaxanthin is lower [41]. In plants, the tight binding of violaxanthin to a specific binding site of antenna complexes (CP29 complex) strongly limits the rate of violaxanthin de-epoxidation [42]. It is also responsible for the restriction of maximal violaxanthin conversion to

zeaxanthin, which, in plants, can typically reach up to 70% [41]. We note that, even though the maximal de-epoxidation in *C. velia* is rather small if calculated in relative values (approximately 40% of violaxanthin is de-epoxidized to zeaxanthin) [14], the absolute amount of zeaxanthin formed on light is high as a result of the much higher violaxanthin content in dark-adapted *C. velia* cells [14].

In higher plant antenna complexes, three putative violaxanthin binding sites (V1, N1 and L2) have been identified [43–45]. They are different in their affinity for violaxanthin, with loosely-bound violaxanthin situated on the antennae periphery [44]. However, the binding of two out of three of the sites appears to be an artifact as a result of reconstitution (e.g. see crystal structure data [46]; work on mutagenesis [47]; and density functional theory studies [48]) because violaxanthin binds exclusively to site V1 native LHCII. Both the number and the binding sites of violaxanthin in CLH antennae are not known. However, the homology of all light-harvesting antenna complexes would



indicate the presence of several binding sites with various affinities for violaxanthin and also for CLH antennae of *C. velia*. Indeed, violaxanthin has the lowest interaction strength among all of the other carotenoids [44] and the existence of loosely-bound violaxanthin in CLH antennae has been discussed previously [49]. These loosely-bound violaxanthin molecules are most likely situated on the protein periphery, where they are in equilibrium with the lipid phase. This could result in the antennae nonbound violaxanthin that has been already observed in lipid phase of *C. velia* thylakoids [50], which makes *C. velia* similar to diatoms where the lipid-phase xanthophyll (diadinoxanthin) has been already identified [51]. The presence of protein unbound violaxanthin in the antennae of higher plants is still questionable and requires further research [52,53]. In *C. velia*, the lipid-phase violaxanthin could be the cause of the fast rate of violaxanthin de-epoxidation to zeaxanthin [14] because the liberation of violaxanthin from antennae is considered to be the main limiting step of violaxanthin de-epoxidation in plants [54]. In the present study, we propose an additional role of the loosely/weakly protein-bound violaxanthin molecules in *C. velia* thylakoids; we suggest that the action of the violaxanthin fraction in NPQ inhibition *in vivo* is similar to that observed in isolated antenna of *C. velia* (Fig. 4).

The effect of violaxanthin on NPQ in CLH and in LHClI antenna [24,39] has been compared (Fig. 4). By plotting the data together, we identified a common relationship between the Vio/Chl ratio and NPQ in these two different types of antennae; in both cases, the lower the concentration of violaxanthin present, the higher is the observed NPQ, and the relationship can be fitted by a nonlinear exponential decay (Fig. 4). Therefore, the inhibitory effect of violaxanthin on NPQ that we showed in CLH antennae could be a general phenomenon for chlorophyll-binding antennas. Indeed, it was also recently proposed for brown algae [55]. This would indicate that maximal NPQ requires not only violaxanthin de-epoxidation to zeaxanthin, but also the removal of violaxanthin from the vicinity of the protein. However, to validate this hypothesis, more direct *in vitro* experiments using isolated antennae from different species are required.

We do not know the precise molecular mechanism by which violaxanthin affects light-harvesting protein efficiency and inhibits NPQ efficiency in the CLH antennae of *C. velia* (Fig. 4). Violaxanthin has been recognized as a modulator that can also trigger structural changes in the antenna complexes [22,23]. Violaxanthin and zeaxanthin differ markedly in their apparent polarity, as determined empirically by their

tendency to form aggregates in water/ethanol mixtures [56]. It has also been proposed previously [23] that hydrophilic xanthophylls such as violaxanthin make the protein structure less dehydrated and thus less compressed; this state could prevent the formation of closer chlorophyll–chlorophyll or chlorophyll–xanthophyll interactions and thus inhibit the quenching of excited states. Indeed, the extent of quenching could be further affected by other factors (e.g. an effect of aggregation or a different oligomeric state on NPQ) [57–59]. A similar effect has already been proposed for NPQ in light-harvesting antenna from diatoms [60]. However, to study this phenomenon, new experiments are required with a more detailed biochemical analysis. Although the molecular mechanism of the effect of violaxanthin on NPQ is still unknown, it is clear that maximal NPQ in light-harvesting antenna complexes requires more than high zeaxanthin formation. We suggest that the removal of violaxanthin or other hydrophilic xanthophylls (diatoxanthin) from the vicinity of the protein is necessary for stimulation of NPQ.

## Acknowledgements

This research project was supported by the Czech Science Foundation (project GACR P501-12-G055) and by institutional project Algatech Plus (MSMT LO1416) provided by the Czech Ministry of Education, Youth and Sport. AVR would like to acknowledge the grants from The Leverhulme Trust and UK Biotechnology and Biological Sciences Research Council and The Royal Society for the Wolfson Research Merit Award. JK was supported by project Algain (EE2.3.30.0059). We thank Eva Žišková for technical assistance and Jan Pilný for help with violaxanthin isolation.

## Author contributions

RK designed the study, wrote the paper, performed fluorescence lifetime measurements and data analysis and supervised the paper. AVR designed the study; he was involved in intensive results discussion and in the paper corrections. EK and EB carried out biophysical measurements, data analysis, and paper corrections. JK, ET and RS purified antennae proteins and characterized them biochemically. All authors discussed the results and commented on the manuscript.

## References

- 1 Kaňa R and Vass I (2008) Thermoimaging as a tool for studying light-induced heating of leaves correlation of

- heat dissipation with the efficiency of photosystem II photochemistry and non-photochemical quenching. *Environ Exp Bot* **64**, 90–96.
- 2 Ruban AV, Johnson MP and Duffy CDP (2012) The photoprotective molecular switch in the photosystem II antenna. *Biochim Biophys Acta* **1817**, 167–181.
  - 3 Croce R and van Amerongen H (2014) Natural strategies for photosynthetic light harvesting. *Nat Chem Biol* **10**, 492–501.
  - 4 Kirilovsky D, Kana R and Prášil O (2014) Mechanisms modulating energy arriving at reaction centers in cyanobacteria. In *Non-Photochemical Quenching and Thermal Energy Dissipation In Plants, Algae and Cyanobacteria in press* (Demmig-Adams B, Adams W, Garab G and Govindjee, eds), pp. 471–501. Springer, Dordrecht, Netherlands.
  - 5 Kaňa R, Kotabová E, Sobotka R and Prášil O (2012) Non-photochemical quenching in cryptophyte alga *Rhodomonas salina* is located in chlorophyll a/c antennae. *PLoS One* **7**, e29700.
  - 6 Stalleva H, Komenda J, Shukla MK, Slouf V, Kana R, Polivka T and Sobotka R (2015) Mechanism of photoprotection in the cyanobacterial ancestor of plant antenna proteins. *Nat Chem Biol* **11**, 287–291.
  - 7 Li XP, Bjorkman O, Shih C, Grossman AR, Rosenquist M, Jansson S and Niyogi KK (2000) A pigment-binding protein essential for regulation of photosynthetic light harvesting. *Nature* **403**, 391–395.
  - 8 Bonente G, Ballottari M, Truong TB, Morosinotto T, Ahn TK, Fleming GR, Niyogi KK and Bassi R (2011) Analysis of LhcSR3, a protein essential for feedback de-excitation in the green alga *Chlamydomonas reinhardtii*. *PLoS Biol* **9**, e1000577.
  - 9 Alboresi A, Gerotto C, Giacometti GM, Bassi R and Morosinotto T (2010) *Physcomitrella patens* mutants affected on heat dissipation clarify the evolution of photoprotection mechanisms upon land colonization. *Proc Natl Acad Sci USA* **107**, 11128–11133.
  - 10 Bailleul B, Rogato A, de Martino A, Coesel S, Cardol P, Bowler C, Falcitore A and Finazzi G (2010) An atypical member of the light-harvesting complex stress-related protein family modulates diatom responses to light. *Proc Natl Acad Sci USA* **107**, 18214–18219.
  - 11 Niyogi KK, Bjorkman O and Grossman AR (1997) The roles of specific xanthophylls in photoprotection. *Proc Natl Acad Sci USA* **94**, 14162–14167.
  - 12 Demmig-Adams B (1990) Carotenoids and photoprotection in plants: a role for the xanthophyll zeaxanthin. *Biochim Biophys Acta* **1020**, 1–24.
  - 13 Lavaud J, Rousseau B, van Gorkom HJ and Etienne AL (2002) Influence of the diadinoxanthin pool size on photoprotection in the marine planktonic diatom *Phaeodactylum tricoratum*. *Plant Physiol* **129**, 1398–1406.
  - 14 Kotabová E, Kana R, Jaresova J and Prasil O (2011) Non-photochemical fluorescence quenching in *Chromera velia* is enabled by fast violaxanthin de-epoxidation. *FEBS Lett* **585**, 1941–1945.
  - 15 Obornik M and Lukes J (2013) Cell biology of chromerids: autotrophic relatives to apicomplexan parasites. In *International Review of Cell and Molecular Biology*, Vol 306 (Jeon KW, ed.), pp. 333–369. Elsevier Academic Press Inc., San Diego, CA.
  - 16 Cheregi O, Kotabová E, Prášil O, Schröder WP, Kaňa R and Funk C (2015) Presence of state transitions in the cryptophyte alga *Guillardia theta*. *J Exp Bot* **66**, 6461–6470.
  - 17 Krupnik T, Kotabová E, van Bezouwen LS, Mazur R, Garstka M, Nixon PJ, Barber J, Kaňa R, Boekema EJ and Kargul J (2013) A reaction centre-dependent photoprotection mechanism in a highly robust photosystem II from an extremophilic red alga *Cyanidioschyzon merolae*. *J Biol Chem* **288**, 23529–23542.
  - 18 Kaňa R, Kotabová E, Lukeš M, Papáček Š, Matonoha C, Liu L-N, Prášil O and Mullineaux CW (2014) Phycobilisome mobility and its role in the regulation of light harvesting in red algae. *Plant Physiol* **165**, 1618–1631.
  - 19 Ahn TK, Avenson TJ, Ballottari M, Cheng YC, Niyogi KK, Bassi R and Fleming GR (2008) Architecture of a charge-transfer state regulating light harvesting in a plant antenna protein. *Science* **320**, 794–797.
  - 20 Ruban AV and Horton P (1999) The xanthophyll cycle modulates the kinetics of nonphotochemical energy dissipation in isolated light-harvesting complexes, intact chloroplasts, and leaves of spinach. *Plant Physiol* **119**, 531–542.
  - 21 Xu P, Tian L, Kloz M and Croce R (2015) Molecular insights into Zeaxanthin-dependent quenching in higher plants. *Sci Rep*, doi:10.1038/srep13679.
  - 22 Johnson MP, Zia A, Horton P and Ruban AV (2010) Effect of xanthophyll composition on the chlorophyll excited state lifetime in plant leaves and isolated LHClI. *Chem Phys* **373**, 23–32.
  - 23 Ruban AV and Johnson MP (2010) Xanthophylls as modulators of membrane protein function. *Arch Biochem Biophys* **504**, 78–85.
  - 24 Ruban AV, Young A and Horton P (1994) Modulation of chlorophyll fluorescence quenching in isolated light-harvesting complex of photosystem-II. *Biochim Biophys Acta* **1186**, 123–127.
  - 25 Moore RB, Obornik M, Janouskovec J, Chrudimsky T, Vancova M, Green DH, Wright SW, Davies NW, Bolch CJS, Heimann K *et al.* (2008) A photosynthetic alveolate closely related to apicomplexan parasites. *Nature* **451**, 959–963.



- 26 Belgio E, Johnson MP, Juric S and Ruban AV (2012) Higher plant photosystem II light-harvesting antenna, not the reaction center, determines the excited-state lifetime-both the maximum and the nonphotochemically quenched. *Biophys J* **102**, 2761–2771.
- 27 Kaňa R, Prášil O, Komárek O, Papageorgiou GC and Govindjee (2009) Spectral characteristic of fluorescence induction in a model cyanobacterium, *Synechococcus* sp (PCC 7942). *Biochim Biophys Acta* **1787**, 1170–1178.
- 28 Schaegger H (2006) Tricine-SDS-PAGE. *Nat Protoc* **1**, 16–22.
- 29 Quigg A, Kotabova E, Jaresova J, Kana R, Setlik J, Sediva B, Komarek O and Prasil O (2012) Photosynthesis in *Chromera velia* represents a simple system with high efficiency. *PLoS One* **7**, e47036.
- 30 Miloslavina Y, Grouneva I, Lambrev PH, Lepetit B, Goss R, Wilhelm C and Holzwarth AR (2009) Ultrafast fluorescence study on the location and mechanism of non-photochemical quenching in diatoms. *Biochim Biophys Acta* **1787**, 1189–1197.
- 31 Tichy J, Gardian Z, Bina D, Konik P, Litvin R, Herbstova M, Pain A and Vacha F (2013) Light harvesting complexes of *Chromera velia*, photosynthetic relative of apicomplexan parasites. *Biochim Biophys Acta* **1827**, 723–729.
- 32 Kotabova E, Jaresova J, Kaňa R, Sobotka R, Bina D and Prasil O (2014) Novel type of red-shifted chlorophyll a antenna complex from *Chromera velia*. I. Physiological relevance and functional connection to photosystems. *Biochim Biophys Acta* **1837**, 734–743.
- 33 Akhtar P, Dorogi M, Pawlak K, Kovács L, Bóta A, Kiss T, Garab G and Lambrev PH (2015) Pigment interactions in light-harvesting complex II in different molecular environments. *J Biol Chem* **290**, 4877–4886.
- 34 Belgio E, Tumino G, Santabarbara S, Zucchelli G and Jennings R (2012) Reconstituted CP29: multicomponent fluorescence decay from an optically homogeneous sample. *Photosynth Res* **111**, 53–62.
- 35 Belgio E, Duffy CDP and Ruban AV (2013) Switching light harvesting complex II into photoprotective state involves the lumen-facing apoprotein loop. *Phys Chem Chem Phys* **15**, 12253–12261.
- 36 Wentworth M, Ruban AV and Horton P (2000) Chlorophyll fluorescence quenching in isolated light harvesting complexes induced by zeaxanthin. *FEBS Lett* **471**, 71–74.
- 37 Petrou K, Belgio E and Ruban AV (2014) pH sensitivity of chlorophyll fluorescence quenching is determined by the detergent/protein ratio and the state of LHClI aggregation. *Biochim Biophys Acta* **1837**, 1533–1539.
- 38 Walters RG, Ruban AV and Horton P (1994) Higher-plant light-harvesting complexes LHClIa and LHClIc are bound by dicyclohexylcarbodiimide during inhibition of energy-dissipation. *Eur J Biochem* **226**, 1063–1069.
- 39 Ruban AV, Young AJ and Horton P (1996) Dynamic properties of the minor chlorophyll a/b binding proteins of photosystem II, an in vitro model for photoprotective energy dissipation in the photosynthetic membrane of green plants. *Biochemistry* **35**, 674–678.
- 40 Joshi-Deo J, Schmidt M, Gruber A, Weisheit W, Mittag M, Kroth PG and Buechel C (2010) Characterization of a trimeric light-harvesting complex in the diatom *Phaeodactylum tricoratum* built of FcpA and FcpE proteins. *J Exp Bot* **61**, 3079–3087.
- 41 Ruban AV, Young AJ, Pascal AA and Horton P (1994) The effects of illumination on the xanthophyll composition of the photosystem-II light-harvesting complexes of spinach thylakoid membranes. *Plant Physiol* **104**, 227–234.
- 42 Jahns P, Latowski D and Strzalka K (2009) Mechanism and regulation of the violaxanthin cycle: the role of antenna proteins and membrane lipids. *Biochim Biophys Acta* **1787**, 3–14.
- 43 Jahns P, Wehner A, Paulsen H and Hobe S (2001) De-epoxidation of violaxanthin after reconstitution into different carotenoid binding sites of light-harvesting complex II. *J Biol Chem* **276**, 22154–22159.
- 44 Ruban AV, Lee PJ, Wentworth M, Young AJ and Horton P (1999) Determination of the stoichiometry and strength of binding of xanthophylls to the photosystem II light harvesting complexes. *J Biol Chem* **274**, 10458–10465.
- 45 Wehner A, Grasses T and Jahns P (2006) De-epoxidation of violaxanthin in the minor antenna proteins of photosystem II, LHCB4, LHCB5, and LHCB6. *J Biol Chem* **281**, 21924–21933.
- 46 Liu ZF, Yan HC, Wang KB, Kuang TY, Zhang JP, Gui LL, An XM and Chang WR (2004) Crystal structure of spinach major light-harvesting complex at 2.72 angstrom resolution. *Nature* **428**, 287–292.
- 47 Lokstein H, Tian L, Polle JEW and DellaPenna D (2002) Xanthophyll biosynthetic mutants of *Arabidopsis thaliana*: altered nonphotochemical quenching of chlorophyll fluorescence is due to changes in Photosystem II antenna size and stability. *Biochim Biophys Acta* **1553**, 309–319.
- 48 Duffy CDP and Ruban AV (2012) A theoretical investigation of Xanthophyll-protein hydrogen bonding in the photosystem II antenna. *J Phys Chem B* **116**, 4310–4318.
- 49 Bina D, Gardian Z, Herbstova M, Kotabova E, Konik P, Litvin R, Prasil O, Tichy J and Vacha F (2014) Novel type of red-shifted chlorophyll a antenna complex from *Chromera velia*: II. Biochemistry and spectroscopy. *Biochim Biophys Acta* **1837**, 802–810.
- 50 Mann M, Hoppenz P, Jakob T, Weisheit W, Mittag M, Wilhelm C and Goss R (2014) Unusual features of the

- high light acclimation of *Chromera velia*. *Photosynth Res* **122**, 159–169.
- 51 Lepetit B, Volke D, Gilbert M, Wilhelm C and Goss R (2010) Evidence for the existence of one antenna-associated, lipid-dissolved and two protein-bound pools of diadinoxanthin cycle pigments in diatoms. *Plant Physiol* **154**, 1905–1920.
- 52 Hartel H, Lokstein H, Grimm B and Rank B (1996) Kinetic studies on the xanthophyll cycle in barley leaves - Influence of antenna size and relations to nonphotochemical chlorophyll fluorescence quenching. *Plant Physiol* **110**, 471–482.
- 53 Dall'Osto L, Cazzaniga S, Havaux M and Bassi R (2010) Enhanced photoprotection by protein-bound vs free xanthophyll pools: a comparative analysis of chlorophyll b and xanthophyll biosynthesis mutants. *Mol Plant* **3**, 576–593.
- 54 Morosinotto T, Caffarri S, Dall'Osto L and Bassi R (2003) Mechanistic aspects of the xanthophyll dynamics in higher plant thylakoids. *Physiol Plant* **119**, 347–354.
- 55 Ocampo-Alvarez H, Garcia-Mendoza E and Govindjee (2013) Antagonist effect between violaxanthin and de-epoxidated pigments in nonphotochemical quenching induction in the qE deficient brown alga *Macrocystis pyrifera*. *Biochim Biophys Acta* **1827**, 427–437.
- 56 Ruban AV, Horton P and Young AJ (1993) Aggregation of higher-plant xanthophylls – differences in absorption-spectra and in the dependency on solvent polarity. *J Photochem Photobiol B* **21**, 229–234.
- 57 Holzwarth AR, Miloslavina Y, Nilkens M and Jahns P (2009) Identification of two quenching sites active in the regulation of photosynthetic light-harvesting studied by time-resolved fluorescence. *Chem Phys Lett* **483**, 262–267.
- 58 Belgio E, Kapitonova E, Chmeliov J, Duffy CDP, Ungerer P, Valkunas L and Ruban AV (2014) Economic photoprotection in photosystem II that retains a complete light-harvesting system with slow energy traps. *Nat Commun* **5**, article number: 4433.
- 59 Ware MA, Giovagnetti V, Belgio E and Ruban AV (2015) PsbS protein modulates non-photochemical chlorophyll fluorescence quenching in membranes depleted of photosystems. *J Photochem Photobiol B*, **152**, 301–307.
- 60 Büchel C (2014) Fucoxanthin-chlorophyll-proteins and non-photochemical fluorescence quenching of diatoms. In *Non-Photochemical Quenching and Energy Dissipation in Plants, Algae and Cyanobacteria* (Demmig-Adams B, Garab G, Adams W III and Govindjee, eds), pp. 259–275. Springer, Netherlands.

## Supporting information

Additional Supporting Information may be found online in the supporting information tab for this article:

**Fig. S1.** Absorbance spectrum of isolated antenna protein fractions from *C. velia*.

**Fig. S2.** *K* fluorescence emission spectra of fractions from sucrose gradient.

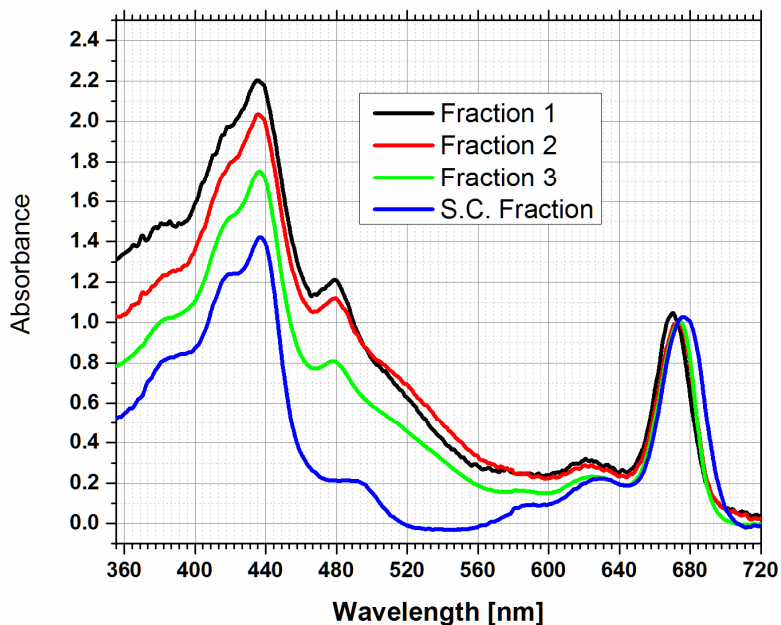
**Fig. S3.** Bar chart showing the different violaxanthin/chlorophyll *a* molar ratio in distinct antenna fractions.

**Fig. S4.** Scheme showing the procedure for inducing quenching of antenna complexes from *C. velia*.

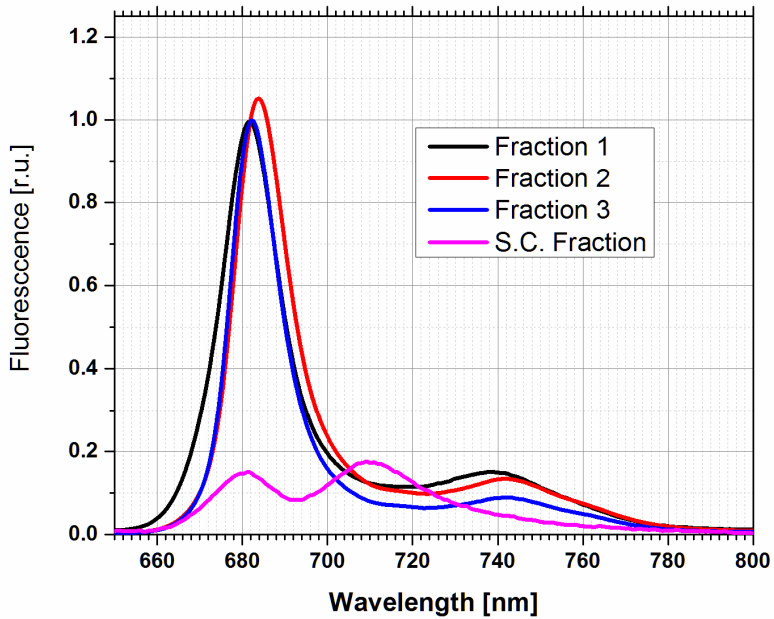
**Fig. S5.** Inhibitory effect of free violaxanthin on NPQ in isolated CLH fraction no. 1.

**Data S1.** Supplementary materials and methods.

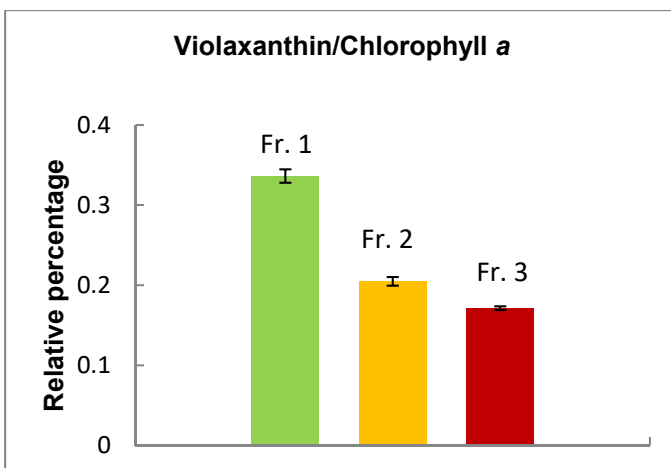
## Supplementary figures:



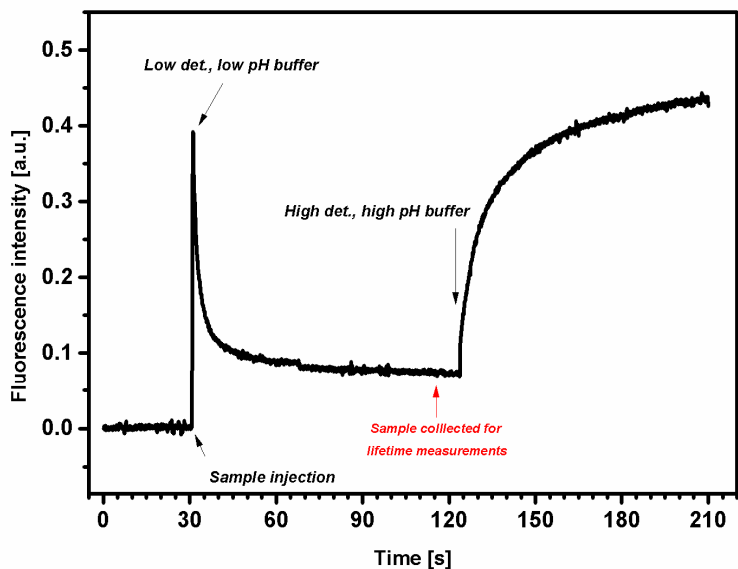
**Supplementary Figure 1: Absorbance spectrum of isolated antenna protein fractions from *Chromera velia*.** Protein fractions were isolated from sucrose gradient (see Figure 2) CLH Fraction 1,2, 3, and Supercomplex fraction. Spectra are normalised at 670 nm.



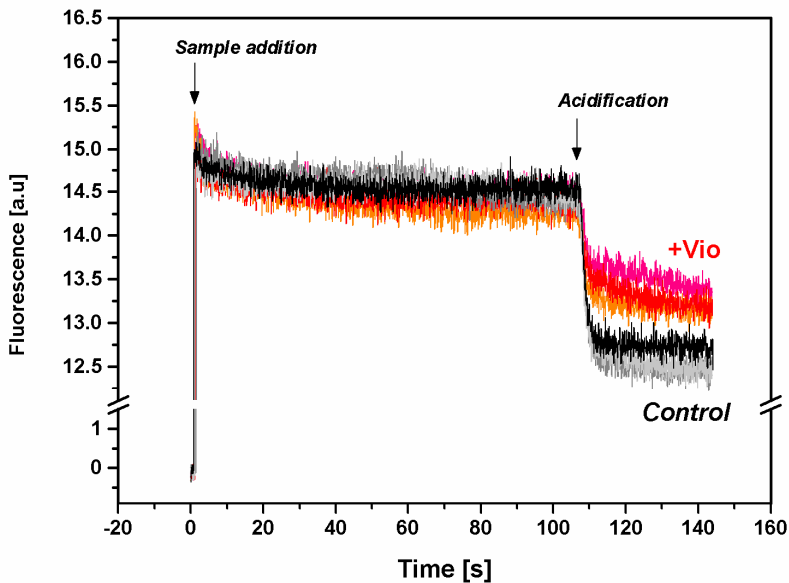
**Supplementary Figure 2: 77 K fluorescence emission spectra of fractions from sucrose gradient.** Light-harvesting antennae fractions 1, 2, and 3 (normalised to the maximum ~ 685 nm) together with Supercomplex band (S.C. – fraction). Excitation was 457 nm. Same spectra were obtained with 425 nm excitation.



**Supplementary Figure 3: Bar chart showing the different violaxanthin/chlorophyll *a* molar ratio in distinct antenna fractions.** Antenna fractions were isolated from sucrose gradients, as shown in Figure 2. Pigment extraction was done in 80% methanol, followed by quantification via HPLC.



**Supplementary Figure 4: Scheme showing the procedure for inducing quenching of antenna complexes from *Chromera velia*.** Quenching was induced by injection of CHL complexes in a buffer containing low detergent (8  $\mu\text{M}$  final concentration DM) and low pH (5.5). At steady state, sample where collected and immediately used for lifetime measures (see the red arrow). Quenching was completely reversible by high detergent, high pH buffer (800  $\mu\text{M}$  DM, pH 7.8). Sample integrity was verified by absorption/fluorescence spectroscopy throughout the entire process.



**Supplementary Figure 5.** Inhibitory effect of free violaxanthin on non-photochemical quenching in isolated CLH fraction no. 1. Quenching was induced by injection of CHL complexes in a buffer (pH 7.8) containing low detergent (6  $\mu\text{M}$  final concentration DM), see left arrow). The second arrow indicates the time when the pH of the medium was changed from 7.8 to 5.5 by addition of small drops of HCl (see acidification). Gray lines represent control samples (no violaxanthin addition, see “Control”), colored lines represents antenna sample previously mixed with additional violaxanthin (final concentration 5  $\mu\text{M}$ ). Violaxanthin was purified as it is described in supplementary materials.

## Supplementary methods

### Preparation of pure violaxanthin

Violaxanthin was purified from *Chromera velia* cells (strain RM 12) grown in an artificial seawater medium supplemented with f/2 nutrient. Irradiation was provided by fluorescence tubes ( $100 \mu\text{mol m}^{-2} \text{s}^{-1}$ , continual light cycle) and cells were continuously bubbled by air. Harvested cells were re-suspended in 25 mM Hepes buffer, pH 7.8 and broken by glass beads using Mini-Bead-Beater (BioSpec, USA). Thylakoid membrane fraction was separated by centrifugation, re-suspended in 1 ml of distilled water, mixed with 9 ml of methanol and incubated for one hour in dark under room temperature. Extract was clarified by centrifugation and the remaining pellet was extracted again by 10 ml of 90% methanol. Both supernatants were pooled and completely evaporated by a vacuum evaporator. Pigments were dissolved in methanol and separated by HPLC (Agilent 1200) on a semi-preparative reverse phase column (Eclipse XDB-C8  $5\mu\text{m}$ ,  $250 \times 9.4$  mm, Agilent, USA) with 35% methanol and 15% acetonitrile in 0.25M pyridine (solvent A) and 20% methanol and 20% acetone in acetonitrile as solvent B. Pigments were eluted by 80 % of solvent B at a flow rate of  $3 \text{ mL min}^{-1}$  at  $40^\circ\text{C}$ . The peak corresponding to violaxanthin was collected and its concentration was calculated from dry weight.



**ARTICLE II**

**High light acclimation of *Chromera velia* points to photoprotective  
NPQ**

Belgio, E., Trsková, E., Kotabová, E., Ewe, D., Prášil, O., and Kaňa, R.

(2018)

*Photosynthesis Research* **135**, 263-274. IF = 3.057

\* Erica Belgio and Eliška Trsková have contributed equally to this work.



## High light acclimation of *Chromera velia* points to photoprotective NPQ

Erica Belgio<sup>1</sup> · Eliška Trsková<sup>1,2</sup> · Eva Kotabová<sup>1</sup> · Daniela Ewe<sup>1</sup> · Ondřej Prášil<sup>1,2</sup> · Radek Kaňa<sup>1,2</sup>

Received: 30 December 2016 / Accepted: 6 April 2017 / Published online: 12 April 2017  
© Springer Science+Business Media Dordrecht 2017

**Abstract** It has previously been shown that the long-term treatment of *Arabidopsis thaliana* with the chloroplast inhibitor lincomycin leads to photosynthetic membranes enriched in antennas, strongly reduced in photosystem II reaction centers (PSII) and with enhanced nonphotochemical quenching (NPQ) (Belgio et al. Biophys J 102:2761–2771, 2012). Here, a similar physiological response was found in the microalga *Chromera velia* grown under high light (HL). In comparison to cells acclimated to low light, HL cells displayed a severe re-organization of the photosynthetic membrane characterized by (1) a reduction of PSII but similar antenna content; (2) partial uncoupling of antennas from PSII; (3) enhanced NPQ. The decrease in the number of PSII represents a rather unusual acclimation response compared to other phototrophs, where a smaller PSII antenna size is more commonly found under high light. Despite the diminished PSII content, no net damage could be detected on the basis of the Photosynthesis versus irradiance curve and electron transport rates pointing at the excess capacity of PSII. We therefore concluded that the photoinhibition is minimized under high light by a lower

PSII content and that cells are protected by NPQ in the antennas.

**Keywords** Nonphotochemical quenching · Photoinhibition · *Chromera velia* alga · High light acclimation · Uncoupling of antennas from Photosystem II.

### Abbreviations

NPQ	Nonphotochemical quenching
PSII	Photosystem II reaction centers
HL	High light
LL	Low light
$\Delta pH$	Trans-thylakoid membrane proton gradient
$F_m$	Variable fluorescence
$F_m$	Maximum fluorescence
$P_{max}$	Maximal photosynthetic rate or photosynthetic capacity
TL	Thermoluminescence
FRRF	Fast repetition rate fluorescence
ETR	Electron transport rates
$\sigma PSII$	Effective antenna size of PSII
$I_k$	Photosynthetic limiting light
$I_{sat}$	Light intensity where photosynthetic saturation starts
$\alpha$ -DM	<i>n</i> -Dodecyl $\alpha$ -D-maltoside
DES	De-epoxidation state

Erica Belgio and Eliška Trsková have contributed equally to this work.

**Electronic supplementary material** The online version of this article (doi:10.1007/s11120-017-0385-8) contains supplementary material, which is available to authorized users.

✉ Erica Belgio  
belgio@alga.cz

<sup>1</sup> Centre Algatech, Institute of Microbiology, Academy of Sciences of the Czech Republic, Opatovický mlýn, 379 81 Třeboň, Czech Republic

<sup>2</sup> Faculty of Science, University of South Bohemia, Branišovská 31, 37005 Czech Budejovice, Czech Republic

### Introduction

Changes in the quantity and quality of the light, to which photosynthetic organisms are exposed, occur both periodically, due to the position of the Earth and stochastically, due to weather variations. Aquatic organisms, moreover, need to cope with variations related to water circulation and

optical effects induced by the waves at the surface (Dera and Gordon 1968; Falkowski and Wirick 1981). In order to overcome light changes with minimum effect on photosynthetic efficiency, phototrophs evolved several mechanisms to keep their photosynthetic yields high even in the most heterogeneous environments. Long-term regulations involve gene expression and protein degradation of both, photosynthetic and nonphotosynthetic processes. They lead to macroscopic changes including the amount and composition of pigments per cell; re-arrangements of the photosynthetic units in terms of their size or number of units per cell; and changes in electron carriers and carboxylases rates (Havelková-Doušová et al. 2004; Kagawa et al. 2001; Kirk 1994; Schöttler and Tóth 2014; Walters 2005).

On a relatively shorter term, i.e., seconds to minutes, more localized, transient, and usually reversible changes occur within the photosynthetic complexes like the de-epoxidation of xanthophyll cycle pigments, the nonphotochemical quenching of fluorescence (NPQ), and state transitions (see i.e., Demmig-Adams 1990; Finazzi and Minagawa 2014; Kaňa and Vass 2008; Ruban et al. 2012).

High light acclimation usually includes morphological changes in the cell structure, an increased Photosystem I to Photosystem II stoichiometry and reduced total chlorophyll content (Boardman 1977; Kendrick and Kronenberg 1994; Lichtenthaler et al. 1981; Oguchi et al. 2003; Pyke 2009; Terashima et al. 2001). Often the size of the photosynthetic antenna is also regulated during acclimation to high light intensities (Anderson and Osmond 2001; Anderson et al. 1988; Ballottari et al. 2007; Caffarri et al. 2009; Hogewoning et al. 2012; Kouřil et al. 2012; Morosinotto et al. 2006; Niyogi 1999; Pesaresi et al. 2009; Tikkanen et al. 2006; Wientjes et al. 2013). However, adjustment of the antenna to reaction center ratio does not appear to be mandatory to all phototrophs as it seems to be species-dependent, especially for aquatic organisms (Anderson et al. 1988; Bailey et al. 2004; Bonente et al. 2012; Falkowski and Owens 1980; Hogewoning et al. 2012; Kouřil et al. 2012, 2013; Leong and Anderson 1984; Lichtenthaler et al. 1981; Ware et al. 2015; Wientjes et al. 2013).

Despite the regulatory adjustments, high light in combination with adverse environmental factors that reduce CO<sub>2</sub> assimilation rate (nutrient starvation, etc.) can compromise the photosynthetic functionality. The oxidative damage occurs primarily at Photosystem II [see i.e., (Aro et al. 1993; Hakala et al. 2005; Ohnishi et al. 2005; Prášil et al. 1992)]. It occurs at all light intensities; however, under saturating lights, the repair mechanisms of Photosystem II do not keep the pace and a net decrease of the photosynthetic rate can be observed (Aro et al. 2005), a process called photoinhibitory damage (Barber 1995; Kok 1956; Powles 1984) as it reflects the sustained decline of the photosynthetic efficiency.

Quantitative estimates of photoinhibition are often based on the ratio between variable and maximal fluorescence ( $F_v/F_m$ ) and on the decline of  $F_m$ , broadly known as nonphotochemical quenching (Bose and Fork 1988; Car-taxana et al. 2013; Kolber and Falkowski 1993; Ruban 2013; Tyystjarvi and Aro 1996). However, also the opposite mechanism, i.e., photoprotection, competes for chlorophyll excited states, thus equally resulting in quenching of maximal fluorescence. Some distinctive features exist: photoprotective quenching is usually reversible in the dark (in the absence of zeaxanthin, see Demmig-Adams and Adams 1992) and it is dependent upon the level of the transmembrane proton gradient ( $\Delta pH$ ); photoinhibition, on the contrary, lasts also in the dark (i.e., Giovagnetti and Ruban 2015) and is active also in the absence of  $\Delta pH$  (Johnson et al. 2011; Roach and Krieger-Liszskay 2014). However, it is often difficult, if not impossible, to distinguish between the two processes based on fluorescence measurements only (Kolber and Falkowski 1993; Ruban and Murchie 2012).

In the present paper, we investigated the NPQ mechanisms of high light (HL)-acclimated *Chromera velia*. The colpodellid, unicellular alga isolated from Sydney bay (Moore et al. 2008) has been reported to display a violaxanthin-based NPQ mechanism (Kotabová et al. 2011; Mann et al. 2014). Despite the unusual NPQ kinetics found in the alga, characterized by fast formation and slow relaxation, NPQ was previously shown to be dependent on  $\Delta pH$  and its kinetics linearly correlated with the de-epoxidation state (DES) of the cells (Kotabová et al. 2011; Mann et al. 2014). Here, we found that HL acclimation brought about an unusual response in *C. velia*, different from other model organisms, including higher plants. This mainly involved a strong reduction in the number of Photosystem II reaction centers (PSII) without decrease in the antenna size. As a consequence, part of the antenna was energetically poorly connected to the few remaining PSII, and NPQ greatly enhanced. As the diminished number of PSII did not affect the photosynthetic capacity of HL cells (i.e., maximal photosynthetic rate), this pointed at an “excess capacity” of PSII (see e.g. Behrenfeld et al. 1994; Kaňa et al. 2002). We propose that reducing the number of PSII while increasing photoprotective NPQ in the antennas may represent a strategy to avoid photoinhibitory damage under HL.

## Materials and methods

### Cell growth

*Chromera velia* strain RM 12 originally isolated from the stony coral *Plesiastrea versipora* in Sydney Harbour (Moore et al. 2008), was obtained from Dr. M. Obornik

(University of South Bohemia). The strain was grown at 28 °C in artificial seawater medium with supplementation of *f*/2 nutrients as described previously (Kotabová et al. 2011). Cell stocks (20  $\mu\text{mol m}^{-2} \text{s}^{-1}$  continuous light) were transferred to aerated glass flasks for a minimum of 3 weeks in semi-continuous batch growth with 24-h irradiation by fluorescence tubes (20 or 200  $\mu\text{mol m}^{-2} \text{s}^{-1}$ ) and nutrient-saturating concentrations. Cell size was determined with a calibrated Coulter Counter (Beckman Multi-sizer III) equipped with a 50- $\mu\text{m}$  aperture. All physiological measurements were performed with cultures harvested in late exponential phase.

### Variable fluorescence measurements

Chlorophyll fluorescence was measured using a double-modulation fluorometer FL-3000 (Photon System Instruments, Czech Republic) on whole cells (chlorophyll concentration 0.7  $\mu\text{g ml}^{-1}$ ). Cells were dark adapted for 30 min before the measurements to oxidize the electron transport chain. A multiple turnover saturating flash was applied to measure the maximum quantum yield of photochemistry of Photosystem II ( $F_v/F_m$ ) according to  $(F_m - F_0)/F_m$ , where the difference between the maximum ( $F_m$ ) and minimal fluorescence ( $F_0$ ) is used to calculate the variable fluorescence ( $F_v$ ) (van Kooten and Snel 1990). Cells were then illuminated with an orange actinic light (625 nm, 250, or 750  $\mu\text{mol photons m}^{-2} \text{s}^{-1}$ ), during which periodical saturating flashes were applied. NPQ was calculated as  $(F_m - F_m')/F_m'$ , where  $F_m'$  is the maximum fluorescence measured in the presence of actinic light.

### Photosystem II functional antenna size, electron transport rates, and connectivity

The effective antenna size of photosystem II ( $\sigma_{\text{PSII}}$ ) was measured with a custom designed fluorometer FL3500 (Photon Systems Instruments, Czech Republic) using a fast repetition rate fluorescence protocol. A single-turnover was induced by application of a series of 80 short blue sub-saturating flashes (1  $\mu\text{s}$  long,  $\lambda=463$  nm) to dark-adapted samples. Single turnover flashes were then measured during sequential exposure to background blue actinic light (463 nm, 11 steps with increasing intensities, 0–1023  $\mu\text{mol photons m}^{-2} \text{s}^{-1}$ ). The measured fluorescence rise during the single turnover flash was fitted according to the model described earlier (Kolber et al. 1998), giving the connectivity of RC PSII and effective PSII cross-section parameter  $\sigma_{\text{PSII}}$ . These parameters were used for calculation of the electron transport rate as follows:

$$\text{ETR} = \sigma_{\text{PSII}} \times n_{\text{PSII}} \times (F'_q/F'_v) / (F_v/F_m) \times I,$$

where  $F_m$  is the maximal fluorescence in the dark and  $F_m'$  that in the light;  $F_v$  is the variable fluorescence in the dark and  $F_v'$  is the one in the light;  $F'_q$  equals  $F_m' - F'$ , where  $F'$  represents steady state value of fluorescence at a given irradiance;  $I$  is the light intensity; and  $n_{\text{PSII}}$  gives the ratio of functional PSII to total chlorophyll *a*. The value  $1/n_{\text{PSII}}=500$  [mol chlorophyll *a*/mol PSII] was used (see (Suggett et al. 2010) for details).

### Thermoluminescence

Thermoluminescence (TL) glow curves were recorded using a thermoluminescence system TL 400/PMT (Photon Systems Instruments, Czech Republic). Cell suspension (0.5–2 ml) was filtered through a Prapo 5 nitrocellulose membrane filter (pore size  $0.6 \pm 0.1$   $\mu\text{m}$ ; Pragochema, Czech Republic) that was placed on the instrumental sample holder. After 2 min of incubation at 28 °C in the dark, the samples were cooled down to 3 °C where two subsequent saturating single turnover flashes (80  $\mu\text{s}$  long, 200 ms apart,  $\lambda=625$  nm) were applied prior to the start of the heating/recording phase. TL curves were recorded from 3 to 65 °C with a linear heating rate of  $0.5$  °C  $\text{s}^{-1}$ . The amount of active photosystem II was quantified by integrating the area under the glow curves and normalized per chlorophyll concentration, in agreement with Küpper et al. (2002).

### Pigment extraction and quantification

Cells were collected on GF/F filters (Whatman, England), soaked in 100% methanol overnight at  $-20$  °C, and disrupted using a mechanical tissue grinder. Filter and cell debris were then removed by centrifugation (12,000 g, 15 min) and the supernatant used for absorbance measurements at 652, 665, and 730 nm. Chlorophyll estimation was done according to an already established method (Porra et al. 1989).

Violaxanthin-to-chlorophyll molar ratio was determined from high-performance liquid chromatography (HPLC) analysis on Agilent 1200 chromatography system equipped with the diode array detector as described in Kotabová et al. (2011). Pigments were separated on Phenomenex column (Luna 3u C8(2), size 100 x 4.6 mm) by applying the 0.028 M ammonium acetate/MeOH gradient (20/80). Eluted pigments were quantified at 440 nm using the relative extinction coefficients.

### 77 K Fluorescence

77 K fluorescence emission spectra were measured using an Aminco–Bowman Series 2 spectrofluorometer (Thermo Fisher Scientific, USA) as described previously (Kaňa et al. 2009). The excitation wavelength

was 435 nm and slit width 4 nm. The emission spectra were recorded in 0.4 nm steps from 600 to 800 nm, with 1 nm slit width. The instrument function was corrected by dividing raw emission spectra by simultaneously recorded signal from the reference diode. Spectra were normalized around 690 nm.

### Gel chromatography

Fast protein liquid chromatography (FPLC) analysis was performed on fresh thylakoid membranes prepared as described in Kaňa et al. (2016). The detergent solubilization and sample separation was performed as described in Belgio et al. (2012). Briefly, membranes were suspended to a final chlorophyll concentration of 0.7 mg ml<sup>-1</sup> and partially solubilized by the addition of n-dodecyl  $\alpha$ -D-maltoside ( $\alpha$ -DM) to a final concentration of 0.7%, incubated 1 min on ice, and then centrifuged 3 min at 16,000 g. The supernatant was filtered through a 0.45-mm filter and loaded onto a gel filtration Amersham-Pharmacia Äcta purifier system, including a Superdex 200 HR 10/30 column at 4 °C. The same amount of chlorophyll was loaded for low and high light samples. This was also verified by a similar integral calculated for the whole chromatogram. The buffer used throughout the whole procedure contained 0.03%  $\alpha$ -DM, 20 mM Hepes pH 7.8, 5 mM MgCl<sub>2</sub>. Complex identification was based on SDS-PAGE, western blotting, and spectroscopy data in comparison with published protein profiles and spectra (Mann et al. 2014; Tichý et al. 2013) and was in line with previous gel filtration results (Ruban et al. 2006).

### SDS-PAGE and western blotting

Proteins were resolved by SDS-PAGE using a denaturing gel gradient of 16–20% acrylamide (acrylamide to bis-acrylamide ratio = 60), using the method described in (Knoppová et al. 2016). Low light and high light membranes were adjusted to the same chlorophyll concentration. The amount of chlorophyll loaded in each lane is indicated in Fig. 2b. Separated proteins were visualized by staining with Coomassie Brilliant Blue or transferred onto nitrocellulose membrane and incubated with antibody against D1 protein. The primary antibody against D1 used in this study was previously described (Dobáková et al. 2007; Komenda et al. 2004). Detection was performed using the Luminata Crescendo Western HRP substrate (Merk Millipore). Densitometry analysis of the signals was done using NIH Image-J software and associated plugins (<http://rsb.info.nih.gov/ij/>), taking the low light sample as 100%.

### Photosynthesis versus Irradiation curve

The photosynthetic limiting light ( $I_k$ ), the light intensity where photosynthetic saturation starts ( $I_{sat}$ ), and the photosynthetic capacity (i.e., maximum photosynthetic rate  $P_{max}$ ) were obtained as described previously (Eilers and Peeters 1988) from the measured oxygen light curves using the “GRG nonlinear solver calculator” from Excel. Oxygen evolution of *C. velia* cells was measured under eleven different light intensities, ranging from 0 to 1017  $\mu\text{mol m}^{-2} \text{s}^{-1}$ , using the Hansatech DW1 Oxygen Electrode Chamber (Hansatech Instruments Ltd, Narborough, UK), coupled to the PSI OxyCorder 401 A/D signal transducer equipped with the PSI OxyWin software (Photon Systems Instruments, Brno, Czech Republic). The desired light intensities were attained using LEDs of the Act2 Systems (Chelsea Technologies Group Ltd, Surrey, UK). The maximal turnover rate of a Photosynthetic unit ( $1/\tau$ ) was calculated from Photosystem II cross-section ( $\sigma$ PSII) and  $I_k$  values, according to the equation (Falkowski and Raven 2007).

$$I_k = 1/(\sigma PSII \times \tau).$$

### Results

#### Feature of high light acclimation in *C. velia*: enhanced NPQ

Cultivation of *C. velia* cells under high light (HL) induced a decrease in total chlorophyll and lowered the  $F_v/F_m$  ratio (Table 1), in agreement with a previous report (Quigg et al. 2012). These changes were accompanied by alterations of the fluorescence induction trace (Fig. 1). At the turning on of the actinic light, the fluorescence signal of HL cells dropped below  $F_0$ , reaching maximal fluorescence quenching in less than 2 min, due to a fast-forming, slowly-relaxing, nonphotochemical quenching (NPQ). Such a fast NPQ activation was previously attributed to an unusually rapid xanthophyll de-epoxidation in *C. velia* (Kotabová et al. 2011). NPQ in HL cells was about 2.4 (Figure S1 and Table 1), i.e., 10 times greater than in LL cells. A very similar change in the fluorescence induction trace was previously observed in higher plants after long-term treatment with the antibiotics lincomycin (Fig. 1b inset). Also in that case, the actinic light induced a strong decrease of the fluorescence signal, twice lower than  $F_0$  level due to an enhanced NPQ (see also Belgio et al. 2012). On the other hand, NPQ relaxation was different in HL *C. velia* in comparison with lincomycin-treated plants, as the strong quenching was still present after 5-min dark relaxation. This was previously reported to be due to the slow zeaxanthin re-epoxidation in the dark (see Mann et al. 2014 and

**Table 1** Summary of physiological responses of low and high light-acclimated *Chromera velia* cells

Parameter	Low light cells (LL)	High light cells (HL)
Growing light intensity, $\mu\text{mol photons m}^{-2} \text{s}^{-1}$	20	200
Chlorophyll/cell, pg	$0.6 \pm 0.1$	$0.3 \pm 0.1$
$F_v/F_m$	$0.60 \pm 0.04$	$0.40 \pm 0.03$
NPQ at $250 \mu\text{mol m}^{-2} \text{s}^{-1}$	$0.1 \pm 0.2$	$0.8 \pm 0.3$
NPQ at $750 \mu\text{mol m}^{-2} \text{s}^{-1}$	$0.24 \pm 0.12$	$2.4 \pm 0.6$
ETR, $\mu\text{mol electron mg chl}^{-1} \text{h}^{-1}$	$822 \pm 22$	$1108 \pm 126$
Vioxanthin/chlorophyll, $\text{mol mol}^{-1}$	$0.27 \pm 0.01$	$0.42 \pm 0.01$
$\sigma\text{PSII}$ , $\text{\AA}/\text{quantum}$	$328 \pm 8.3$	$453 \pm 16$
$I_{\text{sat}}$ , $\mu\text{mol photons m}^{-2} \text{s}^{-1}$	$256 \pm 105$	$547 \pm 8$
$I_k$ , $\mu\text{mol photons m}^{-2} \text{s}^{-1}$	$56 \pm 11$	$85 \pm 2.7$
$1/\tau^*$ , $\text{ms}^{-1}$	0.111	0.232
$P_{\text{max}}$ , $\mu\text{mol O}_2 \text{mg chl}^{-1} \text{h}^{-1}$	$239 \pm 60$	$406 \pm 30$

Nonphotochemical quenching of fluorescence (NPQ) was calculated as  $(F_m - F_m')/F_m'$ , where  $F_m'$  was measured after 5 min of actinic light at the intensity indicated ( $250$  or  $750 \mu\text{mol m}^{-2} \text{s}^{-1}$ ) using the protocol shown in Fig. 1. ETR, electron transport rates;  $\sigma\text{PSII}$ , effective antenna size of PSII from FRRF measurements;  $I_k$ , photosynthetic limiting light;  $I_{\text{sat}}$  light intensity where photosynthetic saturation starts;  $1/\tau^*$  maximal turnover rate of a Photosynthetic unit calculated from  $\sigma\text{PSII}$  and  $I_k$  as described in “Materials and Methods”;  $P_{\text{max}}$ , maximum photosynthetic rate, i.e., photosynthetic capacity (experimental values from Photosynthesis vs. irradiance experiments)

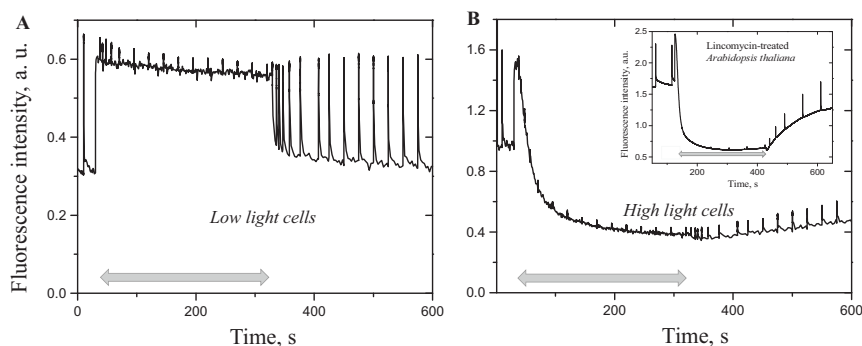


**Fig. 1** Representative chlorophyll *a* fluorescence quenching kinetic analysis of low (a) and high (b) light-acclimated *C. velia* cells illuminated with  $250 \mu\text{mol m}^{-2} \text{s}^{-1}$  actinic light (arrow). Cells were dark adapted for 30 min before the measurements. Inset chlorophyll fluo-

rescence trace of a lincomycin-treated *Arabidopsis thaliana* leaf illuminated with  $200 \mu\text{mol m}^{-2} \text{s}^{-1}$  actinic light (small arrow) (modified from Belgio et al. 2012)

“Discussion”). The HPLC data confirmed the presence of more than 50% DES at this stage of the fluorescence induction kinetics (data not shown).

**Feature of high light acclimation in *C. velia*: reduced PSII content**

We tested whether like lincomycin-treated plants, also HL *C. velia* cells carried a modified antenna to Photosystem II reaction centers (PSII) ratio, possible cause of the observed fluorescence changes. Light acclimation

resulted in a different gel filtration profile of the two types of membranes. Gel filtration is a gentle and incisive way to separate different green complexes on the basis of size (larger complexes elute first). Photosynthetic complex identification was based on SDS-PAGE, western blotting, and spectroscopic analysis of the eluted fractions (Figure S2 and S3), according to the published data (Mann et al. 2014; Tichý et al. 2013). The order of elution of protein complexes (PSI, PSII, antenna fraction) was similar to that of higher plants (Ruban et al. 2006). The membranes isolated from HL cells displayed three main differences

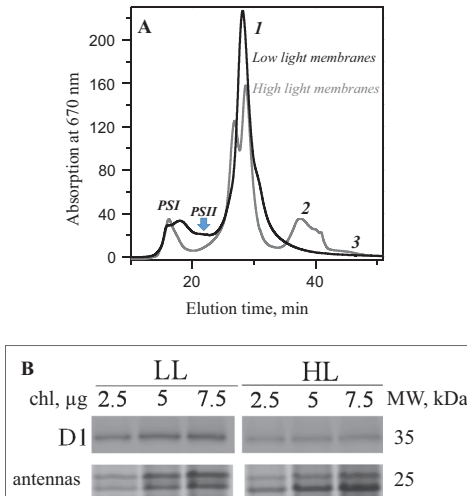


**Fig. 2** a Profile of mildly solubilized membranes isolated from low (black) and high (gray) light-acclimated cells eluted by gel filtration chromatography. Identification of the peaks was performed according to the method of Belgio et al. (2012) and verified by SDS-PAGE (data not shown). For the decomposition of the relative chromatograms, see supplementary Figure S2. PSI, Photosystem I; PSII, Photosystem II core; 1, oligomeric antenna; 2, monomeric antenna; 3, free pigments. The arrow points at the decrease in PSII band in high light. b Typical SDS-PAGE and Western blotting results of low (LL) and high (HL) light membranes. Numbers on top of the lanes correspond to the amount of chlorophyll per lane. D1 represents the signal detected using  $\alpha$ -D1 antibody; antennas represent Coomassie Brilliant Blue staining results. Gel preparation was according to the method of Komenda et al. (2004) and Dobáková et al. (2007). Signals were analyzed using Image-J program as described in “Materials and methods.” MW, approximate molecular weight in kDa

compared to LL cell (Fig. 2a). One of the most noticeable was a decrease of the PSII-related fraction, eluted around 20 min. PSII elution seemed to occur slightly earlier in HL than LL. We cannot exclude that this could be due to a slight difference in the size of PSII, in terms of a slightly bigger PSII in HL cells. Interestingly, PSII band was about three times smaller in HL than LL membranes based on the decomposition of the relative chromatograms [Figure S4, for more details, see “Materials and Methods” and Belgio et al. (2012)]. Besides this, the elution profile of the antenna complexes was also altered. In place of one main peak in LL membranes, eluted between 25 and 40 min and attributed to oligomeric antennas, two distinct peaks were found in HL membranes at 27 and 30 min. Moreover, one broad monomeric antenna fraction appeared between 35 and 40 min, absent in LL membranes. This band balanced the decrease in PSII content

in HL, so that the total area below the chromatogram, and therefore the total chlorophyll loaded, was the same in the two types of sample. Despite the changes in antenna oligomerization, the total amount of antenna was similar in HL and LL cells.

The change in PSII content was verified by SDS-PAGE and Western Blotting analysis. The amount of total antenna per chlorophyll was similar in HL compared to LL membranes (Fig. 2b, bottom and Table 2; for a full gel, see Figure S5), in agreement with gel filtration data (Fig. 3a). On the contrary, PSII content (detected using  $\alpha$ -D1 antibody) was between three and four times weaker in HL membranes (Fig. 2b, top). Both methods therefore confirmed a strong decrease in the number of PSII per chlorophyll induced by high light acclimation. This result was also additionally confirmed by thermoluminescence (Figure S6) using the method described earlier (Küpper et al. 2002). Based on the FPLC chromatogram decomposition, it was possible to estimate the antenna-to-PSII ratio. This was about five and 15 in LL and HL cells, respectively (Table 2). We stress here that the change in the ratio was caused by a drop in PSII complexes while antenna content remained unaffected (Fig. 2).

### Functional PSII antenna size and connectivity in HL cells

As the total antenna per PSII core was increased under HL (see Table 2), we investigated what proportion of it was efficiently transferring the excitation energy to the remaining Photosystem II reaction centers. For this purpose, we applied fast repetition rate fluorescence (FRRF) technique to HL and LL cells (Kolber et al. 1998), finding that Photosystem II cross-section was increased by ~35% in HL compared to LL cells (Fig. 3, left). This percentage was less than what was expected on the basis of FPLC, SDS-PAGE, and Thermo-luminescence data as the three methods had indicated an antenna per PSII ratio 3 times larger in HL compared to LL (see previous section). We therefore concluded that a large part of the antenna complement (3–1.35) was functionally not well connected to PSII in HL cells. This was estimated to correspond to ~8–9 antennas/PSII on the basis of FPLC chlorophyll ratios (see Table 2). In Fig. 5 a putative model of PSII antenna organization is presented showing the difference between total and coupled PSII antenna in HL cells. The analysis of FRRF data indicated also that PSII connectivity was almost zero in HL cells (Fig. 3, right). As “disconnected” antennas would prevent the efficient energy transfer between PSII units, this result is consistent with the suggestion that a large proportion of antennas weakly coupled to PSII in HL cells (see Fig. 5 and “Discussion”).



**Table 2** Relative content of total antenna, PSII, strongly and loosely bound antenna in low and high light *C. velia* cells based on FPLC and SDS-PAGE results

	Total antenna <sup>a</sup>	PSII <sup>b</sup>	Total antenna/PSII <sup>c</sup>	Strongly bound antenna/PSII <sup>#</sup>	Loosely bound antenna/PSII <sup>##</sup>
LL <i>C. velia</i>	100%	~20%	5	5	0
HLC <i>velia</i>	90–100%	5–8%	~15	6–7	8–9

Percentages refer to chlorophyll ratios obtained from decomposition analysis (see Figure S2) of chromatograms from three independent FPLC runs, taking LL antenna band as 100%

<sup>a</sup>Results in agreement with an unchanged content of antenna polypeptides in HL compared to LL, as quantified from five replicates of Coomassie-stained SDS-PAGE gels using Image-J software

<sup>b</sup>Results in agreement with ~30% PSII content in HL compared to LL based on five Western Blotting replicates against D1 protein (see Fig. 2b) and five Thermoluminescence experiments (Figure S3). Western-blot analysis was performed with Image-J software

<sup>c</sup>Ratios calculated dividing “Total antenna” by “PSII”

<sup>#</sup>Strongly bound antenna/PSII are based on FRRF results, considering 100% for the total antenna/PSII of LL, and consequently 133% for HL

<sup>##</sup>Loosely bound antenna/PSII were calculated as the difference between total antenna and strongly bound antenna

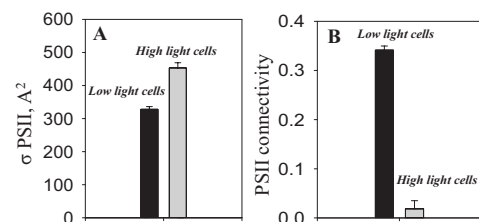


**Fig. 3** Photosystem II functional antenna size (a) and connectivity (b) as derived from fast repetition rate fluorescence (FRRF) measurements (for more details, see Materials and methods) of *C. velia* cells grown under low light (black) or high light (gray). Samples were dark adapted for 30 min before the measurements. Both parameters were obtained based on the fluorescence rise from  $F_0$  to  $F_m$  measured by single turnover flash and fitted according to the model described in Kolber et al. (1998). Data are means  $\pm$  standard deviation from three independent replicates

**Lack of photoinhibition in HL *C. velia* points to photoprotective NPQ**

The reduction in the number of PSII in HL cells prompted us to investigate the possible presence of chronic photoinhibition induced by high light. HL cells displayed slightly higher electron transport rates in comparison to LL cells (Table 1). This pointed at a high photosynthetic capacity notwithstanding the reduced PSII content (see “Discussion”). Additionally, while LL cells started to display signs

of photoinhibition at 200  $\mu\text{mol m}^{-2} \text{s}^{-1}$  (Figure S9), the analysis of the Photosynthesis versus irradiation curve indicated no photoinhibition ( $\beta$ -parameter=0) in HL cells for light intensities of up to 800  $\mu\text{mol m}^{-2} \text{s}^{-1}$  (Fig. 4a); the light intensity corresponding to photosynthetic saturation (“ $I_{\text{sat}}$ ”) was estimated to be  $546 \pm 6 \mu\text{mol m}^{-2} \text{s}^{-1}$ , while the limiting light intensity (“ $I_k$ ”) was  $89 \pm 6 \mu\text{mol m}^{-2} \text{s}^{-1}$  (Table 1). This pointed at a high photosynthetic capacity (see  $P_{\text{max}}$  value in Table 1) notwithstanding the reduced PSII content (see “Discussion”).

These results were interpreted in terms of absence of photoinhibitory damage of PSII in HL cells, which in turn indicated that NPQ was protective for the HL cells. Consistent with this, violaxanthin pool was doubled in HL

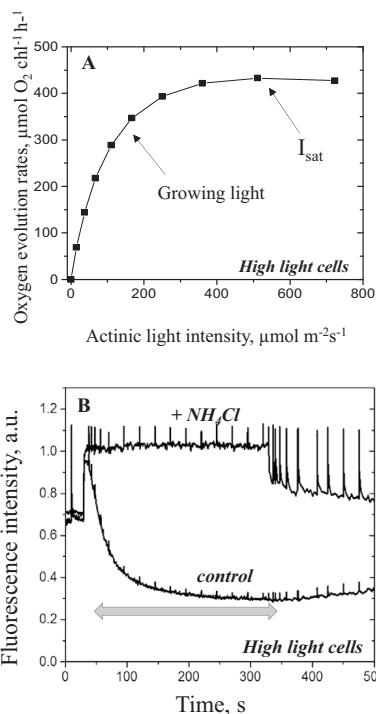


**Fig. 4** a Representative Photosynthesis versus light curve of high light-acclimated cells measured under different actinic light intensities. The growing and saturating ( $I_{\text{sat}}$ ) light intensities are indicated (for more details, see “Materials and methods”). b Representative chlorophyll a fluorescence quenching kinetic analysis showing the effect of the uncoupler  $\text{NH}_4\text{Cl}$  on the NPQ of high light-acclimated *C. velia* cells. Top,  $\text{NH}_4\text{Cl}$  added prior to the illumination; bottom trace, control (no  $\text{NH}_4\text{Cl}$ ). The timing of application of actinic light is marked by an arrow. Protocol as in Fig. 1

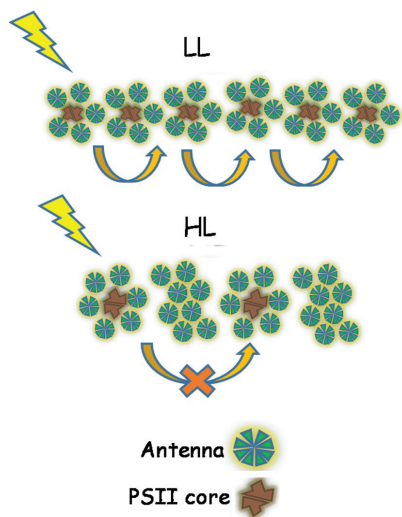


**Fig. 5** Putative organization of Photosystem II (PSII) antenna in low light (LL) and high light (HL)-acclimated *Chromera velia* cells. The model shows diagrammatically the observed difference between total and coupled PSII antenna found in HL cells (see Table 2). Each LL PSII is surrounded by ~5 coupled antenna proteins, while in HL each PSII is surrounded by 6–7 connected antennas plus 8–9 uncoupled antennas. When the excitation energy (lightening) reaches one PSII in closed state, it can still efficiently reach an open PSII nearby in LL (displayed by an orange arrow). In HL, this is not possible due to the longer distance that the excitation energy has to travel to reach another PSII (crossed arrow). This provides a possible explanation for the limited connectivity in HL cells (see also Fig. 3b)

cells compared to LL (Table 1) and NPQ was totally  $\Delta$ pH-dependent (Fig. 4b and S7). We therefore concluded that in HL cells, photoinhibition is minimized by a lower PSII content and NPQ provides further photoprotection.

## Discussion

### Acclimation

The physiological response of *C. velia* grown under high light (i.e., decrease in PSII, unaffected antenna protein content, slight increase in the effective PSII antenna size, see Table 2) represents an unusual strategy in comparison to other phototrophs. For instance, a 30–50% decrease in PSII antenna size has been reported for high light-acclimated *Arabidopsis thaliana* plants (Kouřil et al. 2013; Ware et al. 2015). Similarly, another study (Chukhutsina et al. 2013), reported a smaller overall antenna size (50%) for the high light-acclimated diatom *Cyclotella meneghiniana* (Table 2)

on the basis of fluorescence lifetime measurements. This points to a different regulatory mechanism in *C. velia* as the alga can cope with long-term high light condition by decreasing the number of PSII centers while keeping the antenna protein content unaffected.

Similar response to HL can be found in higher plants after long-term treatment with the antibiotic lincomycin (Figure S8A and B). Although the effect there was more extreme, with a 10 times bigger antenna size (see Table 2), the inhibition of D1-protein (induced by the antibiotic) led to a strong reduction in the number of PSII, without any decrease in the antenna protein content (see also Belgio et al. 2012, 2015).

One might therefore suggest that, like lincomycin-treated plants, *C. velia* is also affected in some of the steps of D1 protein repair. PSII repair involves partial disassembly of damaged complexes, subunit replacement by newly synthesized proteins (a step inhibited by lincomycin), and reassembly. The process requires several indispensable assembly factor proteins (known as Ycf48/Hcf136, Psb27 and Psb28, see Nixon et al. 2010). Our preliminary analysis did not find sequence identity higher than 30% for Ycf48/Hcf136 and Psb27 in *C. velia* (Sobotka et al. work in preparation). Therefore, we can speculate that, in *C. velia*, replacement of D1 protein is ineffective under photoinhibitory conditions (like high light growth) and reducing PSII content is a “surviving” strategy to avoid PSII photodamage. On the other hand, it is more difficult to explain why, in contrast to other organisms (see i.e., Kouřil et al. 2013), *C. velia* keeps a high antenna content under HL. This could be either guarantee efficient light harvesting under fluctuating light intensities (Havelková-Doušová et al. 2004) or provide light harvesting for PSI, that is extremely efficient in *C. velia* (Belgio et al. 2017).

### Poorly coupled antennas

The decrease in PSII contrasted with an unchanged amount of antenna proteins in HL cells (see Fig. 2, diagrammatic scheme in Fig. 5; Table 2). This resulted in antennas poorly coupled to PSII, as previously described for higher plants treated with lincomycin. Energetically poorly bound antennas can in fact provide an explanation for the reduced  $F_v/F_m$ , the drop of variable fluorescence below  $F_0$ , and the increased NPQ (an extensive explanation can be found in Belgio et al. 2012). A confirmation of this can be found in the 77 K fluorescence spectra of HL cells (Figure S8 C and D). Besides the strong reduction in the red tail of emission (~715 nm), attributable to the limited presence of “red” chlorophyll forms (Belgio et al. 2017; Kotabová et al. 2014), in HL cells, a shift from 693 to 689 nm can be clearly noticed. This shift towards the blue can be attributable to antennas poorly coupled to PSII. Also FRRF results

are consistent with a proportion of antennas loosely connected to PSII as poorly coupled limiting the connectivity between PSII units (see Figs. 3b, 5). We cannot exclude that antennas poorly coupled to PSII might be partially connected to Photosystem I (PSI), thus increasing the cyclic electron flow around it (see i.e., Roberty et al. 2014). However, to clarify this point, a direct measurement of PSI antenna size will be necessary.

FPLC revealed that high light adaptation induced a different structural organization of the antennas (Fig. 2). Oligomers separated into two bands, instead of one, and even the milder detergent solubilization yielded a visible “monomeric” antenna band, absent in LL. It is possible that this different fractionation is also connected with the presence of poorly coupled antennas. A less compact Photosystem II supercomplex, in fact, would disaggregate more easily during the detergent-solubilization procedure. Interestingly, antenna proteins of diatoms displayed different oligomeric states also (Beer et al. 2006; Büchel 2003; Gardian et al. 2011; Grouneva et al. 2011; Lavaud et al. 2007; Lepetit et al. 2007) and the partitioning of such antennas onto sucrose gradients seems to depend on light acclimation (Lepetit et al. 2010). Mann et al. (2014) also reported on additional violaxanthin distributed in a lipid phase close to antennas in high light *C. velia* that can further regulate their efficiency (Kaňa et al. 2016). Therefore, we do not exclude a different lipid composition under high light.

### Photoinhibition

High light adaptation induced dramatic changes in the alga, some of which may be interpreted as PSII photodamage. The present results, however, do not support this interpretation. First, slow NPQ relaxation was fully reversed by  $\text{NH}_4\text{Cl}$  (Figure S7), proving that NPQ is  $\Delta\text{pH}$ -dependent. Moreover, it was previously shown that both slow zeaxanthin re-epoxidation and NPQ relaxation can be accelerated by light of weak intensity (Mann et al. 2014), probably because of a limited pool of NADPH and  $\text{H}^+$  co-factors in the dark (Goss et al. 2006; Grouneva et al. 2009). Slow NPQ recovery therefore is not an evidence of photodamage in *C. velia*.

No decrease in the maximal electron transport rates and maximal photosynthetic rates (i.e., photosynthetic capacity) was found in HL *C. velia* cells (see Table 1; Fig. 4), which further pointed to the lack of any photoinhibitory damage of PSII in *C. velia* acclimated to HL. Indeed, we estimated that the maximal turnover rate of a Photosynthetic unit (see Materials and methods and Table 1) in HL cells is twice that of LL. A similar effect of high light acclimation on Photosystem II turnover rate was previously observed in a green alga (*Chlorella*) and in a diatom (*Thalassiosira weissflogii*) (Behrenfeld et al. 1998; Kaňa et al. 2002). In

these phototrophs, it was found that a decrease in the number of reaction centers was compensated by an increased turnover rate, which led to similar photosynthetic capacity with less PSII. The absence of decrease in photosynthetic capacity in spite of reduction in number of PSII centers was rationalized by “excess capacity” of PSII (Behrenfeld et al. 1998; Kaňa et al. 2002). *C. velia* therefore seems to be a clear-cut example of an alga having excess photosynthetic capacity. The molecular mechanism by which this occurs still needs to be clarified.

As a coral symbiont, *Chromera velia* is expected to be mainly exposed to rather “moderate” light intensities, however, as this organism can be also found “free-living” outside the coral, at depths of 3–5 m, light intensities of up to  $1000 \mu\text{mol m}^{-2} \text{s}^{-1}$  are normally experienced on a sunny day (Behrenfeld et al. 1998; Oborník et al. 2011). Thus, the  $150\text{--}200 \mu\text{mol m}^{-2} \text{s}^{-1}$  quanta used in this study and previous studies (see i.e., Mann et al. 2014) are well within the physiological range, and much higher intensities (above  $500 \mu\text{mol m}^{-2} \text{s}^{-1}$ ) are in fact required to saturate photosynthesis (see Fig. 4). Based on the present data, no photoinhibitory damage of PSII occurs in HL-acclimated *C. velia* as photodamage is minimized by a lower PSII content and protective NPQ in the antennas. Nevertheless, excess photosynthetic capacity of PSII guarantees efficient photosynthesis under high light.

**Acknowledgements** The authors thank Dr. Martina Bečková and Ms. Lenka Moravcová for excellent technical help with electrophoresis and Dr. E. Lawrenz for useful discussions. This research project was supported by the Institutional project Algatich Plus (MSMT LO1416) from the Czech Ministry of Education, Youth and Sport. The work of E.B. and E.T. was further supported by The Czech Science Foundation GAČR (Grantová agentura České republiky): 16-10088S granted to R.K. and 17-02363Y granted to E.B.; GAJU 014/2016/P was granted to E.T.

### References

- Anderson J, Osmond B (2001) Sun-shade responses: compromises between acclimation and photoinhibition. Elsevier, Amsterdam
- Anderson JM, Chow WS, Goodchild DJ (1988) Thylakoid membrane organization in sun/shade acclimation. Aust J Plant Physiol 15:11–26
- Aro EM, McCaffery S, Anderson JM (1993) Photoinhibition and D1 protein—degradation in peas acclimated to different growth irradiances. Plant Physiol 103:835–843
- Aro EM et al (2005) Dynamics of photosystem II: a proteomic approach to thylakoid protein complexes. J Exp Bot 56:347–356. doi:10.1093/jxb/eri041
- Bailey S, Horton P, Walters RG (2004) Acclimation of *Arabidopsis thaliana* to the light environment: the relationship between photosynthetic function and chloroplast composition. Planta 218:793–802. doi:10.1007/s00425-003-1158-5
- Ballottari M, Dall’Osto L, Morosinotto T, Bassi R (2007) Contrasting behavior of higher plant photosystem I and II antenna systems

- during acclimation. *J Biol Chem* 282:8947–8958. doi:10.1074/jbc.M606417200
- Barber J (1995) Photosynthesis—short-circuiting the Z-Scheme. *Nature* 376:388–389. doi:10.1038/376388a0
- Beer A, Gundermann K, Beckmann J, Büchel C (2006) Subunit composition and pigmentation of fucoxanthin-chlorophyll proteins in diatoms: evidence for a subunit involved in diadinoxanthin and diatoxanthin binding. *Biochemistry* 45:13046–13053. doi:10.1021/bi061249h
- Behrenfeld MJ, Lee H, Small LF (1994) Interactions between nutritional-status and long-term responses to ultraviolet-b radiation stress in a marine diatom. *Mar Biol* 118:523–530. doi:10.1007/bf00350309
- Behrenfeld MJ, Prášil O, Kolber ZS, Babin M, Falkowski PG (1998) Compensatory changes in Photosystem II electron turnover rates protect photosynthesis from photoinhibition. *Photosynth Res* 58:259–268. doi:10.1023/a:1006138630573
- Belgio E, Johnson MP, Juric S, Ruban AV (2012) Higher plant photosystem II light-harvesting antenna, not the reaction center, determines the excited-state lifetime-both the maximum and the nonphotochemically quenched. *Biophys J* 102:2761–2771. doi:10.1016/j.bpj.2012.05.004
- Belgio E, Ungerer P, Ruban AV (2015) Light-harvesting superstructures of green plant chloroplasts lacking photosystems. *Plant Cell Environ* 38:2035–2047. doi:10.1111/pce.12528
- Belgio E et al (2017) High photochemical trapping efficiency in Photosystem I from the red clad algae *Chromera velia* and *Phaeodactylum tricorutum*. *Biochim Biophys Acta* 1858:56–63. doi:10.1016/j.bbabi.2016.10.002
- Boardman NK (1977) Comparative Photosynthesis of Sun and Shade Plants. *Annu Rev Plant Physiol Plant Mol Biol* 28:355–377. doi:10.1146/annurev.pp.28.060177.002035
- Bonente G, Pippa S, Castellano S, Bassi R, Ballottari M (2012) Acclimation of *Chlamydomonas reinhardtii* to different growth irradiances. *J Biol Chem* 287:5833–5847. doi:10.1074/jbc.M111.304279
- Bose S, Fork DC (1988) Mechanisms of light state transition in photosynthesis of green plants and red algae. *Indian J Biochem Biophys* 25:631–635
- Büchel C (2003) Fucoxanthin-chlorophyll proteins in diatoms: 18 and 19 kDa subunits assemble into different oligomeric states. *Biochemistry* 42:13027–13034
- Caffarri S, Kouril R, Kereiche S, Boekema EJ, Croce R (2009) Functional architecture of higher plant photosystem II supercomplexes. *EMBO J* 28:3052–3063. doi:10.1038/emboj.2009.232
- Cartaxana P, Domingues N, Cruz S, Jesus B, Laviale M, Serodio J, da Silva JM (2013) Photoinhibition in benthic diatom assemblages under light stress. *Aquat Microb Ecol* 70:87–92. doi:10.3354/ame01648
- Chukhutsina VU, Büchel C, van Amerongen H (2013) Variations in the first steps of photosynthesis for the diatom *Cyclotella meneghiniana* grown under different light conditions. *Biochim Biophys Acta* 1827:10–18. doi:10.1016/j.bbabi.2012.09.015
- Demmig-Adams B (1990) Carotenoids and photoprotection in plants: a role for the xanthophyll zeaxanthin. *Biochim Biophys Acta* 1020:1–24
- Demmig-Adams B, Adams WW (1992) Carotenoid composition in sun and shade leaves of plants with different life forms. *Plant Cell Environ* 15:411–419. doi:10.1111/j.1365-3040.1992.tb00991.x
- Dera J, Gordon H (1968) Light field fluctuations in the photic zone. *Limnol Oceanogr* 13:697–699
- Dobáková M, Tichý M, Komenda J (2007) Role of the PsbI protein in photosystem II assembly and repair in the cyanobacterium *Synechocystis* sp PCC 6803. *Plant Physiol* 145:1681–1691. doi:10.1104/pp.107.107805
- Eilers P, Peeters J (1988) A model for the relationship between light-intensity and the rate of photosynthesis in phytoplankton. *Ecol Model* 42:199–215
- Falkowski PG, Owens TG (1980) Light-shade adaptation—2 strategies in marine-phytoplankton. *Plant Physiol* 66:592–595. doi:10.1104/pp.66.4.592
- Falkowski PG, Raven JA (2007) Aquatic photosynthesis. 2nd edn. Princeton University Press, New Jersey
- Falkowski P, Wirick C (1981) A simulation model of the effects of vertical mixing on primary productivity. *Mar Biol* 62:69–75
- Finazzi G, Minagawa J (2014) High light acclimation in green microalgae. In: Demmig-Adams B, Adams WW, Garab G, Govindjee (eds) Non-photochemical quenching and energy dissipation in plants, algae and cyanobacteria. Advances in photosynthesis and respiration—including bioenergy and related processes, vol 40. Springer Netherlands, Dordrecht
- Gardian Z, Tichý J, Vácha F (2011) Structure of PSI, PSII and antennae complexes from yellow-green alga *Xanthonema debile*. *Photosynth Res* 108:25–32
- Giovagnetti V, Ruban AV (2015) Discerning the effects of photoinhibition and photoprotection on the rate of oxygen evolution in Arabidopsis leaves. *J Photochem Photobiol B* 152(Part B):272–278. doi:10.1016/j.jphotobiol.2015.09.010
- Goss R, Lepetit B, Wilhelm C (2006) Evidence for a rebinding of antheraxanthin to the light-harvesting complex during the epoxidation reaction of the violaxanthin cycle. *J Plant Physiol* 163:585–590. doi:10.1016/j.jplph.2005.07.009
- Grouneva I, Jakob T, Wilhelm C, Goss R (2009) The regulation of xanthophyll cycle activity and of non-photochemical fluorescence quenching by two alternative electron flows in the diatoms *Phaeodactylum tricorutum* and *Cyclotella meneghiniana*. *Biochim Biophys Acta* 1787:929–938. doi:10.1016/j.bbabi.2009.02.004
- Grouneva I, Rokka A, Aro EM (2011) The thylakoid membrane proteome of two marine diatoms outlines both diatom-specific and species-specific features of the photosynthetic machinery. *J Proteome Res* 10:5338–5353. doi:10.1021/pr200600f
- Hakala M, Tuominen I, Keranen M, Tyystjärvi T, Tyystjärvi E (2005) Evidence for the role of the oxygen-evolving manganese complex in photoinhibition of Photosystem II. *Biochim Biophys Acta* 1706:68–80. doi:10.1016/j.bbabi.2004.09.001
- Havelková-Doušová H, Prášil O, Behrenfeld M (2004) Photoacclimation of *Dunaliella tertiolecta* (Chlorophyceae) under fluctuating irradiance. *Photosynthetica* 42:273–281
- Hogewoning SW, Wientjes E, Douwstra P, Trouwborst G, van Ieperen W, Croce R, Harbinson J (2012) Photosynthetic quantum yield dynamics: from photosystems to leaves. *Plant Cell* 24:1921–1935. doi:10.1105/tpc.112.097972
- Johnson MP, Goral TK, Duffy CD, Brain AP, Mullineaux CW, Ruban AV (2011) Photoprotective energy dissipation involves the reorganization of photosystem II light-harvesting complexes in the grana membranes of spinach chloroplasts. *Plant Cell* 23:1468–1479. doi:10.1105/tpc.110.081646
- Kagawa T et al (2001) Arabidopsis NPL1: a phototropin homolog controlling the chloroplast high-light avoidance response. *Science* 291:2138–2141
- Kaňa R, Vass I (2008) Thermoimaging as a tool for studying light-induced heating of leaves Correlation of heat dissipation with the efficiency of photosystem II photochemistry and non-photochemical quenching. *Environ Exp Bot* 64:90–96. doi:10.1016/j.envexpbot.2008.02.006
- Kaňa R, Lazár D, Prášil O, Naus J (2002) Experimental and theoretical studies on the excess capacity of Photosystem II. *Photosynth Res* 72:271–284. doi:10.1023/a:1019894720789
- Kaňa R, Prášil O, Komárek O, Papageorgiou G, Govindjee (2009) Spectral characteristic of fluorescence induction in a model

- cyanobacterium, *Synechococcus* sp (PCC 7942). *Biochim Biophys Acta* 1787:1170–1178
- Kaňa R, Kotabová E, Kopečná J, Trsková E, Belgio E, Sobotka R, Ruban AV (2016) Violaxanthin inhibits nonphotochemical quenching in light-harvesting antennae of *Chromera velia*. *FEBS Lett* 590:1076–1085
- Kendrick R, Kronenberg G (1994) *Photomorphogenesis in plants*. 2nd edn. Kluwer Academic Publishers, The Netherlands
- Kirk JT (1994) *Light and photosynthesis in aquatic ecosystems*. 2nd edn. Cambridge University press, Cambridge
- Knoppová J, Jianfeng Y, Koník P, Nixon P, Komenda J (2016) CyanoP is involved in the early steps of Photosystem II assembly in the cyanobacterium *Synechocystis* sp PCC 6803. *Plant Cell Physiol* 57:1921–1931
- Kok B (1956) On the inhibition of photosynthesis by intense light. *Biochim Biophys Acta* 21:234–244. doi:10.1016/0006-3002(56)90003-8
- Kolber Z, Falkowski P (1993) Use of active fluorescence to estimate phytoplankton photosynthesis in situ. *Limnol Oceanogr* 38:1646–1665
- Kolber Z, Prášil O, Falkowski P (1998) Measurements of variable chlorophyll fluorescence using fast repetition rate techniques: defining methodology and experimental protocols. *Biochimica et Biophysica Acta* 1367:88–106
- Komenda J, Reisinger V, Müller BC, Dobáková M, Granvogel B, Eichacker LA (2004) Accumulation of the D2 protein is a key regulatory step for assembly of the photosystem II reaction center complex in *Synechocystis* PCC 6803. *J Biol Chem* 279:48620–48629
- Kotabová E, Kaňa R, Jarešová J, Prášil O (2011) Non-photochemical fluorescence quenching in *Chromera velia* is enabled by fast violaxanthin de-epoxidation. *FEBS Lett* 585:1941–1945 doi:10.1016/j.febslet.2011.05.015
- Kotabová E, Jarešová J, Kaňa R, Sobotka R, Bina D, Prášil O (2014) Novel type of red-shifted chlorophyll alpha antenna complex from *Chromera velia*. I. Physiological relevance and functional connection to photosystems. *Biochim Biophys Acta* 1837:734–743 doi:10.1016/j.bbabi.2014.01.012
- Kouřil R, Dekker JP, Boekema EJ (2012) Supramolecular organization of photosystem II in green plants. *Biochim Biophys Acta* 1817:2–12 doi:10.1016/j.bbabi.2011.05.024
- Kouřil R, Wientjes E, Bultema JB, Croce R, Boekema EJ (2013) High-light vs. low-light: effect of light acclimation on photosystem II composition and organization in *Arabidopsis thaliana*. *Biochim Biophys Acta* 1827:411–419 doi:10.1016/j.bbabi.2012.12.003
- Küpper H, Setlik I, Spiller M, Küpper FC, Prášil O (2002) Heavy metal-induced inhibition of photosynthesis: targets of in vivo heavy metal chlorophyll formation. *J Physiol* 38:429–441. doi:10.1046/j.1529-8817.2002.t01-1-01148.x
- Lavaud J, Strzpek RF, Kroth PG (2007) Photoprotection capacity differs among diatoms: Possible consequences on the spatial distribution of diatoms related to fluctuations in the underwater light climate. *Limnol Oceanogr* 52:1188–1194
- Leong TY, Anderson JM (1984) Adaptation of the thylakoid membranes of pea-chloroplasts to light intensities 0.1. study on the distribution of chlorophyll-protein complexes. *Photosynth Res* 5:105–115. doi:10.1007/bf00028524
- Lepetit B, Volke D, Szabo M, Hoffmann R, Garab GZ, Wilhelm C, Goss R (2007) Spectroscopic and molecular characterization of the oligomeric antenna of the diatom *Phaeodactylum tricornutum*. *Biochemistry* 46:9813–9822. doi:10.1021/bi7008344
- Lepetit B, Volke D, Gilbert M, Wilhelm C, Goss R (2010) Evidence for the existence of one antenna-associated, lipid-dissolved and two protein-bound pools of diadinoxanthin cycle pigments in diatoms. *Plant Physiol* 154:1905–1920. doi:10.1104/pp.110.166454
- Lichtenthaler HK, Burkard G, Kuhn G, Prenzel U (1981) Light-induced accumulation and stability of chlorophylls and chlorophyll-proteins during chloroplast development in radish seedlings. *ZNaturforsch(C)* 36:421–430
- Mann M, Hoppenz P, Jakob T, Weisheit W, Mittag M, Wilhelm C, Goss R (2014) Unusual features of the high light acclimation of *Chromera velia*. *Photosynth Res*. doi:10.1007/s1120-014-0019-3
- Moore RB et al (2008) A photosynthetic alveolate closely related to apicomplexan parasites. *Nature* 451:959–963. doi:10.1038/nature06635
- Morosinotto T, Bassi R, Frigerio S, Finazzi G, Morris E, Barber J (2006) Biochemical and structural analyses of a higher plant photosystem II supercomplex of a photosystem I-less mutant of barley—consequences of a chronic over-reduction of the plastoquinone pool. *FEBS J* 273:4616–4630. doi:10.1111/j.1742-4658.2006.05465.x
- Nixon PJ, Michoux F, Yu JF, Boehm M, Komenda J (2010) Recent advances in understanding the assembly and repair of photosystem II. *Ann Bot* 106:1–16. doi:10.1093/aob/mcq059
- Niyogi KK (1999) Photoprotection revisited: genetic and molecular approaches. *Annu Rev Plant Physiol Plant Mol Biol* 50:333–359 doi:10.1146/annurev.arplant.50.1.333
- Oborník M, Vancová M, Lai DH, Janoušek J, Keeling PJ, Lukeš J (2011) Morphology and ultrastructure of multiple life cycle stages of the photosynthetic relative of apicomplexa, *Chromera velia*. *Protist* 162:115–130. doi:10.1016/j.protis.2010.02.004
- Oguchi R, Hikosaka K, Hirose T (2003) Does the photosynthetic light-acclimation need change in leaf anatomy? *Plant Cell Environ* 26:505–512. doi:10.1046/j.1365-3040.2003.00981.x
- Ohnishi N, Allakhverdiev SI, Takahashi S, Higashi S, Watanabe M, Nishiyama Y, Murata N (2005) Two-step mechanism of photodamage to photosystem II: step 1 occurs at the oxygen-evolving complex and step 2 occurs at the photochemical reaction center. *Biochemistry* 44:8494–8499. doi:10.1021/bi047518q
- Pesaresi P et al (2009) Mutants, overexpressors, and interactors of *Arabidopsis* plastocyanin isoforms: revised roles of plastocyanin in photosynthetic electron flow and thylakoid redox state. *Mol Plant* 2:236–248 doi:10.1093/mp/ssn041
- Porra R, Thompson W, Kriedemann P (1989) Determination of accurate extinction coefficients and simultaneous equations for assaying chlorophylls a and b extracted with four different solvents: verification of the concentration of chlorophyll standards by atomic absorption spectrometry. *Biochim Biophys Acta* 975:384–394
- Powles SB (1984) Photoinhibition of Photosynthesis Induced by Visible-Light. *Annu Rev Plant Physiol Plant Mol Biol* 35:15–44 doi:10.1146/annurev.pp.35.060184.000311
- Prášil O, Adir N, Ohad I (1992) Dynamics of photosystem II: mechanism of photoinhibition and recovery processes. In: Barber J (ed) *The Photosystems: structure, function and molecular biology*, vol 11. Elsevier, Amsterdam, pp 293–348
- Pyke K (2009) *Plastid biology*. *Plastid biology*. Cambridge University Press, Cambridge. doi:10.1017/cbo9780511626715
- Quigg A et al (2012) Photosynthesis in *Chromera velia* represents a simple system with high efficiency. *PLoS ONE* 7:e47036. doi:10.1371/journal.pone.0047036
- Roach T, Krieger-Liszka A (2014) Regulation of photosynthetic electron transport and photoinhibition. *Curr Protein Pept Sci* 15:351–362
- Roberty S, Bailleul B, Berne N, Franck F, Cardol P (2014) PSI Mehler reaction is the main alternative photosynthetic electron pathway in *Symbiodinium* sp., symbiotic dinoflagellates of cnidarians. *New Phytol* 204:81–91. doi:10.1111/nph.12903
- Ruban A (2013) *The photosynthetic membrane*. *Molecular mechanisms and biophysics of light harvesting*. Wiley, United Kingdom

- Ruban AV, Murchie EH (2012) Assessing the photoprotective effectiveness of non-photochemical chlorophyll fluorescence quenching: A new approach. *Biochim Biophys Acta* 1817:977–982. doi:10.1016/j.bbabi.2012.03.026
- Ruban A et al (2006) Plasticity in the composition of the light harvesting antenna of higher plants preserves structural integrity and biological function. *J Biol Chem* 281:14981–14990
- Ruban AV, Johnson MP, Duffy CD (2012) The photoprotective molecular switch in the photosystem II antenna. *Biochim Biophys Acta* 1817:167–181. doi:10.1016/j.bbabi.2011.04.007
- Schöttler MA, Tóth SZ (2014) Photosynthetic complex stoichiometry dynamics in higher plants: environmental acclimation and photosynthetic flux control. *Front Plant Sci* 5. doi:10.3389/fpls.2014.00188
- Suggett DJ, Moore MC, Geider RJ (2010) Estimating aquatic productivity from active fluorescence measurement. In: Suggett DJ PO, Borowitzka MA (eds) *Chlorophyll a fluorescence in aquatic sciences: methods and applications*. Springer, Dordrecht, pp 103–127
- Terashima I, Miyazawa SI, Hanba YT (2001) Why are sun leaves thicker than shade leaves? Consideration based on analyses of CO<sub>2</sub> diffusion in the leaf. *J Plant Res* 114:93–105. doi:10.1007/pl00013972
- Tichý J et al (2013) Light harvesting complexes of *Chromera velia*, photosynthetic relative of apicomplexan parasites. *Biochim Biophys Acta* 1827:723–729. doi:10.1016/j.bbabi.2013.02.002
- Tikkanen M et al (2006) State transitions revisited—a buffering system for dynamic low light acclimation of *Arabidopsis*. *Plant Mol Biol* 62:779–793. doi:10.1007/s11103-006-9044-8
- Tyystjärvi E, Aro EM (1996) The rate constant of photoinhibition, measured in lincomycin-treated leaves, is directly proportional to light intensity. *Proc Natl Acad Sci USA* 93:2213–2218. doi:10.1073/pnas.93.5.2213
- van Kooten O, Snel J (1990) The use of chlorophyll fluorescence nomenclature in plant stress physiology. *Photosynth Res* 25:147–150
- Walters RG (2005) Towards an understanding of photosynthetic acclimation. *J Exp Bot* 56:435–447. doi:10.1093/jxb/eri060
- Ware MA, Belgio E, Ruban AV (2015) Photoprotective capacity of non-photochemical quenching in plants acclimated to different light intensities. *Photosynth Res* 126:261–274. doi:10.1007/s11120-015-0102-4
- Wientjes E, van Amerongen H, Croce R (2013) Quantum yield of charge separation in photosystem II: functional effect of changes in the antenna size upon light acclimation. *J Phys Chem B* 117:11200–11208. doi:10.1021/jp401663w



## Supporting material

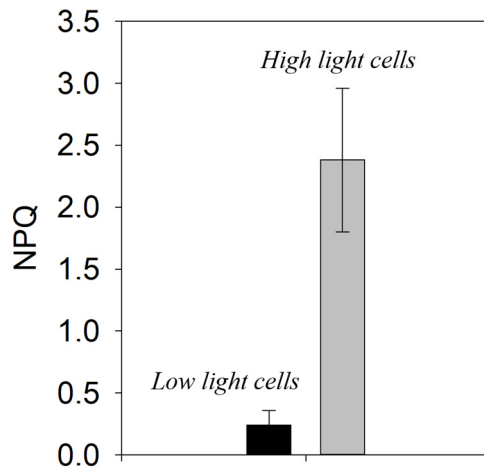


**Figure S1:** Comparison between total NPQ of low and high light adapted *C. velia* cells calculated as  $(F_m - F_m')/F_m'$  at the end of the illumination cycle of the relative fluorescence curves as representatively shown in Figure 1. Actinic light was  $750 \mu\text{mol m}^{-2}\text{s}^{-1}$ . Data are means  $\pm$  standard deviation from at least three independent replicates.

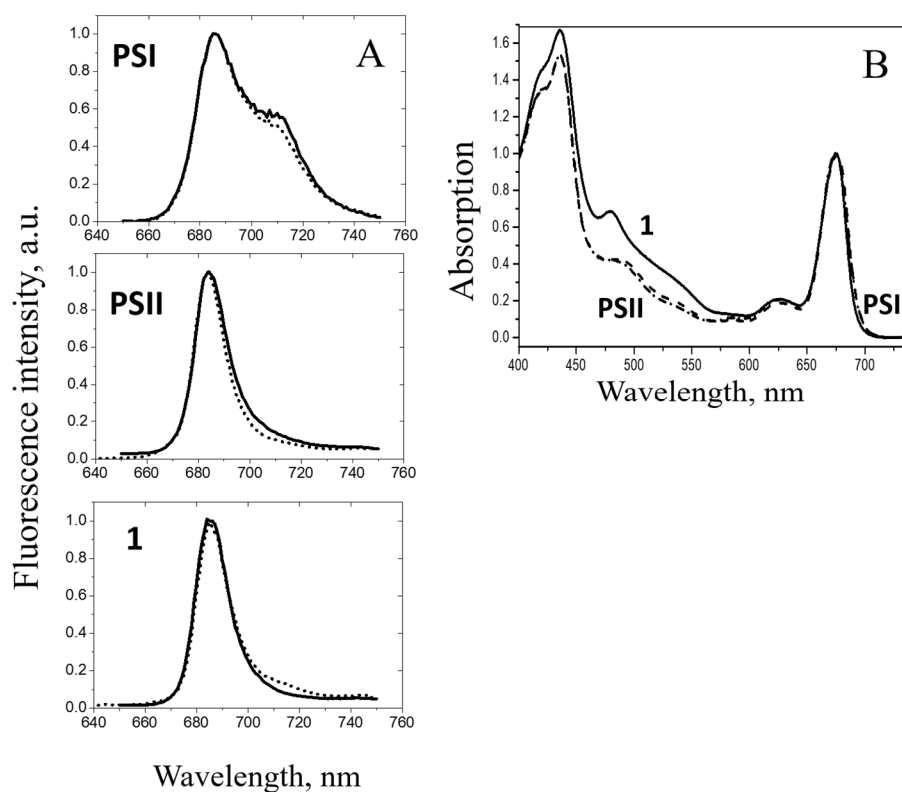


**Figure S2:** Low temperature fluorescence (A) and room temperature absorption (B) spectra of FPLC fractions from Figure 2. The names of the relative fractions are indicated next to the relative spectra. **A:** solid: low light FPLC elutions; dotted, high light FPLC elutions. **B:** low light FPLC spectra. Similar spectra were found for high light fractions.



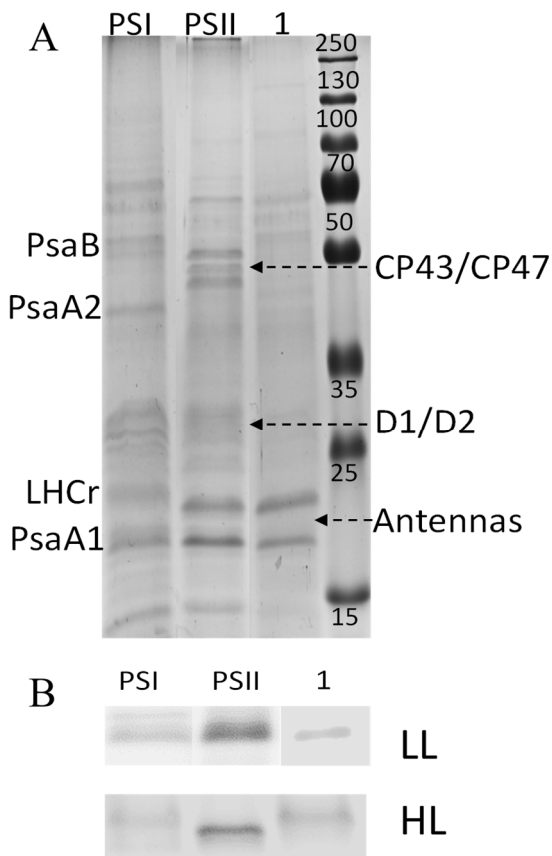


**Figure S3:** Typical SDS-page (A) and Western blotting (B) results of FPLC fractions. Names on top of the lanes correspond to the relative FPLC elutions as presented in Figure 2. The amount of chlorophyll in each lane was 15  $\mu\text{g}$ . (A) Coomassie Brilliant Blue staining result of high light (HL) FPLC fractions. A similar pattern was found for LL. (B) Results from high light (HL) and low light (LL) fractions. Signal detected using  $\alpha$ -D1 antibody. Gel preparation was according to Komenda et al. 2004 and Dobáková et al. 2007.

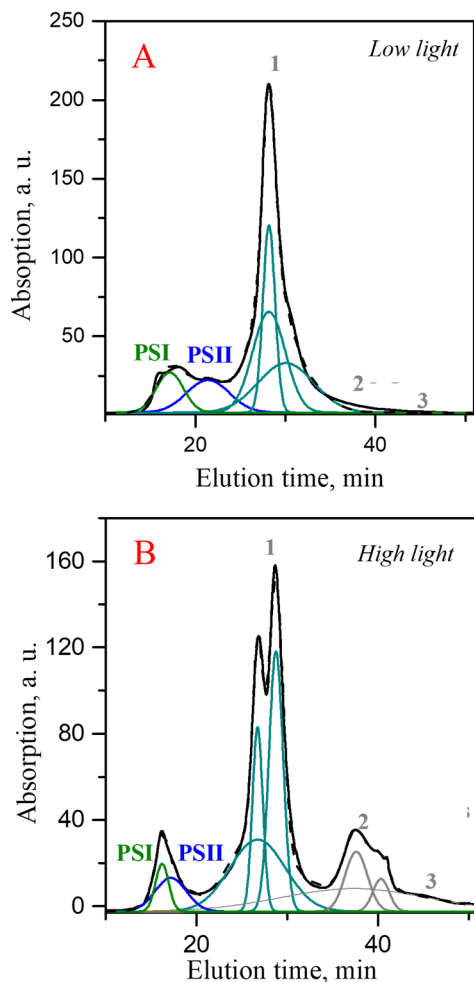


**Figure S4:** Decomposition of the FPLC elution profiles shown in Figure 2 and reported here in solid black line. (A) low light membranes; (B) high light membranes. The fit (dashed black line) was obtained using the Gaussian fit multi-peak option of Originlab program providing the number and positions of the peaks to fit the spectrum. PSI, Photosystem I supercomplex; PSII, Photosystem II complex; 1, oligomeric antenna complexes; 2, monomeric antenna complexes, 3 free pigments.

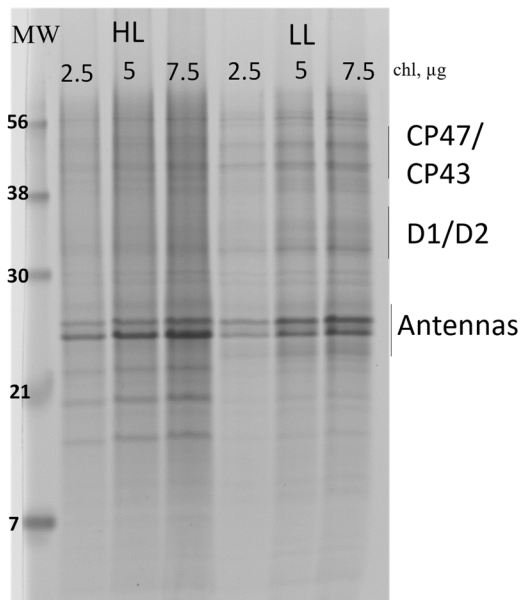


**Figure S5:** Typical SDS-page result of low (LL) and high (HL) light membranes. Numbers on top of the lanes correspond to the amount of chlorophyll per lane (chl,  $\mu\text{g}$ ). Gel preparation was according to (see Komenda et al. 2004 and Dobáková et al. 2007). Signals were analyzed using Image-J program as described in Materials and Methods. MW, approximate molecular weight in kDa.

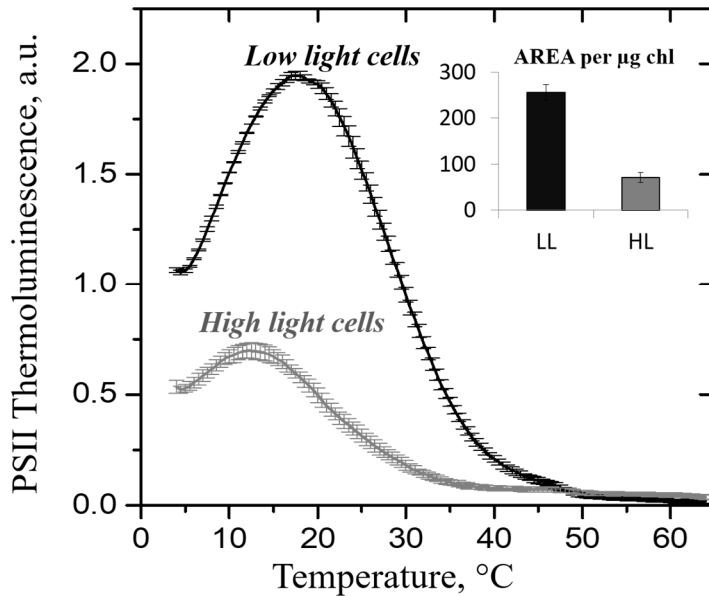


**Figure S6:** Thermo-luminescence signal of high (grey) and low (black) light acclimated *C. velia* cells. Both types of cells were dark-adapted for 30 min before the measurements. The inset shows the calculated area per chlorophyll below each thermo-luminescence trace. For more details, see Materials and Methods and (Küpper et al. 2002).

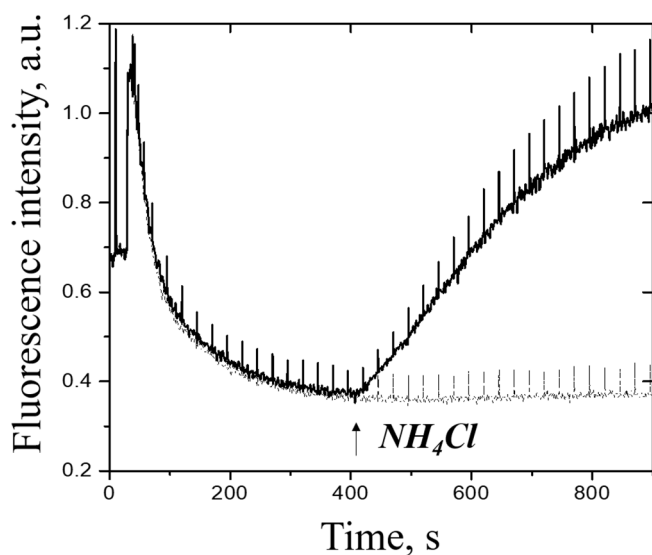


**Figure S7:** Representative chlorophyll *a* fluorescence quenching analysis showing the effect of the uncoupler  $\text{NH}_4\text{Cl}$  during actinic illumination on the NPQ of high light acclimated *C. velia* cells. Dashed, control (no  $\text{NH}_4\text{Cl}$ ); solid line, effect of  $\text{NH}_4\text{Cl}$  addition. The timing of application of  $\text{NH}_4\text{Cl}$  is marked by an arrow. Actinic light was on during the entire experiment.

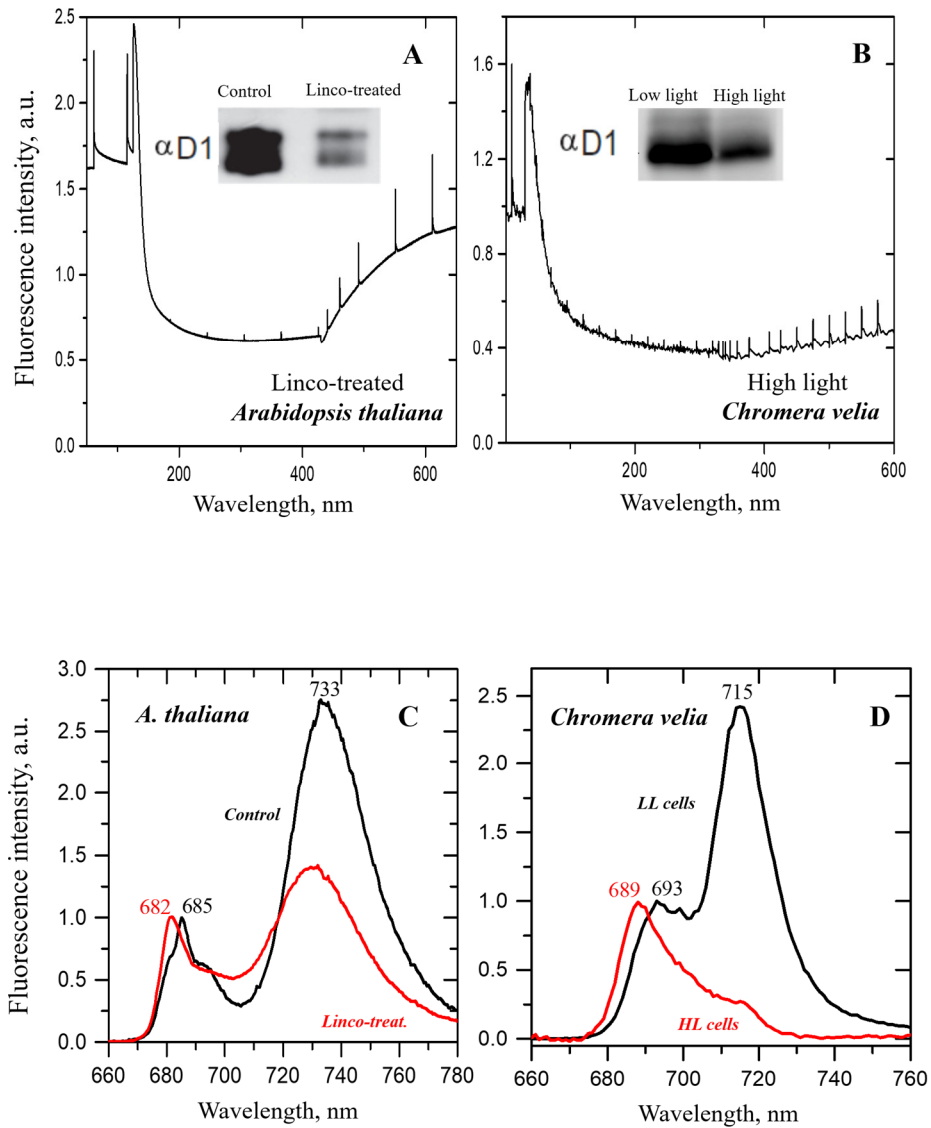


**Figure S8:** Comparison showing similarities between lincomycin-treated *Arabidopsis thaliana* (A, C) and *Chromera velia* (B, D). Top: pulse-modulated fluorimetry traces and Western blotting results; bottom: 77 K fluorescence. Data for *A. thaliana* were taken from Belgio et al. 2012.

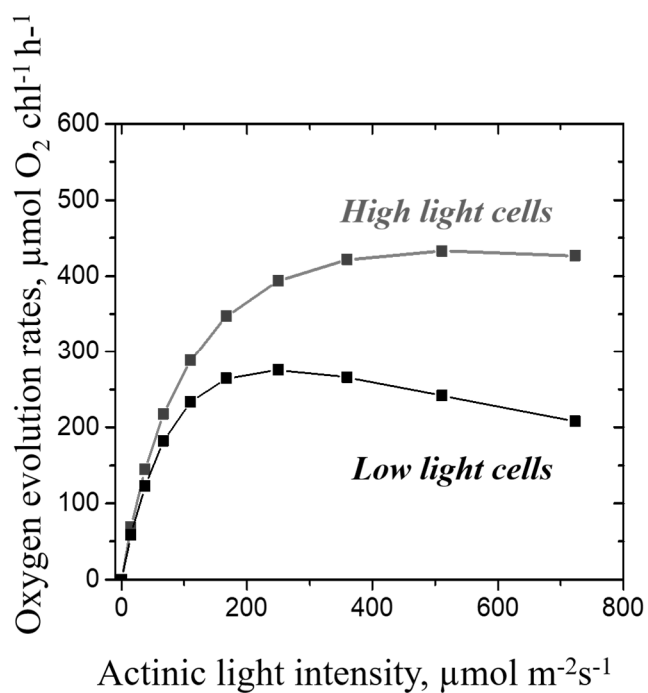


**Figure S9:** Comparison between representative Photosynthesis *versus* light curve of high light and low light acclimated cells measured under different actinic light intensities (for more details, see Materials and Methods).





**ARTICLE III**

**Antenna proton sensitivity determines photosynthetic light  
harvesting strategy**

Kuthanová Trsková, E., Belgio, E., Yeates, A. M., Sobotka, R., Ruban,  
A. V., and Kaňa, R.

(2018)

*Journal of Experimental Botany* **69**, 4483-4493. IF = 5.36





RESEARCH PAPER

# Antenna proton sensitivity determines photosynthetic light harvesting strategy

Eliška Kuthanová Trsková<sup>1,2</sup>, Erica Belgio<sup>1,\*</sup>, Anna M. Yeates<sup>1</sup>, Roman Sobotka<sup>1,2</sup>, Alexander V. Ruban<sup>3</sup> and Radek Kaňa<sup>1,2,\*</sup>

<sup>1</sup> Institute of Microbiology, Academy of Sciences of the Czech Republic, Opatovický mlýn, 379 81 Třeboň, Czech Republic

<sup>2</sup> University of South Bohemia in České Budějovice, Faculty of Science, Branišovská 31a, 370 05 České Budějovice, Czech republic

<sup>3</sup> School of Biological and Chemical Sciences, Queen Mary University of London, London, UK

\* Correspondence: [belgio@alga.cz](mailto:belgio@alga.cz) or [kana@alga.cz](mailto:kana@alga.cz)

Received 7 March 2018; Editorial decision 22 June 2018; Accepted 26 June 2018

Editor: Roland Pieruschka, Forschungszentrum Jülich, Germany

## Abstract

Photoprotective non-photochemical quenching (NPQ) represents an effective way to dissipate the light energy absorbed in excess by most phototrophs. It is often claimed that NPQ formation/relaxation kinetics are determined by xanthophyll composition. We, however, found that, for the alveolate alga *Chromera velia*, this is not the case. In the present paper, we investigated the reasons for the constitutive high rate of quenching displayed by the alga by comparing its light harvesting strategies with those of a model phototroph, the land plant *Spinacia oleracea*. Experimental results and *in silico* studies support the idea that fast quenching is due not to xanthophylls, but to intrinsic properties of the *Chromera* light harvesting complex (CLH) protein, related to amino acid composition and protein folding. The  $pK_a$  for CLH quenching was shifted by 0.5 units to a higher pH compared with higher plant antennas (light harvesting complex II; LHClI). We conclude that, whilst higher plant LHClIs are better suited for light harvesting, CLHs are 'natural quenchers' ready to switch into a dissipative state. We propose that organisms with antenna proteins intrinsically more sensitive to protons, such as *C. velia*, carry a relatively high concentration of violaxanthin to improve their light harvesting. In contrast, higher plants need less violaxanthin per chlorophyll because LHClI proteins are more efficient light harvesters and instead require co-factors such as zeaxanthin and PsbS to accelerate and enhance quenching.

**Keywords:** *Chromera velia*, *in vitro* quenching, light harvesting strategy, non-photochemical quenching, NPQ kinetics, photoprotection, quenching  $pK_a$ , violaxanthin.

## Introduction

Although under low light more than 83% of absorbed photons can be converted into chemical energy (e.g. Jennings *et al.*, 2005; Wientjes *et al.*, 2013), prolonged high light exposure rapidly switches photosystems to energy-dissipating states that release excess energy as heat (Demmig-Adams, 1990; Kaňa and Vass, 2008; Ruban *et al.*, 2012). The switch from light-harvesting

to energy-dissipation mode has long been investigated, resulting in various models for various autotrophs (Demmig-Adams, 1990; Horton *et al.*, 1996; Kaňa *et al.*, 2012; Pinnola *et al.*, 2013; Erickson *et al.*, 2015; Büchel, 2015).

In higher plants, several processes contribute to excess light energy dissipation, but only the pH-dependent one, the

Abbreviations: CLH, *Chromera* light harvesting complex; DCCD, dicyclohexylcarbodiimide; DEPS, xanthophyll cycle de-epoxidation state; LHClI, light harvesting complex II; NPQ, non-photochemical quenching.

© The Author(s) 2018. Published by Oxford University Press on behalf of the Society for Experimental Biology.

This is an Open Access article distributed under the terms of the Creative Commons Attribution License (<http://creativecommons.org/licenses/by/4.0/>), which permits unrestricted reuse, distribution, and reproduction in any medium, provided the original work is properly cited.

so-called energy-dependent quenching mechanism (non-photochemical quenching; NPQ) is considered photoprotective (Demmig-Adams and Adams, 1992; Ruban, 2013). Proof of a strict connection between NPQ and pH is that reverse ATPase activity can stimulate NPQ even in the dark (Gilmore and Yamamoto, 1992). Besides controlling xanthophyll cycle activity, in several phototrophs pH exerts a direct control on NPQ. This is thought to act via a regulation of antennas (e.g. Dekker and Boekema, 2005; Horton *et al.*, 2008; Peers *et al.*, 2009; Grossman *et al.*, 2010). Indeed, a very similar thermal dissipation process to that *in vivo* can be induced *in vitro* in purified antennas by lowering pH and detergent concentration (Ruban *et al.*, 1994a). Starting from this evidence, it was proposed that antenna aggregation is at the basis of the NPQ process (Horton *et al.*, 1996), and subsequent findings employing liposomes started to clarify how pH and ions together with lipids and lipid to antenna ratios control the 'aggregation state' of antennas (Moya *et al.*, 2001; Kirchoff *et al.*, 2008; Akhtar *et al.*, 2015; Kaňa and Govindjee, 2016; Natali *et al.*, 2016; Crisafi and Pandit, 2017). In higher plants, antennas are the site of energy dissipation, whilst xanthophylls and the PsbS protein seem to be simply controllers of the process (Noctor *et al.*, 1991; Walters *et al.*, 1994; Li *et al.*, 2000; Betterle *et al.*, 2009). Evidence that *npq1*, a mutant lacking zeaxanthin, and *npq4*, a mutant without PsbS, could both perform NPQ indicated their dispensability, thus placing antennas and pH as the *only* key elements of the process (Niyogi, 1999; Johnson *et al.*, 2009; Johnson *et al.*, 2011). Nevertheless, xanthophylls play an important role modulating the kinetics of NPQ activation and dissipation (Johnson *et al.*, 2010). Pre-conditioning of leaves with light exposure, for instance, makes NPQ fast and persistent because of the conversion of violaxanthin into zeaxanthin (Ruban and Horton, 1999). Zeaxanthin, a highly hydrophobic pigment, in turn, makes antennas more dehydrated and therefore sensitive to pH and prone to quench compared with violaxanthin-enriched antennas. Interestingly, this idea was put forward not only for higher plant antennas (Ruban *et al.*, 1994a), but also for antennas from distant organisms such as diatoms (Gundermann and Büchel, 2008), brown algae (Ocampo-Alvarez *et al.*, 2013) and alveolates (Kaňa *et al.*, 2016).

The state-of-the-art model of NPQ for plants claims that, under high light, lumen acidification induces antenna protonation, which in turn triggers protein conformational changes, aggregation and energy dissipation. However, it seems that pre-aggregation *in vivo* can affect efficiency of antenna protonation and *vice versa* (e.g. Petrou *et al.*, 2014). Optical changes induced by aggregation can be visualized spectroscopically (Lokstein *et al.*, 2002), specifically as an increase in the fluorescence yield of red-shifted emission from antennas at low temperatures (Ruban *et al.*, 1991; Bassi and Dainese, 1992; Miloslavina *et al.*, 2008; Belgio *et al.*, 2012). Based on dicyclohexylcarbodiimide (DCCD) binding and mutagenesis work (Ruban *et al.*, 1998; Belgio *et al.*, 2013; Ballottari *et al.*, 2016), it was concluded that sensors for low pH are negatively charged residues located in a lumen-exposed antenna protein loop and in the C-terminus. Once protonated, those residues become neutral, thus making the whole protein more hydrophobic and easier to aggregate

and quench. Although *in vitro* fluorescence quenching as a function of pH has been observed for various types of antennas (Gundermann and Büchel, 2012; Kaňa *et al.*, 2012; Schaller-Laudel *et al.*, 2015), identification of putative protonable residues so far concerned mainly antennas from the green lineage (Ruban *et al.*, 1998; Li *et al.*, 2004; Liguori *et al.*, 2013; Belgio *et al.*, 2013; Ballottari *et al.*, 2016).

Despite the progress in our understanding of NPQ in higher plants, this subject has been less explored in algae. The alveolate *Chromera velia* represents an interesting system in this context, as it shows efficient non-photochemical quenching (Kotabová *et al.*, 2011; Quigg *et al.*, 2012; Mann *et al.*, 2014) with similarities on the one side to higher plants, and on the other to brown algae and diatoms (see below). Isolated from stony corals from Sidney harbor, this facultative symbiont is globally distributed in the marine environment at depths not exceeding 5 m (Obornik and Lukes, 2013). The phylogenetic origin of the alga is complex. *C. velia* is an alveolate, and therefore closely related to dinoflagellates and other algae in the SAR clade (such as diatoms and brown algae), but all phylogenetic analyses have invariably demonstrated its genuine relationship to apicomplexan parasites (Obornik *et al.*, 2016). In any case, *C. velia* is considered a 'red-clade' alga, i.e. an alga whose chloroplast was obtained by secondary endosymbiosis from a red algal ancestor (Kotabová *et al.*, 2011; Sobotka *et al.*, 2017). In *C. velia*, NPQ is connected to the xanthophyll cycle (Kotabová *et al.*, 2011) as in brown algae (Ocampo-Alvarez *et al.*, 2013); however, differing from them (Garcia-Mendoza *et al.*, 2011) but similar to diatoms (Ruban *et al.*, 2004; Lavaud and Kroth, 2006; Grouneva *et al.*, 2008), its activation is extremely fast (almost monophasic) and pH-dependent (see Belgio *et al.*, 2018).

In the present paper, we investigated the reasons for the characteristic high rate of quenching displayed by the alga. We compared the NPQ of *C. velia* with that of a higher plant (a well-known system) and showed that the mechanism of heat dissipation and in particular NPQ activation is different in the two evolutionarily distant phototrophs. Our data indicated that the *Chromera* light harvesting complex (CLH) is more sensitive to protons than the higher plant antenna (light harvesting complex II; LHCII). We propose that protonation of the antenna is the basis of the 'constitutively' fast NPQ found in *C. velia* and, as previously suggested for diatoms (Lavaud and Kroth, 2006; Lavaud and Lepetit, 2013),  $\Delta$ pH by itself is important for NPQ activation. This conclusion might also explain the unusual high light acclimation strategy recently reported for *C. velia*, consisting of a decrease in reaction centers whilst still maintaining a full antenna content (Belgio *et al.*, 2018).

## Materials and methods

### Plant material

*Chromera velia* (strain RM12) was grown in artificial sea water with additional *f/2* nutrients (Guillard and Ryther, 1962). Cells were cultivated in glass tubes at 28 °C, in a continuous light regime of 200  $\mu\text{mol m}^{-2} \text{s}^{-1}$  while aerated with air.

*Spinacia oleracea* (spinach) was purchased from a local supermarket. Intact chloroplasts were prepared as previously described (Crouchman *et al.*, 2006).

### Isolation of *C. velia* and plant light harvesting complexes

*C. velia* cells were broken and solubilized as described in Kaňa *et al.* (2016) and then loaded on a fresh, continuous 5–15% sucrose density gradient prepared using a home-made gradient maker in buffer containing 25 mM HEPES pH 7.8 and 0.04% *n*-dodecyl  $\beta$ -D-maltoside ( $\beta$ -DM). The ultracentrifugation was performed at 140 000 *g* at 4 °C for 20 h (with rotor SW28, for 40 ml tubes, of an L8-M ultracentrifuge; Beckmann, USA). The resulting band no. 2 contained a strong double band at 18 and 19 kDa, previously identified as 'fucoxanthin chlorophyll *a/c* binding protein (FCP)-like antenna' (Tichy *et al.*, 2013). The band analysis by Pan *et al.*, (2012) and Tichy *et al.* (2013) placed this antenna protein within the main FCP-like group of light-harvesting complexes and so it was named *Chromera* light harvesting complex (CLH).

After separation by sucrose gradient, the antenna protein was desalted using a PD10 column (GE Healthcare) in a buffer containing 20 mM HEPES (pH 7.6) and 0.01% (w/v)  $\beta$ -DM. Spinach LHCIIb was isolated as previously described (Ruban *et al.*, 1994b) and then purified, desalted and eluted in the same buffer as CLH. In both cases, antennas were isolated from samples dark-adapted for 30–45 min.

### Non-photochemical fluorescence quenching in native cells and isolated chloroplasts

Chlorophyll fluorescence was measured using a double modulation fluorometer FL-3000 (Photon System Instruments, Czech Republic). A multiple turnover saturating flash was applied to measure the maximum quantum yield of the photochemistry of photosystem II ( $F_v/F_m$ ) according to  $(F_m - F_0)/F_m$ , where the difference between the maximum ( $F_m$ ) and minimum ( $F_0$ ) fluorescence is used to calculate the variable fluorescence ( $F_v$ ) (van Kooten and Snel, 1990). Cells were then illuminated with an orange actinic light (625 nm, 500  $\mu$ mol photons  $m^{-2} s^{-1}$ ), during which periodic saturating flashes were applied. NPQ was calculated as  $(F_m - F_m')/F_m$  or  $F_m'$ , where  $F_m'$  is the maximum fluorescence measured in the presence of actinic light. Non-photochemical quenching of fluorescence was measured in whole cells of *C. velia* (chlorophyll concentration 0.7  $\mu$ g  $ml^{-1}$ ) and isolated spinach chloroplasts (chlorophyll concentration 1.4  $\mu$ g  $ml^{-1}$ ). NPQ formation rates (NPQ as a function of time) in different xanthophyll cycle de-epoxidation states (DEPSs) were determined from the measured fluorescence traces as described in the 'Data analysis and model fitting' section.

Where indicated (Fig. 2; Supplementary Fig. S1 at JXB online), the effect of an uncoupler on the fluorescence quenching was examined by adding  $NH_4Cl$  (final concentration of 15 mM) at different time points of the measuring protocol.

### In vitro fluorescence quenching of antennas

Isolated antennas ( $OD_{676}=1 cm^{-1}$ ), solubilized in 0.01% DM, were diluted 20 times, while constantly stirring, in a room temperature buffer containing 10 mM sodium citrate and 10 mM Tris-HCl and adjusted with small drops of HCl to give the desired pH (for further details see Ruban *et al.*, 1994a; Belgio *et al.*, 2013). Chlorophyll fluorescence was continuously monitored using an FL 3000 fluorometer (PSI, Czech Republic, blue excitation at 464 nm, 184  $\mu$ mol  $m^{-2} s^{-1}$ ). The  $pK_a$  values for quenching kinetics were calculated as described in the 'Data analysis and model fitting' section.

### Absorption measurement

Absorption spectra were recorded with a Unicam UV 500 spectrometer (Thermo Spectronic, UK).

### Pigment extraction and HPLC analysis

Cells or chloroplasts were collected on GF/F filters (Whatman, UK) and soaked in 100% methanol (overnight at  $-20$  °C) and disrupted using a mechanical tissue grinder. Filter and cell debris were removed by centrifugation (12 000 *g*, 15 min) and the supernatant used for absorbance measurements at 652, 665, and 730 nm. Chlorophyll concentration was

determined according to Porra *et al.* (1989). HPLC was carried out on an Agilent 1200 chromatography system equipped with a diode array detector. Pigments were separated on a Luna Phenomenex C8 (2) column (particle size, 3  $\mu$ m; pore size, 100 Å; dimensions, 100  $\times$  4.6 mm), by applying a 0.028 M ammonium acetate-MeOH gradient (20/80) as described in (Kotabová *et al.*, 2011) and the eluted pigments were quantified at 440 nm. The de-epoxidation state of the xanthophyll cycle pigments (DEPS) was calculated as: (zeaxanthin+0.5 antheraxanthin)/(violaxanthin+antheraxanthin+zeaxanthin) (Johnson *et al.*, 2009; Kotabová *et al.*, 2011; Oborník *et al.*, 2011). For purified antennas, the same procedure was applied simply skipping the first step of filtration through GF/F filter.

### Zeaxanthin enrichment

Plant chloroplasts and *C. velia* cells with a DEPS of 10% were obtained from dim-light-adapted samples (30 min). Enrichment in zeaxanthin was achieved as described previously (Ruban *et al.*, 1994b; Belgio *et al.*, 2014) by pre-conditioning leaves with 350  $\mu$ mol photons  $m^{-2} s^{-1}$  under 98%  $N_2$  for 20–40 min for 20% and 40% DEPS, respectively. For *C. velia*, 10 min illumination with 500  $\mu$ mol photons  $m^{-2} s^{-1}$  was sufficient to obtain 40% DEPS, in agreement with what has been previously published (Kotabová *et al.*, 2011). DEPS was assessed by immediate incubation in methanol followed by HPLC analysis (see 'Pigment extraction and HPLC analysis' section).

### In silico studies

For *in silico* studies, the LHCIIb structure resolved at 2.5 Å resolution (PDB code: 2BHW; Standfuss *et al.*, 2005) was employed. The structure of the CLH polypeptide (Cvelial\_19753.t1 taken from Tichy *et al.* (2013)) was predicted using Phyre2 (<http://www.sbg.bio.ic.ac.uk/phyre2/html/page.cgi?id=index>) and YASARA software (<http://www.yasara.org>). The protonation states of protein ionizable groups were computed in both cases using the H++ program (<http://biophysics.cs.vt.edu>), an automated system that calculates  $pK_a$  values of ionizable groups in macromolecules and adds missing hydrogen atoms according to the specified pH of the environment. Results shown for LHCIIb are relative to chain A, but results for chains B and C were very similar, in agreement with (Xiao *et al.*, 2012). As recommended for typical physiological conditions and deeply buried residues, the external dielectric value was set to 80, the internal dielectric value to 4, salinity to 0.15 and pH to 7.5.

### Data analysis and model fitting

NPQ formation rates (NPQ in function of time; see Fig. 1) were determined using a well-established methodology valid for both algae and vascular plants (see Seródio and Lavaud (2011) concerning the applicability of the Hill equation to NPQ in algae). Briefly, average data from three to six independent measurements of *C. velia* cells and spinach chloroplasts in different DEPSs were fitted using the sigmoidal Hill equation three-parameter implementation in SigmaPlot 12.5 (Systat Software, Inc., San Jose, CA, USA). The standard error of the estimate was between 0.02 and 0.08, meaning that ~95% of the data fell within 2% of the fitted line; moreover  $R^2$  values were above 0.97, thus confirming the appropriateness of the approach.

In order to determine the quenching  $pK_a$  of antennas, we used a method previously established for various antennas including mutants (Ruban *et al.*, 1994a; Ruban and Horton, 1999; Belgio *et al.*, 2013; Zaks *et al.*, 2013). Briefly, the relationship between quenching kinetics and pH (see Fig. 4) and relative parameters (Table 1) were obtained from experiments like the one shown in Fig. 3 as follows. Quenching kinetics were calculated at each pH point by fitting the measured traces (Fig. 3) with the three-parameter hyperbolic decay function:  $y=(y_0+ab)/(b+x)$  where  $1/b$  represents the rate of the process. Then the data points from Fig. 4 were fitted by the sigmoidal Hill equation  $y=[ax^c]/[e^c+x^c]$  in order to obtain Hill coefficients ( $b$ ),  $pK_a$  values ( $c$ ) and quenching kinetics at pH 4.97 (see also (Johnson *et al.*, 2012; Petrou *et al.*, 2014). The standard error of the estimate was again low (below 0.1) and  $R^2$  above 0.90, confirming the validity of the approach.

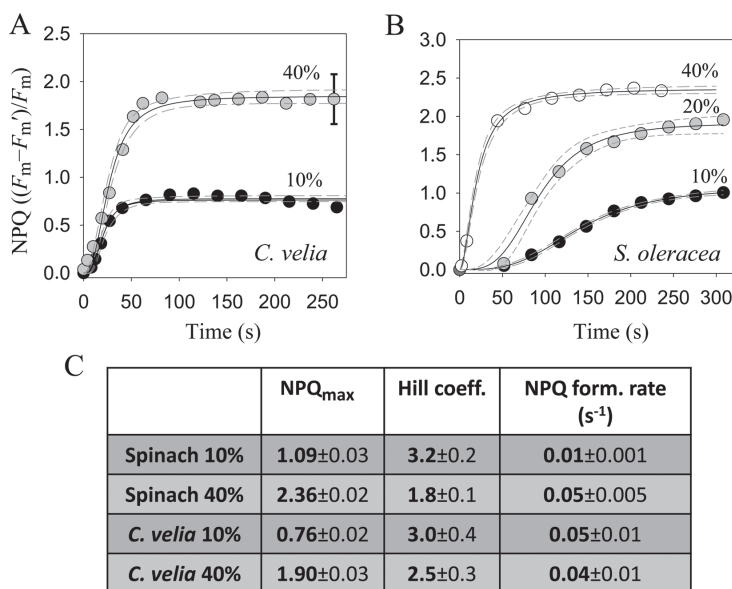


**Fig. 1.** Fast NPQ formation rate in *C. velia*. Comparison between NPQ formation in *C. velia* cells (A) and intact spinach chloroplasts (B) in different de-epoxidation states (10, 20, or 40%). Circles, average data from three to six independent measures; solid lines, fittings; dashed lines, 95% confidence intervals. The error bar shows a typical standard deviation of the data. (C) Fitting parameters and relative errors obtained using the sigmoidal Hill equation  $y=[ax^b]/[c^b+x^b]$ , where  $a$  is NPQ<sub>max</sub>,  $b$  is the sigmoidicity parameter (Hill coefficient) and  $1/c$  is NPQ formation rate (for more details, see 'Materials and methods').

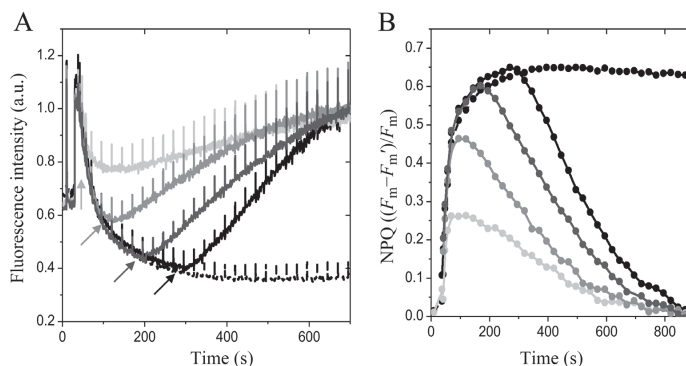


**Fig. 2.** NPQ of *Chromera velia* cells is  $\Delta$ pH-dependent. (A) Representative fluorescence induction traces showing the effect of the uncoupler  $\text{NH}_4\text{Cl}$  on the NPQ of *C. velia* cells. Dashed black, control (no  $\text{NH}_4\text{Cl}$ ); light gray,  $\text{NH}_4\text{Cl}$  added after 45 s; medium gray, uncoupler added after 99 s; dark gray, uncoupler added after 198 s; solid black, uncoupler added after 297 s. The actinic light intensity was  $500 \mu\text{mol m}^{-2} \text{s}^{-1}$ . Samples were dark adapted for 30 min before measurements. Care was taken to ensure that the sample was efficiently stirred throughout the whole experiment. For further information, see 'Materials and methods'. (B) NPQ  $((F_m - F_m')/F_m)$ , calculated from the relative fluorescence traces shown in (A). (This figure is available in colour at JXB online.)

## Results

The kinetics of non-photochemical quenching (NPQ) activation were studied for *C. velia* in different xanthophyll de-epoxidation states (DEPSs) and compared with that of *Spinacia*

*oleracea* (spinach) (Fig. 1). NPQ formation rate positively correlated with the DEPS in spinach as 10, 20, and 40% de-epoxidation yielded significantly different NPQ formation rates of 0.006, 0.011, and  $0.05 \text{ s}^{-1}$ , respectively (Fig. 1B), in agreement

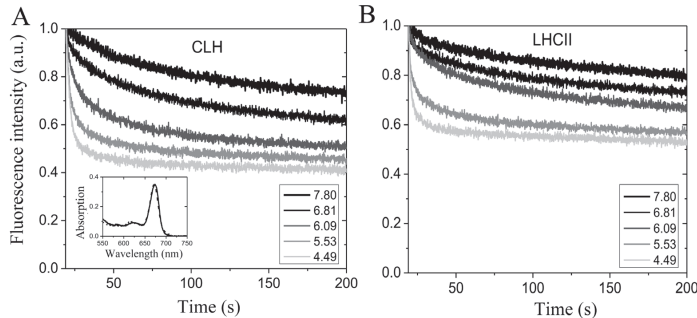


**Fig. 3.** Quenching of *Chromera velia* antennas is highly sensitive to pH. Representative fluorescence time course of CLH (A) and LHCII (B) as a function of pH. Samples were injected into a buffer containing 0.0005%  $\beta$ -DM, 10 mM HEPES and 10 mM sodium citrate (final concentrations). Each buffer had been HCl-buffered to the pH indicated in the figure, prior to sample injection. Data were normalized to the fluorescence maximum. Inset: absorption spectrum of CLH at high (solid line, pH 7.8) and low (dashed line, pH 4.5) pH. (This figure is available in colour at JXB online.)

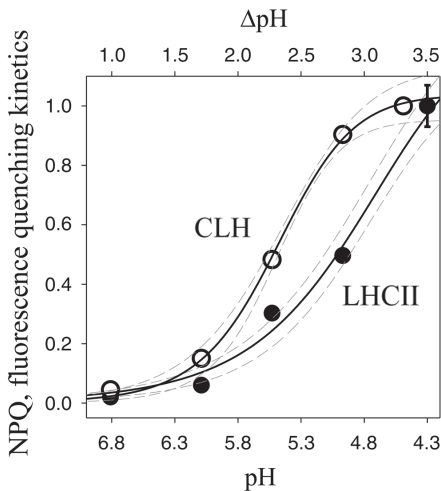


**Fig. 4.** Comparison of pH titration curves for fluorescence quenching of LHCII and CLH. The relationship between percentage of quenching and pH was obtained from traces like those shown in Fig. 3 fitted as described in the 'Data analysis and model fitting' section of 'Materials and methods', using a previously established model (see e.g. Ruban and Horton 1999). Circles, mean averages from at least three independent replicates; solid lines, fittings; dashed lines, 95% confidence intervals. The error bar shows typical standard deviation.

with current NPQ models and previous results from various phototrophs (see e.g. (Demmig-Adams, 1990; Ruban *et al.*, 1994b; Jahns and Holzwarth, 2012; Goss and Lepetit 2015). In contrast, NPQ in *C. velia* formed quickly regardless of the de-epoxidation state (Fig. 1A). Values between 0.04 and 0.05  $s^{-1}$  were thus found for both 10 and 40% DEPS, showing fast NPQ formation, independent of xanthophyll content (Fig. 1C).

The lack of an evident kinetic effect of xanthophylls in *C. velia* can also be seen from the *shape* of the NPQ formation curve. Whilst in spinach the increase in zeaxanthin (zea) concentration from 10 to 40% reduced curve sigmoidicity from 3.2 to 1.8 (Fig. 1B; Table S1), in *C. velia* no evident change could be seen (Fig. 1A) and the Hill coefficients were not significantly different in the two conditions ( $3.0 \pm 0.4$  versus  $2.5 \pm 0.3$ ; see Supplementary Table S1). The increased de-epoxidation (from 10% to 40%; Fig. 1A), therefore, did not seem to affect NPQ kinetics as strongly as in spinach, but it stimulated the total NPQ ( $NPQ_{max}$ ; see Table S1). This is in agreement with a previous report (Kotabová *et al.*, 2011) showing NPQ enhancement by zeaxanthin in *C. velia*.

In *C. velia*, NPQ was induced almost instantaneously with the turning on of the actinic light, and we therefore used  $NH_4Cl$  to investigate the possibility that lumen acidification was the basis of fast NPQ. As with spinach, in *C. velia*  $NH_4Cl$  reversed fluorescence quenching independent of its addition time during irradiation (Fig. 2A), proving a strict link between protons and NPQ in *C. velia*. However, the kinetics of NPQ relaxation at different time points were very different from each other and from those of spinach (Supplementary Fig. S1A). Whilst in spinach NPQ relaxed almost immediately after  $NH_4Cl$  injection, with 70% fluorescence recovery within 10 s, it took at least 500 s to achieve a similar recovery in *C. velia* (Fig. 2B). Interestingly, in *C. velia*, the later  $NH_4Cl$  was added, the faster NPQ relaxed (Fig. 2B). This is in strict contrast to higher plants (Supplementary Fig. S1B), where faster relaxation kinetics were observed at the beginning of NPQ formation (see e.g. Fig. 3A in (Ruban *et al.*, 2004), suggesting a different sensitivity of NPQ to lumen acidification. The connection between NPQ and protons was further investigated *in vitro* using isolated antennas.

'Fluorescence quenching titration' is an efficient way to systematically study the pH dependency of quenching *in vitro*, by injecting purified antennas into buffers of increasingly acidic pH (Ruban *et al.*, 1994b; Wentworth *et al.*, 2000; Kaňa *et al.*, 2012; Belgio *et al.*, 2013). This method was employed

to assess the hypothesis that faster NPQ activation (Fig. 1) related to antenna protonation, rather than to zeaxanthin content. Therefore LHCII and CLH complexes were isolated from dark-adapted material and the absence of zeaxanthin was confirmed by HPLC analysis (see Supplementary Table S1 at JXB online).

Upon injection, CLH displayed a progressive quenching proportional to the acidity of the buffer (Fig. 3A). Sample integrity was constantly monitored by absorption spectroscopy (Fig. 3, inset) and by reversibility of the quenching after detergent addition (data not shown). Besides the general similarity of the process, pointing to a fundamentally conserved quenching mechanism, the differences between the two types of sample are notable. At each pH value, fluorescence quenching was consistently higher in CLH compared with LHCII, with the biggest difference found around pH 6.0. From the traces in Fig. 3, a titration curve of quenching kinetics as a function of pH was constructed (Fig. 4). It shows that, to attain the same rate of fluorescence quenching, a lower pH is required in LHCII compared with CLH. In particular, almost 50% of maximum quenching rate was observed at pH 5.5 in CLH, whilst a pH of 5.0 was necessary to get the same quenching rate in spinach. Similarly, CLH showed almost the maximum quenching rate ( $90 \pm 5\%$ ) at pH 4.97, whereas for LHCII it was only 50%. This was reflected in a shift by 0.5 pH unit to higher values in the calculated quenching  $pK_a$  of CLH compared with LHCII, i.e. from  $5.5 \pm 0.1$  to  $5.0 \pm 0.1$  (Table 1). The  $pK_a$  value for LHCII was in good agreement with that previously reported (see e.g.  $pK_a=4.9$  in Petrou *et al.* (2014)). The Hill coefficient for CLH was not significantly different from that of LHCII ( $7.2 \pm 1.9$  and  $7.5 \pm 1.1$  for LHCII and CLH, respectively; Table 1) and in both cases they were higher than those for *in vivo* quenching (see Fig. 1), consistent with the absence of zeaxanthin (see Supplementary Table S1 and Discussion). In summary, the shift in quenching  $pK_a$  confirmed a higher proton sensitivity of CLH compared with LHCII, independent of xanthophylls.

In order to address possible reasons behind the higher pH sensitivity found in CLH, a comparative *in silico* analysis was conducted using the amino acid sequences of CLH and LHCII (Supplementary Fig. S2). A schematic overview of the two proteins is presented in Supplementary Fig. S3. We have explored in particular the protein luminal loop to identify residues that are protonable within the physiological range. The protein structure predicted for CLH is presented in Fig. 5. We found 24 negatively charged amino acidic residues in total (i.e. aspartic and glutamic acids) in CLH, four of which are located

in the luminal loop (Glu-93, Asp-107, Asp-113, Asp-119) and one in the C-terminus (Glu-205).

The estimated *in situ*  $pK_a$  values were calculated and compared with LHCII (2.5 Å resolution structure from Standfuss *et al.* (2005)) and are presented in Table 2. Results for LHCII are in good agreement with a previous report (Xiao *et al.*, 2012), where two residues in particular (Glu-107 and Asp-215) were indicated as putative pH sensors for NPQ as their quenching  $pK_a$  values are within the thylakoid physiological range (3.9–7.5). The same analysis applied to CLH revealed the presence of three plausible protonable residues: Asp-107, Asp-119 and Glu-205 (see Table 2, Fig. 5 right). Furthermore, their  $pK_a$  values were shifted to higher pH values compared with LHCII, confirming that the luminal loop is more sensitive to protonation in CLH (see Asp-107, Asp-119 and Glu-205 and their  $pK_a$  in Table 2).

An overall comparison between LHCII and CLH protein structures (Table 3) indicated that, despite a similar number of total protonable residues (~11.4–11.5% in both cases), CLH displayed a lower protein charge than LHCII at pH 7.6, that is  $-6$  versus  $-24$ , respectively. This means that LHCII tends to be more charged than CLH and a stronger protein–protein repulsion is expected for LHCII at pH 7.6 (see Discussion). In agreement with this, the CLH isoelectric point was ~0.4 higher than LHCII, implying that ~30 times fewer protons are required to neutralize negatively charged residues compared with LHCII. In summary, the *in silico* results supported the experimental data well and provided theoretical explanations for the faster, more efficient quenching found for CLH.

## Discussion

In the present paper, we investigated reasons for fast NPQ activation in *C. velia*. In higher plants, the kinetics of NPQ induction are influenced by xanthophyll composition (Fig. 1B). Demmig-Adams (1990) was the first to provide evidence for a connection between the xanthophyll cycle and NPQ. She showed that the conversion of violaxanthin into zeaxanthin, stimulated under light by lumen acidification, strongly enhanced NPQ. Later it was noticed (Ruban and Horton, 1999) that the NPQ of zeaxanthin-enriched samples was much faster, as zeaxanthin changed the NPQ dependency (cooperativity) as a function of  $\Delta pH$ , from sigmoidal (violaxanthin) to hyperbolic (zeaxanthin) (see also Horton *et al.*, 2000; Johnson *et al.*, 2009). Here, we confirmed with a control sample (spinach) that the transition into the quenched state is slower for leaves enriched in violaxanthin compared with zeaxanthin (Fig. 1B) as the Hill coefficient

**Table 1.** pH versus quenching titration curve fitting parameters in CLH and LHCII

Sample	Hill coefficient	Estimated $pK_a$	Quenching kinetics at pH 4.97
LHCII	$7.2 \pm 1.9$	$5.0 \pm 0.1$	$0.50 \pm 0.01$
CLH	$7.5 \pm 1.1$	$5.5 \pm 0.1$	$0.90 \pm 0.05$

Titration parameters were determined by fitting measured traces like those represented in Fig. 3 as described in the 'Data analysis and model fitting' section of 'Materials and methods'. Standard fitting errors were provided by SigmaPlot software. (For more details, see Ruban *et al.* 1994a; Ruban and Horton 1999; Petrou *et al.* 2014.)



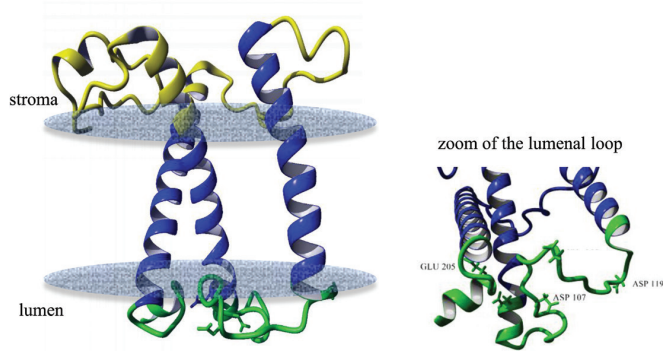


**Fig. 5.** Predicted protein structure for CLH. Predicted structure of the CLH antenna based on sequence homology with LHCII. A zoom of the stranded luminal loop is shown on the right. The putative residues involved in triggering NPQ are labelled in black. Blue, transmembrane helices; green, luminal loop region; yellow, stromal loop. For the prediction of protein structure and the  $pK_a$  of residues, YASARA and H++ programs were used, respectively.

**Table 2.** List of protonable luminal loop residues (Glu, Asp) predicted by the H++ program for LHCII and CLH antenna proteins

LHCII		CLH	
Residue	$pK_a$	Residue	$pK_a$
Glu-94	1.5	Glu-93	1.0
<b>Glu-107</b>	<b>4.4</b>	<b>Asp-107</b>	<b>5.9*</b>
Asp-111	3.4	Asp-113	2.9
Glu-207	2.9	<b>Asp-119</b>	<b>3.9*</b>
Asp-211	3.5	Lys-211	7.4
<b>Asp-215</b>	<b>5.3</b>	<b>Glu-205</b>	<b>&gt;7*</b>

The putative residues that can be protonated within the physiological pH range (3.9–7.5) are in shown bold. Residues in CLH with a higher  $pK_a$  than LHCII have been marked with an asterisk. Set values in the simulation were: for internal dielectric, 4; external dielectric, 80; and salinity, 0.15; in agreement with Xiao *et al.* (2012). Predicted sequences and protein structures are shown in Supplementary Figs S2 and S3, respectively.

decreased in the presence of zeaxanthin. In *C. velia* however, we found a different behavior. Although NPQ was greater in zeaxanthin-enriched samples, confirming the first observations (Kotabová *et al.*, 2011), its rate was insensitive to xanthophyll composition (Fig. 1A, C), indicating that the reason for the fast NPQ in *C. velia* resided elsewhere. The  $\text{NH}_4\text{Cl}$ -infiltration experiment (Fig. 2) following the procedure of Ruban *et al.* (2004) and Lavaud *et al.* (2002), suggested that fast NPQ related to lumen acidification and protons. Incomplete diffusion of the uncoupler was in fact ruled out by previous evidence of efficient  $\text{NH}_4\text{Cl}$  penetration in *C. velia* cells (see Fig. 4b in Belgio *et al.*, 2018). The titration of NPQ as a function of pH confirmed that CLH was significantly more sensitive to protons than LHCII (Figs 2, 3). Most importantly, the rate of quenching was increased, especially between pH 5 and 6.5. Within this pH range a very rapid quenching formed almost instantly upon injection of a CLH sample (Fig. 3A). This resulted in a shift in quenching  $pK_a$  of CLH to higher pH values than LHCII (Table 1). Therefore, to attain 50% of maximum quenching kinetics, a 0.5 unit lower pH

value (corresponding to 3.16 times more protons) was required for LHCII than CLH, indicating that the latter had an increased sensitivity to acidification. The high level of structural similarity between CLH and LHC protein families (Pan *et al.*, 2012; Tichy *et al.*, 2013; see also Supplementary Fig. S3) prompted an *in silico* comparison between luminal loop residues. The analysis identified five protonable (i.e. negative) residues in the luminal loop of CLH (Table 2). Three of them were predicted to be protonable within the physiological range (assuming a chloroplast lumen pH ranging between 3.9 and 7.5 (Peltier *et al.*, 2002). Compared with the corresponding residues in LHCII, the quenching  $pK_a$  values of these three residues are significantly higher in CLH (Table 2), which is consistent with the shift in the quenching  $pK_a$  found from experimental data (Fig. 4). We propose that during lumen acidification and *in vitro* quenching (Fig. 3), these residues shift from negative to neutral (i.e. become protonated) and this occurs earlier (i.e. at higher pH values) in CLH than in LHCII. This mechanism would explain the faster quenching (Fig. 3) and the shift to higher values of CLH quenching  $pK_a$  found experimentally (Fig. 4). Interestingly, the  $pK_a$  of Lys-211 (which in standard conditions has a  $pK_a$  of 10.67) was found to be reduced to 7.4 in CLH (Table 2). If confirmed by further studies, this means that this luminal loop residue can also be protonated during lumen acidification and therefore might play a role in NPQ activation in *C. velia*. The comparison between LHCII and CLH (Table 3) indicated also that the algal antenna is less charged at physiological pH than LHCII. As protein clustering proved to be crucial for efficient quenching of LHCII (Betterle *et al.*, 2009; Johnson *et al.*, 2011; Belgio *et al.*, 2012; Petrou *et al.*, 2014), an overall less charged protein like CLH could be more prone to aggregate and therefore quench more easily, due to a minor protein–protein electrostatic repulsion. The predicted isoelectric point is consistent with this. For CLH, in fact, a  $\sim 0.4$  lower  $pI$  was found (Table 3), corresponding to 30–40 less protons required for charge shielding. Considering the *in vitro* and *in silico* results together, we suggest that the increased NPQ formation kinetics relate to inbuilt antenna properties, in terms of

both a higher number of lumen-exposed protonable residues and an overall increased protein hydrophobicity. We hypothesize that this applies also to other similar antennas, such as diatom FCPs. In fact, although CLH binds only chlorophyll *a* and xanthophylls (see Kotabová *et al.*, 2011), due to its structural properties, this protein was classified as ‘FCP-like’, i.e. closely related to antennas from dinoflagellates, brown algae, and diatoms (Lepetit *et al.*, 2010; Pan *et al.*, 2012; Tichy *et al.*, 2013). Moreover diatoms can also be characterized by fast NPQ activation (Ruban *et al.*, 2004; Lavaud and Kroth, 2006; Grouneva *et al.*, 2008).

It was experimentally shown for brown algae (Nitschke *et al.*, 2012), alveolates (Belgio *et al.*, 2018), and other microalgae (Goss and Jakob, 2010) that the habitat and particularly the light conditions affect NPQ capabilities of algae from the SAR clade. As a coral symbiont, *C. velia* is expected to be mainly exposed to rather ‘moderate’ light intensities.

**Table 3.** Comparison of total charges between LHClI and CLH

	LHClI	CLH
Protonable residues	25/218 (11.5%)	24/211 (11.4%)
pI	4.61	4.97
Charge at pH 7.6	-24	-6

Total number of protonable residues, the isoelectric point (pI) and the total protein charge of LHClI and CLH antenna proteins, as predicted by the H++ program. Relative sequences and protein structures are shown in Supplementary Figs S2 and S3, respectively.

However, as this organism can be also found ‘free-living’ outside the coral, at depths of 3–5 m, light intensities of up to 1000  $\mu\text{mol m}^{-2} \text{s}^{-1}$  are normally experienced on a sunny day (Behrenfeld *et al.*, 1998; Oborník *et al.*, 2011). We can speculate that, due to fast quenching of antennas, in *C. velia* there was no selective pressure towards proteins capable of enhancing NPQ rate such as PsbS or Lhcsr (Pan *et al.*, 2012). These proteins in fact have a role as NPQ enhancers in vascular plants and green microalgae, respectively (Goss and Lepetit 2015). Spinach and *C. velia* seem therefore to have evolved very different ‘antenna behaviors’ in relation to different acclimation strategies. They can be summarized as follows (Fig. 6):

- *Chromera velia* carries antenna proteins that are ‘natural quenchers’; PsbS, a strong NPQ enhancer (Li *et al.*, 2000), is absent (Pan *et al.*, 2011) and the thylakoid membrane is highly enriched in violaxanthin, an ‘anti-quenching’ pigment (Kaňa *et al.*, 2016). As a consequence its NPQ kinetics are characterized by fast formation/slow relaxation.
- Higher plant antenna proteins, here represented by spinach LHClI, are ‘natural light harvesters’, so PsbS is required for effective but in particular fast quenching (Johnson and Ruban, 2011) and little or no free violaxanthin is present in the membranes (Dall’Osto *et al.*, 2010; Xu *et al.*, 2015). The NPQ kinetics are characterized by slow formation/fast relaxation.

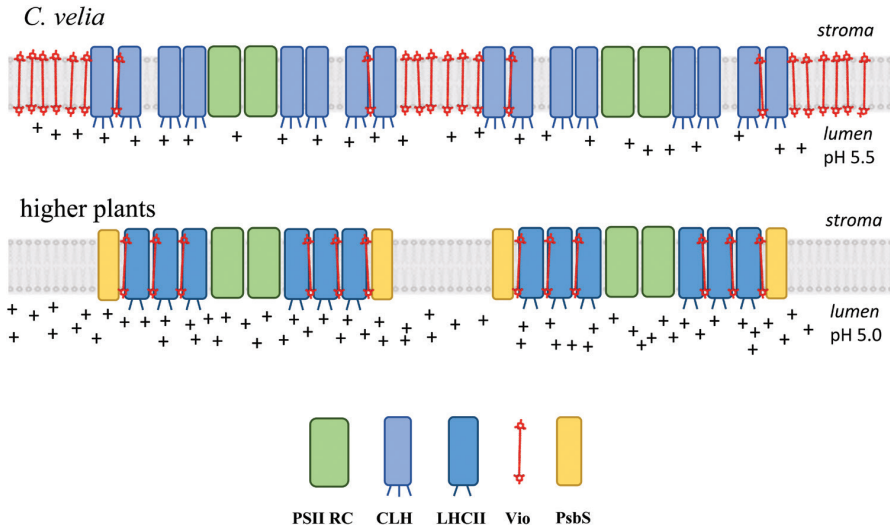


**Fig. 6.** Scheme showing the different light harvesting strategies of *C. velia* and higher plants. The *C. velia* thylakoid membrane carries CLH proteins that are ‘natural quenchers’ with three protonable lumen-facing residues, D107, D119, and E205 (indicated by small protrusions). The membrane is highly enriched in unbound, ‘anti-quenching’, violaxanthin pigments, and PsbS protein is absent. The higher plant thylakoid membrane supports the LHClI protein, a ‘natural light harvester’ with two protonable lumen-facing residues. PsbS protein is required for effective quenching, and the amount of unbound violaxanthin in the membrane is negligible. The scheme does not represent real stoichiometries/proportions. For more details, see main text.

In this scenario, 'free' violaxanthin plays a role of quenching inhibitor, particularly important for *C. velia* and less crucial for LHCII. A similar role of violaxanthin was previously suggested for some brown algae (Ocampo-Alvarez *et al.*, 2013). It explains the abundance of violaxanthin in algae like *C. velia*, where the violaxanthin to Chl *a* ratio is  $\sim 0.36$  (mol mol<sup>-1</sup>),  $\sim 8$  times higher than in plants (see e.g. Kotabová *et al.*, 2011), which is supported by work showing quenching modulation by 'free', i.e. not firmly bound to protein, xanthophylls (Ruban *et al.*, 1994; Lepetit *et al.*, 2010; Mann *et al.*, 2014; Xu *et al.*, 2015; Kaňa *et al.*, 2016).

Finally, the model presented (Fig. 6) provides an explanation also for the unusual acclimation strategy observed in *C. velia*: whilst plants (carrying 'natural harvester' antennas) protect themselves from high light by reducing their antenna size (see Kouřil *et al.*, 2013), in *C. velia* (characterized by 'natural quencher' antenna proteins) the antenna size is unaffected even after days of exposure to high light (Belgio *et al.*, 2018). This evidence, at first puzzling, seems now more logical in view of the results presented here.

## Conclusions

In conclusion, we have shown a similar quenching mechanism in antennas from a higher plant compared with those from an alveolate. In both cases the trigger is low pH and the likely sensors are protonable luminal residues. However, the actual sensitivity to lowering pH is different for the two proteins as CLH is more sensitive to protons than LHCII. We propose that this is due to subtle differences in the amino acid composition of the protein luminal loop. As a result, CLH switches into a dissipative quenched state more easily than LHCII and therefore the higher plant antenna protein can be considered a 'natural light harvester' whilst the CLH protein is a 'natural quencher'.

## Supplementary data

Supplementary data are available at *JXB* online.

Fig. S1. NH<sub>4</sub>Cl induces fast NPQ relaxation in spinach chloroplasts.

Fig. S2. Sequence of LHCIIb and CLH used in the present study.

Fig. S3. Schematic overview of LHCII (left) and CLH (right) antenna protein structures used in the present study.

Table S1. Pigment composition of antennas isolated from *C. velia* and spinach.

## Acknowledgements

This research project was mainly supported by The Czech Science Foundation GAČR (Grantová agentura České republiky) 17-02363Y (EB). Further support was from the Institutional project Algatech Plus (MSMT LO1416) from the Czech Ministry of Education, Youth and Sport. AVR was supported by The Royal Society Wolfson Research Merit Award. The authors thank Dr Petra Ungerer for LHCIIb protein preparation and Mr Filip Charvát for technical help during HPLC sample preparation.

## Author contributions

RK, EKT and EB conceived the project; EKT and EB performed the experiments and analyzed the data; AMY provided HPLC technical assistance; RS provided experimental advice concerning protein isolation; EB, RK and EKT wrote the article with contributions from all the co-authors; EB, EKT and AMY prepared the Figures. AVR supervised and complemented the work.

## References

- Akhtar P, Dorogi M, Pawlak K, Kovács L, Bóta A, Kiss T, Garab G, Lambrev PH. 2015. Pigment interactions in light-harvesting complex II in different molecular environments. *The Journal of Biological Chemistry* **290**, 4877–4886.
- Ballottari M, Truong TB, De Re E, Erickson E, Stella GR, Fleming GR, Bassi R, Niyogi KK. 2016. Identification of pH-sensing sites in the light harvesting complex stress-related 3 protein essential for triggering non-photochemical quenching in *Chlamydomonas reinhardtii*. *The Journal of Biological Chemistry* **291**, 7334–7346.
- Bassi R, Dainese P. 1992. A supramolecular light-harvesting complex from chloroplast photosystem-II membranes. *European Journal of Biochemistry* **204**, 317–326.
- Behrenfeld MJ, Prášil O, Kolber ZS, Babin M, Falkowski PG. 1998. Compensatory changes in Photosystem II electron turnover rates protect photosynthesis from photoinhibition. *Photosynthesis Research* **58**, 259–268.
- Belgio E, Duffy CD, Ruban AV. 2013. Switching light harvesting complex II into photoprotective state involves the lumen-facing apoprotein loop. *Physical Chemistry Chemical Physics* **15**, 12253–12261.
- Belgio E, Johnson MP, Juríć S, Ruban AV. 2012. Higher plant photosystem II light-harvesting antenna, not the reaction center, determines the excited-state lifetime—both the maximum and the nonphotochemically quenched. *Biophysical Journal* **102**, 2761–2771.
- Belgio E, Kapitonova E, Chmeliov J, Duffy CD, Ungerer P, Valkunas L, Ruban AV. 2014. Economic photoprotection in photosystem II that retains a complete light-harvesting system with slow energy traps. *Nature Communications* **5**, 4433.
- Belgio E, Trsková E, Kotabová E, Ewe D, Prášil O, Kaňa R. 2018. High light acclimation of *Chromera velia* points to photoprotective NPQ. *Photosynthesis Research* **135**, 263–274.
- Betterle N, Ballottari M, Zorzan S, de Bianchi S, Cazzaniga S, Dall'Osto L, Morosinotto T, Bassi R. 2009. Light-induced dissociation of an antenna hetero-oligomer is needed for non-photochemical quenching induction. *The Journal of Biological Chemistry* **284**, 15255–15266.
- Büchel C. 2015. Evolution and function of light harvesting proteins. *Journal of Plant Physiology* **172**, 62–75.
- Crisafi E, Pandit A. 2017. Disentangling protein and lipid interactions that control a molecular switch in photosynthetic light harvesting. *Biochimica et Biophysica Acta* **1859**, 40–47.
- Crouchman S, Ruban A, Horton P. 2006. PsbS enhances nonphotochemical fluorescence quenching in the absence of zeaxanthin. *FEBS Letters* **580**, 2053–2058.
- Dall'Osto L, Cazzaniga S, Havaux M, Bassi R. 2010. Enhanced photoprotection by protein-bound vs free xanthophyll pools: a comparative analysis of chlorophyll b and xanthophyll biosynthesis mutants. *Molecular Plant* **3**, 576–593.
- Dekker JP, Boekema EJ. 2005. Supramolecular organization of thylakoid membrane proteins in green plants. *Biochimica et Biophysica Acta* **1706**, 12–39.
- Demmig-Adams B. 1990. Carotenoids and photoprotection in plants: a role for the xanthophyll zeaxanthin. *Biochimica et Biophysica Acta* **1020**, 1–24.
- Demmig-Adams B, Adams WW. 1992. Carotenoid composition in sun and shade leaves of plants with different life forms. *Plant Cell and Environment* **15**, 411–419.
- Erickson E, Wakao S, Niyogi KK. 2015. Light stress and photoprotection in *Chlamydomonas reinhardtii*. *The Plant Journal* **82**, 449–465.

- Garcia-Mendoza E, Ocampo-Alvarez H, Govindjee.** 2011. Photoprotection in the brown alga *Macrocystis pyrifera*: evolutionary implications. *Journal of Photochemistry and Photobiology. B, Biology* **104**, 377–385.
- Gilmore AM, Yamamoto HY.** 1992. Dark induction of zeaxanthin-dependent nonphotochemical fluorescence quenching mediated by ATP. *Proceedings of the National Academy of Sciences, USA* **89**, 1899–1903.
- Goss R, Jakob T.** 2010. Regulation and function of xanthophyll cycle-dependent photoprotection in algae. *Photosynthesis Research* **106**, 103–122.
- Goss R, Lepetit B.** 2015. Biodiversity of NPQ. *Journal of Plant Physiology* **172**, 13–32.
- Grossman AR, Karpowicz SJ, Heinnickel M, et al.** 2010. Phylogenomic analysis of the *Chlamydomonas* genome unmasks proteins potentially involved in photosynthetic function and regulation. *Photosynthesis Research* **106**, 3–17.
- Grouneva I, Jakob T, Wilhelm C, Goss R.** 2008. A new multicomponent NPQ mechanism in the diatom *Cyclotella meneghiniana*. *Plant & Cell Physiology* **49**, 1217–1225.
- Guillard RR, Ryther JH.** 1962. Studies of marine planktonic diatoms. I. *Cyclotella nana* Husted, and *Detonula confervacea* (Cleve) Gran. *Canadian Journal of Microbiology* **8**, 229–239.
- Gundermann K, Büchel C.** 2008. The fluorescence yield of the trimeric fucoxanthin-chlorophyll-protein FCPa in the diatom *Cyclotella meneghiniana* is dependent on the amount of bound diatoxanthin. *Photosynthesis Research* **95**, 229–235.
- Gundermann K, Büchel C.** 2012. Factors determining the fluorescence yield of fucoxanthin-chlorophyll complexes (FCP) involved in non-photochemical quenching in diatoms. *Biochimica et Biophysica Acta* **1817**, 1044–1052.
- Horton P, Johnson MP, Perez-Bueno ML, Kiss AZ, Ruban AV.** 2008. Photosynthetic acclimation: does the dynamic structure and macro-organisation of photosystem II in higher plant grana membranes regulate light harvesting states? *The FEBS Journal* **275**, 1069–1079.
- Horton P, Ruban AV, Walters RG.** 1996. Regulation of light harvesting in green plants. *Annual Review of Plant Physiology and Plant Molecular Biology* **47**, 655–684.
- Horton P, Ruban AV, Wentworth M.** 2000. Allosteric regulation of the light-harvesting system of photosystem II. *Philosophical Transactions of the Royal Society of London. Series B, Biological Sciences* **355**, 1361–1370.
- Jahns P, Holzwarth AR.** 2012. The role of the xanthophyll cycle and of lutein in photoprotection of photosystem II. *Biochimica et Biophysica Acta* **1817**, 182–193.
- Jennings RC, Engelmann E, Garlaschi F, Casazza AP, Zuccherli G.** 2005. Photosynthesis and negative entropy production. *Biochimica et Biophysica Acta* **1709**, 251–255.
- Johnson MP, Goral TK, Duffy CD, Brain AP, Mullineaux CW, Ruban AV.** 2011. Photoprotective energy dissipation involves the reorganization of photosystem II light-harvesting complexes in the grana membranes of spinach chloroplasts. *The Plant Cell* **23**, 1468–1479.
- Johnson MP, Pérez-Bueno ML, Zia A, Horton P, Ruban AV.** 2009. The zeaxanthin-independent and zeaxanthin-dependent qE components of nonphotochemical quenching involve common conformational changes within the photosystem II antenna in *Arabidopsis*. *Plant Physiology* **149**, 1061–1075.
- Johnson MP, Ruban AV.** 2011. Restoration of rapidly reversible photoprotective energy dissipation in the absence of PsbS protein by enhanced ΔpH. *The Journal of Biological Chemistry* **286**, 19973–19981.
- Johnson MP, Zia A, Horton P, Ruban AV.** 2010. Effect of xanthophyll composition on the chlorophyll excited state lifetime in plant leaves and isolated LHClI. *Chemical Physics* **373**, 23–32.
- Johnson MP, Zia A, Ruban AV.** 2012. Elevated ΔpH restores rapidly reversible photoprotective energy dissipation in *Arabidopsis* chloroplasts deficient in lutein and xanthophyll cycle activity. *Planta* **235**, 193–204.
- Kaňa R, Govindjee.** 2016. Role of ions in the regulation of light-harvesting. *Frontiers in Plant Science* **7**, 1–17.
- Kaňa R, Kotabová E, Kopečná J, Trsková E, Belgio E, Sobotka R, Ruban AV.** 2016. Violaxanthin inhibits nonphotochemical quenching in light-harvesting antenna of *Chromera velia*. *FEBS Letters* **590**, 1076–1085.
- Kaňa R, Kotabová E, Sobotka R, Prášil O.** 2012. Non-photochemical quenching in cryptophyte alga *Rhodomonas salina* is located in chlorophyll a/c antennae. *PLoS One* **7**, e29700.
- Kaňa R, Vass I.** 2008. Thermomaging as a tool for studying light-induced heating of leaves: Correlation of heat dissipation with the efficiency of photosystem II photochemistry and non-photochemical quenching. *Environmental and Experimental Botany* **64**, 90–96.
- Kirchhoff H, Haferkamp S, Allen JF, Epstein DB, Mullineaux CW.** 2008. Protein diffusion and macromolecular crowding in thylakoid membranes. *Plant Physiology* **146**, 1571–1578.
- Kotabová E, Kaňa R, Jarešová J, Prášil O.** 2011. Non-photochemical fluorescence quenching in *Chromera velia* is enabled by fast violaxanthin de-epoxidation. *FEBS Letters* **585**, 1941–1945.
- Kouřil R, Wientjes E, Bultema JB, Croce R, Boekema EJ.** 2013. High-light vs. low-light: effect of light acclimation on photosystem II composition and organization in *Arabidopsis thaliana*. *Biochimica et Biophysica Acta* **1827**, 411–419.
- Lavaud J, Kroth PG.** 2006. In diatoms, the transthylakoid proton gradient regulates the photoprotective non-photochemical fluorescence quenching beyond its control on the xanthophyll cycle. *Plant & Cell Physiology* **47**, 1010–1016.
- Lavaud J, Lepetit B.** 2013. An explanation for the inter-species variability of the photoprotective non-photochemical chlorophyll fluorescence quenching in diatoms. *Biochimica et Biophysica Acta* **1827**, 294–302.
- Lavaud J, Rousseau B, van Gorkom HJ, Etienne AL.** 2002. Influence of the diadinoxanthin pool size on photoprotection in the marine planktonic diatom *Phaeodactylum tricatumum*. *Plant Physiology* **129**, 1398–1406.
- Lepetit B, Volke D, Gilbert M, Wilhelm C, Goss R.** 2010. Evidence for the existence of one antenna-associated, lipid-dissolved and two protein-bound pools of diadinoxanthin cycle pigments in diatoms. *Plant Physiology* **154**, 1905–1920.
- Li XP, Björkman O, Shih C, Grossman AR, Rosenquist M, Jansson S, Niyogi KK.** 2000. A pigment-binding protein essential for regulation of photosynthetic light harvesting. *Nature* **403**, 391–395.
- Li XP, Gilmore AM, Caffarri S, Bassi R, Golan T, Kramer D, Niyogi KK.** 2004. Regulation of photosynthetic light harvesting involves intrathylakoid lumen pH sensing by the PsbS protein. *The Journal of Biological Chemistry* **279**, 22866–22874.
- Liguori N, Roy LM, Opacic M, Durand G, Croce R.** 2013. Regulation of light harvesting in the green alga *Chlamydomonas reinhardtii*: the C-terminus of LHCSR is the knob of a dimmer switch. *Journal of the American Chemical Society* **135**, 18339–18342.
- Lokstein H, Tian L, Polle JE, DellaPenna D.** 2002. Xanthophyll biosynthetic mutants of *Arabidopsis thaliana*: altered nonphotochemical quenching of chlorophyll fluorescence is due to changes in Photosystem II antenna size and stability. *Biochimica et Biophysica Acta* **1553**, 309–319.
- Mann M, Hoppenz P, Jakob T, Weisheit W, Mittag M, Wilhelm C, Goss R.** 2014. Unusual features of the high light acclimation of *Chromera velia*. *Photosynthesis Research* **122**, 159–169.
- Miloslavina Y, Wehner A, Lambrev PH, Wientjes E, Reus M, Garab G, Croce R, Holzwarth AR.** 2008. Far-red fluorescence: a direct spectroscopic marker for LHClI oligomer formation in non-photochemical quenching. *FEBS Letters* **582**, 3625–3631.
- Moya I, Silvestri M, Vallon O, Cinque G, Bassi R.** 2001. Time-resolved fluorescence analysis of the photosystem II antenna proteins in detergent micelles and liposomes. *Biochemistry* **40**, 12552–12561.
- Natali A, Gruber JM, Dietzel L, Stuart MC, van Grondelle R, Croce R.** 2016. Light-harvesting complexes (LHCs) cluster spontaneously in membrane environment leading to shortening of their excited state lifetimes. *The Journal of Biological Chemistry* **291**, 16730–16739.
- Nitschke U, Connan S, Stengel DB.** 2012. Chlorophyll a fluorescence responses of temperate Phaeophyceae under submergence and emersion regimes: a comparison of rapid and steady-state light curves. *Photosynthesis Research* **114**, 29–42.
- Niyogi KK.** 1999. Photoprotection revisited: genetic and molecular approaches. *Annual Review of Plant Physiology and Plant Molecular Biology* **50**, 333–359.
- Noctor G, Rees D, Young A, Horton P.** 1991. The relationship between zeaxanthin, energy-dependent quenching of chlorophyll fluorescence,

- and trans-thylakoid pH gradient in isolated chloroplasts. *Biochimica et Biophysica Acta* **1057**, 320–330.
- Obornik M, Kručinská J, Esson H.** 2016. Life cycles of chromerids resemble those of colpodellids and apicomplexan parasites. *Perspectives in Phycology* **3**, 21–27.
- Obornik M, Lukes J.** 2013. Cell biology of chromerids: autotrophic relatives to apicomplexan parasites. *International Review of Cell and Molecular Biology* **306**, 333–369.
- Obornik M, Vancová M, Lai DH, Janoušek J, Keeling PJ, Lukeš J.** 2011. Morphology and ultrastructure of multiple life cycle stages of the photosynthetic relative of apicomplexa, *Chromera velia*. *Protist* **162**, 115–130.
- Ocampo-Alvarez H, García-Mendoza E, Govindjee.** 2013. Antagonist effect between violaxanthin and de-epoxidated pigments in nonphotochemical quenching induction in the qE deficient brown alga *Macrocystis pyrifera*. *Biochimica et Biophysica Acta* **1827**, 427–437.
- Pan H, Slapeta J, Carter D, Chen M.** 2012. Phylogenetic analysis of the light-harvesting system in *Chromera velia*. *Photosynthesis research* **111**, 19–28.
- Pan X, Li M, Wan T, Wang L, Jia C, Hou Z, Zhao X, Zhang J, Chang W. J.** 2011. Structural insights into energy regulation of light-harvesting complex CP29 from spinach. *Nature Structural & Molecular Biology* **18**, 309–315.
- Peers G, Truong TB, Ostendorf E, Busch A, Elrad D, Grossman AR, Hippler M, Niyogi KK.** 2009. An ancient light-harvesting protein is critical for the regulation of algal photosynthesis. *Nature* **462**, 518–521.
- Peltier JB, Emanuelsson O, Kalume DE, et al.** 2002. Central functions of the luminal and peripheral thylakoid proteome of *Arabidopsis* determined by experimentation and genome-wide prediction. *The Plant Cell* **14**, 211–236.
- Petrou K, Belgio E, Ruban AV.** 2014. pH sensitivity of chlorophyll fluorescence quenching is determined by the detergent/protein ratio and the state of LHCII aggregation. *Biochimica et Biophysica Acta* **1837**, 1533–1539.
- Pinnola A, Dall'Osto L, Gerotto C, Morosinotto T, Bassi R, Alboresi A.** 2013. Zeaxanthin binds to light-harvesting complex stress-related protein to enhance nonphotochemical quenching in *Physcomitrella patens*. *The Plant Cell* **25**, 3519–3534.
- Porra R, Thompson W, Kriedemann P.** 1989. Determination of accurate extinction coefficients and simultaneous equations for assaying chlorophylls *a* and *b* extracted with four different solvents: Verification of the concentration of chlorophyll standards by atomic absorption spectrometry. *Biochimica et Biophysica Acta* **975**, 384–394.
- Quigg A, Kotabová E, Jarešová J, Kaňa R, Setlík J, Sedivá B, Komárek O, Prášil O.** 2012. Photosynthesis in *Chromera velia* represents a simple system with high efficiency. *PLoS One* **7**, e47036.
- Ruban A.** 2013. The photosynthetic membrane. Molecular mechanisms and biophysics of light harvesting. Chichester, UK: John Wiley & Sons, Ltd.
- Ruban AV, Horton P.** 1999. The xanthophyll cycle modulates the kinetics of nonphotochemical energy dissipation in isolated light-harvesting complexes, intact chloroplasts, and leaves of spinach. *Plant Physiology* **119**, 531–542.
- Ruban AV, Johnson MP, Duffy CD.** 2012. The photoprotective molecular switch in the photosystem II antenna. *Biochimica et Biophysica Acta* **1817**, 167–181.
- Ruban A, Lavaud J, Rousseau B, Guglielmi G, Horton P, Etienne AL.** 2004. The super-excess energy dissipation in diatom algae: comparative analysis with higher plants. *Photosynthesis Research* **82**, 165–175.
- Ruban AV, Pesaresi P, Wacker U, Irrgang KD, Bassi R, Horton P.** 1998. The relationship between the binding of dicyclohexylcarbodiimide and quenching of chlorophyll fluorescence in the light-harvesting proteins of photosystem II. *Biochemistry* **37**, 11586–11591.
- Ruban AV, Rees D, Noctor GD, Young A, Horton P.** 1991. Long-wavelength chlorophyll species are associated with amplification of high-energy-state excitation quenching in higher-plants. *Biochimica et Biophysica Acta* **1059**, 355–360.
- Ruban AV, Young A, Horton P.** 1994a. Modulation of chlorophyll fluorescence quenching in isolated light-harvesting complex of Photosystem-II. *Biochimica et Biophysica Acta* **1186**, 123–127.
- Ruban AV, Young AJ, Pascal AA, Horton P.** 1994b. The effects of illumination on the xanthophyll composition of the photosystem II light-harvesting complexes of spinach thylakoid membranes. *Plant Physiology* **104**, 227–234.
- Seródio J, Lavaud J.** 2011. A model for describing the light response of the nonphotochemical quenching of chlorophyll fluorescence. *Photosynthesis Research* **108**, 61–76.
- Schaller-Laudel S, Volke D, Redlich M, Kansy M, Hoffmann R, Wilhelm C, Goss R.** 2015. The diadinoxanthin diatoxanthin cycle induces structural rearrangements of the isolated FCP antenna complexes of the pennate diatom *Phaeodactylum tricornutum*. *Plant Physiology and Biochemistry* **96**, 364–376.
- Sobotka R, Esson HJ, Konik P, Tršková E, Moravcová L, Horák A, Dufková P, Obornik M.** 2017. Extensive gain and loss of photosystem I subunits in chromerid algae, photosynthetic relatives of apicomplexans. *Scientific Reports* **7**, 13214.
- Standfuss J, Terwisscha van Scheltinga AC, Lamborghini M, Kühlbrandt W.** 2005. Mechanisms of photoprotection and nonphotochemical quenching in pea light-harvesting complex at 2.5 Å resolution. *The EMBO Journal* **24**, 919–928.
- Tichý J, Gardian Z, Bina D, Konik P, Litvin R, Herbštova M, Pain A, Vacha F.** 2013. Light harvesting complexes of *Chromera velia*, photosynthetic relative of apicomplexan parasites. *Biochimica et Biophysica Acta* **1827**, 723–729.
- van Kooten O, Snel JF.** 1990. The use of chlorophyll fluorescence nomenclature in plant stress physiology. *Photosynthesis Research* **25**, 147–150.
- Walters RG, Ruban AV, Horton P.** 1994. Higher plant light-harvesting complexes LHCIIa and LHCIIc are bound by dicyclohexylcarbodiimide during inhibition of energy dissipation. *European Journal of Biochemistry* **226**, 1063–1069.
- Wentworth M, Ruban AV, Horton P.** 2000. Chlorophyll fluorescence quenching in isolated light harvesting complexes induced by zeaxanthin. *FEBS Letters* **471**, 71–74.
- Wientjes E, van Amerongen H, Croce R.** 2013. Quantum yield of charge separation in photosystem II: functional effect of changes in the antenna size upon light acclimation. *The Journal of Physical Chemistry B* **117**, 11200–11208.
- Xiao FG, Ji HF, Shen L.** 2012. Insights into the region responding to ΔpH change in major light harvesting complex. *Journal of Photochemistry and Photobiology. B, Biology* **111**, 35–38.
- Xu P, Tian L, Kloz M, Croce R.** 2015. Molecular insights into Zeaxanthin-dependent quenching in higher plants. *Scientific Reports* **5**, 13679.
- Zaks J, Amarnath K, Sylak-Glassman EJ, Fleming GR.** 2013. Models and measurements of energy-dependent quenching. *Photosynthesis Research* **116**, 389–409.



## **Supplemental file**

### **Antenna proton sensitivity determines photosynthetic light harvesting strategy**

Eliška Kuthanová Trsková, Erica Belgio, Anna M. Yeates, Roman Sobotka, Alexander V. Ruban, and Radek Kaň

	<b>Neo</b>	<b>Vio</b>	<b>Ant</b>	<b>Lut (LHCII) Isofuco(CLH)</b>	<b>Zea</b>	<b>DEPs</b>	<b>xan/ chl</b>
<b>LHCIIb</b>	29±1	4±1	0	67±1	0	0	0.35
<b>CLH</b>	0	30±1	0	69±3	0	0	0.9

**Table S1: Pigment composition of isolated LHCIIb and CLH.** Neo, Vio, Ant, Lut, Isofuco, Zea, DEPs: neoxanthin, violaxanthin, antheraxanthin, lutein, isofucoxanthin, zeaxanthin, de-epoxidation state ( $Z + 0.5A$ )/(V+A+Z) and xanthophyll/chlorophyll molar ratios. Data are presented as (xanthophyll/total xanthophyll) % and are means  $\pm$  SD from 3 replicates, xan/chl: xanthophyll/chlorophyll molar ratio.



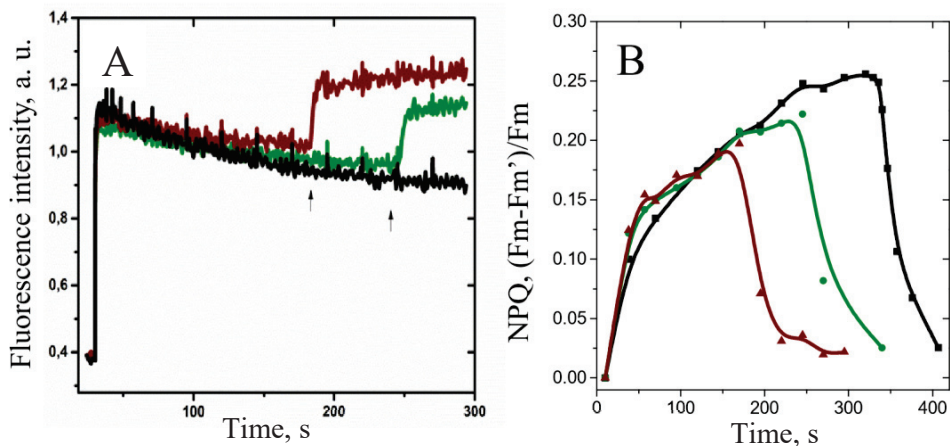


**Figure S1.  $\text{NH}_4\text{Cl}$  induces fast NPQ relaxation in spinach chloroplasts.**

**Panel A.** Representative fluorescence traces showing the uncoupler-dependent reversibility of NPQ in intact chloroplasts isolated from spinach. Black, control (no  $\text{NH}_4\text{Cl}$ ); red,  $\text{NH}_4\text{Cl}$  added at 188 s; green, uncoupler added after 250 s. The actinic light intensity was  $500 \mu\text{mol m}^{-2}\text{s}^{-1}$ . **Samples were dark adapted for 30 min before measurements.** Care was taken to ensure sample mixing throughout the whole procedure. For further information, see materials and methods. **Panel B.** NPQ,  $(F_m - F_m')/F_m$  calculated from the relative fluorescence traces in panel A.

>2BHW:A|PDBID|CHAIN|SEQUENCE

RKSATTKKVASSGSPWYGPDRVKYLGPFSGESPSYLTGEFPGDYGWDTAGLS  
ADPETFSKNRELEVIHSRWAMLGALGSVFPELLSRNGVKFGEAVWFKAGSQI  
FSEGGLDYLGNP SLVHAQSILAIWATQVILMGAVEGYRIAGGPLGEVVDPLY  
PGGSFDPLGLADDPEAF AELKVKELKNGRLAMFSMFGFFVQAIVTGKGPLEN  
LADHLADPVNNNAWSYATNFVPGK

>CveliaI\_19753.t1|Fucoxanthin-chlorophyll a-c binding protein

MKTVAATVCAFAAVSVDAFTLGGVKPVAR SARSEMKMSFDDAPGSGKYGL  
PGFPIFNPFDLSP EDEKFKEYRLKELKNGRLAMLGILGLAATELGARLPGNLN  
AGFDLPFKQDGP AFSDIPGGFAAFPALPAAGWAQVALFVALMDQVFYKQTD  
ADEVAPGITYGKPEDPEEYLDLRNKELNNGRIAMIGLLAMTFQYYIGGATEFP  
YISK

**Figure S2. Sequence of LHCIIb and CLH used in the present study.** Sequence of LHCIIb (DB code: 2BHW, Standfuss et al. 2005) and CLH (CveliaI\_19753.t1 taken from Tichý et al. 2013) polypeptides employed for *in silico* analysis.

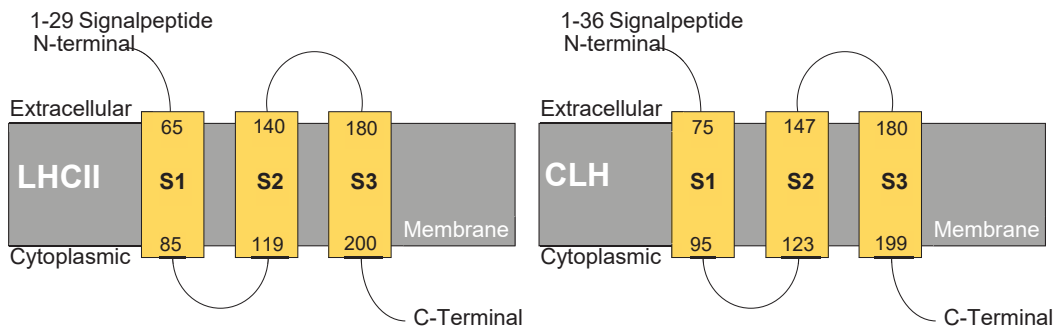


**Figure S3. Schematic overview of LHCII (left) and CLH (right) antenna protein structures used in the present study.** Structures were predicted using PHYRE 2 software. Transmembrane helices are represented as yellow rectangles whilst stromal



**ARTICLE IV**

**Isolation and characterization of CAC antenna proteins and  
photosystem I supercomplex from the cryptophytic alga *Rhodomonas  
salina***

Kuthanová Trsková, E., Bína, D., Santabarbara, S., Sobotka, R., Kaňa,  
R., and Belgio, E.

(2019)

*Physiologia Plantarum* **166**, 309-319. IF (2018) = 3.0



# Isolation and characterization of CAC antenna proteins and photosystem I supercomplex from the cryptophytic alga *Rhodomonas salina*

Eliška Kuthanová Trsková<sup>a,b</sup>, David Bína<sup>b,c</sup>, Stefano Santabarbara<sup>d</sup>, Roman Sobotka<sup>a,b</sup>, Radek Kaňa<sup>a,b</sup> and Erica Belgio<sup>a,\*</sup>

<sup>a</sup>Institute of Microbiology, Academy of Sciences of the Czech Republic, 379 81, Třeboň, Czech Republic

<sup>b</sup>Faculty of Science, University of South Bohemia in České Budějovice, 370 05, České Budějovice, Czech Republic

<sup>c</sup>Institute of Plant Molecular Biology, Biology Centre CAS, 370 05, České Budějovice, Czech Republic

<sup>d</sup>Photosynthesis Research Unit, Centro Studi sulla Biologia Cellulare e Molecolare delle Piante, 20133, Milan, Italy

## Correspondence

\*Corresponding author,  
e-mail: belgio@alga.cz

Received 15 January 2019

doi:10.1111/ppl.12928

In the present paper, we report an improved method combining sucrose density gradient with ion-exchange chromatography for the isolation of pure chlorophyll *a/c* antenna proteins from the model cryptophytic alga *Rhodomonas salina*. Antennas were used for in vitro quenching experiments in the absence of xanthophylls, showing that protein aggregation is a plausible mechanism behind non-photochemical quenching in *R. salina*. From sucrose gradient, it was also possible to purify a functional photosystem I supercomplex, which was in turn characterized by steady-state and time-resolved fluorescence spectroscopy. *R. salina* photosystem I showed a remarkably fast photochemical trapping rate, similar to what recently reported for other red clade algae such as *Chromera velia* and *Phaeodactylum tricorutum*. The method reported therefore may also be suitable for other still partially unexplored algae, such as cryptophytes.

## Introduction

Together with stramenopiles (or heterokonts), alveolates and haptophytes, cryptophytes have long been considered as part of the Chromalveolata supergroup (Cavalier-Smith 1999), with plastids originated from single secondary endosymbiosis with a red alga (Lane and Archibald 2008, Keeling 2009). Like haptophytes, stramenopiles and dinoflagellates, cryptophytes are characterized by the unique presence of chlorophyll *c* (Jeffrey 1976, Cavalier-Smith 2018). Plastids from these groups also share a common structure with four membranes, the outermost of which is connected to the endo-membrane and to the nuclear envelope (Cavalier-Smith 1999, Cavalier-Smith 2018). However,

a consensus is emerging that the Chromalveolata supergroup is not monophyletic and now the four original subgroups have been split at least into two categories: one comprises the stramenopiles and the alveolates, to which the rhizaria are now usually added to form the stramenopiles (heterokonts), alveolates, and rhizaria (SAR) group; the other comprises the cryptophytes and the haptophytes (Burki et al. 2008, Kim and Graham 2008). Recent phylo-genomic analysis by Burki et al. (2012) even indicated that cryptophytes are not even sister group to SAR, as they seem to branch with plants. Cryptophytes are indeed distinguished from other algae by the presence of characteristic extrusomes called ejectisomes or ejectosomes, which allow algae to move away from disturbance like light stress. Moreover, they

**Abbreviations** –  $\beta$ -DM, dodecyl- $\beta$ -maltoside; CAC, chlorophyll *a/c*; CN-PAGE, clear native polyacrylamide gel electrophoresis; DAS, decay-associated spectra; DCPIP, dichlorophenolindophenol; FWHM, full width at half maximum; IRF, instrument response function; NPQ, non-photochemical quenching; PSI, photosystem I; PSII, photosystem II.

are the only known lineage that still harbors a red-algal endo-symbiont nucleus (so-called nucleomorph). For all these reasons, cryptophytes are of pivotal importance to study endosymbiosis and evolution (see, e.g. Burki et al. 2012).

Cryptophytes are peculiar in many ways. In the context of evolution, they carry a unique light harvesting system composed of phycobiliproteins and chlorophyll *a/c* (CAC) antenna proteins. Phycobiliproteins differ from phycobilisomes of red algae and cyanobacteria in several aspects, from their location to their structure and type of phycoerythrin/phycoerythrin bound (Green and Parson 2003, Overkamp et al. 2014). CAC proteins can be considered as the cryptophytic equivalent of light harvesting complex (LHC), because they are membrane intrinsic, three- $\alpha$ -helix proteins, evolutionarily closely related to LHCs of red algae (Green and Parson 2003). Cryptophytes are the only known algae that displays a flexible and effective photoprotective non-photochemical quenching (NPQ) (Kaňa et al. 2012) co-regulated with state transitions in function of the growth stage (Cheregi et al. 2015). At the molecular level, the cryptophytic photosystem I (PSI) binds few of the so-called red chlorophyll forms, with important implications on chlorophyll-chlorophyll energy transfer (Belgio et al. 2017). Finally, CAC proteins do not bind any xanthophyll cycle pigments, but they are instead characterized by unusual carotenenes. The major one, alloxanthin, is the only known carotene with two triple bonds in photosynthetic organisms, and it was recently studied by advanced spectroscopic methods (West et al. 2016).

Despite this, cryptophytes have not been thoroughly studied yet, partially because no standardized biochemical methods are currently available for the purification of photosynthetic complexes from them. The main issue of any such protocols is the minimization of contaminants, especially in isolated antennas, and the maintenance of supercomplex functionality in case of photosystems. Here, we improved isolation of CAC proteins by coupling sucrose gradient to ion-exchange chromatography and antennas were employed for *in vitro* quenching by detergent removal. At the same time, sucrose gradient allowed isolation of functional PSI supercomplex from *Rhodomonas salina*, which was characterized by steady-state and time-resolved spectroscopy. The method therefore proved useful to get new insight on various biophysical and ecological aspects of cryptophytes.

## Materials and methods

### Membrane preparation

Thylakoid membranes were extracted from *R. salina* cells by a procedure described previously in Kaňa et al.

(2016). Briefly, harvested cells were resuspended in 25-mM 4-(2-hydroxyethyl)-1-piperazineethanesulfonic acid (HEPES) pH 7.8 and broken by glass beads, membranes were separated from cell extracts by centrifugation (40 000 g for 20 min) and washed twice to get rid of residuals of phycobiliproteins.

### Sucrose density ultracentrifugation

Thylakoid membranes (1 mg of chlorophyll) were solubilized with 2% dodecyl- $\beta$ -maltoside ( $\beta$ -DM), for 1 h on ice, loaded onto continuous sucrose gradient (5–20% sucrose in 25-mM HEPES pH 7.8, 0.04%  $\beta$ -DM) and ultracentrifuged using SW 28 rotor (L8-M ultracentrifuge; Beckmann, Brea, California, USA) at 4°C for 20 h at 141118 g (based on Kaňa et al. 2012).

### Ion-exchange chromatography

Two millimeter of fraction 2 (PP2) and 3 (PP3) collected from sucrose gradient (Fig. 1) were loaded into a Pharmacia fast protein liquid chromatography (FPLC) system equipped with UV/Vis detector (SPD 20AV; Shimadzu, Kyoto, Japan). Proteins were separated on an anion-exchange column (UnoQ-6; Bio-Rad, Hercules, California, USA) and their absorbance recorded at 450 and 670 nm. The proteins were eluted by a protocol starting with 15 min of isocratic washing with buffer A (20-mM HEPES, 0.04%  $\beta$ -DM, pH 8) followed by 45 min of a linear gradient of  $MgCl_2$  (0–0.25 M) in buffer A. The concentration of  $MgCl_2$  was finally increased from 0.25 to 0.5 M in a 5 min ramp to elute the remaining proteins from the column. The separation was carried out at 8°C at the constant flow rate of 1 ml min<sup>-1</sup>.

### Absorption and fluorescence steady-state spectroscopy

77-K fluorescence emission spectra were measured using an Aminco–Bowman Series 2 spectrofluorometer (Thermo Fisher Scientific, Waltham, Massachusetts, USA). For fluorescence emission, the excitation wavelength was 435 nm and the slit width 4 nm. The emission spectra were recorded in 0.4-nm steps from 600 to 800 nm, with 1-nm slit width. The instrument function was corrected by dividing raw emission spectra by simultaneously recorded signal from the reference diode. Absorption spectra were detected by Unicam UV/vis 500 spectrometer (Thermo Spectronic, Loughborough, UK) in the standard cuvette setup from 340 to 760 nm (1-nm bandwidth, 0.5-nm steps).

### In vitro quenching of purified CAC proteins

CAC proteins ( $OD_{676} = 0.5 \text{ cm}^{-1}$  in 20-mM HEPES 0.01%  $\beta$  DM, pH 8) were injected into a fluorescence



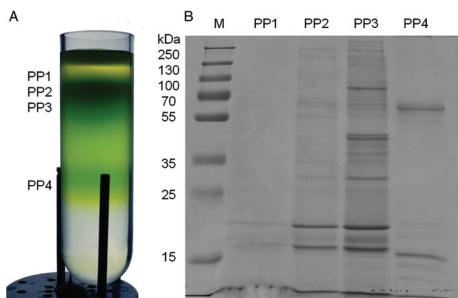


**Fig. 1.** Isolation and characterization of photosynthetic complexes of *Rhodomonas salina*. Panel A. CAC proteins and PSI supercomplex in a native state were isolated by ultracentrifugation in a sucrose gradient (5–15% sucrose in 25-mM HEPES, pH 7.8, 0.04%  $\beta$ -DM) yielding four bands (PP1–PP4), which were subsequently characterized by 12% standard SDS-PAGE as seen in panel B. The resulting protein pattern was assigned based on Kaňa et al. (2012): PP1, mainly free pigments; PP2 and PP3, CAC proteins (18–20 kDa); PP4, PSI supercomplex.

measuring chamber, and adsorbent beads (0.15 g; Bio-Beads SM-2, Bio-Rad) were added under constant stirring. Chlorophyll fluorescence was continuously monitored using a Dual PAM 100 Fluorometer (Walz, Effeltrich, Germany).

### Time-resolved fluorescence spectroscopy

The time-resolved fluorescence spectroscopy of PSI was measured and processed as previously described in Belgio et al. (2017). Briefly, the excited-state decay kinetics were detected using a laboratory assembled time-correlated single-photon counting setup. The PSI samples, at an optical density  $0.1 \text{ cm}^{-1}$  at maximal absorption, were placed in a 3-mm path-length cuvette (at  $10^\circ\text{C}$ ). They were incubated with  $10\text{-}\mu\text{M}$  dichlorophenolindophenol and  $100\text{-}\mu\text{M}$  ascorbate in 25-mM HEPES, pH 7.2 to ensure photochemically open state of PSI (P700). The emission was detected by a cooled microchannel plate photomultiplier (R5916U-51; Hamamatsu photonics, Hamamatsu City, Japan). The decay kinetics were collected and stored by an integrated board (SPC-330; Becker & Hickl, Berlin, Germany). The excitation is provided by a pulsed diode laser (PicoQuant 800B, Berlin, Germany), centered at 632 nm [full width at half maximum (FWHM) 3 nm], operating at a repetition rate of 20 MHz. The intensity was kept sufficiently weak (2 pJ/pulse) to avoid non-linear absorption processes and building-up of long-lived metastable species. Moreover, the excitation conditions were verified on the present samples, by varying the pulse repetition rate and intensity, using neutral density filter. The kinetics were not affected by changing the average excitation flux by over one order of magnitude. The instrument response function (IRF), measured using 1,1'-diethyl-2,2'-carbocyanine iodide, was 110 ps FWHM, that after numerical deconvolution, allows resolving lifetimes of the order of 10 ps.

Lifetimes of unquenched and quenched CAC proteins were measured by a FluoTime 300 using LDH-P-C-485 excitation laser, PMA-C-192 detector and TimeHarp 260 PICO TCSPC board (PicoQuant, Berlin, Germany). Data were analyzed using FluoFit software (PicoQuant).

### Time-resolved data analysis of PSI

For PSI analysis, the excited-state decay was analyzed by convoluting the IRF and a decay model function, consisting in a sum of weighted exponential functions, using the global analysis approach by a laboratory developed software named multiexp (see Belgio et al. 2017 for more details). The outputs of the fit are the wavelength independent lifetimes and their associated, wavelength dependent, pre-exponential, amplitudes which define the decay-associated spectra (DAS). The presented DAS are the weighted means from two to three independent purifications of PSI. The average trapping time was calculated from the fit solutions as previously described in Belgio et al. (2017). As previously demonstrated in Jennings et al. (2004), this parameter represents the effective trapping time of the photochemistry.

### Pigment analysis

Pigments analysis was performed on an Agilent-1200 HPLC device as essentially described in Shukla et al. (2018). Samples (CAC proteins and PSI supercomplex) were extracted with 90% methanol and the extract was separated on a reverse phase column (4.6  $\mu\text{m}$ , 100 mm; Zorbax Eclipse Plus C18, Agilent technologies, Santa Clara, California, USA) with 35% methanol and 15% acetonitrile in 0.25-M pyridine (solvent A) and 20% methanol, 20% acetone in acetonitrile as solvent B. Pigments were eluted with a linear gradient of solvent B (60–100% in 25 min) followed by 100% of solvent B at a flow rate of  $0.8 \text{ ml min}^{-1}$  at  $40^\circ\text{C}$ . Eluted pigments were monitored by their absorption at 440 nm, and their

spectra were determined according to the literature. The pigment contents were calculated as ratios between integrated peak areas.

### Analysis of protein complexes by 2D electrophoresis

Analysis of native complexes from sucrose gradient was performed using clear native (CN) electrophoresis as described previously (Dobáková et al. 2007, Wittig and Schagger 2008). Isolated complexes were separated on 4 to 14% CN-polyacrylamide gel electrophoresis (PAGE), and individual proteins were subsequently resolved in the second dimension by sodium dodecyl sulfate (SDS)-PAGE in a 12 to 20% linear gradient polyacrylamide gel containing 7-M urea. Protein spots were stained by Coomassie Blue. As the annotated genome of *R. salina* is not available, we assigned the relevant PSI and photosystem II (PSII) subunits based on previous studies on *R. salina* (Kaňa et al. 2012) and *Chromera velia* (Sobotka et al. 2017) using a typical pattern of these proteins as they comigrate with given complexes (D1, D2, CP43, CP47 protein for PSII and PsaA/B for PSI).

### Results

Thylakoid membranes were prepared from *R. salina* cells, solubilized by  $\beta$ -DM and the obtained protein complexes separated by ultracentrifugation by a method described previously in Kaňa et al. (2016); see also section Materials and methods. Four pigmented bands (PP1–4, counted from the top of the gradient) were collected and analyzed by SDS-PAGE (Fig. 1). The upper band PP1 consisted mainly of free pigments, PP2 and PP3 bands showed a similar protein pattern as they both contained CAC proteins, in agreement with Kaňa et al. (2012), with PP3 more enriched with photosystems (Fig. S1). Band PP4 contained a ‘large’ PSI supercomplex (‘PSI L’ of Fig. 2), of around 750-kDa size, as confirmed by 2D CN/SDS electrophoresis. This fraction was used for time-resolved/steady-state spectroscopy measurements without any further purification step, while bands PP2 and PP3 were further purified to obtain high-quality CAC proteins. In order to get rid of contamination from photosystems, these two bands were loaded into an FPLC system and ion-exchange chromatography was performed as described in section Materials and methods. The resulting chromatogram is presented in Fig. 3. Pigment-protein complexes were separated into four major peaks: unbound free pigments; reaction centers (peak 1 of Fig. 3); CAC proteins with contamination of higher molecular weight proteins (peak 2); CAC proteins (peak 3).

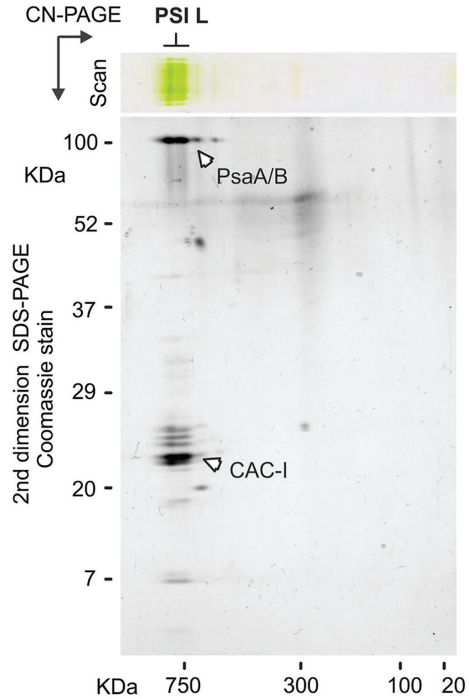


**Fig. 2.** 2D CN/SDS electrophoresis of the PSI complex (band PP4) isolated by sucrose gradient. The PP4 fraction (see Fig. 1) was first separated by a native 4–12% gradient polyacrylamide gel that was scanned in true colors by Canon CanoScan 8800F scanner (Scan). Gel strip from CN-PAGE was further separated in a second dimension by SDS-PAGE and stained with Coomassie blue. PSI L indicates the isolated PSI core complex associated with CAC proteins with a total estimated mass around 750 kDa. A smaller PSI complex designated PSI S was identified in the sucrose gradient PP3 fraction (see Fig. S1). Spots of PsaA/B and the PSI-associated CAC proteins were assigned according to previous analysis of PSI complexes of *Rhodomonas salina* (Kaňa et al. 2012) and *Chromera velia* (Sobotka et al. 2017).

The isolated photosynthetic complexes, ‘PSI L’ from sucrose gradient (from this moment on referred to as PSI) and CAC proteins from ion-exchange chromatography were first analyzed by steady-state spectroscopy (Fig. 4) and their pigment composition determined (Tables 1 and 2). The values obtained for CAC proteins consists mainly of chlorophyll a, chlorophyll c and alloxanthin in approximately 10:10:7 M ratio, with the other xanthophylls present only in substoichiometric amounts, similar to what previously published by Kaňa et al. (2012). Compared to CAC proteins, PSI supercomplex contained

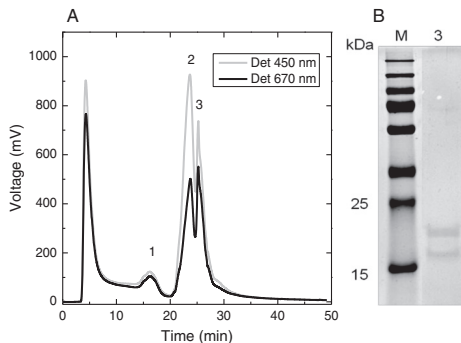


**Fig. 3.** Purification of CAC proteins. (A) Fractions PP2 and PP3 from sucrose gradient were loaded onto ion exchange chromatography column (UnoQ-6; Bio-Rad) in Pharmacia FPLC system equipped with UV/Vis detector (detection at 450 nm and 670 nm). The photosynthetic complexes were eluted with a linear gradient (0–0.25 M) of  $MgCl_2$  at constant flow rate  $1\text{ ml min}^{-1}$  and constant temperature of  $8^\circ\text{C}$ . The complexes were eluted in four distinct peaks: Unbound free pigments; reaction centers (peak 1); CAC proteins with contamination of higher molecular weight proteins (peak 2); CAC proteins (peak 3). (B) 12% SDS-PAGE of peak 3 from ion-exchange chromatography showed antenna proteins without the previous contamination from higher molecular weight proteins (molecular weights of corresponding protein standards are marked).

less chlorophyll *c* and alloxanthin and it was enriched in  $\beta$ -carotene (see also relative chromatograms in Fig. S2). The absorption maximum of PSI was at 682 nm (see Fig. 4), because of slightly red-shifted chlorophylls typical of PSI and visible in low temperature fluorescence at 712 nm (Fig. 4B). In both complexes, the presence of chlorophyll *c* determines a structured absorption at 467 nm, while the shoulder at 493 nm can be attributed to carotenenes, especially alloxanthin (see Kereiche et al. 2008). The low temperature fluorescence spectra have emission maximum at 682 and 712 nm for CAC proteins and PSI, respectively. A secondary emission peak at 682 nm in PSI is due to residual emission from the bulk of antenna and, possibly, to a minor contamination of energy uncoupled PSI-antenna complement.

CAC proteins were used for the *in vitro* study of the NPQ mechanism. Using a standard methodology (Ruban et al. 1997, van Oort et al. 2007, Belgio et al. 2013), an antenna sample was injected into a buffer were polystyrene bio-beads, acting as detergent adsorbants (see, e.g. Lambrev et al. 2011, Akhtar et al. 2015, Enriquez et al. 2015), were added, while monitoring fluorescence emission using a modulated fluorimeter (Fig. 5). This induced a 5 times decrease in the

steady-state emission of the sample, showing that like in higher plant antennas, also in CAC proteins quenching sites can be induced by detergent removal. Absorption spectra of antennas in unquenched and quenched states were measured and compared (Fig. 6). The obtained absorption difference spectrum indicated that the main changes occurred in the Soret region at 405 and 509 nm (Fig. 6, blue). However, the quenched state of CAC proteins also involved changes in the Qy region as the 77K emission spectrum was broader and by 4 nm red-shifted (Fig. 7). The unquenched versus quenched antennas were also analyzed and compared in terms of fluorescence lifetimes (Fig. 5B). In the unquenched sample approximately 80% of emission was due to a 3.5-ns component, while a very fast component (0.2 ns) represented most of the decay (66%) under quenched conditions. Time-resolved changes occurring upon quenching onset in CAC proteins were, therefore, very similar to those occurring in light harvesting complex II (LHCII) antennas (see section Discussion).

In order to verify the functionality (trapping efficiency) of *R. salina* PSI, band 4 from sucrose gradient was characterized by time-resolved spectroscopy (Fig. 8). Four components were needed to describe the time-resolved fluorescence decay: 13, 80, 2179 and 5222 ps. The two fast components (13 and 80 ps) represent the decay of the PSI as they have a maximum emission at approximately 685 nm, while the emission of the two slow components (2179 and 5222 ps) is shifted to shorter wavelengths (approximately 675 nm), which is typical of impurities (partially decoupled antennas and/or free chlorophyll). The present description of the decay is similar to the one previously found for *C. velia* and *Phaeodactylum tricornutum* PSI complexes in Belgio et al. (2017); it resulted in estimated trapping times of around 30 ps across the whole emission spectrum (670–750 nm, Fig. 8B). These trapping times are shorter than those found for intact PSI from higher plants (Fig. 8B). The present analysis therefore indicates that the *R. salina* PSI is one of the most efficient so far reported and that a high trapping efficiency is due to a low red form content (see section Discussion).

## Discussion

Isolation of pure but intact photosynthetic complexes is a crucial step in understanding of pigment-protein bioenergetics. It is generally more challenging to isolate native complexes from algal species than from higher plants because they often display peculiar thylakoid structure, lack of grana-stroma differentiation and therefore require specific solubilization conditions, without mentioning problems with cell disruption in general.

**Fig. 4.** Spectral analysis of CAC proteins and PSI. Panel A. Room temperature absorption spectrum of isolated *Rhodomonas salina* CAC proteins (solid line) and PSI complexes (dashed – Dotted line) with marked position of particular maxima. Spectra were recorded in the standard cuvette setup from 340 to 760 nm with 1-nm bandwidth and 0.5-nm steps. Spectra were normalized to the maximum in the Qy region. Panel B. Low temperature (77 K) fluorescence emission spectrum of isolated *R. salina* CAC proteins (solid line) and PSI complexes (dashed – Dotted line) were recorded after excitation at 435 nm and with the slit width of 4 nm. The spectra were normalized to the maximum.

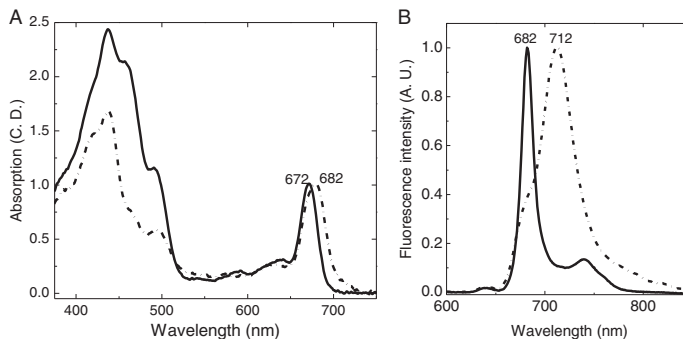


**Table 1.** Pigment content in isolated CAC proteins and PSI supercomplex of *Rhodomonas salina* based on HPLC data. Number represents integrated peak areas relative to total chlorophyll (Chl).

Sample	Chl a	Chl c	Alloxanthin	Monodoxanthin	Crocoxanthin	Carotene
CAC proteins	0.500 ± 0.002	0.500 ± 0.002	0.720 ± 0.007	0.120 ± 0.001	0.120 ± 0.001	0.030 ± 0.002
PSI supercomplex	0.899 ± 0.005	0.101 ± 0.005	0.280 ± 0.012	0.048 ± 0.002	0.067 ± 0.001	0.129 ± 0.034

**Table 2.** Pigment content of isolated CAC antenna and the PSI supercomplex of *Rhodomonas salina*, expressed as mol/100 mol chlorophyll (Chl) a.

Sample	Chl a	Chl c	Alloxanthin	Monodoxanthin	Crocoxanthin	Carotene
CAC proteins	100	100	68	8	8	2
PSI supercomplex	100	9	21	4	5	9

Compared to the available isolation protocol, a ‘washing’ step was added after cell disruption to get rid of phycobiliproteins, which can undermine gradient separation (Kaňa et al. 2012). Then different approaches were tested to improve the purity of isolated antennas. Using of alternative detergents to  $\beta$ -DM (i.e.  $\alpha$ -DM, Triton X100 etc.) or a combination of detergents did not yield any significant improvement; antenna proteins were always contaminated with higher molecular weight proteins and they lost their intactness. This observation seems to imply stronger bonds between antennas and reaction centers in *R. salina* (or other cryptophytes; see, e.g. Janssen and Rhiel 2008, Kereiche et al. 2008) than in higher plants, as previously also found for other red clade species in general (see, e.g. Büchel 2003, Kaňa et al. 2016). On the other hand, it may relate to the fact that chlorophyll c-containing antennas seem to be more delicate (see, i.e. Büchel 2003) and therefore sensitive to detergents. A combination of sucrose gradient density centrifugation and ion-exchange chromatography therefore

appears to be an appropriate method to eliminate contaminations without affecting CAC protein integrity. It was, therefore, possible to use the isolated antenna for in vitro quenching experiment (Fig. 5), which suggested that protein–protein aggregation, by changing relative distances/positions of pigments, induces formation of quenching sites within CAC proteins, in a possibly very similar way to what previously observed for higher plant antennas (Horton et al. 2000). Concomitant spectral changes in the absorption spectrum were mainly observed in the Soret region, at 455 and 509 nm, and in the Qy region, at 662, 673 and 682 nm. It is interesting to note that the latter changes were almost identical to those occurring in quenched LHCII (662, 670 and 681 nm; see, i.e. Ruban et al. 1992, Iliaia et al. 2008), suggesting involvement of similar rearrangements of chlorophyll pigments in the quenched antenna proteins. In agreement with this, the emission spectrum of quenched CAC proteins was broader and red-shifted (by 4 nm) compared to the unquenched one. This is a typical quenching feature of higher plant antennas, where red shifts up to 710 nm can be found (Ruban et al. 1997, van Oort et al. 2007). On the other hand, the different absorption changes compared to LHCII in the Soret region may be related to the fact that xanthophylls cycle pigments are not involved in quenching of CAC proteins (Kaňa et al. 2012). *R. salina*, in fact, carries xanthophylls which are not common in photosynthetic organisms with unusual chemical properties related to

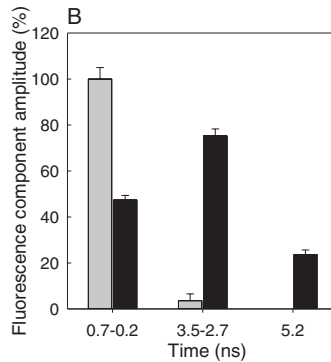
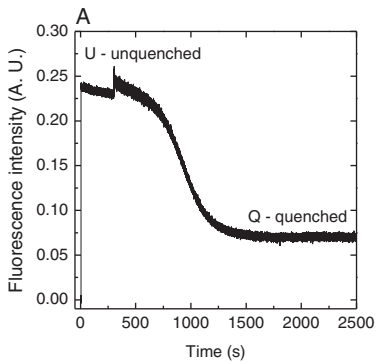


**Fig. 5.** In vitro quenching of purified CAC proteins: Quenching of CAC proteins induced by protein aggregation. (A) CAC proteins were injected into a fluorescence measuring chamber and bio-beads added under constant stirring. After 25 min, antennas fluorescence was reduced to 1/5 of the beginning. (B) Analysis of the chlorophyll fluorescence lifetime in harvesting and photoprotective states. Relative time-resolved fluorescence lifetime component amplitudes of unquenched (black) and quenched (gray) antennas. Data are means from three replicates  $\pm$  s.d.

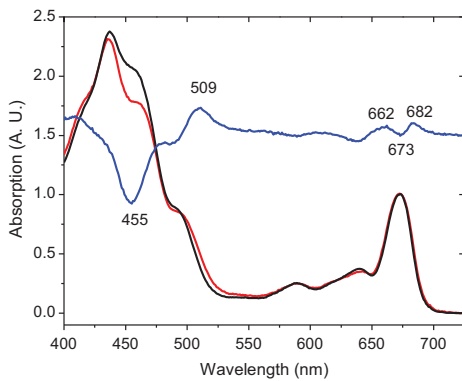


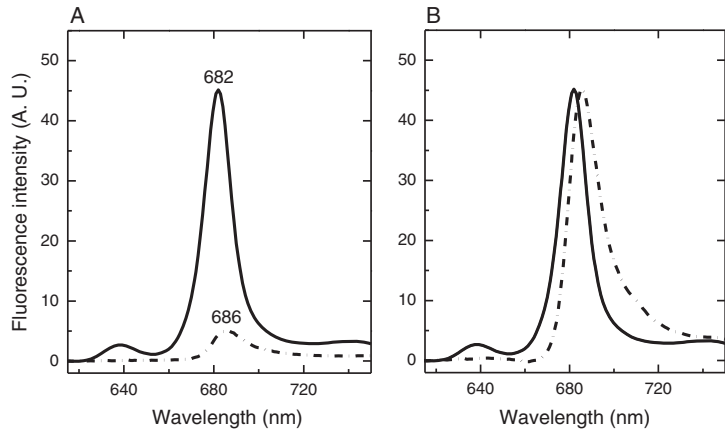
**Fig. 6.** Absorption spectrum of CAC proteins in unquenched/quenched states. Room temperature absorption spectrum of CAC proteins in unquenched (black) and quenched (red) states, corresponding to point U and Q of Fig. 5, respectively, were recorded in the standard cuvette setup from 340 to 760 nm with 1-nm bandwidth and 0.5-nm steps. The spectra were normalized to the maximum of absorption in the Qy region. The blue line represents quenched minus unquenched difference spectrum.

the presence of three triple bonds (see Fig. S2 and S3 for chromatogram and structure of alloxanthin, monadoxanthin and crocoxanthin). The exact role of triple bonds in light harvesting remains unknown, nevertheless, their presence have important consequences for excited-state dynamics and it cannot be excluded that alloxanthin, the main carotene of CAC proteins, may play a role in photoprotective quenching (West et al. 2016).

Fluorescence lifetime analysis of CAC proteins revealed that the unquenched sample was mainly characterized by a 3.5-ns component, similar to LHClI

antennas (see, e.g. Ide et al. 1987, Bassi et al. 1991). However, for the CAC proteins, one longer lifetime of approximately 5.2 ns representing approximately 20% of the emission was also required to fit the decay. Spectral analysis (data not shown) indicated that the spectrum of the two components was identical, with the maximum of emission around 680 nm, both components, therefore, represent emission from antennas and not from impurities. Their origin is most probably related to different oligomeric states of the CAC proteins, similar to fucoxanthin chlorophyll *a/c* binding protein (FCP) antennas from diatoms as seen in Büchel (2003). The average lifetime of unquenched CAC proteins (3.9 ns) is in the range of those previously reported for LHClI and minor antenna complexes of higher plants (Crimi et al. 2001, Moya et al. 2001, van Oort et al. 2007, Belgio et al. 2012). Besides shortening the two components down to 2.7 ns (2.4%) and 0.7 ns (31%), the detergent removal induced appearance of a very fast component (0.2 ns), which represented most of the decay (66%) under quenched conditions. As a result, the average fluorescence lifetime was 0.4 ns (quenching  $K_d \sim 9$ ). As loss of pigment leads to long (>4 ns) fluorescence lifetimes, both evidence, red-shift of 77K fluorescence spectrum and shortening of lifetimes, indicate that very limited protein unfolding occurred upon quenching onset (see, e.g. Illoia et al. 2008, Natali et al. 2016). The current analysis is overall very similar to that of LHClI antennas (see, i.e. Petrou et al. 2014), it therefore allows suggesting that protein aggregation may be a plausible mechanism of quenching without xanthophylls cycle also in *R. salina*. Nevertheless, in order to confirm that aggregational quenching is physiological mechanism of photoprotection for the alga, further studies will be required.

**Fig. 7.** Low temperature fluorescence spectrum of unquenched/quenched CAC proteins. (A) Low temperature (77 K) fluorescence emission spectrum of unquenched (solid line) versus quenched (dashed line) state of CAC proteins, corresponding to point U and Q of Fig. 5, respectively, were recorded after excitation at 435 nm and with the slit width of 4 nm, position of particular maxima are marked. (B) Fluorescence emission spectra from Panel A normalized to the maximum.



There were at least two forms of PSI purified by sucrose gradient: PSI L, ‘large’, in band PP4, used for all further analysis, was around 750-kDa size (protein assignment based on Kaňa et al. 2012 and Sobotka et al. 2017) while band PP3 contained ‘small’ PSI (PSI S of Fig. S1), binding a lower number of antennas. Although the presence of two different types/aggregation states of PSI-CAC supercomplexes has been previously reported as a physiological condition in *Rhodomonas* SP24 (Kereiche et al. 2008), we cannot exclude that, in the present case, fraction PP3 can be instead an artifact of the solubilization procedure, inducing loss of antennas from PSI.

Looking at the pigment data (Table 2), it is possible to get an estimate of the pigment composition of PSI antenna, built on the assumption that *R. salina* PSI core, like all known PSI cores, binds approximately 20 carotenes +100 Chl a. For instance, utilizing red-algal

PSI core value of 21 +97 (Pi et al. 2018) after normalizing to carotene, one gets approximately 230 Chl a per PSI supercomplex, a standard value for PSI supercomplexes from a broad phylogenetic range, from red algae, heterokonts to green algae (Kargul et al. 2003, Ikeda et al. 2008, Thangaraj et al. 2011, Bína et al. 2016). The pigment content of PSI antenna can then be computed by the difference (Table 3). The pigment ratio thus obtained differs from that of CAC proteins, where the most conspicuous difference is the approximately 12-fold decrease of chlorophyll c to a ratio. While this does not exclude the possibility that some CAC proteins form a part of the PSI-bound antenna in zone PP4, it strongly suggests that the light harvesting system of *R. salina* consists of two spectrally distinct pools of pigment-protein complexes. The relative depletion of chlorophyll c in the PSI-bound antenna

**Fig. 8.** Trapping efficiency of *Rhodomonas salina* PSI. (A) Representative DAS of *R. salina* PSI resulting from the global analysis of the excited-state decay kinetics recorded at room temperature. (B) Spectral dependence of the average lifetime,  $\tau_{av}$ , calculated as  $\sum A_i \tau_i / \sum A_i$ , in the isolated PSI of *R. salina* (black), where the two fastest components (approximately 13 and approximately 80 ps) were considered. Higher plant PSI is also shown for comparison (value for plants are from Belgio et al. 2017). The error bars were estimated from the propagated confidence levels.

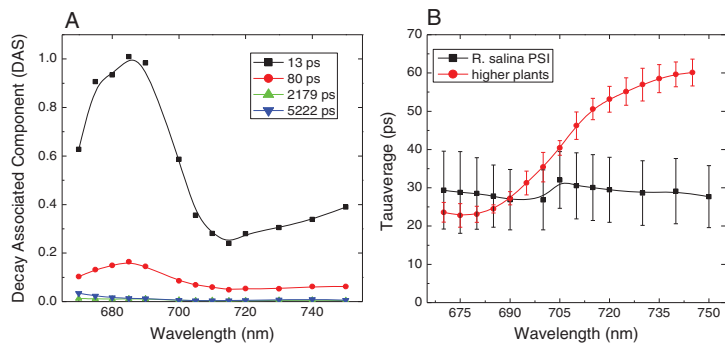




**Table 3.** Estimated pigment content per PSI core of the PSI supercomplex and PSI antenna calculated using measured values taken from Table 2 (shaded lines) and assuming 97 Chl a and 21 carotene molecules per PsaA/B dimer (see, e.g. Pi et al. 2018). \*From red algae (Pi et al. 2018).

	Chl a	Chl c	Alloxanthin	Monodoxanthin	Crocoxanthin	Carotene	
	CAC proteins	100	107.9	68.3	7.7	8.4	1.5
	PSI supercomplex	100	8.6	20.5	3.5	4.8	9.1
Theoretical <sup>a</sup>	PSI core	97	0	0	0	0	21
Per PSI core	PSI supercomplex	231	20	47	8	11	21
Per PSI core	PSI antenna	134	20	47	8	11	0

pool corresponds to the situation previously observed in other chlorophyll *c*-containing organisms of the red lineage (Bína et al. 2016). As for the number of antenna complexes bound to the PSI in *R. salina*, present data allow only for a rough estimate. However, it can be noted that a number of previous studies on the systems binding similar amount of pigments, such as largest red-algal PSI supercomplexes (Thangaraj et al. 2011, Haniewicz et al. 2018) and related heterokont systems (Bína et al. 2017) estimated nine LHC proteins. Moreover, the apparent mass of the PSI-LHC supercomplex of *R. salina* (approximately 750 kDa) corresponds quite well to the size of the PSI-Lhca complex, also containing nine antenna subunits, from the green alga *Chlamydomonas reinhardtii* (approximately 770 kDa, Drop et al. 2011).

The emission spectrum of *R. salina* PSI was very similar to that of other algae with limited number of red-forms (see, i.e. Belgio et al. 2017). The overall description of the decay is similar to that previously obtained for *C. velia* and *P. tricornutum* PSI core-antenna supercomplexes. The decay is largely dominated by a lifetime of approximately 15 ps. A second lifetime of 80 ps, showing spectral characteristic typical of PSI emission is also retrieved from the analysis, which is faster than the approximately 180-ps component observed in *C. velia* and *P. tricornutum* and has a larger relative amplitude. This might relate to different average energy transfer time for the moderately red-shifted chlorophyll forms in *R. salina* with respect to the *C. velia* and *P. tricornutum*. As already discussed in Belgio et al. (2017), the limited presence of the so-called ‘red’ chlorophyll forms in *R. salina*, *C. velia* and *P. tricornutum* PSI complexes, results in a weak dependence of the fluorescence average lifetime (tau average) upon wavelength across the whole emission band. On the contrary, PSI trapping is wavelength-dependent in higher plant and cyanobacterial PSI complexes, both harboring significant amounts of red-forms (see also Fig. 8B). As a result, in place of a similar cross section in terms of total chlorophyll bound to the PSI-antenna supercomplex, the overall photochemical trapping, calculated from the two fastest component over the entire emission band, is faster (approximately 22 ps) in *R. salina* PSI than that of higher

plants (40–45 ps, see, i.e. Jennings et al. 2013 and Santabarbara et al. 2017 for more details).

In conclusion, the study here presented shows that CAC proteins act similar to higher plant antennas during *in vitro* quenching, suggesting that, despite the absence of xanthophylls cycle, a similar quenching model may be applied. On the other hand, *R. salina* PSI displays high trapping efficiency that is more typical of red clade algae (second endosymbionts). The results altogether point at the complexity of algae still partially unexplored, like cryptophytes, which thanks to current method can be better characterized and understood.

### Author contributions

E.B. and E.K.T. conceived the project; E.K.T. and E.B. performed the experiments and analyzed the data; R.S. provided experimental advice on 2D/CN gels and chromatographic techniques; D.B. provided assistance with lifetime measurements of CAC proteins and HPLC data; S.S. provided assistance with lifetime measurements of PSI complex; E.B. and E.K.T. wrote the article with contributions from all the co-authors; R.K. supervised and complemented the work.

*Acknowledgements* – This research project was mainly supported by the Czech Science Foundation, project 17-02363Y (E.B.). Further support was from the Institutional project Algatex Plus (MSMT LO1416) of the Czech Ministry of Education, Youth and Sport. D.B. acknowledges Institutional support RVO:60077344. The authors thank Jan Pilný and Jana Zahradníková for their technical help with pigment analysis and gel electrophoresis.

### References

- Akhtar P, Dorogi M, Pawlak K, Kovacs L, Bota A, Kiss T, Garab G, Lambrev PH (2015) Pigment interactions in light-harvesting complex II in different molecular environments. *J Biol Chem* 290: 4877–4886
- Bassi R, Silvestri M, Dainese P, Moya I, Giacometti GM (1991) Effects of a nonionic detergent on the spectral properties and aggregation state of the light-harvesting chlorophyll - a/b protein complex (LHCII). *J Photochem Photobiol B-Biol* 9: 335–354

- Belgio E, Johnson MP, Juric S, Ruban AV (2012) Higher plant photosystem II light-harvesting antenna, not the reaction center, determines the excited-state lifetime—both the maximum and the nonphotochemically quenched. *Biophys J* 102: 2761–2771
- Belgio E, Duffy CD, Ruban AV (2013) Switching light harvesting complex II into photoprotective state involves the lumen-facing apoprotein loop. *Phys Chem Chem Phys* 15: 12253–12261
- Belgio E, Santabarbara S, Břina D, Trsková E, Herbstová M, Kaňa R, Zucchelli G, Prášil O (2017) High photochemical trapping efficiency in photosystem I from the red clade algae *Chromera velia* and *Phaeodactylum tricorutum*. *Biochim Biophys Acta* 1858: 56–63
- Břina D, Herbstová M, Gardian Z, Vácha F, Litvín R (2016) Novel structural aspect of the diatom thylakoid membrane: lateral segregation of photosystem I under red-enhanced illumination. *Sci Rep* 6: 25583
- Břina D, Gardian Z, Herbstová M, Litvín R (2017) Modular antenna of photosystem I in secondary plastids of red algal origin: a *Nannochloropsis oceanica* case study. *Photosynth Res* 131: 255–266
- Büchel C (2003) Fucoxanthin-chlorophyll proteins in diatoms: 18 and 19 kDa subunits assemble into different oligomeric states. *Biochemistry* 42: 13027–13034
- Burki F, Shalchian-Tabrizi K, Pawlowski J (2008) Phylogenomics reveals a new ‘megagroup’ including most photosynthetic eukaryotes. *Biol Lett* 4: 366–369
- Burki F, Okamoto N, Pombert JF, Keeling PJ (2012) The evolutionary history of haptophytes and cryptophytes: phylogenomic evidence for separate origins. *Proc Biol Sci* 279: 2246–2254
- Cavalier-Smith T (1999) Principles of protein and lipid targeting in secondary symbiogenesis: euglenoid, dinoflagellate, and sporozyan plastid origins and the eukaryote family tree. *J Eukaryot Microbiol* 46: 347–366
- Cavalier-Smith T (2018) Kingdom Chromista and its eight phyla: a new synthesis emphasising periplastid protein targeting, cytoskeletal and periplastid evolution, and ancient divergences. *Protoplasma* 255: 297–357
- Cheregi O, Kotabová E, Prášil O, Schröder W, Kaňa R, Funk C (2015) Presence of state transitions in the cryptophyte alga *Guillardia theta*. *J Exp Bot* 66: 6461–6470
- Crimi M, Dorra D, Bosinger CS, Giuffra E, Holzwarth AR, Bassi R (2001) Time-resolved fluorescence analysis of the recombinant photosystem II antenna complex CP29. Effects of zeaxanthin, pH and phosphorylation. *Eur J Biochem* 268: 260–267
- Dobáková M, Tichý M, Komenda J (2007) Role of the PsbI protein in photosystem II assembly and repair in the cyanobacterium *Synechocystis sp* PCC 6803. *Plant Physiol* 145: 1681–1691
- Drop B, Webber-Birungi M, Fusetti F, Kouril R, Redding KE, Boekema EJ, Croce R (2011) Photosystem I of *Chlamydomonas reinhardtii* contains nine light-harvesting complexes (Lhca) located on one side of the core. *J Biol Chem* 286: 44878–44887
- Enriquez MM, Akhtar P, Zhang C, Garab G, Lambrev PH, Tan HS (2015) Energy transfer dynamics in trimers and aggregates of light-harvesting complex II probed by 2D electronic spectroscopy. *J Chem Phys* 142: 212432
- Green B, Parson W (2003) *Light-Harvesting Antennas in Photosynthesis*, Vol. 13. Kluwer Academic Publishers, Dordrecht
- Haniewicz P, Abram M, Nosek L, Kirkpatrick J, El-Mohsnawy E, Olmos JDJ, Kouril R, Kargul JM (2018) Molecular mechanisms of photoadaptation of photosystem I supercomplex from an evolutionary cyanobacterial/algal intermediate. *Plant Physiol* 176: 1433–1451
- Horton P, Ruban AV, Wentworth M (2000) Allosteric regulation of the light-harvesting system of photosystem II. *Philos Trans R Soc Lond Ser B-Biol Sci* 355: 1361–1370
- Ide JP, Klug DR, Kühlbrandt W, Giorgi LB, Porter G (1987) The state of detergent solubilized light-harvesting chlorophyll-a/b protein complex as monitored by picosecond time-resolved fluorescence and circular-dichroism. *Biochim Biophys Acta* 893: 349–364
- Ikeda Y, Komura M, Watanabe M, Minami C, Koike H, Itoh S, Kashino Y, Satoh K (2008) Photosystem I complexes associated with fucoxanthin-chlorophyll-binding proteins from a marine centric diatom, *Chaetoceros gracilis*. *Biochim Biophys Acta* 1777: 351–361
- Ilioaia C, Johnson MP, Horton P, Ruban AV (2008) Induction of efficient energy dissipation in the isolated light-harvesting complex of photosystem II in the absence of protein aggregation. *J Biol Chem* 283: 29505–29512
- Janssen J, Rhiel E (2008) Evidence of monomeric photosystem I complexes and phosphorylation of chlorophyll a/c-binding polypeptides in *Chromonas* sp strain LT (Cryptophyceae). *Int Microbiol* 11: 171–178
- Jeffrey SW (1976) The occurrence of chlorophyll c1 and c2 in algae. *J Phycol* 12: 349–354
- Jennings RC, Zucchelli G, Engelmann E, Garlaschi FM (2004) The long-wavelength chlorophyll states of plant LHCI at room temperature: a comparison with PSI-LHCI. *Biophys J* 87: 488–497
- Jennings RC, Zucchelli G, Santabarbara S (2013) Photochemical trapping heterogeneity as a function of wavelength, in plant photosystem I (PSI-LHCI). *Biochim Biophys Acta* 1827: 779–785
- Kaňa R, Kotabová E, Sobotka R, Prášil O (2012) Non-photochemical quenching in cryptophyte alga *Rhodomonas salina* is located in chlorophyll a/c antennae. *PLoS One* 7: e29700
- Kaňa R, Kotabová E, Kopečná J, Trsková E, Belgio E, Sobotka R, Ruban AV (2016) Violaxanthin inhibits nonphotochemical quenching in light-harvesting antennae of *Chromera velia*. *FEBS Lett* 590: 1076–1085
- Kargul J, Nield J, Barber J (2003) Three-dimensional reconstruction of a light-harvesting complex



- I-photosystem I (LHCI-PSI) supercomplex from the green alga *Chlamydomonas reinhardtii*. Insights into light harvesting for PSI. *J Biol Chem* 278: 16135–16141
- Keeling PJ (2009) Chromalveolates and the evolution of plastids by secondary endosymbiosis. *J Eukaryot Microbiol* 56: 1–8
- Kereiche S, Kouril R, Oostergetel GT, Fusetti F, Boekema EJ, Doust AB, van der Weij-de Wit CD, Dekker JP (2008) Association of chlorophyll a/c(2) complexes to photosystem I and photosystem II in the cryptophyte *Rhodomonas* CS24. *Biochim Biophys Acta* 1777: 1122–1128
- Kim E, Graham LE (2008) EEF2 analysis challenges the monophyly of Archaeplastida and Chromalveolata. *PLoS One* 3: e2621
- Lambrev PH, Schmitt F-J, Kussin S, Schoengen M, Várkonyi Z, Eichler HJ, Garab G, Renger G (2011) Functional domain size in aggregates of light-harvesting complex II and thylakoid membranes. *Biochim Biophys Acta* 1807: 1022–1031
- Lane CE, Archibald JM (2008) The eukaryotic tree of life: endosymbiosis takes its TOL. *Trends Ecol Evol* 23: 268–275
- Moya I, Silvestri M, Vallon O, Cinque G, Bassi R (2001) Time-resolved fluorescence analysis of the photosystem II antenna proteins in detergent micelles and liposomes. *Biochemistry* 40: 12552–12561
- Natali A, Gruber JM, Dietzel L, Stuart MCA, van Grondelle R, Croce R (2016) Light-harvesting complexes (LHCs) cluster spontaneously in membrane environment leading to shortening of their excited state lifetimes. *J Biol Chem* 291: 16730–16739
- van Oort B, van Hoek A, Ruban AV, van Amerongen H (2007) Aggregation of light-harvesting complex II leads to formation of efficient excitation energy traps in monomeric and trimeric complexes. *FEBS Lett* 581: 3528–3532
- Overkamp KE, Gasper R, Kock K, Herrmann C, Hofmann E, Frankenberg-Dinkel N (2014) Insights into the biosynthesis and assembly of cryptophycean phycobiliproteins. *J Biol Chem* 289: 26691–26707
- Petrou K, Belgio E, Ruban AV (2014) pH sensitivity of chlorophyll fluorescence quenching is determined by the detergent/protein ratio and the state of LHClI aggregation. *Biochim Biophys Acta* 1837: 1533–1539
- Pi X, Tian L, Dai H-E, Qin X, Cheng L, Kuang T, Sui S-F, Shen J-R (2018) Unique organization of photosystem I–light-harvesting supercomplex revealed by cryo-EM from a red alga. *Proc Natl Acad Sci USA* 115: 4423–4428
- Ruban A, Rees D, Pascal AA, Horton P (1992) Mechanism of  $\Delta$ pH-dependent dissipation of absorbed excitation energy by photosynthetic membranes. II. The relationship between LHClI aggregation in vitro and qE in isolated thylakoids. *Biochim Biophys Acta* 1102: 39–44
- Ruban AV, Calkoen F, Kwa SLS, van Grondelle R, Horton P, Dekker JP (1997) Characterisation of LHC II in the aggregated state by linear and circular dichroism spectroscopy. *Biochim Biophys Acta* 1321: 61–70
- Santabarbara S, Tibiletti T, Remelli W, Caffarri S (2017) Kinetics and heterogeneity of energy transfer from light harvesting complex II to photosystem I in the supercomplex isolated from Arabidopsis. *Phys Chem Chem Phys* 19: 9210–9222
- Shukla MK, Llansola-Portoles MJ, Tichy M, Pascal AA, Robert B, Sobotka R (2018) Binding of pigments to the cyanobacterial high-light-inducible protein HlIC. *Photosynth Res* 137: 29–39
- Sobotka R, Esson HJ, Konik P, Trskova E, Moravcova L, Horak A, Dufkova P, Obornik M (2017) Extensive gain and loss of photosystem I subunits in chromerid algae, photosynthetic relatives of apicomplexans. *Sci Rep* 7: 13214
- Thangaraj B, Jolley CC, Sarrou I, Bultema JB, Greyslak J, Whitelegge JP, Lin S, Kouril R, Subramanyam R, Boekema EJ, Fromme P (2011) Efficient light harvesting in a dark, hot, acidic environment: the structure and function of PSI-LHCl from *Galdieria sulphuraria*. *Biophys J* 100: 135–143
- West R, Kesan G, Trsková E, Sobotka R, Kaňa R, Fuciman M, Polívka T (2016) Spectroscopic properties of the triple bond carotenoid alloxanthin. *Chem Phys Lett* 653: 167–172
- Wittig I, Schagger H (2008) Features and applications of blue-native and clear-native electrophoresis. *Proteomics* 8: 3974–3990

## Supporting Information

Additional supporting information may be found online in the Supporting Information section at the end of the article.

**Fig. S1.** 2D CN/SDS electrophoresis of PP3 fraction isolated by sucrose gradient.

**Fig. S2.** Typical HPLC chromatogram of pigments extracted from *Rhodomonas salina* PSI supercomplex.

**Fig. S3.** Structure of pigments typical of *Rhodomonas salina*.

Edited by C. Spetea

## Supporting information

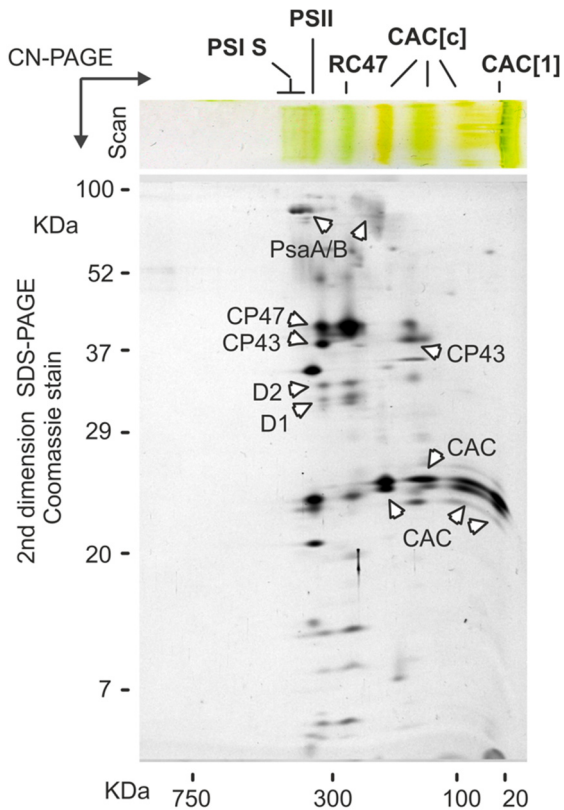


**Figure S1:** 2D CN/SDS electrophoresis of PP3 fraction isolated by sucrose gradient. The obtained fraction (see Fig. 1A) was first separated by a native 4–12% gradient polyacrylamide gel, which was scanned in true colours by Canon CanoScan 8800F scanner (Scan). Gel strip from CN-electrophoresis was further separated in a second dimension on a SDS-gel and stained with Coomassie blue. CAC[1] indicates monomeric CAC proteins; CAC[c] – oligomeric CAC protein assemblies; PSII – Photosystem II; RC47 – a disassembled PSII lacking the CP43 subunit. PSI S marks a PSI core complex associated with CAC proteins, which total mass is however smaller than the isolated PSI presented in Fig. 2. Individual protein spots were assigned according to previous analysis of thylakoid membranes complexes of *R. salina* (Kaňa et al. 2012) and *Chromera velia* (Sobotka et al. 2017).

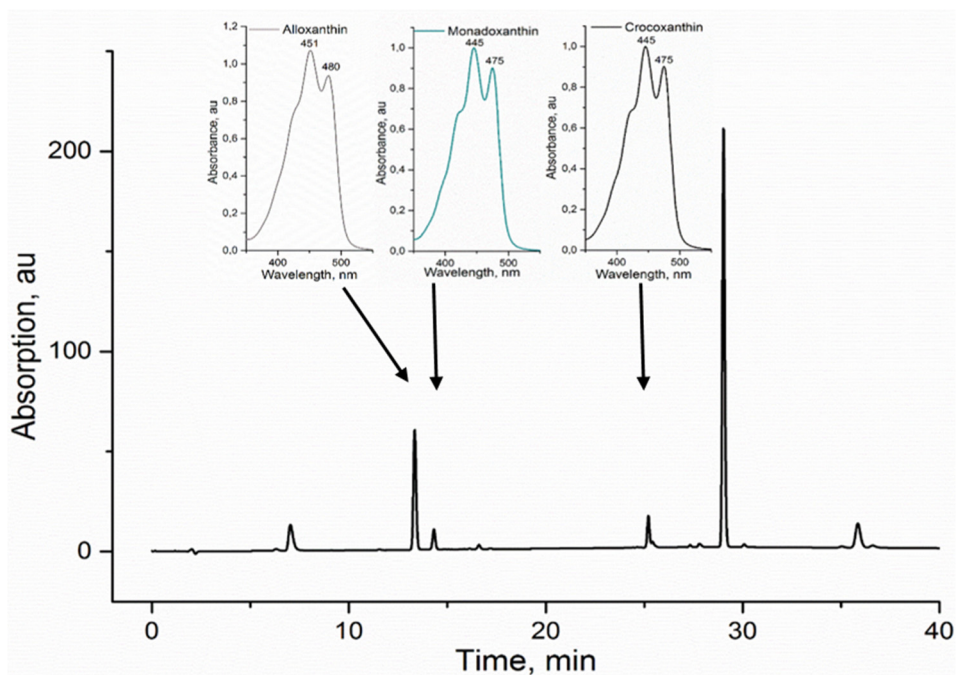


**Figure S2: Typical HPLC chromatogram of pigments extracted from *R. salina* PSI supercomplex.** Pigments extraction and analysis were performed essentially as described in Shukla et al. (2018). Pigments were eluted using a linear gradient (60–100% in 25 min) of 20% methanol, 20% acetone in acetonitrile followed by 100% of the same solvent at a flow rate of 0.8 mL min<sup>-1</sup> at 40 °C. Eluted pigments were monitored by their absorption at 440 nm and their spectra were determined according to the literature (Jeffrey et al. 1997). Retention times were: 7, 13, 14, 25, 29 and 35 minutes for chlorophyll *c*, alloxanthin, monadoxanthin, crocoxanthin, chlorophyll *a* and  $\beta$ -carotene, respectively. Inset: absorption spectra of alloxanthin, crocoxanthin, monadoxanthin. Relative pigment structures are presented in Figure S3.

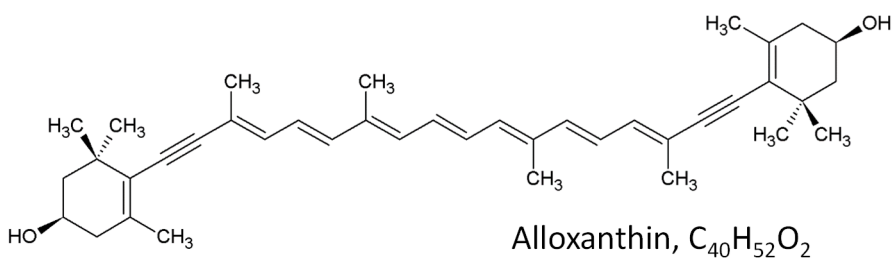
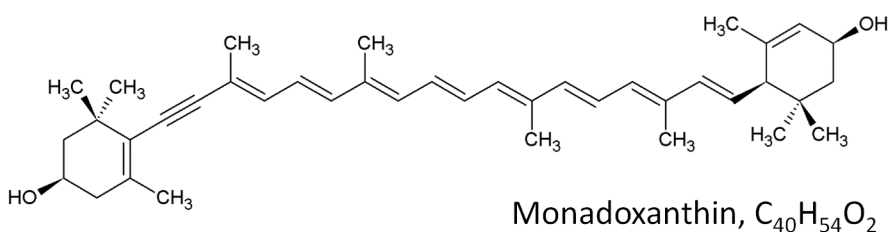
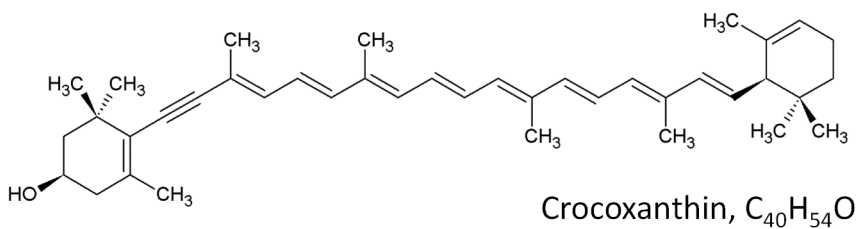


**Figure S3: Structure of pigments typical of *R. salina*.** Structures of alloxanthin, monadoxanthin, crocoxanthin extracted from PSI supercomplex as described in Figure S2 and eluted from HPLC at times: 13, 14 and 25 minutes, respectively. Absorption spectra are presented in Figure S2. Structures drawn using Chemsketch software and reference book (Jeffrey et al. 1997).

**Photoprotective strategies in the motile cryptophyte alga  
*Rhodomonas salina* – role of non-photochemical quenching, ions,  
photoinhibition and cell motility**

Kaňa, R., Kotabová, E., Šedivá, B., and Kuthanová Trsková, E.  
(2019)

*Folia Microbiologica* **64**, 691-703, IF (2018) = 1.31





# Photoprotective strategies in the motile cryptophyte alga *Rhodomonas salina*—role of non-photochemical quenching, ions, photoinhibition, and cell motility

Radek Kaňa<sup>1</sup> · Eva Kotabová<sup>1</sup> · Barbora Šedivá<sup>1</sup> · Eliška Kuthanová Trsková<sup>1,2</sup>

Received: 1 February 2019 / Accepted: 15 July 2019 / Published online: 27 July 2019  
© Institute of Microbiology, Academy of Sciences of the Czech Republic, v.v.i. 2019

## Abstract

We explored photoprotective strategies in a cryptophyte alga *Rhodomonas salina*. This cryptophytic alga represents phototrophs where chlorophyll *a/c* antennas in thylakoids are combined with additional light-harvesting system formed by phycobiliproteins in the chloroplast lumen. The fastest response to excessive irradiation is induction of non-photochemical quenching (NPQ). The maximal NPQ appears already after 20 s of excessive irradiation. This initial phase of NPQ is sensitive to  $\text{Ca}^{2+}$  channel inhibitor (diltiazem) and disappears, also, in the presence of non-actin, an ionophore for monovalent cations. The prolonged exposure to high light of *R. salina* cells causes photoinhibition of photosystem II (PSII) that can be further enhanced when  $\text{Ca}^{2+}$  fluxes are inhibited by diltiazem. The light-induced reduction in PSII photochemical activity is smaller when compared with immotile diatom *Phaeodactylum tricoratum*. We explain this as a result of their different photoprotective strategies. Besides the protective role of NPQ, the motile *R. salina* also minimizes high light exposure by increased cell velocity by almost 25% percent (25% from 82 to 104  $\mu\text{m/s}$ ). We suggest that motility of algal cells might have a photoprotective role at high light because algal cell rotation around longitudinal axes changes continual irradiation to periodically fluctuating light.

## Introduction

Photosynthetic organisms have colonized almost all environments on earth that are illuminated with visible light. They occupy all types of waters (fresh waters and marine); land including extreme conditions like soils, muds, and snow; or hypersaline environments (see, e.g., Lee 2008). Many of these environments are exposed to periods of excessive irradiations that can possibly lead to formation of reactive oxygen intermediates and result in damage to pigments, proteins, and lipids (Asada 2006; Li et al. 2009). Therefore, photosynthetic

organisms have evolved several mechanisms to cope with changing light environment and to optimize light photosynthetic reactions based on metabolic demands (see, e.g., Cruz et al. 2005; Derks et al. 2015; Giovagnetti and Ruban 2018; Goss and Lepetit 2014; Magdaong and Blankenship 2018).

One of the fastest responses to excessive irradiation is non-photochemical quenching (NPQ) of fluorescence. It represents a feedback regulatory mechanism that can dissipate excessive light (Croce and van Amerongen 2014; Horton and Ruban 2005; Ruban et al. 2012). The process of NPQ involves de-excitation of chlorophyll excited states and can be routinely detected by analysis of chlorophyll fluorescence induction (Muller et al. 2001) rather than by direct detection of NPQ-induced heating of the samples (Kaňa and Vass 2008). NPQ proceeds mostly at the level of photosystem II light-harvesting antennas (see, e.g., Belgio et al. 2012; Kuthanová Trsková et al. 2018). There is only minor effect of the reaction centrum quenching (Ivanov et al. 2008; Vass and Cser 2009) especially in extremophile algae (Krupnik et al. 2013; Ohad et al. 2010). The non-photochemical quenching at the level of chlorophyll *a/c* antennas has been already described also for cryptophytes (Kaňa et al. 2012), and it has shown its variability based on species (compare studies with *Rhodomonas salina* (Kaňa et al.

Dedicated to the memory of Dr. Ivan Šetlík

**Electronic supplementary material** The online version of this article (<https://doi.org/10.1007/s12223-019-00742-y>) contains supplementary material, which is available to authorized users.

✉ Radek Kaňa  
kana@alga.cz

<sup>1</sup> Institute of Microbiology, Centre ALGATECH, Czech Academy of Sciences, Třeboň, Czech Republic

<sup>2</sup> Student of Faculty of Science, University of South Bohemia, Branišovská 31, 370 05 Ceske Budejovice, Czech Republic

2012) and *Guillardia theta* (Funk et al. 2011)). NPQ also depends on growth phase when other photoprotective mechanisms, like state transitions, need to be taken into account (Cheregi et al. 2015).

In general, currently, there are few main model organisms to study mechanisms of NPQ: higher plants (Belgio et al. 2015; Horton et al. 2008; Xu et al. 2015), green algae (Berteotti et al. 2016; Finazzi et al. 2006; Liguori et al. 2013; Peers et al. 2009), and diatoms (see, e.g., Grouneva et al. 2009; Grouneva et al. 2011; Lavaud and Kroth 2006; Lavaud and Lepetit 2013). Recently, mechanism of NPQ has been intensively studied also in some other species including brown algae (Garcia-Mendoza et al. 2011; Li et al. 2014), dinoflagellates (Slavov et al. 2016), or the photosynthetic colpodelid alga *Chromera velia* (Belgio et al. 2018; Kotabová et al. 2011; Kuthanová Trsková et al. 2018), which exhibit simple photosynthetic system with high efficiency (Quigg et al. 2012). The photoprotective NPQ is also present in prokaryotic cyanobacteria, where it has, however, different mechanisms connected with orange carotenoid protein, a light sensor that is triggered by blue light (see, e.g., Kirilovsky et al. 2014). In contrast to the OCP-dependent quenching in cyanobacteria, the process of energy dissipation by NPQ in algae is triggered by thylakoid lumen acidification (Krause et al. 1983) which affects light-harvesting antennas (Ballottari et al. 2016; Belgio et al. 2013; Kuthanová Trsková et al. 2018; Walters et al. 1996). It results in conformational change measurable by single-molecule spectroscopy (Kruger et al. 2011), and the process ends up in formation of energy quenchers that dissipate excited states of pigments (see, e.g., review (Ruban et al. 2012) for details). The molecular mechanism of NPQ is still an open question; several quenching mechanisms have been already proposed for light-harvesting antennas: charge-transfer quenching requiring energy transfer from bulk of chlorophylls to chlorophyll-zeaxanthin heterodimer (Ahn et al. 2008; Holt et al. 2005), chlorophyll excited state quenching via direct energy transfer to carotenoids (Ruban et al. 2007; Staleva et al. 2015) or quenching due to excitonic interaction between chlorophylls and carotenoid (Bode et al. 2009). The mechanism of reaction center quenching in photosystem II (PSII) then requires some process of charge recombination (Vass 2011). The above mentioned energy dissipation by NPQ is further modulated by several allosteric regulators (see the details of the concept in Ruban et al. 2012) including the PsbS protein (see, e.g., Johnson and Ruban 2010; Li et al. 2000) or xanthophylls (e.g., zeaxanthin, violaxanthin (Kaňa et al. 2016; Niyogi et al. 1998; Xu et al. 2015)). However, this mechanism is absent in cryptophytes, as no xanthophyll cycle has been detected in these species (Funk et al. 2011; Kaňa et al. 2012).

NPQ involves processes with different kinetics; apart from a very fast energetic quenching (qE) that forms and relaxes (in dark) rapidly in a few minutes in response to lumen

acidification, there is also a slower photoinhibitory quenching (qI) that represents less flexible reaction to excessive irradiation appearing later on, after prolonged exposure to excessive light that sometimes kinetically overlapped with the so-called sustained quenching (Ruban and Horton 1995). The slower response to excessive irradiation involves also reorganization at the level of thylakoid membrane, e.g., pigment-protein dissociation (Betterle et al. 2009) or formation of quenching aggregates under severe stress conditions in general (Tang et al. 2007). The slower part of NPQ can also appear together with photoinhibition that represents complex phenomenon inducing decrease in PSII photosynthetic activity (Kale et al. 2017; Li et al. 2018; Prášil et al. 1992). It starts with changes on the acceptor side of photosystem II (Vass 2012) that are followed by degradation of the D1 protein, a central protein subunit of PSII. Afterwards, newly synthesized copy of the D1 protein is incorporated to restore PSII activity (for review, see, e.g., Li et al. 2018; Yamamoto et al. 2008). In fact, D1 protein sacrifices itself in order to avoid complete PSII damage (Mulo et al. 2012) due to amino acid oxidation of PSII subunits by oxygen radicals (Kale et al. 2017). We have to note that the process of D1 damage occurs at all light intensities however only at saturating lights; D1 repair mechanisms do not keep the pace with its degradation and a net decrease of the photosynthetic rate can be observed (Aro et al. 2005; Kaňa et al. 2002); this process is then often called photoinhibitory damage of PSII (Kok 1956). However, the high light-induced decline in PSII activity (e.g., deduced from fluorescence parameters) can be easily misinterpreted as photoinhibition in some non-green algae species and therefore needs to be interpreted carefully with the help of other proteomics methods (see discussion in Belgio et al. 2018). The process of photoinhibition (in a meaning of excessive D1 protein degradation) is affected by several factors including thylakoid membrane organization (Khatoun et al. 2009), protein mobility (Goral et al. 2010), protein phosphorylation (Tikkanen and Aro 2012), and presence of several auxiliary proteins (Komenda et al. 2006; Krynicka et al. 2015). Some of these factors differ between species (Belgio et al. 2018; Mulo et al. 2012), and this makes the extent of PSII photoinactivation species-dependent (see, e.g., Campbell and Tyystjarvi 2012). Recently, it has been noted that photoinhibition connected with the fast D1 protein turnover is probably less important in some algae like diatoms (Havurinne and Tyystjarvi 2017; Ting and Owens 1994) or chromerids (Belgio et al. 2018). For instance, PSII reaction centers in diatoms are not particularly well protected against the primary damage of photoinhibition by fast D1 turnover in diatoms (Havurinne and Tyystjarvi 2017; Ting and Owens 1994) or the process of photoinhibitory D1 protein turnover on high light is missing in *Chromera velia* as some assemble factors are missing in its genome (Belgio et al. 2018). It pointed to so-called excess capacity of PSII in these organisms (Behrenfeld et al. 1998) that can overcome decrease in the



active PSII center due to photoinhibitory treatment by the increased turnover rate of remaining PSII centers (Kaňa et al. 2002).

Additional strategy against light stress exists that has not been that well studied, especially nowadays—stress avoidance due to the cell motility. In higher plants, the controlled chloroplast movement has been already proved (see Suetsugu and Wada 2007; Suetsugu et al. 2010 or review (Wada 2016)) as chloroplast has the ability to move into shade of other chloroplast under conditions of excess light when blue-light photoreceptors activate chloroplast avoidance movements (Cazzaniga et al. 2013; Dall’Osto et al. 2014; Suetsugu et al. 2010). Similarly, blue and green light photoreceptors cause motile algae to swim away from intense light. The positive and negative phototaxis has been already observed at higher irradiancies in some cryptophytes (see, e.g., Kaneda and Furuya 1986). In *Cryptomonas maculate*, both positive phototaxis and negative phototaxis have been found (Häder et al. 1987). The precise mechanism of light sensing in cryptophytes is still an open question; in some representatives, an eyespot was found that is nevertheless missing in others (Erata et al. 1995). The phototactic response depends on light and also on dark periods between light pulses (Watanabe and Furuya 1978; Watanabe and Furuya 1982). Interestingly, it also depends on concentration of calcium ions (Kaneda and Furuya 1987a). Action spectrum of cryptophyte phototaxis usually resembles maximum absorption of phycoerythrins in contrast to other flagellated algae (see, e.g., Häder et al. 1987; Watanabe and Furuya 1974; Watanabe and Furuya 1982). However, the direct involvement of phycoerythrin in this process was excluded (Erata et al. 1995). Interestingly, a rhodopsin-mediated photoreception has been described in cryptophytes (Sineshchekov et al. 2005). One striking example of the protein is the rhodopsin from phototactic marine cryptophyte alga *Guillardia theta* that has been recently sequenced (Curtis et al. 2012). Interestingly, rhodopsins act as light-gated anion channels when expressed in animal cells and therefore have been named anion channelrhodopsins - ACRs (Govorunova et al. 2015). Even though there is probably no direct connection between photosynthesis and phototaxis (Watanabe et al. 1976) controlled by rhodopsin, phototaxis seems to play an indirect role in avoidance from excessive irradiance in algae as it has been already proven for chloroplast (Cazzaniga et al. 2013; Dall’Osto et al. 2014; Suetsugu et al. 2010).

We surveyed various photoprotective mechanisms in this cryptophyte alga *Rhodomonas salina* that contains chlorophyll a/c antennas in thylakoid membranes together with additional light-harvesting system formed by phycobiliproteins tightly embedded in a lumen (Kaňa et al. 2009); this antenna composition (membrane type of antennas together with phycobillin-type antenna in a lumen) makes cryptophytes a unique model organism. The previous studies have already

clarified pH dependency of NPQ in cryptophytes (Kaňa et al. 2012) that is mostly localized in their thylakoid membrane CAC (chlorophyll a/c binding) antennas and not in phycoerythrins situated in the lumen (Kaňa 2018; Kaňa et al. 2012). Moreover, redistribution of antennas in state transitions plays a role in regulation of light harvesting of some cryptophytes (Cheregi et al. 2015). Here we further show that *R. salina* possess an effective and very flexible NPQ. The fastest part of NPQ is sensitive to  $\text{Ca}^{2+}$  fluxes and the gradient of monovalent ions across thylakoid membranes. We also found that PSII of flagellated cryptophyte algae is less affected by prolonged periods of photoinhibitory light in contrast to immotile diatoms. We suggest that this is due to the combination of effective NPQ, effective D1 protein turnover, and the ability of cryptophytes to avoid high light by rapid movement.

## Materials and methods

### Cell growth and sample treatment

The cryptophyte alga *Rhodomonas salina* (strain CCAP 978/27) and *Phaeodactylum tricorutum* were cultivated in artificial seawater medium with f/2 nutrient addition in a temperature-controlled bath ( $t = 18\text{ }^{\circ}\text{C}$ ). The cell suspension was continually bubbled with air and illuminated by dimmable fluorescence tubes with intensity  $35\text{ }\mu\text{mol photons m}^{-2}\text{ s}^{-1}$  (day-night cycle 12/12 h) (Havelková-Doušová et al. 2004). All experiments were carried out with cells in exponential growth phase.

### Measurements of variable fluorescence

Variable chlorophyll a fluorescence was detected by FL-3000 (Photon System Instrument, Czech Republic) in the spectral range 690–710 nm. For fluorescence quenching analysis, samples were dark adapted for 20 min before applying low-intensity measuring light ( $2\text{ }\mu\text{mol photons m}^{-2}\text{ s}^{-1}$ , 622 nm) for the detection of intrinsic fluorescence of the dark-adapted sample— $F_0$  (minimal fluorescence). Maximal fluorescence for the dark ( $F_M$ ) and light-adapted sample ( $F_M'$ ) has been measured during 200-ms multiple turnover saturating flashes. Actinic light during light period was provided by orange light ( $700\text{ }\mu\text{mol photons m}^{-2}\text{ s}^{-1}$ , 622 nm). Fluorescence parameters were calculated as follows: maximal PSII efficiency as  $F_v/F_M = (F_M - F_0) / F_M$  and non-photochemical quenching based on Stern-Volmer formalism as  $\text{NPQ} = (F_M - F_M') / F_M$ .

### Photoinhibitory and post-photoinhibitory treatment

The photoinhibition was induced by high light treatment of cell suspension using white light-emitting diode array that provided intensity of  $1000\text{ }\mu\text{mol photons m}^{-2}\text{ s}^{-1}$  inside the

culture. Cell suspension was exposed to the high light for 75 min and subsequently shifted to the growth light conditions ( $35 \mu\text{mol photons m}^{-2} \text{s}^{-1}$ ) to provide recovery from high light treatment. During treatment, suspension was continuously stirred to avoid cell settling. The degree of photoinhibition was assessed by variable fluorescence measurement from maximal PSII efficiency ( $F_V/F_M$ , see above). Fluorescence parameters were measured: (i) 20 min in dark before the light treatment and (ii) after 5 min of dark adaptation during and after light treatment.

### Detection of cell velocity and phototaxis

Cell velocity was measured by epifluorescence microscopy (Zeiss Imager Z1, Objective Zeiss Apochromat  $\times 20$  with NA 0.75) equipped with digital camera (pixel resolution  $512 \times 512$ ) that can measure single picture every 100 ms. Fluorescence was excited by white fluorescence diode and detected above 680 nm. Before measurements,  $15 \mu\text{L}$  of cell suspension was placed on the glass plate, covered by the slit and sealed with enamel. This allowed us to make chamber suitable for cell movement in 2D space. The velocity of cells was measured either under low light ( $\sim 30 \mu\text{mol photons m}^{-2} \text{s}^{-1}$ ) or high light conditions ( $\sim 500 \mu\text{mol photons m}^{-2} \text{s}^{-1}$ ) for 1 min. Pictures were processed in the open-source ImageJ software (Abramoff et al. 2003) by means of its “tracking object” tool.

The same epifluorescence microscopy setup was also used to characterize negative and positive phototaxis of *R. salina* cells within irradiated visual field. The pictures characterizing the number of cells inside the visual field were taken every second during period of low white light ( $\sim 30 \mu\text{mol photons m}^{-2} \text{s}^{-1}$ , for 20 s) followed by high light ( $\sim 500 \mu\text{mol photons m}^{-2} \text{s}^{-1}$  for 200 s) and again low light ( $\sim 30 \mu\text{mol photons m}^{-2} \text{s}^{-1}$ , for 20 s). The obtained pictures were collected, and the number of cells was counted by ImageJ software automatically (Abramoff et al. 2003).

## Results

### Non-photochemical quenching—role of ions

Fluorescence quenching analysis of *Rhodomonas salina* showed a typical curve (Fig. 1). It confirmed the presence of NPQ of fluorescence in this alga as its maximal fluorescence during orange actinic light ( $F_M'$ ) decreased very fast (Fig. 1). The kinetics of NPQ revealed the presence of two phases (insert of Fig. 1); fast increase of NPQ with the maximum at 40 s ( $\sim 1.5$ ) was followed by slight decrease that leveled off to the steady-state value of NPQ around 1.2. In the dark, NPQ recovered very fast—this is a usual sign of pH-dependent

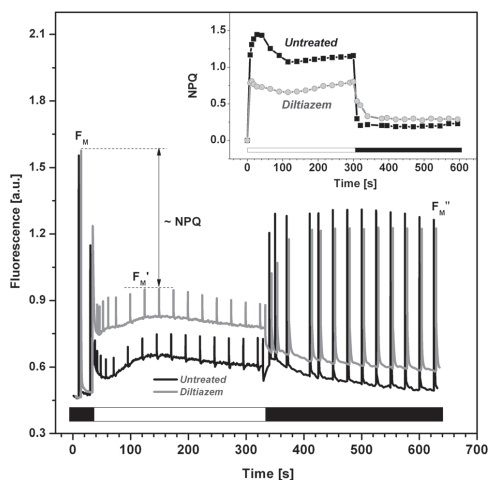


**Fig. 1** Role of calcium channel inhibitor on non-photochemical quenching of fluorescence (NPQ) in *R. salina*. Curves were obtained after addition of calcium channel inhibitor, diltiazem (concentration of  $20 \mu\text{mol/L}$ ), and compared with control, untreated cells. The extent of NPQ was calculated as  $(F_M' - F_M'')/F_M'$  for every saturating flash. The value of maximal PSII efficiency ( $F_V/F_M$ ) was 0.7 for both curves. NPQ was detected during 5 min of orange actinic light ( $622 \text{ nm}$ ,  $600 \mu\text{mol photons m}^{-2} \text{s}^{-1}$ ; white bar) and in dark period afterwards (see black bar). Cells were dark adapted for 20 min before measurements; data represent typical curves

energetic quenching and is in line with the results described previously (Kaňa et al. 2012).

We newly focused on a possible role of ions as they have been proved to be connected with the regulation of light-harvesting efficiency (see, e.g., review Kaňa and Govindjee 2016). We have tested calcium ions ( $\text{Ca}^{2+}$ ) that are present in lower concentrations than other divalent ion  $\text{Mg}^{2+}$ . Even though it is a well-known signal molecule that regulates photosynthesis (Hochmal et al. 2015), the role of  $\text{Ca}^{2+}$  in NPQ regulation in cryptophytes has not been explored yet. We have clearly shown that application of the calcium channel blocker, diltiazem (non-dihydropyridine), that inhibits non-potential  $\text{Ca}^{2+}$  influx into chloroplast (Roh et al. 1998) diminished the fast burst of NPQ and reduced the steady-state NPQ value. Moreover, NPQ recovery in the dark was also significantly slower in the presence of diltiazem (insert of Fig. 1). Therefore, blocking of  $\text{Ca}^{2+}$  influx/efflux in the chloroplast slows down the reaction of *R. salina* to high light. It is in line with the proposed role of  $\text{Ca}^{2+}$  in regulation of the  $\text{K}^+/\text{H}^+$  two-pore potassium channel AtTPK3; the absence of the channel diminishes building of  $\Delta\text{pH}$  (Carraretto et al. 2013) that is required for fast qE.

We further explored sensitivity of the fast NPQ phase to ions by using an ionophore for monovalent cations—non-actin. This cyclic ionophore reversibly binds to thylakoid

membrane and abolishes gradient of monovalent ions (Schmid and Junge 1975). Thirty-micromole/liter concentration of non-actin added before irradiation blocked the fastest phase of NPQ (Fig. 2) even more than diltiazem (insert of Fig. 1). At the end of light phase, the steady-state value of NPQ decreased to half of its original value. Non-actin also reduced maximal efficiency of photosystem II (PSII) photochemistry  $F_V/F_M$  (see legend of Fig. 2) from 0.75 (for untreated cells) to 0.64. Interestingly, non-actin has a similar effect on NPQ kinetics as glycine betaine (Fig. 2) that acts as hyperosmotic compound draining water out of the cell (Papageorgiou et al. 1998). As glycine betaine affects the fast phase of NPQ, so water/ion activities are important. If we additionally block specifically the flux of monovalent cations with non-actin, the NPQ kinetics are similarly affected, which would suggest that it is mainly the monovalent cation flux that is important in the mechanism for this fast NPQ phase. These hyperosmotic conditions were able to destroy the fastest phase of NPQ without any effect on the steady-state value of NPQ and without any reduction of  $F_V/F_M$  (see legend of Fig. 2). It means that water activities around the membrane together with gradients of monovalent cations across membranes (probably thylakoid membrane) are both necessary for the fast phase of NPQ in *R. salina*.

### Photoinhibitory treatment of *R. salina* cells

We have further explored an effect of extended periods of high light on PSII photochemistry. It has been shown (Kaňa et al. 2012) that there is no light-induced xanthophyll cycle in

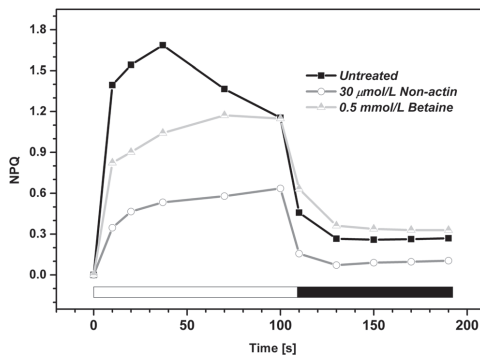


**Fig. 2** Effect of hyperosmosis and potassium ion ionophore (non-actin) on NPQ of *R. salina*. Hyperosmosis was induced by addition of glycine betaine (0.5 mol/L); gradient of monovalent potassium channels ( $K^+$ ) was inhibited by addition of non-actin (30  $\mu\text{mol/L}$ ). NPQ was measured during orange irradiation (622 nm, 600  $\mu\text{mol photons m}^{-2} \text{s}^{-1}$ ; white bar) and during following darkness (see black bar). The calculated values of maximal efficiency of PSII photochemistry ( $F_V/F_M$ ) were 0.75 for untreated sample, 0.64 with non-actin, and 0.74 with glycine betaine. Cells were dark adapted for 20 min before measurements; data represent typical curves

*R. salina*, in contrast to the presence of diadinoxanthin cycle in diatoms (Goss et al. 2010). In diatoms, xanthophyll cycles play a crucial role in light stress (Lavaud et al. 2002a; Lavaud et al. 2003). Therefore, we have intentionally compared the cryptophyte alga *R. salina* without any xanthophyll cycle and the representative of diatoms, *Phaeodactylum tricoratum*, to prolonged period of excessive irradiation that can induce photoinhibitory damage of PSII (Li et al. 2018; Prášil et al. 1992). In *R. salina*, the high light treatment caused biphasic reduction in maximal PSII photochemical efficiency (see  $F_V/F_M$  in Fig. 3a). The very fast phase of the decrease was visible already after 2-min exposure to high light and reflects non-photochemical reduction of PSII photochemistry due to some irreversible component of NPQ. This effect is also visible in Fig. 1 in the value of  $F_M''$  that is not fully reversible in the

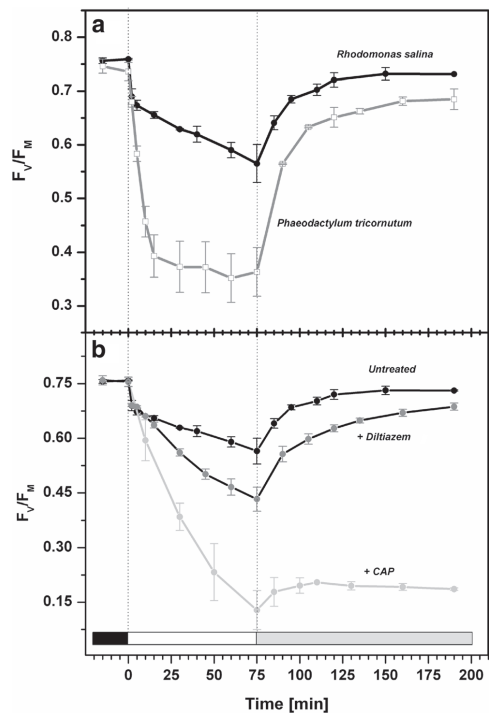


**Fig. 3** Maximal efficiency of photosystem II photochemistry ( $F_V/F_M$ ) during light stress in *Rhodomonas salina* and in the diatom *Phaeodactylum tricoratum*. Samples were dark adapted for 20 min (black bar) and then exposed to high irradiance 1000  $\mu\text{mol photons m}^{-2} \text{s}^{-1}$  for 75 min (see white bar).  $F_V/F_M$  recovery at low irradiance (30  $\mu\text{mol photons m}^{-2} \text{s}^{-1}$ ) was detected for the following 2 h (see gray bar). **a** Progress of light stress in cryptophyte algae *R. salina* and in the diatom *P. tricoratum*. **b** Effect of protein synthesis inhibition (chloramphenicol—see “CAP”) and calcium channel inhibition (diltiazem) in *R. salina*

dark. Exposure of *R. salina* to high light for more than 2 min caused further linear decrease in maximal PSII photochemistry (Fig. 3) that is a typical sign of photoinhibition (see, e.g., Kosugi et al. 2018; Tyystjarvi and Aro 1996). After 75 min at high light,  $F_v/F_M$  decreased from 0.78 to 0.56, and this decrease was reversible in low light (Fig. 3). This result indicates the presence of photoinhibition of the PSII reaction centers, where the D1 protein is the most sensitive target of this reversible damage (Prášil et al. 1992). The relatively small change in maximal PSII photochemistry ( $F_v/F_M$ ) in *R. salina* indicates the protective role of D1 protein turnover in this alga. This was confirmed by the addition of chloramphenicol (CAP), the chloroplast protein synthesis inhibitor that enhanced reduction of  $F_v/F_M$  in *R. salina* several times (Fig. 4b). Therefore, we assume that, also in cryptophytes, D1 protein undergoes continual photoinactivation and its fast repair that is a key factor required for effective protection of PSII during photoinhibitory conditions in many other phototrophs (Yamamoto et al. 2008). We do not know if the reduction in the number of active PSII centers results in decrease of whole photosynthesis (e.g., measured by carbon assimilation) or if there is an excess capacity of PSII that keeps photosynthetic rate unchanged in some green algae (Kaňa et al. 2002) or in *Chromera velia* (Belgio et al. 2018). We found that the negative effect of high irradiation on  $F_v/F_M$  was also enhanced by the calcium channel blocker diltiazem (Fig. 3) that inhibits non-potential  $Ca^{2+}$  influx into chloroplasts (Roh et al. 1998). It started the reduction of maximal PSII photochemistry after 20 min of irradiations that indicates negative long-term effect after inhibition of  $Ca^{2+}$  fluxes (for details, see “Discussion”).

This type of photoprotection observed in *R. salina* was different in comparison with the diatom, *Phaeodactylum*

*tricornutum*, where pronounced decrease in PSII efficiency is visible already after 20 min of irradiation (Fig. 3a). This is because of the activity of the xanthophyll cycle in *Phaeodactylum tricornutum* (Lavaud et al. 2002b) that allowed fast quenching of excessive irradiation and resulted in  $F_v/F_M$  value 0.4 already after 20 min of irradiation. As there was no further decrease in  $F_v/F_M$  with prolonged irradiation (Fig. 3a), we conclude that there is almost no photoinhibition in *Phaeodactylum tricornutum* in line with previous results (Havurinne and Tyystjarvi 2017; Ting and Owens 1994).

### Cell motility of cryptophytes

Photoinhibitory experiments presented in Fig. 3 proved different strategies of photoprotection in cryptophytes and in diatoms that both belong to chromalveolate algae (Green 2011). Moreover, in comparison with, e.g., green algae (Kaňa et al. 2002), *R. salina* could cope relatively well with 75 min of high light. These results have brought a question if there is any other protective mechanism in cryptophytes except effective NPQ (Kaňa et al. 2012) and fast D1 protein turnover (Fig. 3). In contrast to *Phaeodactylum tricornutum*, *R. salina* is a motile alga. Therefore, we checked if motility of *R. salina* could play an additional protective role during the light stress (see Figs. 4 and 5).

Microscopic measurements showed that different types of trajectory patterns of *R. salina* cells exist (Fig. 4a). We could visualize the helical path of *R. salina* cell (see “trajectory of Cell no. 1” in Fig. 4a). This type of trajectory is typical for most of motile algae including green algae, dinoflagellates, or Euglenophyta (for review, see, e.g., Barsanti and Gualtieri 2006). There were also cells with narrower helical path that

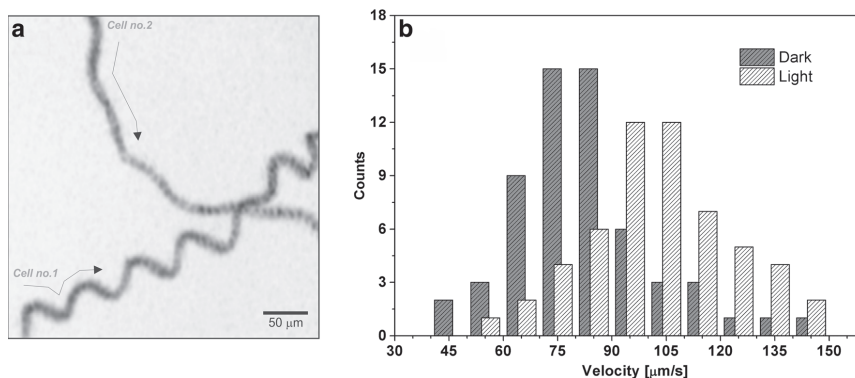


**Fig. 4** Irradiance-induced changes in the velocity of *Rhodomonas salina*. **a** Typical trajectory pattern of *R. salina* movements in solution. Picture shows movements of two different cells (see arrows) in a visual field of a fluorescence microscope for 9-s-long integration; 50-µm scale bar is marked. **b** Distribution in cell velocities in the dark (“Dark”) and in light

(“Light”) samples measured by particle tracking routine. Mean values (with standard deviation) of “Dark” and “Light” samples were  $82 \pm 19$  µm/s and  $104 \pm 22$  µm/s, respectively. Values were calculated from measurements of 60 cells with 1500 tracking events

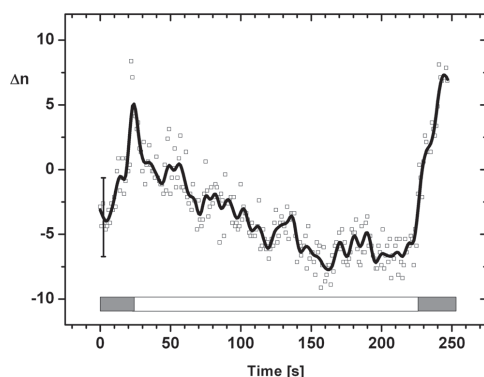


**Fig. 5** Changes in the number of cells ( $\Delta n$ ) in a visual field of an epifluorescence microscope. Cells were counted at low light (see gray bars) and at high light (see white bar). Total amount of cells in the visual field was around 50; bar represent standard deviation from 4 repetitions

resemble rather straight movement (see “trajectory of Cell no. 2” in Fig. 4a). This result showed heterogenic behavior in cell suspension. Generally, motile algae also rotate few times per second around a longitudinal axis during swimming (Polin et al. 2009); however, this movement was not detectable by epifluorescence microscopy. Therefore, we focused on detection of cell velocity and its change on light as they are triggered by blue and green light photoreceptors (Allorent and Petroustos 2017).

In green motile algae *Chlamydomonas reinhardtii*, phototaxis signaling is mediated by the photoreceptors channel rhodopsin (1 and 2), light-gated proton, and calcium channels (Nagel et al. 2002, 2003) that seem to be dominant receptors for photophobic responses (Govorunova et al. 2004; Hegemann 1997). We exposed *R. salina* to high white light to see if short periods of irradiation can accelerate motility of cells. We have confirmed helical pattern of *R. salina* movement (see Fig. 4a, supplementary movie 1). Cell velocity was detected by epifluorescence microscopy with continuous detection of the movement of cells in the visual field during sudden irradiation by high light. The velocity of particular cell was calculated from known distances and frequency of detection (for details, see “Materials and Methods”). Indeed, these measurements showed slight, but significant, light-induced increase in the distribution of cell velocities (Fig. 4b). The velocity in the light increased from 82  $\mu\text{m/s}$  in the dark to 104  $\mu\text{m/s}$  (see the legend of Fig. 4b). This swimming speed is in line with values previously described for cryptophytes (Barsanti and Gualtieri 2006), and its increase during the high light strongly suggests a role of negative phototaxis of cryptophytes in avoidance of excessive irradiation. We also tested whether the observed acceleration in swimming velocity is connected with the movement out of the light source. We

focused high light to the visual field of a microscope and counted the number of cells (Fig. 5). At low light, before high light treatment, there was a slight increase in the number of cells in field of view (by 10–20%). On the contrary, high light caused decrease in the number cells in the irradiated part (see Fig. 5). The results pointed at the presence of negative phototaxis during period of high light in *R. salina*.

## Discussion

It has been already shown that non-photochemical quenching in cryptophytes proceeds in the chlorophyll a/c binding antennas (CAC) that are associated with photosystem II that resembles efficient energetic quenching of higher plants (Kaňa et al. 2012). This photoprotection of PSII is not connected with any quenching in phycoerythrobilins (Kaňa 2018) that are firmly bound to the luminal side of these antennas (Kaňa et al. 2009). Further, the cryptophytic PSI turned out to be one from the fastest (i.e., the most efficient) so far measured (Kuthanová Trsková et al. 2019), and cryptophytes are able to regulate distribution of light between photosystem PSI and PSII (protected by NPQ) by state transitions (Cheregi et al. 2015). All these show that cryptophytes have evolved a unique combination of photoprotective strategies that probably lead to significant dominants of cryptophyte algae in case of highly illuminated conditions of some coastal waters (Mendes et al. 2018). Here, we have further explored properties of this unique NPQ with the main focus on the role of ions ( $\text{Ca}^{2+}$  and monovalent ions), protective role of NPQ during longer period of excessive irradiation in comparison to diatoms and green algae, and finally also on the possible role of cell motility in light stress avoidance.

We have found that the fastest burst of NPQ is affected by inhibition of  $\text{Ca}^{2+}$  channels by diltiazem (Fig. 1). This is a compound that is able to inhibit potential-stimulated  $\text{Ca}^{2+}$  influx into chloroplast of higher plants (Roh et al. 1998). The  $\text{Ca}^{2+}$  influx into chloroplast proceeds on light stimulus (for reviews, see, e.g., Johnson et al. 2006; McAinsh and Pittman 2009; Verret et al. 2010). However, as there is no significant increase in free  $\text{Ca}^{2+}$  in the chloroplast stroma after irradiation, it is supposed that  $\text{Ca}^{2+}$  coming into chloroplast is apparently rapidly bound to thylakoid and/or rapidly transferred into a lumen (Johnson et al. 2006). This is facilitated by  $\text{Ca}^{2+}/\text{H}^{+}$  antiporter that has been already identified in thylakoid membrane (Ettinger et al. 1999) and even proven to have an important effect onto the pH homeostasis and function of PSII in higher plants (Wang et al. 2016). High concentration of  $\text{Ca}^{2+}$  inside of the thylakoid lumen is crucial for activity of oxygen-evolving complex (Miqyass et al. 2007). Calcium ions have also several other functions. Dilley and co-workers suggested (for review, see, e.g., Dilley 2004) that  $\text{Ca}^{2+}$  can mediate stress response of thylakoids to high light



by switching between localized and de-localized energy-coupling mode, and thus form ATP either from proton gradient localized close to thylakoid membrane (“localized mode”), or from the whole bulk in a lumen (“de-localized mode”) (Ewy and Dilley 2000).  $\text{Ca}^{2+}$  can thus modulate extent of lumen acidification and therefore stress response (for review, see, e.g., Dilley 2004). The mechanism of such an action is based on reversible binding of  $\text{Ca}^{2+}$  to 8-kDa protein  $\text{CF}_0$  proton channel in ATPase (Van Walraven et al. 2002). In de-localized state,  $\text{Ca}^{2+}$  is displaced from the  $\text{CF}_0$  proton channel of ATPase that allows free access of  $\text{H}^+$  into a lumen and triggering of stress response. Such a role of  $\text{Ca}^{2+}$  in the fast stress response has been already shown for violaxanthin de-epoxidation that is necessary for NPQ in higher plants (Jahns et al. 2009) that proceeds only in de-localized mode (Pan and Dilley 2000). However, there is no xanthophyll cycle in cryptophytes (Kaňa et al. 2012), and in contrast to Pan and Dilley (2000), inhibition of  $\text{Ca}^{2+}$  fluxes into a lumen by diltiazem rather inhibits NPQ (Fig. 1) not the opposite. Therefore, there must be some other mechanism in  $\text{Ca}^{2+}$  action in cryptophytes.

Interestingly, there are some older results showing that  $\text{Ca}^{2+}$  pH-dependent release of  $\text{Ca}^{2+}$  from photosystem II plays a role in reversible energy dissipation (Johnson and Krieger 1994; Krieger et al. 1992; Krieger and Weis 1993). We do not have experimental data proving that the released  $\text{Ca}^{2+}$  could reversibly bind to light-harvesting antennas of cryptophytes where presence of NPQ has been proven (Kaňa et al. 2012). However, it is known that  $\text{Ca}^{2+}$  can bind to proteins important for NPQ in higher plants like CP29 and PsbS (Dominici et al. 2002; Jegerschold et al. 2000). Interestingly, it has been already confirmed that the chloroplast calcium sensor (CAS) is required for photoacclimation in *Chlamydomonas reinhardtii* (Petroustos et al. 2011), and photoreceptors are important for response to high light stress in general (Allorent and Petroustos 2017).

To resolve if  $\text{Ca}^{2+}$  can bind directly to chlorophyll a/c antennas or there is some indirect effect of  $\text{Ca}^{2+}$  on NPQ, more experiments with isolated antennas complexes are necessary. Our measurements only indicate a signal role of calcium fluxes in NPQ (Fig. 1) in line with the proposed signal role of  $\text{Ca}^{2+}$  in chloroplasts (Johnson et al. 2006). Ion fluxes catalyzed by channels/transporters in thylakoids (Höhner et al. 2016) interfere with the proton gradients (a key factor for NPQ), and the actual concentration of ions (especially  $\text{Ca}^{2+}$ ) then might contribute to shape proton gradient between localized and de-localized mode (e.g., switching between localized/de-localized  $\Delta\text{pH}$  by  $\text{Ca}^{2+}$  (see Dilley 2004)). Alternatively,  $\text{Ca}^{2+}$  can directly interact with newly described thylakoid membrane voltage-gated channels and transporters (Höhner et al. 2016), namely, with (1)  $\text{H}^+/\text{K}^+$  KEA antiporters (Armbruster et al. 2014; Kunz et al. 2014); (2) chloride channel (Herdean et al. 2016a; Herdean et al. 2016b); and (3) two-

pore potassium channel (TPK, see, e.g. Carraretto et al. 2013). Indeed,  $\text{Ca}^{2+}$  can directly bind TPK potassium channel (Carraretto et al. 2013). Our data indicates some connection of NPQ with monovalent ion channels (see Fig. 2) as the fast burst of NPQ was inhibited when monovalent concentration of cations (mostly  $\text{K}^+$ ) across membranes is equilibrated by non-actin. However, to prove a direct connection between the KEA antiporter and/or TPK channel inhibition and  $\text{Ca}^{2+}$  concentration, more experiments are necessary. In any cases, experiments with the calcium channel blocker, diltiazem (non-dihydropyridine), clearly showed that the fast burst of NPQ and the steady-state NPQ value (Fig. 1) are somehow controlled by  $\text{Ca}^{2+}$  in cryptophytes.

We have also tested importance of  $\text{Ca}^{2+}$  concentrations ( $\text{Ca}^{2+}$  channels were inhibited by diltiazem) for prolonged periods of high irradiation (Fig. 3b) in line with previous experiments (Fig. 1). In control sample, the prolonged exposition to high light reduced maximal PSII photochemistry for about 20% that was fully reversible in the dark (Fig. 3b). Reduction in maximal PSII photochemistry was mostly due to photoinhibition of the PSII reaction centers due to reversible damage of the D1 protein since, in case of inhibition in this D1 protein turnover by CAP, the  $F_v/F_M$  dropped to very low values (Fig. 3b). Therefore, the fast D1 protein turnover in cryptophytes keeps maximal PSII activity relatively high in comparison with diatoms (see *Phaeodactylum tricoratum* in Fig. 3b) or green algae (Kaňa et al. 2002) treated at same conditions. Interestingly, faster D1 protein turnover in higher plants can be observed in a case of grana de-stacking (Khatoun et al. 2009) so it is a question if the minimal reduction in PSII photochemistry, in comparison with diatoms and green plants, is due to a more fluid membrane organization in cryptophytes. We also found that inhibition in  $\text{Ca}^{2+}$  by diltiazem further reduced PSII efficiency (Fig. 3b). We do not know if the effect of diltiazem reduces  $F_v/F_M$  at high light just due to its effect on NPQ (Fig. 1) or by some other mechanism of action. As algal motility is affected by calcium flux (Hill et al. 2000; Smith 2002), we cannot exclude that diltiazem-induced change in motility response on single cell level results in some macroscopic changes in fluorescence values in Fig. 3. However, this is rather improbable, and we tend to suggest a direct influence of  $\text{Ca}^{2+}$  fluxes on photoprotection in *R. salina*.

The observed effect of prolonged exposure to high light is different than in diatoms, as only a limited sign of photoinhibition can be usually detected (see, e.g., *Phaeodactylum tricoratum* in Ting and Owens 1994) probably due to the operation of very effective xanthophyll cycle (Lavaud et al. 2002b) and cyclic electron flow around PSII (Lavaud et al. 2002c). It brings a question of how cryptophytes protect themselves against longer period of excessive irradiation. Our data newly show that one possible strategy could be the avoidance from light stress by active movement (see Figs. 4 and 5). Cryptophytes are flagellates

and are able to move very fast (with velocity more than 100  $\mu\text{m/s}$ , Fig. 4), in contrast to immotile diatoms that are passively moved by water turbulences. In nature, cryptophytes are able to adjust their position in the water column during the diel cycle to optimize acquisition of nutrients and exposure to irradiance (Arvola et al. 1991). Therefore, we suggest that a reduction in exposition time to excessive irradiation by active movement (due to negative phototaxis, see Fig. 5) could play a protective role in cryptophytes as they do not operate any xanthophyll cycle (Kaňa et al. 2012) that would further stimulate NPQ for prolonged periods of irradiation as can be seen in diatoms (Lavaud et al. 2002b). Similar positive and negative phototaxis has been already proved for *Cryptomonas maculata* (Häder et al. 1987). Interestingly, motile algae, apart from swimming in helical paths, also do rotate few times per second around a longitudinal axis during swimming (around 2 Hz, see, e.g., Kaneda and Furuya 1987b). Therefore, motile algae like cryptophytes, in contrast to immotile diatoms, are exposed rather to fluctuating light conditions which we can refer to a regime of periodically changing light intensity. We tend to suggest that this rotation plays an additional protective role in motile algae; however, its real importance has to be addressed by future studies.

**Acknowledgments** We want to thank Ondřej Prášil and Aurelie Crepin for critical reading of the manuscript. We want to acknowledge Jiří Šetlík for his long-term technical assistance during experiments and for skillful adaptation of biophysical instruments.

**Funding information** This research project was supported by the Czech Science Foundation (GAČR) (Grantová agentura České republiky) project GACR 16-10088S. The work at center ALGATECH has been supported by the institutional projects Algatech Plus (MSMT LO1416) and Algamic (CZ 1.05/2.1.00/19.0392) from the Czech Ministry of Education, Youth and Sport.

**Abbreviations** CAP, chloramphenicol;  $F_M$ , maximal chlorophyll a fluorescence for dark-adapted sample;  $F_M'$ , maximal chlorophyll a fluorescence for light-adapted sample;  $F_M''$ , maximal chlorophyll a fluorescence measured in the dark following short light period;  $F_V/F_M$ , maximal efficiency of PSII photochemistry; NPQ, non-photochemical quenching of fluorescence; PSII, photosystem II

## References

- Abramoff MD, Magelhaes PJ, Ram SJ (2004) Image processing with ImageJ. *Biophoton Int* 11:36–42
- Ahn TK, Avenson TJ, Ballottari M, Cheng Y-C, Niyogi KK, Bassi R, Fleming GR (2008) Architecture of a charge-transfer state regulating light harvesting in a plant antenna protein. *Science* 320:794–797. <https://doi.org/10.1126/science.1154800>
- Allort G, Petroustos D (2017) Photoreceptor-dependent regulation of photoprotection. *Curr Opin Plant Biol* 37:102–108. <https://doi.org/10.1016/j.pbi.2017.03.016>
- Armbruster U, Carrillo LR, Venema K, Pavlovic L, Schmidtman E, Kornfeld A, Jahns P, Berry JA, Kramer DM, Jonikas MC (2014) Ion antiport accelerates photosynthetic acclimation in fluctuating light environments. *Nat Commun* 5:5. <https://doi.org/10.1038/ncomms6439>
- Aro EM et al (2005) Dynamics of photosystem II: a proteomic approach to thylakoid protein complexes. *J Exp Bot* 56:347–356. <https://doi.org/10.1093/jxb/eri041>
- Arvola L, Ojala A, Barbosa F, Heaney SI (1991) Migration behaviour of three cryptophytes in relation to environmental gradients: an experimental approach. *Br Phycol J* 26:361–373. <https://doi.org/10.1080/00071619100650331>
- Asada K (2006) Production and scavenging of reactive oxygen species in chloroplasts and their functions. *Plant Physiol* 141:391–396. <https://doi.org/10.1104/pp.106.082040>
- Ballottari M et al (2016) Identification of pH-sensing sites in the light harvesting complex stress-related 3 protein essential for triggering non-photochemical quenching in *Chlamydomonas reinhardtii*. *J Biol Chem* 291:7334–7346. <https://doi.org/10.1074/jbc.M115.704601>
- Barsanti L, Gualtieri P (2006) Algae: anatomy, biochemistry, and biotechnology. Taylor & Francis Group, Boca Raton
- Behrenfeld MJ, Prasil O, Kolber ZS, Babin M, Falkowski PG (1998) Compensatory changes in photosystem II electron turnover rates protect photosynthesis from photoinhibition. *Photosynth Res* 58:259–268. <https://doi.org/10.1023/a:1006138630573>
- Belgio E, Johnson MP, Juric S, Ruban AV (2012) Higher plant photosystem II light-harvesting antenna, not the reaction center, determines the excited-state lifetime—both the maximum and the nonphotochemically quenched. *Biophys J* 102:2761–2771. <https://doi.org/10.1016/j.bpj.2012.05.004>
- Belgio E, Duffy CDP, Ruban AV (2013) Switching light harvesting complex II into photoprotective state involves the lumen-facing apoprotein loop. *Phys Chem Chem Phys* 15:12253–12261. <https://doi.org/10.1039/c3cp51925b>
- Belgio E, Ungerer P, Ruban AV (2015) Light-harvesting superstructures of green plant chloroplasts lacking photosystems. *Plant Cell Environ* 38:2035–2047. <https://doi.org/10.1111/pce.12528>
- Belgio E, Trskova E, Kotabova E, Ewe D, Prasil O, Kana R (2018) High light acclimation of *Chromera velia* points to photoprotective NPQ. *Photosynth Res* 135:263–274. <https://doi.org/10.1007/s11120-017-0385-8>
- Berteotti S, Ballottari M, Bassi R (2016) Increased biomass productivity in green algae by tuning non-photochemical quenching. *Sci Rep* 6:21339. <https://doi.org/10.1038/srep21339>
- Betterle N et al (2009) Light-induced dissociation of an antenna heterooligomer is needed for non-photochemical quenching induction. *J Biol Chem* 284:15255–15266. <https://doi.org/10.1074/jbc.M808625200>
- Bode S et al (2009) On the regulation of photosynthesis by excitonic interactions between carotenoids and chlorophylls. *Proc Natl Acad Sci U S A* 106:12311–12316. <https://doi.org/10.1073/pnas.0903536106>
- Campbell DA, Tyystjarvi E (2012) Parameterization of photosystem II photoinactivation and repair. *Biochim Biophys Acta* 1817:258–265. <https://doi.org/10.1016/j.bbabi.2011.04.010>
- Carraretto L et al (2013) A thylakoid-located two-pore K<sup>+</sup> channel controls photosynthetic light utilization in plants. *Science* 342:114–118. <https://doi.org/10.1126/science.1242113>
- Cazzaniga S, Dall’Osto L, Kong SG, Wada M, Bassi R (2013) Interaction between avoidance of photon absorption, excess energy dissipation and zeaxanthin synthesis against photooxidative stress in *Arabidopsis*. *Plant J* 76:568–579. <https://doi.org/10.1111/tpj.12314>
- Cheregi O, Kotabová E, Prášil O, Schröder WP, Kaňa R, Funk C (2015) Presence of state transitions in the cryptophyte alga *Guillardia theta*. *J Exp Bot* 66:6461–6470. <https://doi.org/10.1093/jxb/erv362>
- Croce R, van Amerongen H (2014) Natural strategies for photosynthetic light harvesting. *Nat Chem Biol* 10:492–501. <https://doi.org/10.1038/nchembio.1555>

- Cruz JA, Avenson TJ, Kanazawa A, Takizawa K, Edwards GE, Kramer DM (2005) Plasticity in light reactions of photosynthesis for energy production and photoprotection. *J Exp Bot* 56:395–406. <https://doi.org/10.1093/jxb/eri022>
- Curtis BA et al (2012) Algal genomes reveal evolutionary mosaicism and the fate of nucleomorphs. *Nature* 492:59–65. <https://doi.org/10.1038/nature11681>
- Dall'Osto L, Cazzaniga S, Wada M, Bassi R (2014) On the origin of a slowly reversible fluorescence decay component in the Arabidopsis npq4 mutant. *Philos Trans R Soc B Biol Sci* 369. <https://doi.org/10.1098/rstb.2013.0221>
- Derks A, Schaven K, Bruce D (2015) Diverse mechanisms for photoprotection in photosynthesis. Dynamic regulation of photosystem II excitation in response to rapid environmental change. *Biochim Biophys Acta* 1847:468–485. <https://doi.org/10.1016/j.bbabi.2015.02.008>
- Dilley RA (2004) On why thylakoids energize ATP formation using either delocalized or localized proton gradients - a Ca<sup>2+</sup> mediated role in thylakoid stress responses. *Photosynth Res* 80:245–263
- Dominici P, Caffarri S, Arnenante F, Ceoldo S, Crimi M, Bassi R (2002) Biochemical properties of the PsbS subunit of photosystem II either purified from chloroplast or recombinant. *J Biol Chem* 277:22750–22758. <https://doi.org/10.1074/jbc.M200604200>
- Erata M, Kubota M, Takahashi T, Inouye I, Watanabe M (1995) Ultrastructure and phototactic action spectra of two genera of cryptophyte flagellate algae. *Cryptomonas Chromonas* 188:258–266. <https://doi.org/10.1007/BF01280378>
- Ettinger WF, Clear AM, Fanning KJ, Peck ML (1999) Identification of a Ca<sup>2+</sup>/H<sup>+</sup> antiport in the plant chloroplast thylakoid membrane. *Plant Physiol* 119:1379–1385
- Ewy RG, Dilley RA (2000) Distinguishing between luminal and localized proton buffering pools in thylakoid membranes. *Plant Physiol* 122:583–596. <https://doi.org/10.1104/pp.122.2.583>
- Finazzi G, Johnson GN, Dall'Osto L, Zito F, Bonente G, Bassi R, Wollman FA (2006) Nonphotochemical quenching of chlorophyll fluorescence in *Chlamydomonas reinhardtii*. *Biochemistry* 45:1490–1498. <https://doi.org/10.1021/bi0521588>
- Funk C, Alami M, Tibiletti T, Green BR (2011) High light stress and the one-helix LHC-like proteins of the cryptophyte *Guillardia theta*. *Biochim Biophys Acta* 1807:841–846. <https://doi.org/10.1016/j.bbabi.2011.03.011>
- Garcia-Mendoza E, Ocampo-Alvarez H, Govindjee (2011) Photoprotection in the brown alga *Macrocystis pyrifera*: evolutionary implications. *J Photochem Photobiol B Biol* 104:377–385. <https://doi.org/10.1016/j.jphotobiol.2011.04.004>
- Giovagnetti V, Ruban AV (2018) The evolution of the photoprotective antenna proteins in oxygenic photosynthetic eukaryotes. *Biochem Soc Trans* 46:1263–1277. <https://doi.org/10.1042/bst20170304>
- Goral TK, Johnson MP, Brain AP, Kirchhoff H, Ruban AV, Mullineaux CW (2010) Visualizing the mobility and distribution of chlorophyll proteins in higher plant thylakoid membranes: effects of photoinhibition and protein phosphorylation. *Plant J* 62:948–959. <https://doi.org/10.1111/j.0960-7412.2010.04207.x>
- Goss R, Lepetit B (2014) Biodiversity of NPQ. *J Plant Physiol* 172:13–32. <https://doi.org/10.1016/j.jplph.2014.03.004>
- Goss R, Lepetit B, Volke D, Gilbert M, Wilhelm C (2010) Evidence for the existence of one antenna-associated, lipid-dissolved and two protein-bound pools of diadinoxanthin cycle pigments in diatoms. *Plant Physiol* 154:1905–1920. <https://doi.org/10.1104/pp.110.166454>
- Govorunova EG, Jung KH, Sineshchekov OA, Spudich JL (2004) *Chlamydomonas* sensory rhodopsins A and B: cellular content and role in photophobic responses. *Biophys J* 86:2342–2349. [https://doi.org/10.1016/s0006-3495\(04\)74291-5](https://doi.org/10.1016/s0006-3495(04)74291-5)
- Govorunova EG, Sineshchekov OA, Janz R, Liu XQ, Spudich JL (2015) Natural light-gated anion channels: a family of microbial rhodopsins for advanced optogenetics. *Science* 349:647–650. <https://doi.org/10.1126/science.aaa7484>
- Green BR (2011) After the primary endosymbiosis: an update on the chromalveolate hypothesis and the origins of algae with Chl c. *Photosynth Res* 107:103–115. <https://doi.org/10.1007/s11120-010-9584-2>
- Grouneva I, Jakob T, Wilhelm C, Goss R (2009) The regulation of xanthophyll cycle activity and of non-photochemical fluorescence quenching by two alternative electron flows in the diatoms *Phaeodactylum tricornutum* and *Cyclotella meneghiniana*. *Biochim Biophys Acta* 1787:929–938. <https://doi.org/10.1016/j.bbabi.2009.02.004>
- Grouneva I, Rokka A, Aro EM (2011) The thylakoid membrane proteome of two marine diatoms outlines both diatom-specific and species-specific features of the photosynthetic machinery. *J Proteome Res* 10:5338–5353. <https://doi.org/10.1021/pr200600f>
- Häder D-P, Rhiel E, Wehmeyer W (1987) Phototaxis in the marine flagellate *Cryptomonas maculata*. *J Photochem Photobiol B Biol* 1:115–122. [https://doi.org/10.1016/1011-1344\(87\)80011-8](https://doi.org/10.1016/1011-1344(87)80011-8)
- Havelková-Doušová H, Prášil O, Behrenfeld M (2004) Photoacclimation of *Dunaliella tertiolecta* (Chlorophyceae) under fluctuating irradiance. *Photosynthetica* 42:273–281
- Havurinne V, Tyystjärvi E (2017) Action spectrum of photoinhibition in the diatom *Phaeodactylum tricornutum*. *Plant Cell Physiol* 58:2217–2225. <https://doi.org/10.1093/pcp/pcx156>
- Hegemann P (1997) Vision in microalgae. *Planta* 203:265–274. <https://doi.org/10.1007/s004250050191>
- Herdean A, Nziengui H, Zsiros O, Solymski K, Garab G, Lundin B, Spetea C (2016a) The arabidopsis thylakoid chloride channel AtCLCe functions in chloride homeostasis and regulation of photosynthetic electron transport. *Front Plant Sci* 7:7. <https://doi.org/10.3389/fpls.2016.00115>
- Herdean A, Teardo E, Nilsson AK, Pfeil BE, Johansson ON, Ünneper R, Nagy G, Zsiros O, Dana S, Solymski K, Garab G, Szabó I, Spetea C, Lundin B (2016b) A voltage-dependent chloride channel fine-tunes photosynthesis in plants. *Nat Commun* 7:11. <https://doi.org/10.1038/ncomms11654>
- Hill K, Hemmler R, Kovermann P, Calenberg M, Kreimer G, Wagner R (2000) A Ca<sup>2+</sup>- and voltage-modulated flagellar ion channel is a component of the mechanoshock response in the unicellular green alga *Spermatozopsis similis*. *Biochim Biophys Acta Biomembr* 1466:187–204. [https://doi.org/10.1016/S0005-2736\(00\)00200-5](https://doi.org/10.1016/S0005-2736(00)00200-5)
- Hochmal AK, Schulze S, Trompelt K, Hippler M (2015) Calcium-dependent regulation of photosynthesis. *Biochim Biophys Acta* 1847:993–1003. <https://doi.org/10.1016/j.bbabi.2015.02.010>
- Höhner R, Aboukila A, Kunz H-H, Venema K (2016) Proton Gradients and Proton-Dependent Transport Processes in the Chloroplast. *Front Plant Sci* 7:7. <https://doi.org/10.3389/fpls.2016.00218>
- Holt NE, Zigmantas D, Valkunas L, Li XP, Niyogi KK, Fleming GR (2005) Carotenoid cation formation and the regulation of photosynthetic light harvesting. *Science* 307:433–436. <https://doi.org/10.1126/science.1105833>
- Horton P, Ruban A (2005) Molecular design of the photosystem II light-harvesting antenna: photosynthesis and photoprotection. *J Exp Bot* 56:365–373. <https://doi.org/10.1093/jxb/eri023>
- Horton P, Johnson MP, Perez-Bueno ML, Kiss AZ, Ruban AV (2008) Photosynthetic acclimation: does the dynamic structure and macro-organisation of photosystem II in higher plant grana membranes regulate light harvesting states? *FEBS J* 275:1069–1079. <https://doi.org/10.1111/j.1742-4658.2008.06263.x>
- Ivanov AG, Sane PV, Hurry V, Oquist G, Huner NP (2008) Photosystem II reaction centre quenching: mechanisms and physiological role. *Photosynth Res* 98:565–574. <https://doi.org/10.1007/s11120-008-9365-3>
- Jahns P, Latowski D, Strzalka K (2009) Mechanism and regulation of the violaxanthin cycle: The role of antenna proteins and membrane



- lipids. *Biochim Biophys Acta* 1787:3–14. <https://doi.org/10.1016/j.bbabi.2008.09.013>
- Jegerschold C, Rutherford AW, Mattioli TA, Crimi M, Bassi R (2000) Calcium binding to the photosystem II subunit CP29. *J Biol Chem* 275:12781–12788
- Johnson G, Krieger A (1994) Thermoluminescence as a probe of Photosystem II in intact leaves: Non-photochemical fluorescence quenching in peas grown in an intermittent light regime. *Photosynth Res* 41:371–379. <https://doi.org/10.1007/BF02183039>
- Johnson MP, Ruban AV (2010) Arabidopsis plants lacking PsbS protein possess photoprotective energy dissipation. *Plant J* 61:283–289. <https://doi.org/10.1111/j.1365-3113X.2009.04051.x>
- Johnson CH, Shingles R, Ettinger WF (2006) Regulation and role of calcium fluxes in the chloroplast. In: Wise RR, Hooper JK (eds) *The structure and function of plastids*. Springer Netherlands, Dordrecht, pp 403–416. [https://doi.org/10.1007/978-1-4020-4061-0\\_20](https://doi.org/10.1007/978-1-4020-4061-0_20)
- Kale R, Hebert AE, Frankel LK, Sallans L, Bricker TM, Pospisil P (2017) Amino acid oxidation of the D1 and D2 proteins by oxygen radicals during photoinhibition of photosystem II. *Proc Natl Acad Sci U S A* 114:2988–2993. <https://doi.org/10.1073/pnas.1618922114>
- Kaňa R (2018) Application of spectrally resolved fluorescence induction to study light-induced nonphotochemical quenching in algae. *Photosynthetica* 56:132–138. <https://doi.org/10.1007/s11099-018-0780-1>
- Kaňa R, Govindjee (2016) Role of ions in the regulation of light-harvesting. *Front Plant Sci* 7:7. <https://doi.org/10.3389/fpls.2016.01849>
- Kaňa R, Vass I (2008) Thermoimaging as a tool for studying light-induced heating of leaves: correlation of heat dissipation with the efficiency of photosystem II photochemistry and non-photochemical quenching. *Environ Exp Bot* 64:90–96. <https://doi.org/10.1016/j.envexpbot.2008.02.006>
- Kaňa R, Lazár D, Prášil O, Naus J (2002) Experimental and theoretical studies on the excess capacity of photosystem II. *Photosynth Res* 72:271–284. <https://doi.org/10.1023/a:1019894720789>
- Kaňa R, Prášil O, Mullineaux CW (2009) Immobility of phycobilins in the thylakoid lumen of a cryptophyte suggests that protein diffusion in the lumen is very restricted. *FEBS Lett* 583:670–674
- Kaňa R, Kotabová E, Sobotka R, Prášil O (2012) Non-photochemical quenching in cryptophyte alga *Rhodomonas salina* is located in chlorophyll a/c antennae. *PLoS One* 7:e29700. <https://doi.org/10.1371/journal.pone.0029700>
- Kaňa R, Kotabová E, Kopečná J, Trsková E, Belgio E, Sobotka R, Ruban AV (2016) Violaxanthin inhibits nonphotochemical quenching in light-harvesting antenna of *Chromera velia*. *FEBS Lett* 590:1076–1085. <https://doi.org/10.1002/1873-3468.12130>
- Kaneda H, Furuya M (1986) Temporal changes in swimming direction during the phototactic orientation of individual cells in *Cryptomonas* sp. *Plant Cell Physiol* 27:265–271. <https://doi.org/10.1093/oxfordjournals.pcp.a077099>
- Kaneda H, Furuya M (1987a) Effect of calcium-ions on phototactic orientation of individual cryptomonas cells. *Plant Sci* 48:31–35
- Kaneda H, Furuya M (1987b) Effects of the timing of flashes of light during the course of cellular rotation on phototactic orientation of individual cells of *Cryptomonas*. *Plant Physiol* 84:178–181
- Khatoun M et al (2009) Quality control of photosystem II: thylakoid unstacking is necessary to avoid further damage to the D1 protein and to facilitate D1 degradation under light stress in spinach thylakoids. *J Biol Chem* 284:25343–25352. <https://doi.org/10.1074/jbc.M109.007740>
- Kirilovsky D, Kaňa R, Prášil O (2014) Mechanisms modulating energy arriving at reaction centers in cyanobacteria. In: Demmig-Adams B, Garab G, Adams III W, Govindjee (eds) *Non-photochemical quenching and energy dissipation in plants, algae and cyanobacteria*, Advances in photosynthesis and respiration, vol 40. Springer, Netherlands, pp 471–501. [https://doi.org/10.1007/978-94-017-9032-1\\_22](https://doi.org/10.1007/978-94-017-9032-1_22)
- Kok B (1956) On the inhibition of photosynthesis by intense light. *Biochim Biophys Acta* 21:234–244. [https://doi.org/10.1016/0006-3002\(56\)90003-8](https://doi.org/10.1016/0006-3002(56)90003-8)
- Komenda J, Barker M, Kuvikova S, de Vries R, Mullineaux CW, Tichy M, Nixon PJ (2006) The FtsH protease slr0228 is important for quality control of photosystem II in the thylakoid membrane of *Synechocystis* sp. PCC 6803. *J Biol Chem* 281:1145–1151. <https://doi.org/10.1074/jbc.M503852200>
- Kosugi M et al (2018) A comparative study of wavelength-dependent photoinactivation in photosystem II of drought-tolerant photosynthetic organisms in Antarctica and the potential risks of photoinhibition in the habitat. *Ann Bot*. <https://doi.org/10.1093/aob/mcy139>
- Kotabová E, Kaňa R, Jarešova J, Prášil O (2011) Non-photochemical fluorescence quenching in *Chromera velia* is enabled by fast violaxanthin de-epoxidation. *FEBS Lett* 585:1941–1945. <https://doi.org/10.1016/j.febslet.2011.05.015>
- Krause GH, Briantais JM, Vermette C (1983) Characterization of chlorophyll fluorescence quenching in chloroplasts by fluorescence spectroscopy at 77-K. 1.  $\Delta$ pH-dependent quenching. *Biochim Biophys Acta* 723:169–175. [https://doi.org/10.1016/0005-2728\(83\)90116-0](https://doi.org/10.1016/0005-2728(83)90116-0)
- Krieger A, Weis E (1993) The role of calcium in the pH-dependent control of photosystem II. *Photosynth Res* 37:117–130. <https://doi.org/10.1007/bf02187470>
- Krieger A, Moya I, Weis E (1992) Energy-dependent quenching of chlorophyll a fluorescence: effect of pH on stationary fluorescence and picosecond-relaxation kinetics in thylakoid membranes and photosystem II preparations. 1102. [https://doi.org/10.1016/0167-4838\(92\)90507-A](https://doi.org/10.1016/0167-4838(92)90507-A)
- Kruger TPJ, Wientjes E, Croce R, van Grondelle R (2011) Conformational switching explains the intrinsic multifunctionality of plant light-harvesting complexes. *Proc Natl Acad Sci U S A* 108:13516–13521. <https://doi.org/10.1073/pnas.1105411108>
- Krupnik T et al (2013) A reaction centre-dependent photoprotection mechanism in a highly robust photosystem II from an extremophilic red alga *Cyanidioschyzon merolae*. *J Biol Chem* 288:23529–23542. <https://doi.org/10.1074/jbc.M113.484659>
- Krynicka V, Shao S, Nixon PJ, Komenda J (2015) Accessibility controls selective degradation of photosystem II subunits by FtsH protease. *Nat Plants* 1:15168. <https://doi.org/10.1038/nplants.2015.168>
- Kunz HH, Gierth M, Herdean A, Satoh-Cruz M, Kramer DM, Spetea C, Schroeder JI (2014) Plastidial transporters KEA1, -2, and -3 are essential for chloroplast osmoregulation, integrity, and pH regulation in *Arabidopsis*. *Proc Natl Acad Sci U S A* 111:7480–7485. <https://doi.org/10.1073/pnas.1323899111>
- Kuthanová Trsková E, Belgio E, Yeates AM, Sobotka R, Ruban AV, Kaňa R (2018) Antenna proton sensitivity determines photosynthetic light harvesting strategy. *J Exp Bot* 69:4483–4493. <https://doi.org/10.1093/jxb/ery240>
- Kuthanová Trsková E, Bína D, Santabarbara S, Sobotka R, Kaňa R, Belgio E (2019) Isolation and characterization of CAC antenna proteins and photosystem I supercomplex from the cryptophyte alga *Rhodomonas salina*. *Physiol Plant* 166:309–319. <https://doi.org/10.1111/ppl.12928>
- Lavaud J, Kroth PG (2006) In diatoms, the transthylakoid proton gradient regulates the photoprotective non-photochemical fluorescence quenching beyond its control on the xanthophyll cycle. *Plant Cell Physiol* 47:1010–1016. <https://doi.org/10.1093/pcp/pcj058>
- Lavaud J, Lepetit B (2013) An explanation for the inter-species variability of the photoprotective non-photochemical chlorophyll fluorescence quenching in diatoms. *Biochim Biophys Acta* 1827:294–302. <https://doi.org/10.1016/j.bbabi.2012.11.012>

- Lavaud J, Rousseau B, Etienne AL (2002a) In diatoms, a transthylakoid proton gradient alone is not sufficient to induce a non-photochemical fluorescence quenching. *FEBS Lett* 523:163–166
- Lavaud J, Rousseau B, van Gorkom H, Etienne A (2002b) Influence of the diadinoxanthin pool size on photoprotection in the marine planktonic diatom *Phaeodactylum tricoratum*. *Plant Physiol* 129:1398–1406
- Lavaud J, van Gorkom HJ, Etienne A-L (2002c) Photosystem II electron transfer cycle and chlororespiration in planktonic diatoms. *Photosynth Res* 74:51–59. <https://doi.org/10.1023/A:1020890625141>
- Lavaud J, Rousseau B, Etienne AL (2003) Enrichment of the light-harvesting complex in diadinoxanthin and implications for the nonphotochemical fluorescence quenching in diatoms. *Biochemistry* 42:5802–5808. <https://doi.org/10.1021/bi027112i>
- Lee RE (2008) *Phycology*, 4th edn. Cambridge University Press, Cambridge. <https://doi.org/10.1017/CBO9780511812897>
- Li XP, Bjorkman O, Shih C, Grossman AR, Rosenquist M, Jansson S, Niyogi KK (2000) A pigment-binding protein essential for regulation of photosynthetic light harvesting. *Nature* 403:391–395
- Li ZR, Wakao S, Fischer BB, Niyogi KK (2009) Sensing and responding to excess light. *Annu Rev Plant Biol* 60:239–260. <https://doi.org/10.1146/annurev.arplant.58.032806.103844>
- Li XM, Zhang QS, Tang YZ, Yu YQ, Liu HL, Li LX (2014) Highly efficient photoprotective responses to high light stress in *Sargassum thunbergii* gemmlings, a representative brown macroalga of intertidal zone. *J Sea Res* 85:491–498. <https://doi.org/10.1016/j.seares.2013.08.004>
- Li L, Aro EM, Millar AH (2018) Mechanisms of photodamage and protein turnover in photoinhibition. *Trends Plant Sci* 23:667–676. <https://doi.org/10.1016/j.tplants.2018.05.004>
- Liguori N, Roy LM, Opacic M, Durand G, Croce R (2013) Regulation of light harvesting in the green alga *Chlamydomonas reinhardtii*: the C-terminus of LHCSR is the knob of a dimmer switch. *J Am Chem Soc* 135:18339–18342. <https://doi.org/10.1021/ja4107463>
- Magdaong NCM, Blankenship RE (2018) Photoprotective, excited-state quenching mechanisms in diverse photosynthetic organisms. *J Biol Chem* 293:5018–5025. <https://doi.org/10.1074/jbc.TM117.000233>
- McAinsh MR, Pittman JK (2009) Shaping the calcium signature. *New Phytol* 181:275–294. <https://doi.org/10.1111/j.1469-8137.2008.02682.x>
- Mendes CRB, Tavano VM, Dotto TS, Kerr R, de Souza MS, Garcia CAE, Secchi ER (2018) New insights on the dominance of cryptophytes in Antarctic coastal waters: a case study in Gerlache Strait. *Deep-Sea Res II Top Stud Oceanogr* 149:161–170. <https://doi.org/10.1016/j.dsr2.2017.02.010>
- Miqyass M, van Gorkom HJ, Yocum CF (2007) The PSII calcium site revisited. *Photosynth Res* 92:275–287. <https://doi.org/10.1007/s11120-006-9124-2>
- Muller P, Li XP, Niyogi KK (2001) Non-photochemical quenching. A response to excess light energy. *Plant Physiol* 125:1558–1566
- Mulo P, Sakurai I, Aro EM (2012) Strategies for psbA gene expression in cyanobacteria, green algae and higher plants: from transcription to PSII repair. *Biochim Biophys Acta* 1817:247–257. <https://doi.org/10.1016/j.bbabi.2011.04.011>
- Nagel G, Ollig D, Fuhrmann M, Kateriya S, Musti AM, Bamberg E, Hegemann P (2002) Channelrhodopsin-1: a light-gated proton channel in green algae. *Science* 296:2395–2398. <https://doi.org/10.1126/science.1072068>
- Nagel G et al (2003) Channelrhodopsin-2, a directly light-gated cation-selective membrane channel. *Proc Natl Acad Sci U S A* 100:13940–13945. <https://doi.org/10.1073/pnas.1936192100>
- Niyogi KK, Grossman AR, Bjorkman O (1998) Arabidopsis mutants define a central role for the xanthophyll cycle in the regulation of photosynthetic energy conversion. *Plant Cell* 10:1121–1134. <https://doi.org/10.2307/3870716>
- Ohad I, Raanan H, Keren N, Tchernov D, Kaplan A (2010) Light-induced changes within photosystem II protects *Microcoleus* sp in biological desert sand crusts against excess light. *PLoS One* 5:e11000. <https://doi.org/10.1371/journal.pone.0011000>
- Pan RS, Dilley RA (2000) Influence of Ca<sup>2+</sup> on the thylakoid lumen violaxanthin de-epoxidase activity through Ca<sup>2+</sup> gating of H<sup>+</sup> flux at the CFoH<sup>+</sup> channel. *Photosynth Res* 65:141–154
- Papageorgiou GC, Alygizaki-Zorba A, Ladas N, Murata N (1998) A method to probe the cytoplasmic osmolality and osmotic water and solute fluxes across the cell membrane of cyanobacteria with chlorophyll a fluorescence: experiments with *Synechococcus* sp. PCC7942 103:215–224. <https://doi.org/10.1034/j.1399-3054.1998.1030209.x>
- Peers G et al (2009) An ancient light-harvesting protein is critical for the regulation of algal photosynthesis. *Nature* 462:518–U215. <https://doi.org/10.1038/nature08587>
- Petroutsos D et al (2011) The chloroplast calcium sensor CAS is required for photoacclimation in *Chlamydomonas reinhardtii*. *Plant Cell* 23:2950–2963. <https://doi.org/10.1105/tpc.111.087973>
- Polin M, Tuval I, Drescher K, Gollub JP, Goldstein RE (2009) *Chlamydomonas* swims with two “gears” in a eukaryotic version of run-and-tumble locomotion. *Science* 325:487–490. <https://doi.org/10.1126/science.1172667>
- Prášil O, Adir N, Ohad I (1992) Dynamics of photosystem II: mechanism of photoinhibition and recovery processes. In: Barber J (ed) *The photosystems: structure, function and molecular biology*, vol 11. Elsevier Science, Oxford, pp 295–348
- Quigg A et al (2012) Photosynthesis in *Chromera velia* represents a simple system with high efficiency. *PLoS One* 7:e47036. <https://doi.org/10.1371/journal.pone.0047036>
- Roh MH, Shingles R, Cleveland MJ, McCarty RE (1998) Direct measurement of calcium transport across chloroplast inner-envelope vesicles. *Plant Physiol* 118:1447–1454. <https://doi.org/10.1104/pp.118.4.1447>
- Ruban AV, Horton P (1995) An investigation of the sustained component of nonphotochemical quenching of chlorophyll fluorescence in isolated-chloroplasts and leaves of spinach. *Plant Physiol* 108:721–726
- Ruban AV et al (2007) Identification of a mechanism of photoprotective energy dissipation in higher plants. *Nature* 450:575–U522. <https://doi.org/10.1038/nature06262>
- Ruban AV, Johnson MP, Duffy CDP (2012) The photoprotective molecular switch in the photosystem II antenna. *Biochim Biophys Acta* 1817:167–181. <https://doi.org/10.1016/j.bbabi.2011.04.007>
- Schmid R, Junge W (1975) Current-voltage studies on the thylakoid membrane in the presence of ionophores. *Biochim Biophys Acta* 394:76–92
- Sineshchekov OA, Govorunova EG, Jung KH, Zauner S, Maier UG, Spudich JL (2005) Rhodopsin-mediated photoreception in cryptophyte flagellates. *Biophys J* 89:4310–4319. <https://doi.org/10.1529/biophysj.105.070920>
- Slavov C et al (2016) “Super-quenching” state protects Symbiodinium from thermal stress - implications for coral bleaching. *Biochim Biophys Acta* 1857:840–847. <https://doi.org/10.1016/j.bbabi.2016.02.002>
- Smith EF (2002) Regulation of flagellar dynein by calcium and a role for an axonemal calmodulin and calmodulin-dependent kinase. *Mol Biol Cell* 13:3303–3313. <https://doi.org/10.1091/mbc.e02-04-0185>
- Staleva H, Komenda J, Shukla MK, Slouf V, Kana R, Polivka T, Sobotka R (2015) Mechanism of photoprotection in the cyanobacterial ancestor of plant antenna proteins. *Nat Chem Biol* 11:287–291. <https://doi.org/10.1038/nchembio.1755>
- Suetsugu N, Wada M (2007) Chloroplast photorelocation movement mediated by phototropin family proteins in green plants. *Biol Chem* 388:927–935. <https://doi.org/10.1515/bc.2007.118>

- Suetsugu N, Yamada N, Kagawa T, Yonekura H, Uyeda TQP, Kadota A, Wada M (2010) Two kinesin-like proteins mediate actin-based chloroplast movement in *Arabidopsis thaliana*. *Proc Natl Acad Sci U S A* 107:8860–8865. <https://doi.org/10.1073/pnas.0912773107>
- Tang Y, Wen X, Lu Q, Yang Z, Cheng Z, Lu C (2007) Heat stress induces an aggregation of the light-harvesting complex of photosystem II in spinach plants. *Plant Physiol* 143:629–638. <https://doi.org/10.1104/pp.106.090712>
- Tikkanen M, Aro EM (2012) Thylakoid protein phosphorylation in dynamic regulation of photosystem II in higher plants. *Biochim Biophys Acta* 1817:232–238. <https://doi.org/10.1016/j.bbabi.2011.05.005>
- Ting CS, Owens TG (1994) The effects of excess irradiance on photosynthesis in the marine diatom *Phaeodactylum-tricornutum*. *Plant Physiol* 106:763–770
- Tyystjarvi E, Aro EM (1996) The rate constant of photoinhibition, measured in lincomycin-treated leaves, is directly proportional to light intensity. *Proc Natl Acad Sci U S A* 93:2213–2218. <https://doi.org/10.1073/pnas.93.5.2213>
- Van Walraven HS, Scholts MJC, Zakharov SD, Kraayenhof R, Dilley RA (2002) pH-dependent Ca<sup>2+</sup> binding to the F-0 c-subunit affects proton translocation of the ATP synthase from *Synechocystis* 6803. *J Bioenerg Biomembr* 34:455–464
- Vass I (2011) Role of charge recombination processes in photodamage and photoprotection of the photosystem II complex. *Physiol Plant* 142:6–16. <https://doi.org/10.1111/j.1399-3054.2011.01454.x>
- Vass I (2012) Molecular mechanisms of photodamage in the photosystem II complex. *Biochim Biophys Acta* 1817:209–217. <https://doi.org/10.1016/j.bbabi.2011.04.014>
- Vass I, Cser K (2009) Janus-faced charge recombinations in photosystem II photoinhibition. *Trends Plant Sci* 14:200–205. <https://doi.org/10.1016/j.tplants.2009.01.009>
- Verret F, Wheeler G, Taylor AR, Farnham G, Brownlee C (2010) Calcium channels in photosynthetic eukaryotes: implications for evolution of calcium-based signalling. *New Phytol* 187:23–43. <https://doi.org/10.1111/j.1469-8137.2010.03271.x>
- Wada M (2016) Chloroplast and nuclear photorelocation movements. *Proc Jpn Acad Ser B Phys Biol Sci* 92:387–411. <https://doi.org/10.2183/pjab.92.387>
- Walters RG, Ruban AV, Horton P (1996) Identification of proton-active residues in a higher plant light-harvesting complex. *Proc Natl Acad Sci U S A* 93:14204–14209
- Wang C et al (2016) A putative chloroplast-localized Ca<sup>2+</sup>/H<sup>+</sup> antiporter CCHA1 is involved in calcium and pH homeostasis and required for PSII function in *Arabidopsis*. *Mol Plant* 9:1183–1196. <https://doi.org/10.1016/j.molp.2016.05.015>
- Watanabe M, Furuya M (1974) Action spectrum of phototaxis in a cryptomonad alga, *Cryptomonas* sp. *Plant Cell Physiol* 15:413–420. <https://doi.org/10.1093/oxfordjournals.pcp.a075021>
- Watanabe M, Furuya M (1978) Phototactic responses of cell population to repeated pulses of yellow light in a phytoflagellate *Cryptomonas* sp. *Plant Physiol* 61:816–818
- Watanabe M, Furuya M (1982) Phototactic behaviour of individual cells of *Cryptomonas* sp. in response to continuous and intermittent light stimuli. *Photochem Photobiol* 35:559–563. <https://doi.org/10.1111/j.1751-1097.1982.tb02609.x>
- Watanabe M, Miyoshi Y, Furuya M (1976) Phototaxis in *Cryptomonas* sp. under condition suppressing photosynthesis. *Plant Cell Physiol* 17:683–690. <https://doi.org/10.1093/oxfordjournals.pcp.a075324>
- Xu P, Tian L, Kloz M, Croce R (2015) Molecular insights into zeaxanthin-dependent quenching in higher plants. *Sci Rep* 5:13679. <https://doi.org/10.1038/srep13679>
- Yamamoto Y et al (2008) Quality control of photosystem II: impact of light and heat stresses. *Photosynth Res* 98:589–608. <https://doi.org/10.1007/s1120-008-9372-4>

**Publisher's note** Springer Nature remains neutral with regard to jurisdictional claims in published maps and institutional affiliations.

# *Curriculum vitae*

---

## **Eliška Kuthanová (Trsková)**

Institute of Microbiology, Czech Academy of Sciences  
Department of Autotrophic Microorganisms, Laboratory of  
Photosynthesis  
CZ-379 81 Třeboň, Czech Republic  
Email: kuthanova@alga.cz, Phone: +420 384 340 442

### **ACADEMIC QUALIFICATION:**

- PhD study – **Plant Physiology - University of South Bohemia** (2015- present). Topic: Regulation of photochemical activity in pigment-proteins of thylakoid membrane, supervisor: Mgr. Radek Kaňa, PhD
- Master study of **Genetics - University of South Bohemia** (2013-2015). Topic: Mechanism of photoprotection in photosynthetic proteins, supervisor: Mgr. Radek Kaňa, PhD
- Bachelor study **Biological chemistry - Johannes Kepler University** Linz, Austria (2010-2013). Topic: Purification of isotopically labeled PsbP from *Spinacia oleracea*.
- Bachelor study of **Biological chemistry - University of South Bohemia** České Budějovice, Czech Republic (2010-2013). Topic: Organic pollutants in constructed wetlands

### **CONFERENCES:**

- **International congress of Biophysics of photosynthesis (from molecules to the field)**, Rome, Italy, poster: *NPQ without xanthophyll cycle –the effect of pH and ions on in vitro quenching of cryptophytic antennas* (2019)
- **Plant biology 2019**, České Budějovice, presentation: *Antenna sensitivity to protons determines photosynthetic light harvesting strategy* (2019)
- **First European Congress on Photosynthesis Research, ePS-1**, Uppsala, Sweden, Poster and selected flash poster presentation: *Antenna sensitivity to protons determines photosynthetic light harvesting strategy* (2018)

- **The 17th International Congress on Photosynthesis Research**, Maastricht, The Netherlands: Poster: *Unique NPQ mechanism in Chromera velia: from native cells to in vitro* (2016)
- **Chromera meeting**, České Budějovice: Poster: *Non-photochemical quenching in isolated complexes of Chromera velia: the role of pH in vitro* (2014)

### **ABROAD STAYS AND COLLABORATIONS:**

- **Prof. Alexander Ruban laboratory** - Queen Mary university of London, 1 month (2017)
- **Prof. Alexander Ruban laboratory** - Queen Mary university of London - 2 weeks, September 2014
- International **Bachelor program of Biological Chemistry** in Linz, Austria – three semesters in Austria (between 2010-2013)

### **WORKING EXPERIENCE**

- **Research assistant**, Department of Autotrophic Microorganisms, Laboratory of Photosynthesis, The Czech Academy of Sciences (2014 – present)
- **Involvement in the project of Czech Science foundation:** *Photoprotective antenna protein dynamics: from live cells to algal proteoliposomes*, member of the team, GAČR 17-02363Y
- **Involvement in the project of Czech Science foundation:** *Mobility of photosynthetic proteins*, member of the team, GAČR P501-12-0304

### **GRANTS AND FELLOWSHIPS**

- **GAJU scholarship** for 1-year research project as a fellow PhD student (2018)
- **FEBS short term fellowship** for 1 month stay at the at the Ruban Laboratory, Queen Mary University of London (2017)
- **GAJU scholarship** for 1-year individual research project (2016)
- **Rectors award for outstanding results** – University of South Bohemia (2015)
- **Top-up Scholarship of Excellence - Innovatives** Oberösterreich 2010 PLUS (2013)

## **PUBLICATIONS:**

- Kaňa, R., Kotabová, E., Šedivá, B., and **Kuthanová Trsková, E.** (2019). Photoprotective strategies in the motile cryptophyte alga *Rhodomonas salina* – role of non-photochemical quenching, ions, photoinhibition and cell motility. *Folia Microbiologica* 64, 691-703.
- **Kuthanová Trsková, E.**, Bína, D., Santabarbara, S., Sobotka, R., Kaňa, R., and Belgio, E. (2019). Isolation and characterization of CAC antenna proteins and photosystem I supercomplex from the cryptophytic alga *Rhodomonas salina*. *Physiologia Plantarum* **166**, 309-319.
- **Kuthanová Trsková E**, Belgio E, Yeates AM, Sobotka R, Ruban AV, Kaňa R (2018) Antenna proton sensitivity determines photosynthetic light harvesting strategy. *J Exp Bot* 69: 4483-4493
- Belgio E, **Trsková E**, Kotabová E, Ewe D, Prášil O, Kaňa R (2018) High light acclimation of *Chromera velia* points to photoprotective NPQ. *Photosynthesis Research* 135: 263-274
- Sobotka R, Esson HJ, Koník P, **Trsková E**, Moravcová L, Horák A, Dufkova P, Oborník M (2017) Extensive gain and loss of photosystem I subunits in chromerid algae, photosynthetic relatives of apicomplexans. *Sci Rep* 7: 13214
- Belgio E, Santabarbara S, Bína D, **Trsková E**, Herbstová M, Kaňa R, Zucchelli G, Prášil, O (2017) High photochemical trapping efficiency in Photosystem I from the red clade algae *Chromera velia* and *Phaeodactylum tricorutum*. *Biochimica et Biophysica Acta (BBA) - Bioenergetics* 1858:56-63
- Kaňa R, Kotabová E, Kopečná J, **Trsková E**, Belgio E, Sobotka R, Ruban AV (2016) Violaxanthin inhibits nonphotochemical quenching in light-harvesting antennae of *Chromera velia*. *FEBS letters* 590:1076-1085
- West R, Kesan G, **Trsková E**, Sobotka R, Kaňa R, Fuciman M, Polívka T (2016) Spectroscopic properties of the triple bond carotenoid alloxanthin. *Chemical Physics Letters* 653:167-172

© for non-published parts Eliška Kuthanová

[kuthanova@alga.cz](mailto:kuthanova@alga.cz)

Regulation of photosynthetic activity of pigment-protein complexes in thylakoid membranes. Ph.D. Thesis Series, 2020, No. 13

All rights reserved

For non-commercial use only

Printed in the Czech Republic by Typodesign

Edition of 20 copies

University of South Bohemia in České Budějovice

Faculty of Science

Branišovská 1760

CZ-37005 České Budějovice, Czech Republic

Phone: +420 387 776 201

[www.prf.jcu.cz](http://www.prf.jcu.cz), e-mail: [sekret-fpr@prf.jcu.cz](mailto:sekret-fpr@prf.jcu.cz)